
# Functional consequences of *Setd1a* haploinsufficiency: from gestation to behaviour

by

**Matthew Lee Bosworth**

A thesis submitted for the degree of

**Doctor of Philosophy**

September 2019

## Declarations

### Statement 1

This thesis is being submitted in partial fulfilment of the requirements for the degree of Doctor of Philosophy.

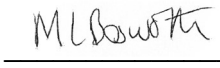
(Matthew Bosworth) Date 24/09/2019

### Statement 2

This work has not been submitted in substance for any other degree or award at this or any other university or place of learning, nor is it being submitted concurrently for any other degree or award (outside of any formal collaboration agreement between the University and a partner organisation)

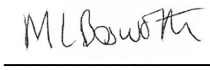
(Matthew Bosworth) Date 24/09/2019

### Statement 3

I hereby give consent for my thesis, if accepted, to be available in the University's Open Access repository (or, where approved, to be available in the University's library and for inter-library loan), and for the title and summary to be made available to outside organisations, subject to the expiry of a University-approved bar on access if applicable.

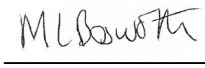
(Matthew Bosworth) Date 24/09/2019

### Declaration

This thesis is the result of my own independent work, except where otherwise stated, and the views expressed are my own. Other sources are acknowledged by explicit references. The thesis has not been edited by a third party beyond what is permitted by Cardiff University's Use of Third Party Editors by Research Degree Students Procedure.

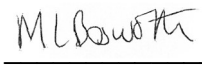
(Matthew Bosworth) Date 24/09/2019

## Summary

Advances in psychiatric genetics are providing opportunities to investigate underlying pathogenic mechanisms. Rare loss of function (LoF) variants that have large effects on risk are of particular interest because they unequivocally implicate LoF of a single gene and are expected to have prominent phenotypic effects. The first LoF variants to be identified for schizophrenia were in the *SETD1A* gene. *SETD1A* catalyses methylation of lysine residue 4 on histone 3 (H3K4) and its pathogenic role is consistent with convergent evidence implicating disrupted H3K4 methylation in schizophrenia and other neurodevelopmental disorders. However, understanding of the biological mechanisms underlying the association between *SETD1A* LoF and psychopathology is lacking. This thesis investigated the functional consequences of *Setd1a* haploinsufficiency using a mouse model.

*Setd1a* haploinsufficiency resulted in modest transcriptomic changes in the developing mouse brain that were enriched for mitochondrial annotations (Chapter 3). However, there was no enrichment for schizophrenia common variant association. Additionally, placental weight was reduced in *Setd1a*$^{+/-}$ mice and sexually dimorphic changes in placental gene expression and postnatal growth were observed in *Setd1a*$^{+/-}$ males but not females (Chapter 4).

Behavioural phenotyping revealed that constitutive *Setd1a* haploinsufficiency caused heightened emotional reactivity and aberrant sensorimotor gating (Chapter 5). The effects on sensorimotor gating were robust and could not be rescued by established antipsychotics (haloperidol and risperidone) (Chapter 6). However, male (but not female) *Setd1a*$^{+/-}$ mice showed an insensitivity to the startle-inhibiting effects of risperidone, potentially indicating 5-HT2A receptor dysfunction. Finally, behavioural phenotyping of a conditional knockout with *Setd1a* haploinsufficiency constrained to the nervous system revealed evidence for a degree of convergence with the constitutive model (Chapter 7).

In conclusion, this thesis provides novel insights into the diverse effects of *Setd1a* haploinsufficiency. These findings warrant further investigation to establish the pathophysiological relevance of effects on the developing brain, placenta, and adult brain function.

## List of Contents

## List of Figures

## List of Tables

## List of Abbreviations

| | |
|---|---|
| 5-HT | Serotonin |
| ANOVA | Analysis of variance |
| ASR | Acoustic startle response |
| ASU | Arbitrary startle units |
| bp | Base pairs |
| cDNA | Complementary DNA |
| CNV | Copy number variant |
| DAO | D-amino acid oxidase |
| DMR | Differentially methylated region |
| DNA | Deoxyribonucleic acid |
| DOI | 2,5-Dimethoxy-4-iodoamphetamine |
| EPM | Elevated plus maze |
| ESC | Embryonic stem cell |
| fMRI | Functional magnetic resonance imaging |
| GABA | Gamma-aminobutyric acid |
| GO | Gene ontology |
| GWAS | Genome-wide association study |
| H3K4me | Histone 3 lysine 4 methylation |
| ICR | Imprinting control region |
| IMPC | International Mouse Phenotyping Consortium |
| IUGR | Intrauterine growth restriction |
| Indel | Insertion or deletion |
| IP | Intraperitoneal |
| kb | Kilobase |
| KDM | Lysine demethylase |

| | |
|---|---|
| KMT | Lysine methyltransferase |
| LoF | Loss of function |
| LSD | Lysergic acid diethylamide |
| MANOVA | Multivariate analysis of variance |
| mRNA | Messenger ribonucleic acid |
| NMDA | *N*-methyl-D-aspartate |
| NOR | Novel object recognition |
| NPC | Neuronal progenitor cell |
| OFT | Open field test |
| PCP | Phencyclidine |
| PCR | Polymerase chain reaction |
| PFC | Prefrontal cortex |
| PPI | Prepulse inhibition |
| RT-qPCR | Real-time quantitative polymerase chain reaction |
| SEM | Standard error of the mean |
| *Setd1a*$^{+/-}$ | Constitutive heterozygous *Setd1a* model |
| *Setd1a* cKO | Conditional heterozygous *Setd1a* model |
| SNP | Single nucleotide polymorphism |
| TCP | Tranylcypromine |
| Tm1a | Targeted mutation 1a (knock-out first allele) |
| Tm1c | Targeted mutation 1c (floxed allele) |
| Tm1d | Targeted mutation 1d (deleted allele) |
| WT | Wild type |

## Acknowledgements

First and foremost, I would like to thank my supervisors: Professor Lawrence Wilkinson, Professor Anthony Isles, and Dr Trevor Humby. Thank you all for your continued support and guidance throughout this PhD and for giving me the academic freedom to pursue my own ideas (but also knowing when to rein me in!) I've learned a great deal from you all and am so grateful for the opportunities you have given me. I am very much looking forward to continuing to work with you all over the next few years.

A special thanks goes to Dr Gráinne McNamara for introducing me to behavioural neuroscience during my rotation year. Thanks also to Dr Hugo Creeth for his invaluable knowledge of the placenta, Dr Nick Clifton for his patience while showing me how to analyse RNA-seq data, and Dr Andrew Pocklington for helpful bioinformatics advice and discussion.

A big thank you to all of the JBIOS staff for taking care of my animals and without whom this work would not be possible. Particular thanks go to Rhys Perry, who was always there whenever I had any questions about animal husbandry. Thank you also to the core team in the IPMCN labs for keeping everything running smoothly.

I am grateful to have shared this PhD journey with many great colleagues and friends. Thanks to other members of the Isles lab (Dr Manni Adam, Dr Kira Rienecker, and Simona Zahova), my BNL office mates (Emma Bubb, Ina Iliescu, and Lucy Lewis) and the rest of the Wellcome Trust cohort (Tommy Freeman, Jasmine Donaldson, Frankie Keefe, Laura Smith, and Juliet Scully) for your help and advice in and out of the lab.

Thank you to my parents and sister for always believing in me and for everything you've done for me to get me to where I am today. This would not have been possible without you.

Last but definitely not least, thank you to my partner, Nick. Thank you for your unwavering support over the past four years. Thank you for always being there for me during the ups and downs. Thank you for your constant tolerance, putting up with me, and never once complaining when I had to work weekends. Thank you for being you.

This work was primarily funded by a Wellcome Trust Integrative Neuroscience PhD studentship. Additional funding was provided by the Medical Research Council for the generation of floxed *Setd1a* mice at MRC Harwell.

## Acknowledgements of assistance received

Initial training in techniques, laboratory practice and subsequent mentoring:

- Professor Lawrence Wilkinson: general advice, guidance, and discussion with reference to behavioural genetics and behavioural neuroscience.
- Professor Anthony Isles: training in all molecular methods and general advice, guidance, and discussion with reference to behavioural genetics and behavioural neuroscience.
- Dr Trevor Humby: training in all behavioural methods and general advice, guidance, and discussion with reference to behavioural genetics and behavioural neuroscience.
- Dr Nick Clifton: training in RNA-seq data analysis.

Data/materials produced by others:

- Placental RT-qPCR data: Dr Hugo Creeth and Annabel Flynn.
- Library preparations and sequencing: Joanne Morgan.
- RNA-seq data analysis scripts: Dr Robert Andrews.

# Chapter 1: General Introduction

## 1.1. Unmet clinical need of schizophrenia

Schizophrenia is a chronically disabling and extremely distressing neuropsychiatric disorder. Mortality rates are high in people with schizophrenia, with a reduction in life expectancy of between 10 and 20 years (Chesney, Goodwin, & Fazel, 2014; Hjorthøj, Stürup, McGrath, & Nordentoft, 2017). High mortality in schizophrenia has been attributed to increased risk of suicide or medical conditions caused by poor lifestyle factors, such as heavy smoking, inadequate diet, and reduced physical activity (Laursen, Nordentoft, & Mortensen, 2014). Despite a relatively low prevalence (McGrath, Saha, Chant, & Welham, 2008), schizophrenia is ranked among the top 20 causes of disability worldwide (Spencer et al., 2018). The economic burden of schizophrenia is substantial, both in terms of the direct costs of care (Mangalore & Knapp, 2007) and indirect costs caused by high levels of unemployment (Marwaha & Johnson, 2004), homelessness (Folsom et al., 2005), and loss of family caregiver work productivity (Mangalore & Knapp, 2007). Recent meta-analyses suggest that recovery rates are low; respectively, only 30 % and 13 % of people with first-episode and multi-episode schizophrenia meet criteria for recovery (Jääskeläinen et al., 2013; Lally et al., 2017).

Symptoms of schizophrenia can be broadly classified into three categories; i) positive or psychotic (detachment from reality, comprising hallucinations and delusions), ii) negative (anhedonia, motivational deficits, and social withdrawal), and cognitive (impairments in executive function, attention, and memory) (Arango & Carpenter, 2011). Onset typically occurs in late adolescence or early adulthood but is usually preceded by a prodromal phase characterised by less severe symptomatology (Lewandowski, Cohen, & Öngur, 2011; Lieberman et al., 2001). As with all other mental disorders, there are currently no clinically viable biomarkers or diagnostic tests for schizophrenia (Owen, Sawa, & Mortensen, 2016). Consequently, diagnosis relies on an assessment of symptom presentation and history, as outlined by the Diagnostic and Statistical Manual of Mental Disorders 5 (American Psychiatric Association, 2013) and International Classification of Diseases (World Health Organization, 1993). However, it is being increasingly recognised that these discrete diagnostic categories do not accurately reflect the underlying pathophysiology or genetic architecture of psychiatric disorders, which may hinder research aimed at understanding their biology (Owen, 2014). The Research Domain Criteria initiative was developed in response to these limitations, with the aim of refocussing research efforts on

investigating the neurobiological substrates of continuous dimensions of psychopathology that span current diagnostic boundaries (Cuthbert, 2015).

There are currently no disease-modifying treatments for schizophrenia (Millan et al., 2016). Limited progress has been made in the development of new treatments since the original discovery of the therapeutic properties of highly specific D2 receptor antagonists, so called first-generation (typical) antipsychotics, over 60 years ago (Creese, Burt, & Snyder, 1976; Seeman, Lee, Chau-Wong, & Wong, 1976). Although second-generation (atypical) antipsychotics target a wider range of receptors, they share this fundamental mechanism of D2 receptor blockade (Kapur & Remington, 2001). The purported advantages of atypical over typical antipsychotics are questionable (Cunningham Owens & Johnstone, 2018), with limited evidence for increased efficacy or tolerability due to adverse side-effects, such as motor disturbance, weight gain, and cardiometabolic symptoms (Geddes, Freemantle, Harrison, & Bebbington, 2000; Huhn et al., 2019; Leucht et al., 2013). Current antipsychotics are also ineffective for treating negative symptoms (Krause et al., 2018) and cognitive symptoms (Buchanan, Freedman, Javitt, Abi-Dargham, & Lieberman, 2007), which are the most disabling (Bowie, Reichenberg, Patterson, Heaton, & Harvey, 2006; Rabinowitz et al., 2012). In addition, approximately 30 % of patients do not respond to antipsychotic treatment (Meltzer, 1997), of which between 70 – 84 % are treatment resistant from illness onset (Demjaha et al., 2017; Lally et al., 2016). Thus, there is a great need for novel therapeutics that are based on a better understanding of pathogenic mechanisms.

### 1.2. Neurobiology of schizophrenia

A comprehensive understanding of the neurobiological underpinnings of schizophrenia remains elusive and the search for neuroimaging biomarkers to aid diagnosis is ongoing (Abi-Dargham & Horga, 2016; Fusar-Poli & Meyer-Lindenberg, 2016). This section reviews current understanding of the neuroanatomical and functional brain changes that occur in schizophrenia.

#### *1.2.1. Neuroanatomical abnormalities*

A number of neuroanatomical changes have been consistently reported in schizophrenia. Post-mortem brain weight is consistently reduced in patients with schizophrenia (Harrison, Freemantle, & Geddes, 2003) and volumetric neuroimaging measures indicate that reduced overall brain volume and enlarged ventricles are recurrently observed (Steen, Mull, Mcclure, Hamer, & Lieberman, 2006). Large-scale meta-analyses of neuroimaging studies conducted by the ENIGMA consortium have

shown reduced grey matter volume in the cerebellum (Moberget et al., 2018), hippocampus, and several subcortical structures, including the amygdala, thalamus, and nucleus accumbens (van Erp et al., 2016). Moreover, decreased cortical thickness and surface area have also been reported, with largest effects in frontal and temporal cortices (van Erp et al., 2018). Post-mortem evidence implicates several of the same brain regions, with marked neuropathology in the dorsolateral prefrontal cortex (PFC), thalamus, and hippocampal formation (Harrison, 2008) that are thought to underlie abnormalities in functional connectivity (Harrison, 1999a). Whole-brain estimates of white matter integrity are also reduced in schizophrenia (Kelly et al., 2018; Klauser et al., 2016), suggesting widespread structural dysconnectivity.

Interpreting how these structural changes relate to pathophysiological mechanisms is challenging. Several studies show a moderating effect of cumulative antipsychotic medication on grey matter volume (Moncrieff & Leo, 2010; van Erp et al., 2016) and cortical thickness (van Erp et al., 2018) but not white matter integrity (Kelly et al., 2018). These effects could also be attributed to natural disease progression, although a longitudinal study has shown that antipsychotic treatment (but not illness duration or severity) correlates with grey matter volume reductions over time (Fusar-Poli et al., 2013). However, preclinical studies suggest that antipsychotics do not produce the hallmark neuropathological changes observed in schizophrenia (Harrison, 1999b).

Some of the neuroanatomical alterations observed in chronic schizophrenia are present in unmedicated individuals with first-episode psychosis (Samartzis, Dima, Fusar-Poli, & Kyriakopoulos, 2014; Shah et al., 2017) and individuals at high genetic risk for schizophrenia (Fusar-Poli et al., 2011), possibly suggesting that these changes precede illness onset and may have a genetic basis. However, there is mixed evidence regarding whether common variant genetic risk for schizophrenia predicts changes in brain morphometry (van der Merwe et al., 2019). One study has shown that schizophrenia-associated copy number variants (CNVs) are associated with decreased volume of some of the subcortical regions previously shown to be reduced in schizophrenia (Warland, Kendall, Rees, Kirov, & Caseras, 2019). Thus, the extent to which neuroanatomical alterations reflect core aspects of schizophrenia pathogenesis and how these changes relate to psychopathology remains unknown.

*1.2.2. Functional brain alterations*

Functional magnetic resonance imaging (fMRI) studies have shown that patients with schizophrenia exhibit aberrant resting-state and task-related activity in several of the brain regions implicated by structural neuroimaging, including prefrontal, cingulate

and temporal cortices, hippocampus, striatum, thalamus, and cerebellum (McGuire, Howes, Stone, & Fusar-Poli, 2008). Meta-analyses of fMRI studies have shown reduced functional connectivity between these brain regions in schizophrenia (Dong, Wang, Chang, Luo, & Yao, 2018; Li et al., 2019), supporting the view that disruption of brain network dynamics contributes to pathogenesis (Friston, Brown, Siemerkus, & Stephan, 2016). However, there is a large degree of heterogeneity in the affected brain regions, effect sizes, and directionality of activity changes across studies, which could be due to differences in patient symptomatology and/or unreliable fMRI measures (Fröhner, Teckentrup, Smolka, & Kroemer, 2019).

Findings from molecular imaging studies have yielded support for the prevailing theory of the neurochemical substrate of schizophrenia. The dopamine hypothesis initially proposed that elevated dopaminergic transmission was central to schizophrenia pathophysiology (Meltzer & Stahl, 1976). This theory has undergone several refinements since its conception, such that it now focuses on the role of dopamine dysregulation in the striatum in relation to positive symptoms (Howes & Kapur, 2009). The nature of this striatal dopaminergic dysfunction comprises increased presynaptic dopamine synthesis (Fusar-Poli & Meyer-Lindenberg, 2013) and elevated dopamine release (Abi-Dargham, van de Giessen, Slifstein, Kegeles, & Laruelle, 2009; Breier et al., 1997; Laruelle et al., 1996), with little evidence for differences in D2/D3 receptor density (Howes et al., 2012). Recent evidence suggests that these effects are larger in the dorsal than limbic striatum (McCutcheon, Beck, Jauhar, & Howes, 2018). These findings challenge the longstanding assumption of dopaminergic dysfunction in mesolimbic pathways, leading to the proposal that nigrostriatal dysfunction may contribute more to pathophysiology (McCutcheon, Abi-Dargham, & Howes, 2019).

The dopamine hypothesis has also been extended to explain cognitive symptoms of schizophrenia as a result of hypodopaminergic function in the PFC (Davis, Kahn, Ko, & Davidson, 1991). There is mixed evidence to support this hypothesis; a meta-analysis of the molecular imaging literature suggests that differences in D1 receptor availability in the PFC of schizophrenia are inconclusive (Kambeitz, Abi-Dargham, Kapur, & Howes, 2014). Conversely, a subsequent study found evidence for deficient dopamine release following amphetamine challenge in the dorsolateral PFC of schizophrenia patients (Slifstein et al., 2015).

Convergent evidence also implicates abnormal glutamatergic signalling in the pathophysiology of schizophrenia (Howes, McCutcheon, & Stone, 2015), particularly

in the hippocampus (Harrison, 2004). Glutamate binds to several receptors, including the *N*-methyl-D-aspartate (NMDA) receptor (Meldrum, 2000). Initial evidence for a pathophysiological role for NMDA receptor hypofunction was provided by preclinical studies showing that administration of NMDA receptor antagonists recapitulates neuropathological changes and behavioural endophenotypes of schizophrenia (Lee & Zhou, 2019; Olney & Farber, 1995). Moreover, NMDA receptor antagonists induce psychotic-like symptoms in healthy controls (Krystal et al., 1994; Lahti, Weiler, Michaelidis, Parwani, & Tamminga, 2001).

There is also evidence that NMDA receptor hypofunction may be caused by a deficiency in D-serine levels. D-serine is the main co-agonist that binds to glycine modulatory sites on synaptic NMDA receptors and is required for receptor opening (Papouin et al., 2012). Reduced D-serine levels have been consistently reported in serum of schizophrenia patients (Cho, Na, Cho, & Kang, 2016). Moreover, decreased expression of the D-serine transporter in the PFC and cerebellum of schizophrenia patients has been suggested to reflect a compensatory mechanism for reduced synaptic availability of D-serine (Burnet et al., 2008a). Several lines of evidence suggest that D-amino acid oxidase (DAO) hyperactivity, an enzyme that metabolises D-serine, may contribute to NMDA receptor hypofunction in schizophrenia by reducing D-serine levels (Burnet et al., 2008b; Verrall, Burnet, Betts, & Harrison, 2010). Two randomised-controlled trials indicate that DOA inhibitors show therapeutic potential in schizophrenia as adjunctive treatments (Lane et al., 2013; Lin et al., 2018) but several questions remain regarding their mechanism of action (Harrison, 2018).

Neuroimmunological evidence also implicates the involvement of the NMDA receptor in schizophrenia pathogenesis (Coutinho, Harrison, & Vincent, 2014). Serum autoantibodies to the NMDA receptor have been reported in patients with first-episode psychosis (Lennox et al., 2017; Pathmanandavel et al., 2015; Scott et al., 2018; Steiner et al., 2013; Zandi et al., 2011) and psychosis is present in 67 % of patients with NMDA receptor antibody encephalitis (Al-Diwani et al., 2019). It has been suggested that this autoimmune response may contribute to pathogenesis by affecting NMDA receptor membrane trafficking (Jézéquel, Johansson, Leboyer, & Groc, 2018).

A meta-analysis of proton magnetic spectroscopy studies has shown that levels of glutamatergic metabolites are elevated in the basal ganglia, thalamus, and medial temporal lobe in schizophrenia (Merritt, Egerton, Kempton, Taylor, & McGuire, 2016). This paradoxical increase in glutamatergic transmission is thought to be caused by

disinhibition of pyramidal neurons as a result of NMDA receptor hypofunction on inhibitory gamma-aminobutyric acid (GABA)-ergic interneurons (Cohen, Tsien, Goff, & Halassa, 2015; Homayoun & Moghaddam, 2007). Interestingly, striatal dopamine synthesis is negatively correlated with glutamate levels in the hippocampus (Stone et al., 2010) and anterior cingulate cortex (Jauhar et al., 2018) in the early stages of schizophrenia, suggesting downstream effects of dysregulated glutamatergic transmission on striatal dopaminergic function. Consistent with this, genetic ablation of the NMDA receptor subunit *Grin1* in parvalbumin-positive GABAergic neurons leads to an enhancement and attenuation of amphetamine-induced dopamine release in the striatum and medial PFC, respectively (Nakao et al., 2019). These findings resemble the effects of amphetamine challenge observed in schizophrenia patients (Abi-Dargham et al., 2009; Breier et al., 1997; Laruelle et al., 1996; Slifstein et al., 2015) and support the hypothesis that dopaminergic dysfunction in schizophrenia is secondary to NMDA receptor hypofunction (Howes et al., 2015).

A more general role for GABAergic dysfunction in schizophrenia (Lewis, Hashimoto, & Volk, 2005) is supported by post-mortem studies showing reduced PFC expression of the GABA-synthesising enzyme glutamic acid decarboxylase 67 (GAD67) in patients (Akbarian et al., 1995; Hashimoto et al., 2003; Volk, Austin, Pierri, Sampson, & Lewis, 2000). In addition, upregulation of $GABA_A$ receptors is consistently observed in post-mortem studies (Benes, Vincent, Marie, & Khan, 1996; Benes, Vincent, Alsterberg, Bird, & SanGiovanni, 1992), suggesting post-synaptic changes that compensate for deficient GABA synthesis. Molecular imaging studies have yielded inconsistent findings regarding whole-tissue GABA concentration and $GABA_A$ receptor availability (Egerton, Modinos, Ferrera, & McGuire, 2017). However, there is evidence from one study using a technique that directly measures GABA levels in the synapse for impaired GABA neurotransmission in the dorsolateral PFC of antipsychotic naïve schizophrenia patients (Frankle et al., 2015). Convergent evidence also implicates GABAergic dysfunction as contributing to hippocampal hyperactivity in schizophrenia (Heckers & Konradi, 2015), which has been suggested to lead to dysregulation of the dopamine system (Grace, 2016). Genetic evidence has shown convergence of schizophrenia CNVs on the $GABA_A$ receptor complex that is independent of an association with the NMDA receptor (Pocklington et al., 2015). Together, these findings suggest a primary role for GABAergic dysfunction in schizophrenia pathogenesis that is distinct from the effects of NMDA receptor hypofunction described above.

Serotonergic dysfunction has also been suggested to contribute to schizophrenia pathogenesis (Geyer & Vollenweider, 2008). Consistent with this, the hallucinogenic drugs lysergic acid diethylamide (LSD) and psilocybin induce psychomimetic states via agonism of the serotonin (5-HT) 2A receptor (Halberstadt & Geyer, 2011). Conversely, many atypical antipsychotics exhibit antagonistic effects at 5-HT2A receptors (Meltzer & Massey, 2011). The role of serotonergic dysfunction in schizophrenia pathogenesis is unclear and could involve modulation of midbrain dopaminergic projections to the limbic system and PFC (Abi-Dargham, 2007) and/or functional interaction between the 5-HT2A receptor and metabotropic glutamate receptor 2 (González-Maeso & Sealfon, 2009). Post-mortem studies consistently report elevated 5-HT1A and reduced 5-HT2A receptor densities in frontal cortex (Burnet, Eastwood, & Harrison, 1996; Harrison, 1999c) and there is evidence for abnormal 5-HT2A receptor expression in cerebellum of schizophrenia patients (Eastwood, Burnet, Gittins, Baker, & Harrison, 2001). However, a schizophrenia-associated polymorphism in the 5-HT2A receptor gene does not influence mRNA expression levels of this receptor in post-mortem cortical regions (Bray, Buckland, Hall, Owen, & O'Donovan, 2004). In addition, findings from molecular imaging studies demonstrating abnormal serotonergic transmission in schizophrenia are inconsistent (Selvaraj, Arnone, Cappai, & Howes, 2014).

In summary, schizophrenia is associated with widespread neuroanatomical and functional alterations in several brain regions. The neurochemical substrates of functional alterations are complex and involve several interacting neurotransmitter systems that are not well understood.

## 1.3. Schizophrenia aetiology

The aetiology of schizophrenia is complex, comprising a myriad of environmental factors and genetic variants. Understanding how these factors interact to ultimately result in the emergence of psychopathology remains a major challenge for research (van Os et al., 2014). This section provides an overview of known environmental risk factors for schizophrenia and current understanding of the genetic architecture.

### *1.3.1. Environmental risk factors*

Epidemiological studies have identified several sociodemographic factors that are associated with increased risk for schizophrenia (van Os, Kenis, & Rutten, 2010). For example, incidence of schizophrenia is higher in urban areas (Vassos, Pedersen, Murray, Collier, & Lewis, 2012). Several explanations for this relationship have been

proposed, including social stress and exposure to other putative environmental risk factors that are more common in urban areas (e.g., pollution, higher rates of infection transmission, and illicit drug use) (Kirkbride, Keyes, & Susser, 2018). Immigration has also been repeatedly linked with an increased risk of schizophrenia, particularly in ethnic minority groups (Jongsma, Turner, Kirkbride, & Jones, 2019; Selten, van der Ven, & Termorshuizen, 2019) and has been suggested to be mediated, in part, by the effects of social exclusion (Selten, van der Ven, Rutten, & Cantor-Graae, 2013). However, the underlying mechanisms linking these sociodemographic factors with risk of schizophrenia are poorly understood (Plana-Ripoll, Pedersen, & McGrath, 2018). Moreover, the extent to which these associations reflect causal effects on schizophrenia risk is questionable due to the possibility of genetic confounding and reverse causation.

Other environmental risk factors for schizophrenia that occur during early life are thought to increase risk by influencing brain development during sensitive periods (Owen, O'Donovan, Thapar, & Craddock, 2011). The human brain undergoes protracted development throughout early life, characterised by profound neurogenesis and neuronal migration *in utero,* followed by gliogenesis, myelination, and synaptogenesis later in gestation and extending into childhood, and extensive synaptic pruning during late childhood and adolescence (Silbereis, Pochareddy, Zhu, Li, & Sestan, 2016). Several prenatal risk factors for schizophrenia have been identified, including nutritional insufficiency (Brown & Susser, 2008; Xu et al., 2009), maternal stress (Khashan et al., 2008; van Os & Selten, 1998) and infection (Brown & Derkits, 2010; Khandaker, Zimbron, Lewis, & Jones, 2013), and obstetric complications (Cannon, Jones, & Murray, 2002). The causative nature of these relationships is supported by animal studies showing that many neurobiological and behavioural endophenotypes of schizophrenia are recapitulated by prenatal stressors (Meyer & Feldon, 2010). Childhood trauma is also linked with increased risk for schizophrenia (McGrath et al., 2017; Varese et al., 2012). Although the complexities of childhood adversity are difficult to model *in vivo*, maternal deprivation and isolation rearing are widely used developmental models of schizophrenia (Fone & Porkess, 2008; Marco et al., 2015). Cannabis use during adolescence has also been suggested to increase risk for schizophrenia (Mustonen et al., 2018) and this is supported by animal models (Renard, Rushlow, & Laviolette, 2016). However, a genetic predisposition for schizophrenia also increases the likelihood of cannabis use (Power et al., 2014), which may suggest some degree of genetic confounding.

### *1.3.2. Genetic architecture*

Preliminary evidence that genetic factors contribute to schizophrenia liability was provided by twin studies showing that up to 80 % of the variance in liability is explained by genetic variance (Sullivan, Kendler, & Neale, 2003). Progress in understanding the genetic architecture of schizophrenia was initially slow, with many findings from linkage and candidate gene studies not being reproducible (Farrell et al., 2015). Recent advances in genomic technologies and formation of international consortia, notably the Psychiatric Genomics Consortium (Sullivan et al., 2018), have enabled the large-scale studies that are needed to detect genetic variants at stringent genome-wide significance levels (Bray & O'Donovan, 2018). It is hoped that these genetic discoveries will provide insights into the biology of schizophrenia, ultimately facilitating the development of more effective treatments (Harrison, 2015a).

#### *1.3.2.1. Common variants*

Genome-wide association studies (GWASs) compare single nucleotide polymorphism (SNP) arrays between cases and controls, enabling an unbiased investigation of genomic regions associated with schizophrenia risk. These studies have confirmed the highly polygenic nature of schizophrenia, involving the contribution of many SNPs that are common in the population (frequency > 5 %). To date, 145 risk loci have been robustly associated with schizophrenia (Pardiñas et al., 2018; Schizophrenia Working Group of the Psychiatric Genomics Consortium, 2014), some of which corroborate the involvement of dopaminergic (*DRD2*) and glutamatergic (*GRIN2A, GRIA1, GRM3,* and *SRR*) mechanisms, and implicating voltage-gated calcium channels (*CACNA1C*, *CACNB2*, and *CACNA1I*) in pathogenesis. However, the *DRD2* risk allele does not affect mRNA levels in post-mortem striatum (Toste et al., 2019), raising questions about the pathophysiological mechanism underlying this association.

It is predicted that several thousand common variants contribute to schizophrenia risk (Ripke et al., 2013) and that the number of SNPs that reach genome-wide significance will increase as sample sizes become larger. Individual SNPs have a small effect on risk (odds ratio < 1.2) but cumulatively account for 23 % of the variance in schizophrenia liability (Cross-Disorder Group of the Psychiatric Genomics Consortium, 2013). Such SNP heritability estimates are considerably lower than heritability estimates from twin studies, which is thought to reflect non-additive genetic effects (epistasis), gene-environment interactions, and the contribution of rare variants (Maher, 2008).

There is a high degree of overlap in common variants associated with schizophrenia and other neuropsychiatric disorders, particularly bipolar disorder and major depressive disorder (Brainstorm Consortium, 2018; Cross-Disorder Group of the Psychiatric Genomics Consortium, 2013; International Schizophrenia Consortium, 2009). This genetic pleiotropy reflects clinical overlap and has important implications for understanding pathophysiology (O'Donovan & Owen, 2016). Pathway analysis of common variant association for schizophrenia, bipolar disorder, and major depressive disorder has shown enrichment for genes involved in histone methylation, synaptic signalling, and immune and neurotrophic factors (Network and Pathway Analysis Subgroup of Psychiatric Genomics Consortium, 2015). Notably, the strongest association across all three disorders was observed for histone methylation and this remained significant when data were analysed separately for schizophrenia.

Recent evidence, perhaps surprisingly, suggests that common variant risk for schizophrenia also affects placental function (Ursini et al., 2018). The placenta mediates maternal-foetal nutrient transfer and is a source of endocrine signals that are essential for prenatal development (Bronson & Bale, 2016; Jansson & Powell, 2007). Interestingly, polygenic risk for schizophrenia predicts the occurrence of obstetric complications and schizophrenia common variants that are differentially expressed in the placenta following early-life complications are enriched for metabolic and cellular stress pathways (Ursini et al., 2018). Obstetric complications are generally regarded as an environmental risk factor for schizophrenia (Cannon et al., 2002). However, these findings may suggest that this relationship might be an indirect consequence of genetic risk for schizophrenia and raise the possibility that genetic risk for schizophrenia has pathogenic effects on *in utero* brain development by affecting placental function.

Uncovering molecular insights into pathogenesis from common variant association is challenging (Harrison, 2015b). Linkage disequilibrium of SNPs within a GWAS discovery locus means that there are several potential candidate genes that could be responsible for the signal at a given locus. Moreover, most SNPs are in non-coding regions of the genome, suggesting that these risk variants impact on regulation of gene expression by altering regulatory element sequences (Bray, 2008). Elucidating the functional consequences of these non-coding SNPs requires integration with functional genomics data and consideration of potential cell-type specific effects operating at particular points in development (Bray & Hill, 2016; Sullivan & Geschwind, 2019).

Work is ongoing to generate brain-specific functional genomics data for this purpose (PsychENCODE Consortium, 2018). Initial findings indicate an over-representation of schizophrenia risk loci in foetal brain regulatory elements (de la Torre-Ubieta et al., 2018; Hannon et al., 2016; Li et al., 2018; O'Brien et al., 2018; Won et al., 2016), suggesting a role for common variants in neurodevelopmental processes. Consistent with this, patterns of differential DNA methylation observed in PFC of patients with schizophrenia are enriched for genes with neurodevelopmental roles and CpG sites at which DNA methylation changes occur during foetal brain development (Pidsley et al., 2014). In addition, single-cell transcriptomics approaches have revealed enrichment for striatal medium spiny neurons, cortical interneurons, and cortical and hippocampal pyramidal neurons in the adult brain (Skene et al., 2018), particularly excitatory neurons (Li et al., 2018; Wang et al., 2018).

*1.3.2.2. Rare variants*

*1.3.2.2.1. Copy number variants*

CNVs are structural variants (i.e., chromosomal deletions or duplications) that range in size from 1 kb to several megabases (Malhotra & Sebat, 2012). Many benign CNVs are present throughout the human genome (Sebat et al., 2004). Pathogenic CNVs are rare (< 1 % frequency) but tend to be large (> 500 kb), gene-rich, and occur *de novo* at recurrent genomic locations via non-allelic homologous recombination (Kirov, 2015). 11 CNVs have been robustly linked with risk of schizophrenia, including 5 duplications (1q21.1, 7q11.23, 15q11.2-q13.1, 16p13.1, and proximal 16p11.2) and 6 deletions (22q11.2, 1q21.1, 2p16.3, 3q29, 15q11.2, and 15q13.3) that have a substantial effect on liability (odds ratios 2 - 60) (Rees et al., 2014a). 8 of these CNVs meet criteria for genome-wide significance in the largest study to date (Marshall et al., 2017). The burden of large CNVs in schizophrenia is increased even after exclusion of known schizophrenia CNVs (Rees et al., 2014b), suggesting that additional, as yet unidentified, CNVs contribute to schizophrenia.

Schizophrenia-associated CNVs also increase risk for other neurodevelopmental disorders, such as autism spectrum disorders and developmental delay, with greater penetrance (Kirov et al., 2014). It is important to note that these CNVs are not fully penetrant, with recent evidence highlighting that common variants play a role in determining phenotypic expression (Bergen et al., 2019; Tansey et al., 2016). Nevertheless, all CNVs that increase risk for schizophrenia are associated with cognitive impairment, even in individuals without a neuropsychiatric diagnosis (Kendall et al., 2019a). It has been suggested that the relative enrichment of

deleterious CNVs across neurodevelopmental and neuropsychiatric disorders reflects the degree of neurodevelopmental aberration and consequent cognitive impairment (Owen & O'Donovan, 2017). Consistent with this, the burden of large CNVs in neuropsychiatric disorders with less of a neurodevelopmental component, such as bipolar disorder (Green et al., 2016) and depression (Kendall et al., 2019b), is lower than for schizophrenia. In addition, there is an increased burden of CNVs associated with intellectual disability in schizophrenia (Rees et al., 2016).

With the exception of deletions at 2p16.3 which selectively affect the *NRXN1* gene, all CNVs encompass multiple genes (Kirov, 2015). Generating mechanistic insights from CNVs therefore requires a pathway analysis approach to identify whether the genes hit by CNVs are over-represented in particular biological processes. In a landmark study, Kirov et al. (2012) demonstrated that genes in *de novo* CNV loci are enriched for the post-synaptic density. Moreover, this effect was principally driven by genes encoding the NMDA receptor complex and, to a lesser extent, activity-regulated cytoskeleton-associated protein. These findings are consistent with prior hypotheses regarding NMDA receptor hypofunction in schizophrenia and support a pathophysiological role for aberrant synaptic plasticity (Hall, Trent, Thomas, O'Donovan, & Owen, 2015; Harrison & Owen, 2003; Harrison & Weinberger, 2005). Subsequent work in a larger sample replicated the over-representation of genes in schizophrenia-associated CNVs in the NMDA receptor complex and provided the first genetic evidence that $GABA_A$ receptors play an independent role in schizophrenia pathogenesis (Pocklington et al., 2015). Interestingly, enrichment was also observed for neurodevelopmental processes (e.g., abnormal neural plate morphology and neuronal differentiation).

*1.3.2.2.2. Loss of function variants*

Recent advances in next generation sequencing technologies have facilitated gene discovery efforts aimed at the identification of rare point mutations, such as single nucleotide variants and insertions or deletions (indels), that are highly penetrant for schizophrenia and, consequently, extremely rare in the population (< 0.1 %). Unlike SNPs and CNVs, rare variants identified by whole exome sequencing unequivocally implicate a single protein-coding gene and the functional consequence of the mutation for gene function can be determined more easily. The majority of exome sequencing studies have not been powered to detect specific variants at exome-wide significance but have shown an increased burden of protein-altering mutations in schizophrenia (Genovese et al., 2016; Singh et al., 2017) that are enriched for

synaptic signalling (Curtis, Coelewij, Liu, Humphrey, & Mott, 2018; Fromer et al., 2014; Purcell et al., 2014), voltage-gated calcium and sodium channels (Purcell et al., 2014; Rees et al., 2019), and histone modifications (Curtis, 2016).

*De novo* loss of function (LoF) variants in the *SETD1A* (SET Domain Containing 1A) gene were first reported in two schizophrenia cases (Takata et al., 2014). Subsequent work confirmed the pathogenic contribution of *SETD1A* LoF variants in the largest exome sequencing study of schizophrenia to date (Singh et al., 2016). The effect size of *SETD1A* LoF was high (odds ratio = 37.6), with mutations being observed in 10 out of 7,776 schizophrenia cases (4 of which occurred *de novo*), whereas only 2 were observed in 58,404 controls. Several of the *SETD1A* LoF carriers had impaired intellectual functioning and 6 additional carriers (2 *de novo*) were observed in children with a range of neurodevelopmental phenotypes, suggesting a role for *SETD1A* LoF in neurodevelopmental disorders more generally. Consistent with this, recent evidence also implicates *de novo* mutations in *SETD1A* in language disorders (Eising et al., 2019) and epilepsy (Yu et al., 2019).

In the Singh et al. (2016) paper, LoF variants were distributed throughout the *SETD1A* gene (Figure 1.1) but all occurred before the catalytic SET domain (exons 16 - 19). Notably, 7 of these variants were the same two-base deletion at the exon 16 splice acceptor site. Transfecting this variant into a human cell line was associated with reduced expression of a fused GFP reporter, which was shown using Sanger sequencing to be a result of aberrant splicing leading to a premature stop codon and truncated protein. The remaining LoF variants were either stop-gain mutations, splice acceptor site point mutations, or frameshifting indels that are predicted to lead to haploinsufficiency.

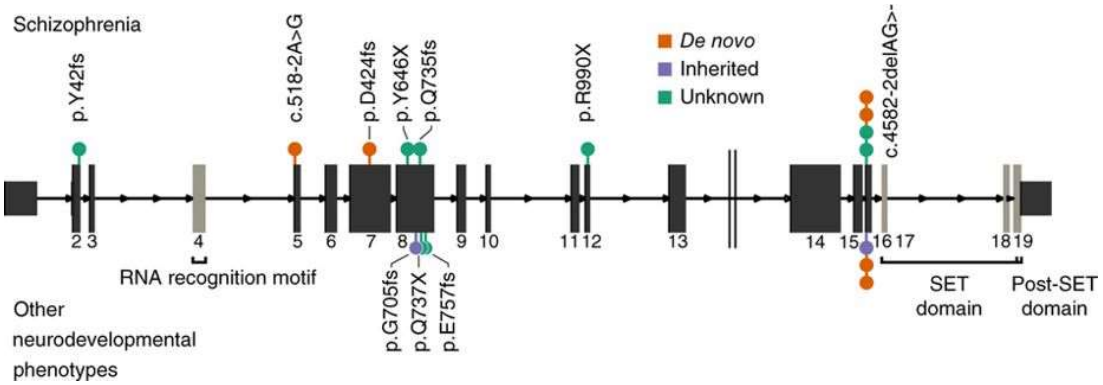


**Figure 1.1. Summary of *SETD1A* LoF mutations observed in schizophrenia and other neurodevelopmental disorders.** Taken from Singh et al. (2016).

#### *1.3.2.3. Summary of genetic findings*

In summary, the genetic architecture of schizophrenia is highly polygenic, comprising a large number of common variants (SNPs) with small, but cumulative, effects on risk, and several CNVs that are rare in the population but increase risk considerably. These have led to several important mechanistic insights regarding schizophrenia pathogenesis and a better understanding of genetic pleiotropy with other neuropsychiatric and neurodevelopmental disorders. Exome sequencing is starting to identify highly damaging, rare LoF variants in specific genes (*SETD1A*) with predictable effects on gene function (haploinsufficiency) that have considerable potential for investigating pathogenic mechanisms using model systems.

### 1.4. *SETD1A*: utility for disease modelling

*SETD1A* is an attractive candidate for disease modelling for several reasons. First, the LoF mutations observed in human carriers are predicted to cause haploinsufficiency, which can be recapitulated in model systems to investigate biologically relevant mechanisms contributing to pathogenesis. Second, *SETD1A* LoF mutations are highly penetrant and, consequently, haploinsufficiency is expected to have substantial phenotypic effects, making it a biologically tractable target. Finally, *SETD1A* encodes a subunit of a histone methyltransferase complex involved in methylation of lysine residue 4 on histone 3 (H3K4) (see section 1.4.4). The convergence of common and rare variants on H3K4 methylation may suggest that studying *SETD1A* could serve as a window into more general biological pathways underlying pathogenesis.

#### *1.4.1. Histone modifications*

Nucleosomes are the repeating unit making up chromatin, each comprising 146 bp of DNA wrapped around a histone octamer with two of each histone protein (H2A, H2B, H3, and H4) (Kornberg & Lorch, 1999). Histones are highly conserved proteins, comprising a globular domain, which interacts with other histones and DNA to form the nucleosome, and protruding N-terminal tails (Luger, Mäder, Richmond, Sargent, & Richmond, 1997). Post-translational modifications of histone tails, such as methylation, acetylation, phosphorylation, and ubiquitylation, change higher-order chromatin structure by affecting interactions between histones and DNA within a nucleosome or between histones of adjacent nucleosomes (Kouzarides, 2007). Histone modifications are broadly classified as either activating (correlated with euchromatin formation and gene expression) or repressive (correlated with heterochromatin formation and gene silencing) (Bannister & Kouzarides, 2011). The

observation that distinct histone modifications correlate with gene expression prompted the proposal that these modifications form the basis of a histone code that lead to the recruitment of transcriptional regulators affecting gene expression (Strahl & Allis, 2000).

### *1.4.2. H3K4 methylation*

H3K4 methylation is generally considered an activating histone mark on the basis that broad H3K4 methylation peaks are observed at regions of euchromatin (Noma, Allis, & Grewal, 2001). There are three types of H3K4 methylation: mono- (H3K4me1), di- (H3K4me2), and tri-methylation (H3K4me3). These marks are all found at transcription start sites of active genes (Barski et al., 2007; Ernst et al., 2011). H3K4 methylation marks serve as binding sites for 'reader' enzymes that bring about downstream changes (e.g., chromatin remodelling and recruitment of transcription factors) that lead to transcriptional activation (Ruthenburg, Allis, & Wysocka, 2007). For example, Transcription factor II D recognises and binds H3K4me3, illustrating its role as a docking site for transcription initiation (Vermeulen et al., 2007). The different forms of H3K4 methylation are also differentially distributed throughout the genome, with enhancers showing enrichment of H3K4me1 (Heintzman et al., 2007; 2009), whereas promoters are marked with H3K4me2 and H3K4me3 (Kim et al., 2005; Mikkelsen et al., 2007).

H3K4 methylation is a labile epigenetic mark that can be removed by lysine demethylases (KDMs). There are 6 mammalian KDMs that have been shown to remove H3K4 methylation (Hyun, Jeon, Park, & Kim, 2017), providing an additional layer of regulatory complexity. Interestingly, H3K4 methylation co-occurs with the repressive H3K27 mark at bivalent domains in embryonic stem cells (ESCs), which is thought to keep genes involved in differentiation in a "poised" state, permitting rapid transcriptional activation by removal of the repressive mark (Bernstein et al., 2006). It is important to note, however, that the causative role of H3K4 methylation in transcriptional activation has recently been questioned (Howe, Fischl, Murray, & Mellor, 2017), raising the possibility that these marks are a consequence of gene expression.

### *1.4.3. H3K4 methylation in the brain*

The work described above suggesting a role for H3K4 methylation in transcriptional activation has mostly been conducted in cell lines. Similar findings have been reported in post-mortem human brain tissue, with positive correlations between levels of promoter H3K4me3 and mRNA levels (Huang & Akbarian, 2007; Stadler et al.,

2005). Notably, H3K4me3 peaks in PFC are enriched for genes involved in putative biological mechanisms of schizophrenia, such as glutamatergic and dopaminergic transmission (Dincer et al., 2015). Moreover, reduced H3K4me3 has been reported at the *Gad1* promoter in post-mortem brain of schizophrenia patients (Huang et al., 2007), which may contribute to previously described GABAergic dysfunction. Single-cell analysis has shown that neuronal H3K4me3 peaks are enriched for schizophrenia common variant association (Girdhar et al., 2018), suggesting a degree of molecular convergence between common and rare variant genetic risk. Consistent with this, knockdown of *SETD1A* in a human neuroblastoma cell line leads to transcriptomic changes that are enriched for schizophrenia common variants (Cameron, Blake, Bray, & Hill, 2019).

The landscape of H3K4 methylation in human brain undergoes dramatic remodelling during the early years of life (Cheung et al., 2010; Shulha, Cheung, Guo, Akbarian, & Weng, 2013), implicating an important role for dynamic regulation of H3K4 methylation in neurodevelopment (Roidl & Hacker, 2014). Indeed, mutations in many other genes from the H3K4 methyltransferase gene family (KMT2) and readers and erasers of H3K4 methylation have been linked with a variety of neurodevelopmental disorders and intellectual disability (Vallianatos & Iwase, 2015). Based on these findings, it might be predicted that *SETD1A* LoF causes disturbed neurodevelopment with downstream consequences for later brain function that contribute to the emergence of psychopathology.

In addition to its role in neurodevelopment, changes in H3K4 methylation contribute to adult brain function. Animal studies have shown that knockout of *KMT2A* (Gupta et al., 2010; Kerimoglu et al., 2017) and *KMT2B* (Kerimoglu et al., 2013; Kerimoglu et al., 2017) cause memory impairments. Both of these genes are involved in regulating H3K4me3 in the hippocampus at promoters of learning-associated genes (Collins, Sweatt, & Greer, 2019). *KMT2A* is also involved in regulating H3K4me3 in the hippocampus and anterior cingulate cortex during memory retrieval (Webb et al., 2017). In addition, conditional knockout of *KMT2A* in the PFC or ventral striatum causes deficient synaptic plasticity (Jakovcevski et al., 2015; Shen et al., 2016). These findings illustrate the involvement of H3K4 methylation in biological processes underlying learning and memory and suggest that the link between *SETD1A* LoF and cognitive impairment might involve similar pathogenic mechanisms.

### *1.4.4. SETD1A biochemical function*

*SETD1A* (also known as *KMT2F*) is a member of the KMT2 family of genes that specifically catalyse H3K4 methylation. In mammals, this gene family contains five other KMTs: *KMT2A* (*MLL1*), *KMT2B* (*MLL2*), *KMT2C* (*MLL3*), *KMT2D* (*MLL4*), and *KMT2G* (*SETD1B*) (Shilatifard, 2008). Each of these enzymes contain a 130-140 amino acid SET (Suppressor of variegation 3-9 (Su(var)3-9), Enhancer of zeste (E(z)), and Trithorax) domain that catalyses the transfer of methyl groups from the cofactor *S*-adenosylmethionine to H3K4 in non-redundant COMPASS (Complex Proteins Associated with Set1) complexes (Miller et al., 2001). There are five common subunits observed in all COMPASS complexes (*ASH2L*, *RBBP5*, *WDR5*, *DPY30,* and *HCFC1*) plus complex-specific subunits; in the *SETD1A* complex, these are *CXXC1* and *WDR82* (Shilatifard, 2012).

The *SETD1A* complex is capable of catalysing H3K4me1, H3K4me2, and H3K4me3 (Lee & Skalnik, 2005). However, knockdown of *SETD1A* in ESCs results in reduced bulk H3K4me3, without affecting levels of H3K4me1 or H3K4me2 (Wu et al., 2008). The genomic targeting of H3K4me3 by the *SETD1A* complex involves coordinated activity of the *CXXC1* and *WDR82* subunits. The *CXXC1* subunit of the *SETD1A* complex recognises non-methylated CpG islands, restricting H3K4 methylation activity of the *SETD1A* complex to euchromatin regions (Clouaire et al., 2012; Tate, Lee, & Skalnik, 2010). The deposition of H3K4me3 at transcription start sites by the *SETD1A* complex is facilitated by the *WDR82* subunit, which is bound to the RNA recognition motif of *SETD1A* and recruits the complex to the Ser-5 phosphorylated C-terminal domain of RNA polymerase II, which is associated with transcription initiation (Lee & Skalnik, 2008).

### *1.4.5. Setd1a and embryonic development*

Homozygous knock-out of *Setd1a* is embryonically lethal (Bledau et al., 2014), highlighting its essential role in embryogenesis. However, its precise role remains unclear with one study suggesting that it is necessary for inner cell mass formation in the blastocyst (Fang et al., 2016), while another suggests that it is required during gastrulation, after inner cell mass formation (Bledau et al., 2014). *Setd1a* plays a role in maintenance of ESC pluripotency through its interaction with *Oct4*, leading to H3K4me3 at the promoters of *Oct4* target genes (Bledau et al., 2014; Fang et al., 2016). This interaction may be mediated indirectly through *Uhrf1*, which binds with both *Setd1a* and *Oct4* to maintain H3K4me3 at bivalent domains in ESCs, particularly at the promoters of genes involved in specifying neuroectodermal lineages (Kim et

al., 2018). Ablation of the catalytic SET domain in ESCs is associated with impaired differentiation but has no effect on self-renewal (Sze et al., 2017). These findings suggest that the aforementioned role of *Setd1a* in ESC maintenance does not depend on its methyltransferase activity but that this is critical for cell-fate specification during differentiation.

There is also evidence to suggest that *Setd1a* plays a role in placental function. Knockdown of *Setd1a* in mouse ESCs leads to transcriptomic changes that are enriched for placental development (Fang et al., 2016). Moreover, *Setd1a* expression is reduced in the mouse placenta following a prenatal high-fat diet (Gabory et al., 2012), a manipulation that is associated with schizophrenia endophenotypes in animal models (Sullivan, Riper, Lockard, & Valleau, 2015). These findings suggest that *Setd1a* LoF may exert pathogenic effects by influencing placental function during prenatal development.

*1.4.6. Setd1a and neurogenesis*

Embryonic neurogenesis involves the asymmetric division of neuronal progenitor cells (NPCs) in the ventricular zone of the developing telencephalon to produce two daughter cells: a self-renewing NPC and a differentiating cell that will terminally differentiate into a post-mitotic neuron (Paridaen & Huttner, 2014). This asymmetric division is essential for maintaining a sufficient pool of NPCs for the production of the vast number of neurons of manifold subtypes and at the right stage of development. A role for *Setd1a* in neurogenesis is supported by evidence for impaired proliferation of NPCs in primary cultures derived from *Setd1a* deficient mice (Bledau et al., 2014). Subsequent work has shown that *Setd1a* is recruited by the histone chaperone HIRA to deposit H3K4me3 at the promoter of the *β-catenin* gene, leading to increased *β-catenin* expression and NPC self-renewal (Li & Jiao, 2017). *β-catenin* is a component of the canonical *Wnt* signalling pathway that regulates cell-fate decisions (Zechner et al., 2003). Li and Jiao (2017) also report that knockdown of *Setd1a* results in premature neuronal differentiation and a reduction in markers of NPC proliferation in the embryonic mouse brain. *Setd1a* is also recruited by *Nap1|1* to deposit H3K4me3 at the promoter of *RassF10*, which has a similar effect on maintaining NPC pluripotency (Qiao et al., 2018). Together, these findings provide convergent evidence for a role for *Setd1a* in regulating the balance between NPC proliferation and differentiation, suggesting that perturbations to this balance may play a role in pathogenic mechanisms of *Setd1a* LoF in neurodevelopmental disorders.

### *1.4.7. Summary: current understanding of Setd1a function*

*Setd1a* is a promising candidate for investigating schizophrenia pathogenesis because it implicates LoF of a single gene of large effect that can be recapitulated in model systems. Convergent evidence supports a role for disrupted H3K4 methylation in schizophrenia and other neurodevelopmental disorders, a process that is important for neurodevelopment and brain function. *Setd1a* is known to be essential for prenatal development, with strong evidence to support a role in embryonic neurogenesis and suggestive evidence for a role in placental function. However, very little is known about the precise biological mechanisms underlying the association between *Setd1a* LoF and risk for psychopathology.

## 1.5. Thesis aims

The aim of this thesis was to investigate the functional consequences of *Setd1a* haploinsufficiency using a mouse model to reproduce the predicted effects of LoF variants on gene function in human carriers. An integrative approach was adopted to assess the effects of *Setd1a* LoF on; i) behavioural endophenotypes of relevance to schizophrenia and other neurodevelopmental disorders, and ii) candidate pathogenic mechanisms, spanning prenatal development and adult brain function. The specific aims of each chapter were as follows:

- Chapter 3: assess the regulatory role of *Setd1a* in the embryonic mouse brain using RNA-seq to determine transcriptomic changes in a constitutive heterozygous knockout mouse line (*Setd1a*$^{+/-}$).
- Chapter 4: investigate effects of *Setd1a* haploinsufficiency on the placenta (i.e., placental weight and gene expression) and growth curves of *Setd1a*$^{+/-}$ mice.
- Chapter 5: perform a comprehensive behavioural characterisation of the *Setd1a*$^{+/-}$ mouse line (i.e., anxiety, activity levels, sensorimotor gating, motoric functioning, and object recognition memory).
- Chapter 6: determine whether sensorimotor gating impairments observed in *Setd1a*$^{+/-}$ mice in Chapter 5 can be rescued using antipsychotics with different pharmacological profiles to probe underlying neurochemical mechanisms.
- Chapter 7: explore the extent to which behavioural effects of *Setd1a* haploinsufficiency observed in Chapter 5 are attributable to effects in the nervous system alone using a Nestin-Cre driver to create a conditional knockout.

## Chapter 2: General Methods

### 2.1. Animal lines

#### *2.1.1. Knockout strategy*

Heterozygous *Setd1a* knockout mice were generated using a 'knockout-first' strategy, as shown in Figure 2.1 (Skarnes et al., 2011). This approach combines the Flp/FRT and Cre-LoxP systems to create a reporter-tagged allele with conditional potential. C57BL/6NTac-*Setd1a*$^{tm1a(EUCOMM)Wtsi}$/WtsiCnrm knockout-first mice were produced by EUCOMM. The tm1a allele was created by insertion of a FRT-flanked LacZ/neomycin reporter cassette into the intronic region between exons 3 and 4 of the *Setd1a* gene, disrupting gene function by splicing to the LacZ cassette. In addition, a critical exon present in all transcript variants (i.e., exon 4) was flanked by LoxP sites, conferring conditional knockout potential. The tm1a allele was converted to a conditional (tm1c) allele by crossing *Setd1a*$^{tm1a}$ mice with a FlpO driver line, leading to excision of the LacZ/neomycin cassette and restoration of gene function. Mice heterozygous for the 'floxed' *Setd1a*$^{tm1c}$ allele were generated and supplied by the Mary Lyon Centre (MRC Harwell) and subsequently crossed with a Cre driver line. Recombination and deletion of the floxed exon by Cre recombinase causes a frameshift mutation in the deleted (tm1d) allele, resulting in loss of *Setd1a* function via nonsense mediated decay.

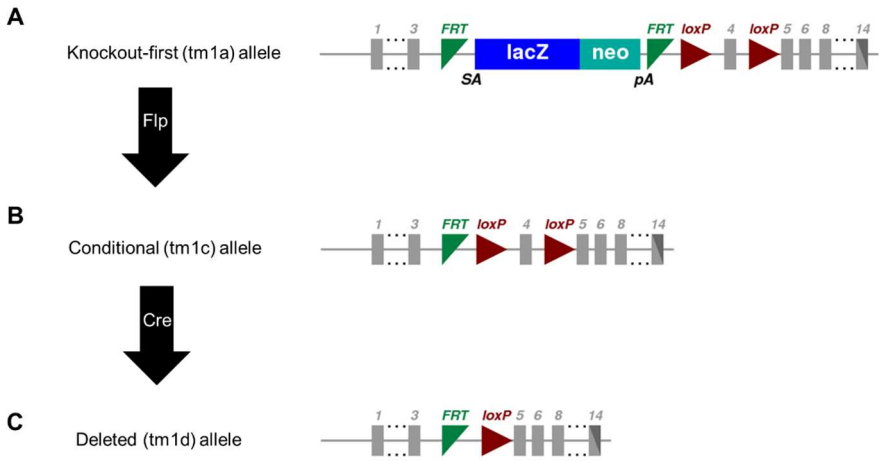


**Figure 2.1. Depiction of the 'knock-out first' strategy used to generate the heterozygous *Setd1a* knockout mouse. A:** The LacZ/neomycin cassette in the tm1a allele disrupts gene function. **B:** Removal of the LacZ/neomycin cassette by Flp recombinase restores gene function and converts the tm1a allele into a conditional tm1c allele. **C:** Excision of the floxed exon by Cre recombinase causes a frameshift mutation, leading to nonsense mediated decay of the tm1d allele. Adapted from: https://www.mousephenotype.org/data/genes/MGI:2446244.

*2.1.2. Animal husbandry*

Offspring were separated from their mothers on postnatal day 28 and an ear biopsy collected for genotyping. Mice were subsequently group housed (2-5 per cage) in single sex cages containing the same environmental enrichment and were cleaned out weekly. Standard chow and water were available *ad libitum* in home cages. Temperature- (21 ± 2 °C) and humidity- (50 ± 10 %) regulated holding rooms were maintained on a 12-hour light-dark cycle (lights on from 08:00-20:00). All procedures were conducted in accordance with the requirements of the UK Animals (Scientific Procedures) Act 1986 (PPL 30/3375).

**2.2. Genotyping**

*2.2.1. DNA extraction*

Tissue biopsies were digested in lysis buffer (0.1 M Tris-HCl pH 8.5, 5 mM EDTA pH 8.0, 0.02 % SDS, 0.2 M NaCl) containing either 100 µg/mL (ear biopsies) or 200 µg/mL (embryo biopsy) Proteinase K (Promega, UK) at 55 °C overnight. Samples were centrifuged at 13,000 rpm for 10 minutes to pellet debris and the supernatant was transferred to a sterile Eppendorf. Samples were treated with an equal volume of phenol (Sigma, UK) to purify nucleic acids, thoroughly mixed by shaking for 10 minutes, centrifuged at 13,000 rpm for 10 minutes and the upper aqueous phase transferred to a new Eppendorf. An equal volume of ice-cold isopropanol (Thermo-Fisher Scientific, UK) was added to all samples and mixed thoroughly to precipitate DNA. DNA was pelleted by centrifugation at 13,000 rpm for 10 minutes at 4 °C. The supernatant was removed and the pellet was washed in 70 % (v/v) ethanol. Samples were vortexed briefly to resuspend the pellet and centrifuged at 13,000 rpm for 5 minutes. Following removal of the supernatant, the pellet was left to air dry and then resuspended in TE buffer (10 mM Tris pH 8.0, 1 mM EDTA pH 8.0). Samples were stored at -20 °C until required.

*2.2.2. PCR*

Animals were genotyped using two separate PCRs to identify the presence of the mutant *Setd1a* allele and the Cre transgene. Tables 2.1 and 2.2 show the contents for the mutant *Setd1a* and Cre PCR reactions, respectively. The cycling conditions for the *Setd1a* PCR were; i) 94 °C for 15 minutes, ii) 94 °C for 30 seconds, iii) 60 °C for 30 seconds, iv) 72 °C for 60 seconds, v) repeat ii-iv 34 times, vi) 72 °C for 2 minutes. The cycling conditions for the Cre PCR were; i) 95 °C for 10 minutes, ii) 94

°C for 30 seconds, iii) 51.7 °C for 30 seconds, iv) 72 °C for 60 seconds, v) repeat ii-iv 34 times, vi) 72 °C for 2 minutes.

**Table 2.1.** PCR reaction contents for the mutant *Setd1a* PCR.

| Reagent | Volume per reaction (µL) |
|---|---|
| 10 X PCR buffer (Qiagen, UK) | 2.0 |
| dNTPs (10 mM) | 0.4 |
| Forward primer (20 µM) AATGATAGCGGCTCCCCAAT | 1.0 |
| Mutant reverse primer (20 µM) GAACTTCGGAATAGGAACTTCG | 1.0 |
| WT reverse primer (20 µM) GAGACAAGACAGAGCCGAGT | 1.0 |
| Hot Start Taq DNA polymerase (Qiagen, UK) | 0.2 |
| DNA template | 1.0 |
| Nuclease-free $H_2O$ | 13.4 |

**Table 2.2.** PCR reaction contents for the Cre PCR.

| Reagent | Volume per reaction (µL) |
|---|---|
| 10 X PCR buffer (Qiagen, UK) | 3.0 |
| dNTPs (10 mM) | 0.6 |
| Cre forward primer (20 µM) GCGGTCTGGCAGTAAAAACTATC | 1.5 |
| Cre reverse primer (20 µM) GTGAAACAGCATTGCTGTCACTT | 1.5 |
| Internal control forward primer (20 µM) CTAGGCCACAGAATTGAAAGATCT | 1.5 |
| Internal control reverse primer (20 µM) GTAGGTGGAAATTCTAGCATCATCC | 1.5 |
| Hot Start Taq DNA polymerase (Qiagen, UK) | 0.2 |
| DNA template | 2.0 |
| Nuclease-free $H_2O$ | 18.2 |

Following completion of the reaction, an appropriate volume of 5X DNA loading buffer (Bioline, UK) was added to PCR products. 20 µL of each reaction and 4 µL of 100 bp Hyperladder™ (Bioline, UK) were loaded onto an agarose gel (3.0 % or 1.5 % for Cre and *Setd1a* PCRs, respectively), which was then run at 100 V for 50 minutes. The gel was visualised under ultraviolet light following separation of the DNA. Mice heterozygous for the *Setd1a* mutant allele were identified by the presence of a mutant band at 143 bp and a WT band at 204 bp (Figure 2.2A). The presence of the Cre transgene was indicated by a band at 100 bp (Figure 2.2B).

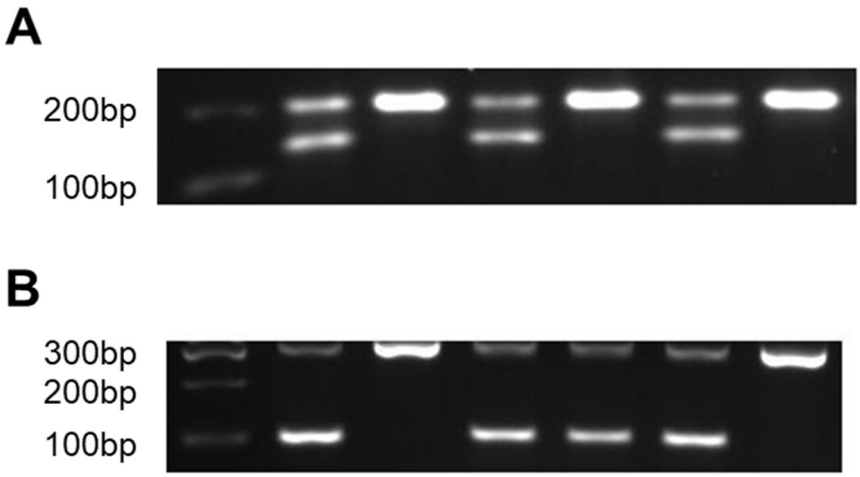


**Figure 2.2. Examples of the mutant *Setd1a* and Cre PCRs. A)** Amplification of wild type *Setd1a* (204 bp) and mutant *Setd1a* (143 bp). **B)** Amplification of the Cre transgene (100 bp) and internal control gene (324 bp).

An additional PCR was used to identify the presence of the *Setd1a*$^{tm1d}$ allele to demonstrate correct recombination and deletion of the floxed exon. The cycling conditions and reaction contents were identical to the *Setd1a* mutant PCR except for the primers; a forward primer was located in the selection cassette (AAGGCGCATAACGATACCAC) and two reverse primers, one in the LoxP site (ACTGATGGCGAGCTCAGACC) and the other in the floxed exon (GAGACAAGACAGAGCCGAGT). The 174 bp amplicon from the forward primer and LoxP site primer is specific to the tm1d allele because the product is too large for amplification in the tm1c allele (Figure 2.3). In addition, a 259 bp band from the forward primer and floxed exon reverse primer will only be observed in the tm1c allele because this region is excised from the tm1d allele following recombination.

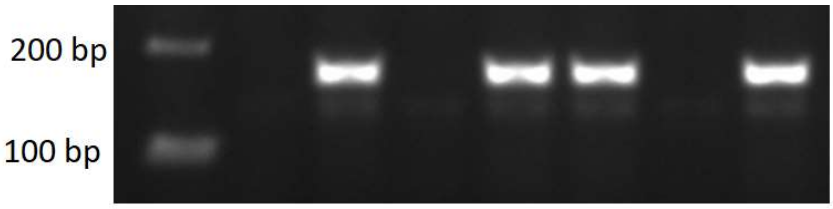


**Figure 2.3. Example of *Setd1a*$^{tm1d}$ PCR**. Amplification of deleted *Setd1a* allele at a band size of 174 bp.

*2.2.3. Embryonic sex determination*

Embryo sex was determined by a multiplex PCR for a Y-linked family of genes (*Ssty*) and an autosomal control gene (*Om1a*). Table 2.3 shows the PCR reaction contents. The PCR conditions for the reaction were; i) 94 °C for 10 minutes, ii) 94 °C for 45 seconds, iii) 61 °C for 45 seconds, iv) 72 °C for 45 seconds, v) repeat ii-iv 34 times, vi) 72 °C for 5 minutes. Gels were visualised as described above. A single band at 245 bp (*Om1a*) indicated female sex and an additional band at 343 bp (*Ssty*) indicated male sex (Figure 2.4).

**Table 2.3.** PCR reaction contents for the sex determination PCR.

| Reagent | Volume per reaction (µL) |
|---|---|
| 10 X PCR buffer (Qiagen) | 2.5 |
| $MgCl_2$ (25 mM) | 2.0 |
| dNTPs (10 mM) | 0.5 |
| *Ssty* forward primer (10 µM) CTGGAGCTCTACAGTGATGA | 1.0 |
| *Ssty* reverse primer (10 µM) CAGTTACCAATCAACACATCAC | 1.0 |
| *Om1a* forward primer (40 µM) TTACGTCCATCGTGGACAGCAT | 0.25 |
| *Om1a* reverse primer (40 µM) TGGGCTGGGTGTTAGTCTTAT | 0.25 |
| Hot Start Taq DNA polymerase (Qiagen) | 0.25 |
| DNA template | 1.0 |
| Nuclease-free $H_2O$ | 16.25 |

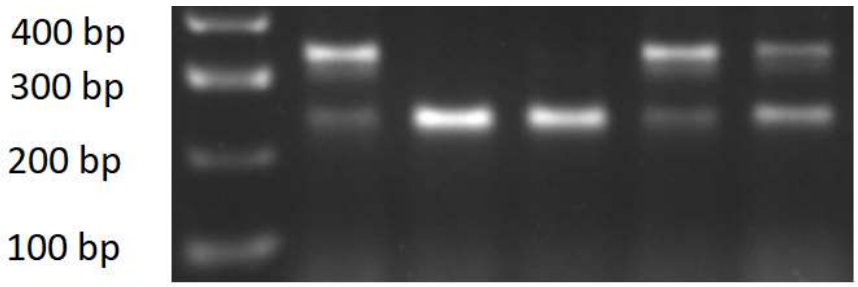


**Figure 2.4. Example of the sex determination PCR.** Amplification of the autosomal control gene *Om1a* (245 bp) and Y-linked gene family *Ssty* (343 bp).

**2.3. Behavioural methods**

Animals were handled daily for at least seven days prior to behavioural testing. Testing started when the animals were 8 weeks old. All animals underwent behavioural tests in the order described here. The time of day that each test was conducted was counterbalanced across genotypes.

*2.3.1. Elevated plus maze*

The elevated plus maze (EPM) was constructed from white Perspex. The apparatus comprised four arms (19 x 8 cm) arranged in the shape of a cross. Two of the opposing arms were open platforms extending outwards from the centre of the apparatus (‘open arms’). The other two opposing arms were enclosed by opaque, 15 cm high walls (‘closed arms’). The maze was elevated 50 cm from the floor and evenly illuminated by a 60 watt lamp positioned above the apparatus and oriented upwards. Mice were placed in the same closed arm at the beginning of the trial and allowed to freely explore the apparatus for five minutes. A camera was positioned above the maze and connected to a computer to record each trial. Ethovision software (Version XT, Noldus, Netherlands) was used to track the animals’ position in the maze (track rate = 17 frames per second), which was divided into five virtual zones; two open arms, two closed arms, and the central region. Measures of anxiety were the proportion of time spent on either of the open arms (relative to the amount of time spent on either of the closed arms), latency of first entry onto an open arm, and the number of entries onto the open arms summed across each arm.

*2.3.2. Open field test*

The open field test (OFT) was conducted under the same conditions as the EPM. The apparatus comprised a square-shaped arena (75 cm x 75 cm) with 45 cm high walls constructed from white Perspex. Animals were placed in the same corner of the arena and allowed to freely explore for ten minutes. The arena was subdivided into two, concentric virtual zones in Ethovision software for tracking: the central 60 cm x 60 cm region ('inner zone') and the surrounding 15 cm ('outer zone'). The amount of time spent in the inner zone, the number of entries into the inner zone, and the latency of first entry into the inner zone were calculated as indices of anxiety.

*2.3.3. Locomotor activity*

Locomotor activity levels were assessed using clear Perspex boxes (21 x 36 x 20 cm) fitted with two transverse infrared beams. The beams were equally spaced (0.3 cm from either end of the box) and positioned 0.1 cm from the floor of the box. The apparatus was connected to a computer and the number of beam breaks during the 120 minute sessions were recorded in 30 minute quartiles using a custom programme (BBC BASIC Version 6). Activity levels were assessed in the dark and at the same time of day over three consecutive days. The primary outcome measures were; i) spontaneous activity levels (i.e., number of beam breaks) in a novel environment and

ii) habituation to a novel environment, indicated by a reduction in activity levels over time both within a session and across consecutive days.

### *2.3.4. Sensorimotor gating*

Acoustic startle response (ASR) and prepulse inhibition (PPI) were measured in a single test session using apparatus from SR-Lab (San Diego Instruments, USA). Mice were placed in a clear Perspex tube (35 mm diameter) mounted on a Perspex plinth in a sound-attenuating chamber. A 70 dB (A scale) white noise stimulus was continuously played during the whole session via a loudspeaker positioned 12 cm above the tube. Each session started with a five minute habituation period. This was followed by two blocks of acoustic stimuli with an average intertrial interval of 16 seconds (pseudorandomly varied between 6 and 24 seconds). In block 1, 6 pulse-alone trials were presented at 120 dB above background, followed by 7 additional pulse-alone trials interspersed with 18 prepulse trials (either 4 dB, 8 dB or 16 dB above background, 6 of each prepulse amplitude) and three no stimulus trials. Three additional no stimulus trials were presented at the end of the block. In block 2, a range of pulse alone trials were presented (80 – 120 dB in 10 dB increments), with three trials of each amplitude in a pseudorandom order with two no stimulus trials at the end of the block. Each pulse-alone trial consisted of a 40 ms acoustic startle stimulus. Prepulse trials comprised a 20 ms acoustic prepulse stimulus followed by a 40 ms acoustic startle stimulus 80 ms after prepulse offset.

The whole-body startle response on each trial was detected by a piezoelectric sensor attached to the plinth, which transduced flexion in the plinth into a digitised signal. The average startle response (Vavg) was recorded in arbitrary startle units using SR-Lab software over the 65 ms period following stimulus onset. Startle data were weight-adjusted by dividing Vavg by body weight. PPI was calculated as the percentage reduction in startle amplitude between prepulse and pulse alone trials (excluding the first 3 pulse-alone trials).

### *2.3.5. Rotarod performance test*

Motor coordination and motor learning were assessed using the Rotarod performance test (Ugo Basile, Italy). The apparatus comprised a circular rod (6 cm diameter) coated with rubber grooves. Mice were placed on the rotating rod, which was suspended 16 cm above levers that triggered a timer to stop and record the latency to fall on each trial. Motor learning was assessed across five accelerating trials lasting 300 seconds each (three trials on day one and two trials the next day). On each

accelerating trial, the speed of rotation increased from 5 rpm to 50 rpm at a constant rate of 0.15 rpm per second. Motor coordination was assessed on day two at 10 fixed rotation speeds. Mice completed two 120 second trials at each speed (20 trials in total). The speed of rotation increased across the test session in 5 rpm increments from 5 rpm to 50 rpm.

*2.3.6. Novel object recognition*

Recognition memory was assessed using the novel object recognition paradigm. Testing was conducted under dimmed lighting in a white Perspex arena (30 x 30 cm) with 30 cm high walls. Ethovision software was used to manually code object exploration (defined as when the head was within 2 cm of and oriented towards the object) using the keyboard. Prior to testing, mice were habituated to the empty arena for 10 minutes per day over three consecutive days to overcome anxiety associated with being in a novel environment and promote object exploration.

Each test session comprised three phases. First, mice were refamiliarised to the empty arena for 10 minutes ('habituation phase'). Second, two identical objects were placed in diagonally opposite quadrants of the arena (10.5 cm from the corners) and mice explored the objects for up to 15 minutes ('acquisition phase'). To control for differences in propensity to explore the objects that could contribute to subsequent memory performance, the total amount of object exploration was timed during the trial by the experimenter. The trial was ended once 40 seconds of object exploration had been reached. Finally, the 'test phase' was conducted after a retention interval of either 30 minutes or 24 hours (within-subjects). Mice were placed back in the arena for 5 minutes with one of the objects that the animals had been exposed to during acquisition ('familiar') and another object that had not been encountered previously ('novel'). The objects were presented in the same locations as the acquisition phase and object exploration was recorded.

At least 24 hours elapsed between the mice being re-tested at the other retention interval. For the second test session, different objects that had not been encountered previously were placed in the quadrants of the arena that were unoccupied in the previous session. The order of the retention interval, location of the objects, and allocation of objects to retention interval were counterbalanced.

## 2.4. Molecular methods

### *2.4.1. Timed-matings and dissections*

Pairings were always set up in the late afternoon. For embryonic timepoints, males were separated from females early the following morning and females were inspected for a vaginal plug to confirm mating. Pregnant dams were culled by cervical dislocation and either whole heads (E11.5) or whole brains (E13.5 and E18.5) were dissected. For postnatal timepoints, day of birth was designated as postnatal day zero (P0). Animals were culled by cervical dislocation and dissected tissue was snap frozen using dry ice and stored at -80 °C until required.

### *2.4.2. RNA extraction*

Tissue was homogenized in an appropriate volume of TRI reagent (Sigma, UK) using Lysing Matrix D tubes (MP Biomedicals, UK). Homogenisation was performed three times for 10 seconds at 6 m/second in a Fast Prep 120 Homogeniser (Thermo Fisher Scientific, UK). Samples were centrifuged for 10 minutes at 13,000 rpm to pellet debris and the supernatant was transferred to a fresh RNase-free Eppendorf. RNA was extracted and DNase treated according to manufacturer's instructions using a Direct-zol™ RNA Miniprep kit (Zymo, UK). RNA purity was assessed using a NanoDrop 8000 spectrophotometer (Thermo Fisher Scientific, UK). RNA concentration was quantified using a Qubit™ RNA HS Assay Kit and Qubit 2.0 Fluorometer (Invitrogen, UK). Samples were stored at -80 °C until required.

### *2.4.3. cDNA synthesis*

RNA to cDNA conversion was performed using RNA to cDNA EcoDry™ Premix (double-primed) kits (Clontech, UK). 1 µg RNA per sample was reverse transcribed according to manufacturer's instructions. cDNA was diluted 1:10 in nuclease-free water and stored at -20 °C until required.

### *2.4.4. RT-qPCR*

Intron-spanning primers (annealing temperature = 58 °C) were designed for *Setd1a* and three housekeeping genes (*Hprt*, *Dynein*, and *B2m*; Table 2.4). Samples were run in triplicate and the same biological replicate was used for amplification of *Setd1a* and all three housekeeping genes. A nuclease-free water no-template control was included on each run. The contents of each 25 µL reaction were: 12.5 µL 2X SensiMix SYBR No-ROX (Bioline, UK), 1.75 µL forward primer, 1.75 µL reverse primer, 5.0 µL template, 4.0 µL nuclease-free $H_2O$. Reactions were performed using a Corbett Rotor

Gene 6000 Real-Time PCR Machine with the following conditions; i) 95 °C for 10 minutes, ii) 95 °C for 20 seconds, iii) 58 °C for 20 seconds, iv) 72 °C for 20 seconds, v) repeat ii-iv 39 times. Subsequently, melt curves were generated by heating the reaction from 50-99 °C in 1 °C increments. These were inspected to confirm a single PCR product for each primer pair. The threshold cycle (Ct) was calculated at an Rn of 0.3 for all RT-qPCR reactions.

RT-qPCR data were analysed using the $2^{-\Delta\Delta CT}$ method. First, data were averaged across the triplicates for each sample. Second, expression data were normalised to the internal control genes by calculating the geometric mean of the three housekeeping genes and subtracting this value from the Ct value for *Setd1a* for each sample. These ΔCt values were used for statistical analysis. Third, $2^{-\Delta CT}$ values were calculated and used to calculate fold-change expression for visualisation ($2^{-\Delta\Delta CT}$) by subtracting the average $2^{-\Delta CT}$ for the reference condition from the other conditions.

**Table 2.4.** RT-qPCR primer sequences and target product sizes for *Setd1a* and three housekeeping genes (*Hprt, Dynein, and B2m*).

| Target | Forward primer | Reverse primer | Product size (bp) |
|---|---|---|---|
| *Setd1a* | CCCTCCCGGTTCCTAAGTTT | CATTGTCATTGAGCCTCGCA | 90 |
| *Hprt* | GCGATGATGAACCAGGTTATGA | GCCTCCCATCTCCTTCATGA | 146 |
| *Dynein* | GACCTCAGGCTCAGACGAAGAC | AAGACGCTCATGGCATCACA | 116 |
| *B2m* | TTCTGGTGCTTGTCTCACTGA | CAGTATGTTCGGCTTCCCATTC | 104 |

### *2.4.5. Protein extraction*

Protein extraction was performed on ice to prevent protein degradation. Tissue was homogenised using Lysing Matrix D tubes (MP Biomedicals, UK) in an appropriate volume of sample buffer, comprising RIPA buffer (Sigma, UK) with one cOmplete™ Mini Protease Inhibitor Cocktail tablet (Roche, Switzerland) per 10 mL of buffer. Homogenisation was performed three times for 10 seconds at 6 m/second in a Fast Prep 120 Homogeniser (Thermo Fisher Scientific, UK). Protein concentration was quantified in triplicate for each sample using a Pierce™ BCA Protein Assay kit (Thermo Scientific, UK) according to manufacturer's instructions. Samples were diluted to 1 µg/µL in sample buffer and treated with 1 % (v/v) Benzonase Nuclease (Millipore, UK) to digest nucleic acids. Samples were stored at -80 °C in 50 µL aliquots to reduce the number of freeze-thaw cycles.

### *2.4.6. Western blotting*

Samples were defrosted on ice and an equal volume of 2X protein loading buffer (LI-COR, UK) containing 0.05 % (v/v) 2-Mercaptoethanol (Sigma, UK) was added.

Samples were heated at 95 °C for 5 minutes to denature proteins. 20 µg of each protein sample and 5 µL Odyssey Protein Molecular Weight Marker (LI-COR, UK) were loaded onto a NuPAGE™ 4-12 % Tris-Acetate gel (Invitrogen, UK). Proteins were separated by SDS-PAGE in NuPAGE™ Tris-Acetate SDS Running Buffer (Invitrogen, UK) at 120 V for 2 hours at room temperature. Proteins were then transferred to a 0.45 µm pore size nitrocellulose membrane (Invitrogen, UK) at 70 V for 3 hours on ice in NuPAGE™ Transfer Buffer (Invitrogen, UK) containing 10 % methanol (Fisher Scientific, UK).

All incubation steps were performed with agitation. Following transfer, the membrane was stained for protein using a REVERT™ Total Protein Stain Kit (LI-COR, UK) and then blocked in Odyssey TBS Blocking Buffer (LI-COR, UK) for 60 minutes at room temperature. The membrane was incubated overnight at 4 °C in primary rabbit polyclonal *Setd1a* antibody (Bethyl Laboratories, USA), diluted 1:1,000 in blocking buffer containing 0.2 % (v/v) Tween 20 (Sigma, UK). Following primary antibody incubation, the membrane was washed four times in TBS-T (1M NaCl, 1M Tris-HCl pH 7.5, 0.2 % (v/v) Tween 20) for five minutes. The membrane was then incubated for one hour at room temperature in IRDye 800CW goat anti-rabbit secondary antibody (LI-COR, UK), diluted 1:10,000 in blocking buffer containing 0.2 % (v/v) Tween 20. Finally, four additional wash steps were performed in TBS-T.

Membranes were imaged using an Odyssey CLx imaging system (LI-COR, UK). Average background-subtracted fluorescence was measured at 700 nm (total protein) and 800 nm (*Setd1a*) using Image Studio software (LI-COR, UK). Relative *Setd1a* protein abundance was quantified using total protein normalisation. The lane normalisation factor was calculated by dividing the total protein signal for each lane by the lane with the highest total protein signal. The normalised signal for *Setd1a* was calculated for each lane by dividing the signal for the *Setd1a* band (268 kDa) by the lane normalisation factor. These normalised values were used for analysis and calculating fold-change values for visualisation.

### 2.5. Data analysis

All data were analysed using IBM SPSS software (version 25) with the exception of the RNA-seq data (Chapter 4). Data are presented as mean and standard error of the mean (SEM) unless otherwise specified. Data were analysed using analysis of variance (ANOVAs) with the between-subjects factors of genotype and sex, with additional factors as required (see relevant chapters for details).

## Chapter 3: Investigating transcriptomic changes in the developing brains of *Setd1a*$^{+/-}$ mice

### 3.1. Introduction

In this chapter, the regulatory role of *Setd1a* in the developing mouse brain was examined using RNA-seq. This work was conducted to assess the effects of *Setd1a* haploinsufficiency on biological processes during prenatal brain development that could be important for understanding pathogenic mechanisms.

The neurodevelopmental hypothesis of schizophrenia posits that disrupted brain development is integral to pathogenesis (Murray & Lewis, 1987; Weinberger, 1987). Consistent with this, common variants for schizophrenia are highly expressed in the prenatal brain (Birnbaum et al., 2015; Clifton et al., 2019; Jaffe et al., 2018). Moreover, foetal brain expression quantitative trait loci are enriched for schizophrenia common variants (O'Brien et al., 2018). These findings suggest a degree of convergence of genetic risk for schizophrenia on biological processes taking place during early brain development. Dynamic regulation of histone modification, particularly H3K4 methylation, is thought to be critical for the precise coordination of extensive changes in gene expression that are essential for cell-fate specification and migratory processes that occur during neurodevelopment (Roidl & Hacker, 2014; Shen, Shulha, Weng, & Akbarian, 2014). Indeed, mutations in several genes involved in the addition, reading, and removal of H3K4 methylation cause a range of neurodevelopmental disorders (Vallianatos & Iwase, 2015). Thus, one mechanism by which *Setd1a* loss of function could serve to increase risk for psychopathology is due to perturbed neurodevelopment as a result of aberrant H3K4 methylation and associated transcriptional dysregulation.

A role for *Setd1a* in neurodevelopment has been reported previously. Specifically, knockdown of *Setd1a* has been shown to result in reduced proliferation of neuronal progenitor cells (NPCs) *in vitro* (Bledau et al., 2014), suggesting a role for *Setd1a* in maintenance of NPC pluripotency. Further evidence to support this is provided by *in vivo* evidence that *Setd1a* knockdown causes increased neurogenesis and a reduction in markers of NPC proliferation in the embryonic mouse brain (Li & Jiao, 2017). These findings suggest that *Setd1a* loss of function may cause premature differentiation and, consequently, a depleted supply of NPCs. Adult *Setd1a*$^{+/-}$ mice have fewer pyramidal neurons in cortical layers 2 and 5 and reduced inhibitory neurons in layer 5 of the medial prefrontal cortex (Mukai et al., 2019). These changes

may be attributed to the aforementioned imbalance between proliferation and differentiation of NPCs that occurs as a result of *Setd1a* loss of function.

Two previous studies have investigated the effects of *Setd1a* loss of function on the transcriptome in neural tissue. A 50 % reduction in *Setd1a* dosage has been shown to cause changes in expression of over 1,000 genes in a neuroblastoma cell line (Cameron et al., 2019). These transcriptional changes were enriched for schizophrenia common variants and gene annotations relating to metabolism, peptidase regulator activity, and cell adhesion. Interestingly, several of the differentially expressed genes (e.g., *Dlx5* and *Dcx*) are known to play a role in neurodevelopment. In another study, approximately 300 differentially expressed genes were identified by RNA-seq of adult prefrontal cortex of *Setd1a*$^{+/-}$ mice (Mukai et al., 2019). However, the biological relevance of these changes and their overlap with other genetic variants for schizophrenia remains unclear. In addition, the effect of *Setd1a* loss of function on the transcriptome of the developing brain has not been investigated previously.

The aim of this chapter was to assess transcriptomic changes in the developing brains of *Setd1a*$^{+/-}$ mice. The trajectory of *Setd1a* expression in the brain was examined across neurodevelopment (from E11.5 to P56), revealing highest expression around mid-gestation (section 3.3.1). Based on these results, RNA-seq was performed on E13.5 whole brain. This is a period of substantial neurogenesis, coinciding with the commencement of the formation of cortical layer 5 neurons (Finlay & Darlington, 1995). Differentially expressed genes were assessed for enrichment of gene ontology (GO) annotations and schizophrenia common variants to investigate over-representation in biological pathways and the degree of convergence with other molecular mechanisms conferring risk for schizophrenia, respectively.

## 3.2 Methods

### *3.2.1. Trajectory of Setd1a expression across neurodevelopment*

Timed-matings and dissections were conducted as described in Chapter 2.4.1. Whole brains (E11.5, E13.5 and E18.5) or hemibrains (P7, P23 and P56) were obtained from F1 progeny of C57BL/6J x C57BL/6NTac parents. Tissue was obtained from at least two separate litters per timepoint.

RNA extraction, cDNA synthesis, and RT-qPCR were conducted as described in Chapter 2.4.2-2.4.3 to examine *Setd1a* mRNA expression levels (N = 6 per

timepoint). Protein extractions and Western blotting were conducted as described in Chapter 2.4.5-2.4.6 to examine *SETD1A* protein levels (N = 5 per timepoint).

### *3.2.2. Generation of the model*

As described in Chapter 2.1.1, a “knock-out first” strategy was used to generate *Setd1a* heterozygous knockout mice. Although the tm1a allele disrupts gene function, it is necessary to remove the LacZ/neomycin cassette to eliminate potential confounding effects of these constructs (Coleman et al., 2015). Expression of LacZ in the central nervous system results in neuropathological changes and behavioural impairments (Reichel et al., 2016). Moreover, insertion of a neomycin cassette can disrupt expression of other genes more than 100 kb from the insertion (Pham, MacIvor, Hug, Heusel, & Ley, 1996). Therefore, mice heterozygous for the *Setd1a*$^{tm1c}$ allele were crossed with a homozygous B6.C-Tg(CMV-cre)1Cgn/J line (referred to as 'CMV-Cre'), purchased from The Jackson Laboratory. Cre recombinase is expressed constitutively in the CMV-Cre line under the control of the human cytomegalovirus promoter. This results in recombination and deletion of the floxed exon in all tissues (including germline cells), leading to a frameshift mutation in the deleted (tm1d) allele and loss of *Setd1a* function via nonsense mediated decay of the mutant transcript.

Cre recombinase has been reported to have excitotoxic effects as a result of DNA damage (Loonstra et al., 2001), possibly arising from recombination at cryptic LoxP sites in the genome (Thyagarajan, Guimarães, Groth, & Calos, 2000). On this basis, a breeding strategy was devised that enabled elimination of the Cre transgene from experimental cohorts. F1 progeny from male *Setd1a*$^{tm1c}$ and female CMV-Cre pairings were genotyped to identify animals that were positive for the tm1d (deleted) allele. Transgenic F1 males were then crossed with wild type C57BL/6J females purchased from Charles River. Since the Cre transgene is X-linked, all F2 male progeny were negative for the Cre transgene. Experimental cohorts were generated by pairing F2 male *Setd1a*$^{+/-}$ mice with wild type C57BL/6J females to eliminate effects of *Setd1a* loss of function on maternal contributions to prenatal environment and maternal care.

### *3.2.3. Model validation*

To confirm whether approximately 50 % knockdown of *Setd1a* had occurred in the constitutive heterozygous model, RT-qPCR (N = 16; 8 WT and 8 KO) was performed on cDNA derived from E13.5 whole brain (see Chapter 2.4.2-2.4.3). As described earlier, the tm1d allele is still transcribed following recombination by Cre recombinase. Therefore, a primer pair that included the deleted exon was designed in order to be sensitive to detect changes at the transcript level (i.e., the sequence of the reverse

primer was complementary to exon 4). In addition, SETD1A protein levels in E13.5 whole brain (N = 10; 5 WT and 5 KO) were examined using Western blot (see Chapter 2.4.5-2.4.6).

### *3.2.4. RT-qPCR and Western blot data analysis*

The $2^{-\Delta\Delta CT}$ method was used to calculate ΔCt values (see Chapter 2.4.4). Normalised Western blot data were calculated as described in Chapter 2.4.6. To assess changes in *Setd1a* expression across neurodevelopment, between-subjects ANOVAs (age: 6 levels) were used followed by Tukey post-hoc tests. Confirmation of *Setd1a* knockdown in *Setd1a*$^{+/-}$ mice was tested using independent t-tests.

### *3.2.5. RNA-seq*

#### *3.2.5.1. RNA extraction and quality control*

RNA was extracted from 16 (8 WT and 8 KO, balanced for sex) E13.5 whole brains using a Direct-zol™ RNA Miniprep kit (Zymo, UK). E13.5 was chosen based on the results of the developmental expression work, which showed highest expression levels at this timepoint (see section 3.3.1). RNA purity was assessed using a NanoDrop 8000 spectrophotometer (Thermo Fisher Scientific, UK). RNA concentration was quantified using a Qubit™ RNA High Sensitivity Assay Kit and Qubit 2.0 Fluorometer (Invitrogen, UK). RNA integrity was assessed using a Bioanalyzer RNA 6000 Nano Assay (Agilent, UK) and 2100 Bioanalyzer system (Agilent, UK). All samples had an RNA Integrity Number of at least 9.7.

#### *3.2.5.2. Library preparations and sequencing*

Library preparations were performed using a KAPA mRNA Hyperprep kit (Roche, Switzerland) according to manufacturer's instructions, with 1 µg total RNA as input. Following library amplification, fragment size (mean = 374.9, SD = 12.5) was determined using a High Sensitivity DNA kit (Agilent, UK). A Qubit™ dsDNA High Sensitivity Assay Kit (Invitrogen, UK) was used to determine library concentration. Libraries were adjusted prior to pooling to achieve a final DNA molarity of 20 nM. Sequencing was performed on a HiSeq 4000 (Illumina, USA) with 75 bp paired-end reads at a read depth of 30 million reads.

#### *3.2.5.3. Analysis pipeline*

Reads were trimmed to remove adapters and low-quality bases using Trimmomatic (Bolger, Lohse, & Usadel, 2014) with default parameters. All samples passed quality control implemented in FastQC (Andrews, 2010). Reads were mapped to the mouse

reference genome (GRCm38) using STAR (Dobin et al., 2013). The mean number of reads mapped was 97.2 % (SD = 0.5 %). Read counts were generated using featureCounts (Liao, Smyth, & Shi, 2014) to allocate reads to genomic features using the mouse Ensembl gene annotation (GRCm.38.95). Coverage at exon 4 of *Setd1a* was substantially reduced in *Setd1a*$^{+/-}$ E13.5 brain, indicating that recombination had occurred (Figure 3.1). Differential expression analysis was performed using DEseq2 (Love, Huber, & Anders, 2014) implemented in R (version 3.5.3). The Benjamini Hochberg correction was used to correct for multiple testing and identify genes that were differentially expressed in *Setd1a*$^{+/-}$ relative to WT ($p_{adj}$ < .05), with sex included as a covariate.

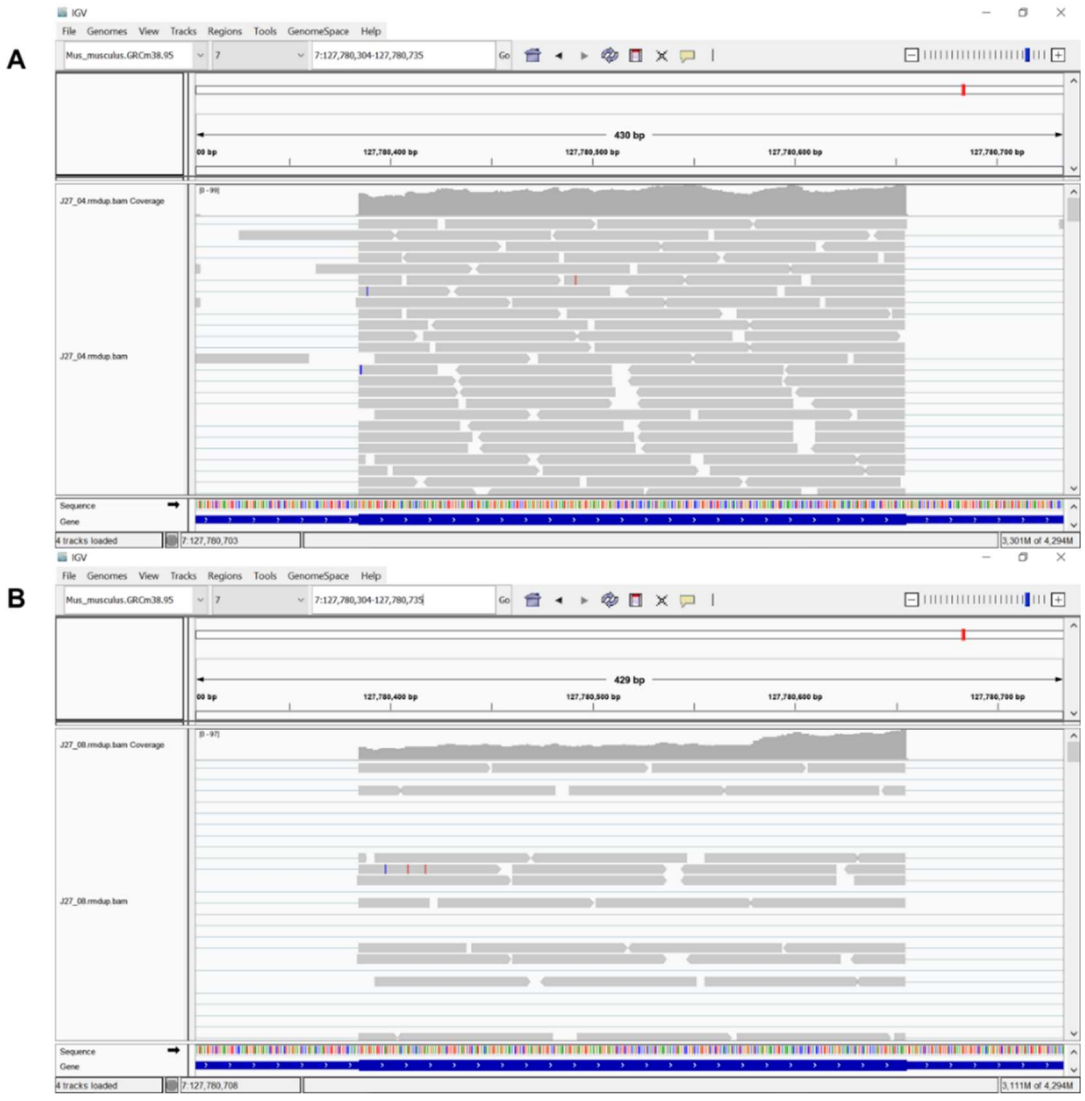


**Figure 3.1. Read alignment at the critical exon of *Setd1a*.** Screenshot from Integrative Genomics Viewer showing substantially more reads aligning to exon 4 in **A)** WTs compared to **B)** *Setd1a*$^{+/-}$ mice.

*3.2.5.4. Gene ontology enrichment analysis*

GO term enrichment analysis was performed using the Database for Annotation, Visualization and Integrated Discovery (Huang, Sherman, & Lempicki, 2009). Only protein-coding genes with entrez IDs (219 genes) were included in the differentially expressed gene-set. A custom background gene-set was created using all expressed genes in the dataset (12,295 genes). This was defined as any gene with a FPKM $\geq$ 1 across 8 samples (i.e., the number of biological replicates in each condition).

*3.2.5.5. Schizophrenia common variant gene set enrichment analysis*

The differentially expressed gene-set was filtered to include only genes with human entrez IDs (205 genes). This gene-set was assessed for enrichment of schizophrenia common variants using MAGMA (de Leeuw, Mooij, Heskes, & Posthuma, 2015) with GWAS summary data from 40,675 cases and 65,643 controls (Pardiñas et al., 2018). SNPs were filtered to include those with a minor allele frequency of greater than 0.01. Annotation of SNPs to genes was performed using an annotation window of 35 kb upstream and 10 kb downstream of each gene. The gene-set analysis function in MAGMA performs a linear regression, testing whether the association of the phenotype with genes in the gene-set is greater than with genes that are not in the gene-set (controlling for gene size, gene density, and linkage disequilibrium).

**3.3. Results**

*3.3.1. Trajectory of Setd1a expression across neurodevelopment*

Analysis of the RT-qPCR data revealed a significant main effect of age ($F(5, 30) = 11.65$, $p < .001$; Figure 3.2A). Post-hoc tests showed that expression levels were significantly higher at E11.5 than all other timepoints (all $p \leq .002$) except at E13.5 ($p = .26$). Expression levels at E13.5 were not significantly different from E18.5 ($p = .32$) or P7 ($p = .08$) but were significantly higher than at P23 ($p = .003$) and P56 ($p = .02$). There was no further significant decline in expression levels after E18.5 (all $p \geq .33$).

Similar results were obtained at the protein level: a significant main effect of age was observed ($F(5, 24) = 6.78$, $p < .001$; Figure 3.2B), which reflected significantly increased expression at E11.5 and E13.5 relative to postnatal timepoints (all $p \leq .02$). No significant difference was observed between E11.5 and E13.5 or E18.5 (both $p \geq .60$). Consistent with the RT-qPCR data, expression levels did not change after E18.5 (all $p \geq .17$). Together, these data suggest that *Setd1a* expression levels are higher in the developing brain during (mid) gestation, followed by down-regulation in the postnatal brain.

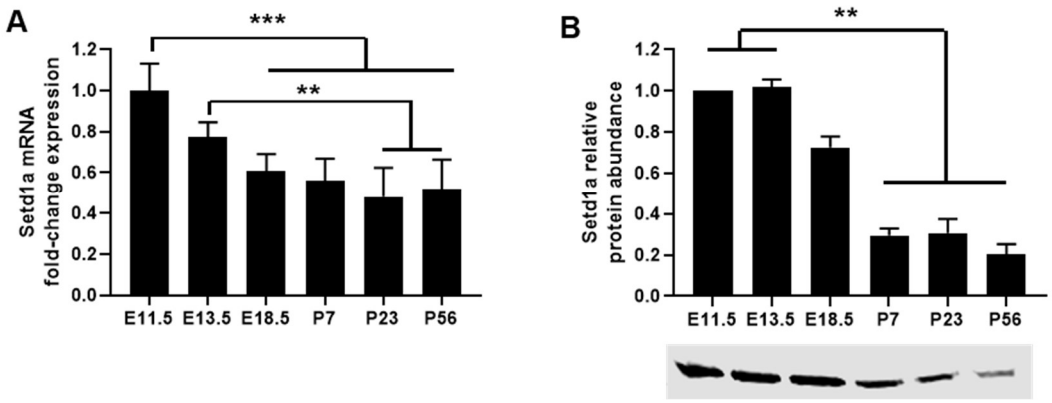


**Figure 3.2. Developmental trajectory of *Setd1a* expression in the brain.** Mean (+/- SEM) fold-change expression (relative to E11.5) of **A)** *Setd1a* mRNA and **B)** SETD1A protein abundance across embryonic and postnatal brain development.

*3.3.2. Model validation*

*Setd1a* mRNA expression in E13.5 brain was reduced by 48.7 % in *Setd1a*$^{+/-}$ mice compared to WTs ($t(14) = 9.19$ $p < .001$; Figure 3.3A). Consistent with this, levels of SETD1A protein were reduced by 46.3 % ($t(8) = 2.71$ $p = .03$; Figure 3.3B). This magnitude of reduction is consistent with haploinsufficiency and confirms that *Setd1a* knockdown was successfully achieved.

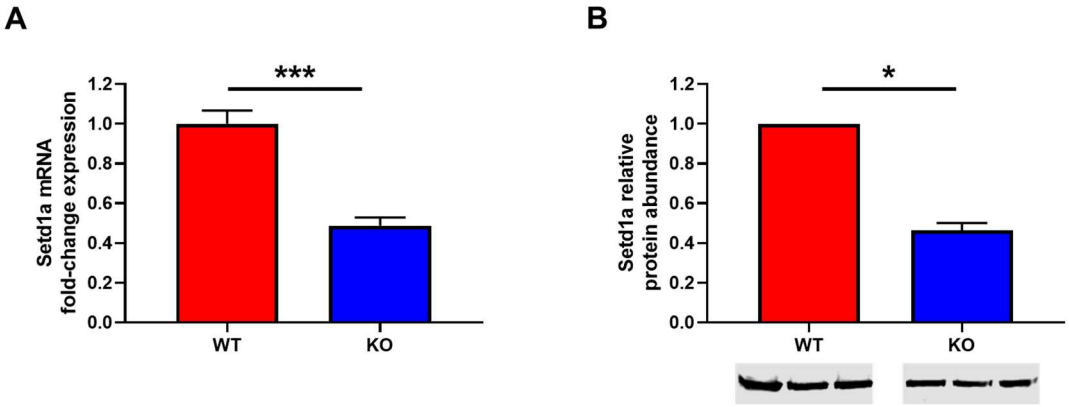


**Figure 3.3. Confirmation of *Setd1a* haploinsufficiency in brains of *Setd1a*$^{+/-}$ mice at E13.5.** Mean (+/- SEM) fold-change expression (relative to WT) of **A)** *Setd1a* mRNA and **B)** SETD1A protein abundance.

### *3.3.3. RNA-seq*

#### *3.3.3.1. Differential expression*

Principal components analysis of differentially expressed genes showed that the samples clustered by genotype on principal component 1 (Figure 3.4A). This component accounted for the highest proportion of variance across samples (67.5%). There were 267 genes (Benjamini Hochberg $p_{adj}$ < .05) that were differentially expressed (234 downregulated and 33 upregulated; Appendix 1) in brains of *Setd1a*$^{+/-}$ mice at E13.5 (Figure 3.4B). Modest changes in gene expression were observed, with log2 fold changes ranging from -0.63 to 1.19. Hierarchical clustering based on normalised read counts was performed using Morpheus (https://software.broadinstitute.org/morpheus) to produce a dendrogram (Figure 3.4C). This showed that samples of the same genotype clustered together, suggesting similar patterns of gene expression changes within each group.

#### *3.3.3.2. Gene ontology enrichment analysis*

Results of the GO term enrichment analysis revealed that the differentially expressed gene-set was significantly enriched for the mitochondrion GO term 0005739 (Benjamini Hochberg $p_{adj}$ = .002). 16 nominally significantly (uncorrected $p$ < .05) associations were observed that did not survive correction for multiple testing (Table 3.1) but included annotations relating to other mitochondrial terms, cilium, and methylation.

#### *3.3.3.3. Schizophrenia common variant gene set enrichment analysis*

Gene-set enrichment analysis revealed that genes that were differentially expressed in *Setd1a*$^{+/-}$ E13.5 brain were not significantly enriched for schizophrenia common variant association ($B$ = 0.004, SE = 0.088, $p$ = .48).

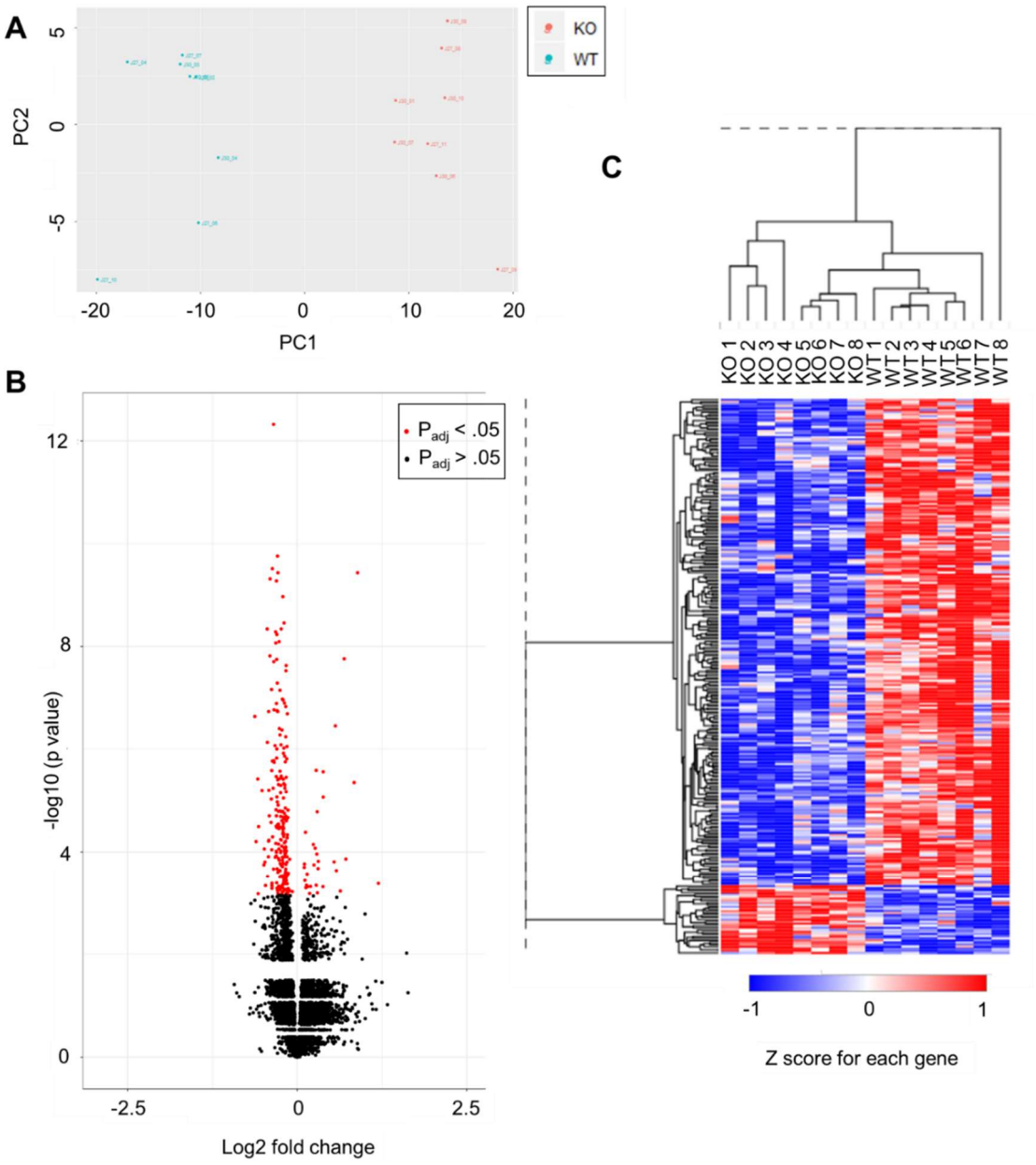


**Figure 3.4. Effects of *Setd1a* haploinsufficiency on transcriptional changes in E13.5 mouse brain. A)** PCA plot of differentially expressed genes (Benjamini Hochberg $p_{adj}$ < .05) showing separation of WT and KO samples along PC1, **B)** volcano plot of differentially expressed genes, and **C)** dendrogram showing clustering of differentially expressed genes according to genotype.

**Table 3.1.** Results of GO term enrichment analysis.

| Category | GO term | Gene count | *P* value | Benjamini Hochberg |
|---|---|---|---|---|
| Cellular component | Mitochondrion (GO: 0005739) | 47 | .00001 | .002 |
| | Cilium (GO: 005929) | 10 | .004 | .35 |
| | Ciliary basal body (GO: 0036064) | 7 | .005 | .30 |
| | Mitochondrial matrix (GO: 0005759) | 8 | .02 | .74 |
| | Integral component of mitochondrial inner membrane (GO: 0031305) | 3 | .04 | .80 |
| Biological process | Peptidyl-lysine deacetylation (GO: 0034983) | 3 | .006 | .98 |
| | Methylation (GO: 0032259) | 8 | .01 | .99 |
| | Cilium morphogenesis (GO: 0060271) | 8 | .01 | .95 |
| | Cell projection organization (GO: 0030030) | 7 | .02 | .97 |
| | Cilium assembly (GO: 0060271) | 6 | .04 | 1.0 |
| | Nucleotide metabolic process (GO: 0009117) | 3 | .04 | 1.0 |
| Molecular Function | Methyltransferase activity (GO: 0008168) | 8 | .009 | .95 |
| | Nucleic acid binding (GO: 0003676) | 26 | .01 | .80 |
| | NAD-dependent histone deacetylase activity (H3-K14 specific) (GO: 0032041) | 3 | .02 | .82 |
| | Transferase activity (GO: 0016740) | 29 | .02 | .84 |
| | Nucleotidyltransferase activity (GO: 0016779) | 5 | .03 | .86 |
| | Aspartate-tRNA ligase activity (GO: 0004815) | 2 | .03 | .82 |

### 3.4. Discussion

This chapter investigated the effects of *Setd1a* haploinsufficiency on the transcriptome of the developing mouse brain at E13.5. The number of differentially expressed genes was moderate (267 genes survived correction for multiple testing) and the magnitude of effect sizes were relatively modest. The majority of differentially expressed genes were downregulated, consistent with a loss of activating H3K4 methylation following *Setd1a* loss of function (Shilatifard, 2012). The differentially expressed genes were enriched for mitochondrion annotations. No enrichment for schizophrenia common variant association was observed.

The observation that *Setd1a* loss of function leads to differential expression of genes that are over-represented in the mitochondrion GO term is consistent with previous reports (Cameron et al., 2019; Hoshii et al., 2018). Mitochondrial dysfunction has been repeatedly implicated in the pathogenesis of schizophrenia (Ben-Shachar, 2017; Flippo & Strack, 2017; Rajasekaran, Venkatasubramanian, Berk, & Debnath, 2015). Further work is needed to determine whether this enrichment is a direct consequence of *Setd1a* loss of function or is attributable to increased cellular stress. No other GO terms survived correction for multiple testing. However, several nominally significant cilium-related GO terms were observed. Cilia play an essential role during neurodevelopment (Guemez-Gamboa, Coufal, & Gleeson, 2014) and knockdown of a range of neuropsychiatric risk genes affects cilia formation *in vitro* (Marley & von Zastrow, 2012). It would be interesting to explore whether *Setd1a* loss of function has similar effects in future work.

The transcriptomic changes observed in *Setd1a*$^{+/-}$ E13.5 mouse brain were not enriched for schizophrenia common variant association. One interpretation of this finding is that *Setd1a* loss of function exerts pathogenic effects via molecular mechanisms that are distinct from common genetic variants. However, this is inconsistent with the results of a previous study conducted in a human neuroblastoma cell line (Cameron et al., 2019). Notably, substantially fewer differentially expressed genes were observed in the present study, which may be due to cellular heterogeneity of the E13.5 mouse brain. The number of differentially expressed genes observed here was similar to what has been reported in the prefrontal cortex of adult *Setd1a*$^{+/-}$ mice (Mukai et al., 2019). One explanation for why fewer changes were observed in mouse brain than *in vitro* is due to differences in gene-targeting approaches. That is, there is likely to be more opportunity for compensatory mechanisms to take place *in vivo* compared to an acute challenge of *Setd1a* knockdown *in vitro* since *Setd1a*$^{+/-}$

mice are haploinsufficient from conception. Other explanations include differences in the transcriptomic effects of *Setd1a* loss of function in different cell types or in the regulatory role of *Setd1a* in mouse and human.

Interestingly, Mukai et al. (2019) used Chip-seq to show that *Setd1a* target genes in WT mouse prefrontal cortex are enriched for schizophrenia common variants. However, very few of these target genes were differentially expressed in their RNA-seq analysis, both of bulk prefrontal cortex and at the single-cell level. This suggests that the observed transcriptomic changes reflect effects downstream of *Setd1a* targets. It would be interesting in future work to assess differential H3K4 methylation in *Setd1a*$^{+/-}$ mice to explore the extent to which *Setd1a* haploinsufficiency results in altered H3K4 methylation of target genes that is not sufficient to cause transcriptional changes but increase vulnerability to transcriptional dysregulation following a second 'hit' (e.g., stress).

A limitation of the present experiment is that subtle gene expression changes may have been masked by the diverse cell types in E13.5 brain tissue. The whole brain transcriptome was assayed due to the lack of available data on cell-type and region specific expression of *Setd1a* in the developing mouse brain. However, it is possible that a stronger signal would be observed in the ventricular zone considering previous evidence demonstrating a role for *Setd1a* in neurogenesis (Bledau et al., 2014; Li & Jiao, 2017). It may be necessary in future work to generate homogeneous cell populations using primary neuron cultures or use single-cell RNA-seq to examine the cell-type specific effects of *Setd1a* loss of function. In addition, although *Setd1a* expression levels in the brain were highest at mid-gestation, robust expression was observed until adulthood. It would be informative to assess transcriptomic effects of *Setd1a* loss of function at other stages of neurodevelopment.

Another limitation of the current design was a lack of power to detect sex-specific effects of *Setd1a* loss of function. When analysed separately, very few differentially expressed genes were identified in males (11 genes) and none survived correction for multiple testing in females. This likely reflects the fact that the magnitude of the changes in gene expression were relatively modest (log2 fold changes ranged from -0.63 to 1.19). Sexually dimorphic effects of *Setd1a* loss of function have been observed in the placenta (Chapter 4) and in the effects of the atypical antipsychotic risperidone on the acoustic startle response (Chapter 6). Thus, further work is needed to determine whether the transcriptomic consequences of *Setd1a* loss of function in the developing brain are also moderated by sex.

In conclusion, this chapter demonstrated that *Setd1a* haploinsufficiency has a modest effect on the transcriptome of the developing mouse brain at E13.5. Gene-set enrichment analyses revealed that differentially expressed genes were enriched for mitochondrion annotations but not for association with schizophrenia common variants. Further work is needed to determine the cell-type specific effects of *Setd1a* loss of function at different stages of neurodevelopment.

## Chapter 4: Gestational compromise in *Setd1a*$^{+/-}$ mice and consequences for growth in the early post-weaning period

### 4.1. Introduction

Recent evidence highlights a role for the placenta in mediating genetic risk for schizophrenia (Ursini et al., 2018). This chapter explored whether the pathogenic effects of *Setd1a* haploinsufficiency may also be mediated by an effect in the placenta and how these effects translate into differences in foetal and postnatal growth.

Many neurodevelopmental and neuropsychiatric disorders have their origins in early life. Epidemiological studies have identified several *in utero* risk factors that increase the likelihood of offspring developing schizophrenia, including prenatal diet (Brown & Susser, 2008; Xu et al., 2009), maternal stress (Khashan et al., 2008; van Os & Selten, 1998) and infection (Brown & Derkits, 2010; Khandaker et al., 2013), and obstetric complications (Cannon et al., 2002). These findings illustrate the susceptibility of the developing brain to prenatal adversity and are consistent with the neurodevelopmental hypothesis of schizophrenia (Birnbaum & Weinberger, 2017; Murray & Lewis, 1987; Weinberger, 1987). Further evidence is provided by animal models showing that many prenatal stressors recapitulate behavioural and neurobiological endophenotypes of schizophrenia (Meyer & Feldon, 2010). It has been suggested that the effects of prenatal insults on risk for neurodevelopmental disorders are mediated by the placenta, which acts as the interface between mother and foetus and is critically important for foetal development (Bronson & Bale, 2016; Jansson & Powell, 2007; Sandovici, Hoelle, Angiolini, & Constância, 2012).

Placental defects in embryonically lethal transgenic mice are a strong predictor of abnormal brain morphology (Perez-Garcia et al., 2018), further suggesting that perturbed placental function has negative consequences for prenatal brain development. Recent evidence also suggests that common variant genetic risk for schizophrenia may be partially mediated by effects on placental function. Specifically, polygenic risk for schizophrenia is higher in the presence of early-life complications and pathway analysis of schizophrenia risk genes that are differentially expressed in the placenta following early-life complications has shown enrichment of metabolic and cellular stress pathways (Ursini et al., 2018). These findings raise the intriguing possibility that rare genetic variants for schizophrenia, such as *Setd1a*, may also exert pathogenic effects by influencing placental function. Preliminary evidence to support this hypothesis comes from a study showing that knockdown of *Setd1a* in embryonic stem cells causes transcriptomic changes that are enriched for placental

development (Fang et al., 2016). In addition, down-regulation of *Setd1a* expression in the placenta has been reported to occur following a prenatal high-fat diet (Gabory et al., 2012), which is also linked with schizophrenia-relevant behavioural alterations (Sullivan et al., 2015). However, the direct effects of *Setd1a* haploinsufficiency on placental phenotypes has not been examined previously.

In eutherian mammals, the placenta plays an integral role in maternal-foetal nutrient and gas exchange, removal of foetal waste products, and endocrine signalling to maintain pregnancy (Watson & Cross, 2005). The mature mouse placenta is formed around mid-gestation and contains two foetally-derived regions (the junctional zone and labyrinth) and the maternally-derived decidua (Georgiades, Ferguson-Smith, & Burton, 2002) (Figure 4.1). The junctional zone is separated from the maternal decidua by a layer of parietal trophoblast giant cells (TGCs) (Simmons, Fortier, & Cross, 2007). It is a major endocrine compartment containing two trophoblast-derived lineages: the spongiotrophoblast and glycogen cells (Coan, Conroy, Burton, & Ferguson-Smith, 2006). The spongiotrophoblast, glycogen cells, and TGCs express several placental lactogen hormones (Simmons, Rawn, Davies, Hughes, & Cross, 2008) that drive maternal physiological adaptations to sustain pregnancy (Bhattacharyya, Lin, & Linzer, 2002; Müller et al., 1999). Maternal-foetal exchange takes place in the labyrinth, which consists of foetal blood vessels surrounded by a trilaminar layer of trophoblast-derived cells comprising syncytiotrophoblast layers (I and II) and sinusoidal TGCs which are in contact with the maternal blood supply (John & Hemberger, 2012). Three additional trophoblast-derived cells line the maternal vasculature in the mouse placenta: spiral artery TGCs (in the maternal decidua), canal TGCs (in the junctional zone), and channel TGCs (beneath the decidua, the exit point of maternal blood) (Gasperowicz, Surmann-Schmitt, Hamada, Otto, & Cross, 2013; Rai & Cross, 2014).

Although there are differences in the morphology and timing of development between the mouse and human placenta, there is considerable homology between the function of the different placental lineages and the molecular mechanisms underpinning their development (Cox et al., 2009; Georgiades et al., 2002). Consequently, the mouse is a widely accepted model system for studying the placenta. Several studies in transgenic mice have shown that genetic manipulations that cause a reduction in the size and/or changes in the cellular composition of the junctional zone or labyrinth are associated with intrauterine growth restriction (IUGR) (Woods, Perez-Garcia, & Hemberger, 2018). IUGR is a risk factor for neurodevelopmental disorders, including schizophrenia (Nielsen et al., 2013). *Setd1a* haploinsufficiency has been reported to

cause decreased fat mass with no effect on overall body weight by the International Mouse Phenotyping Consortium (IMPC). However, it is important to note that body weight measurements were not recorded at birth and were averaged across postnatal development from 3-8 weeks, which may mask IUGR and potential catch-up growth effects.

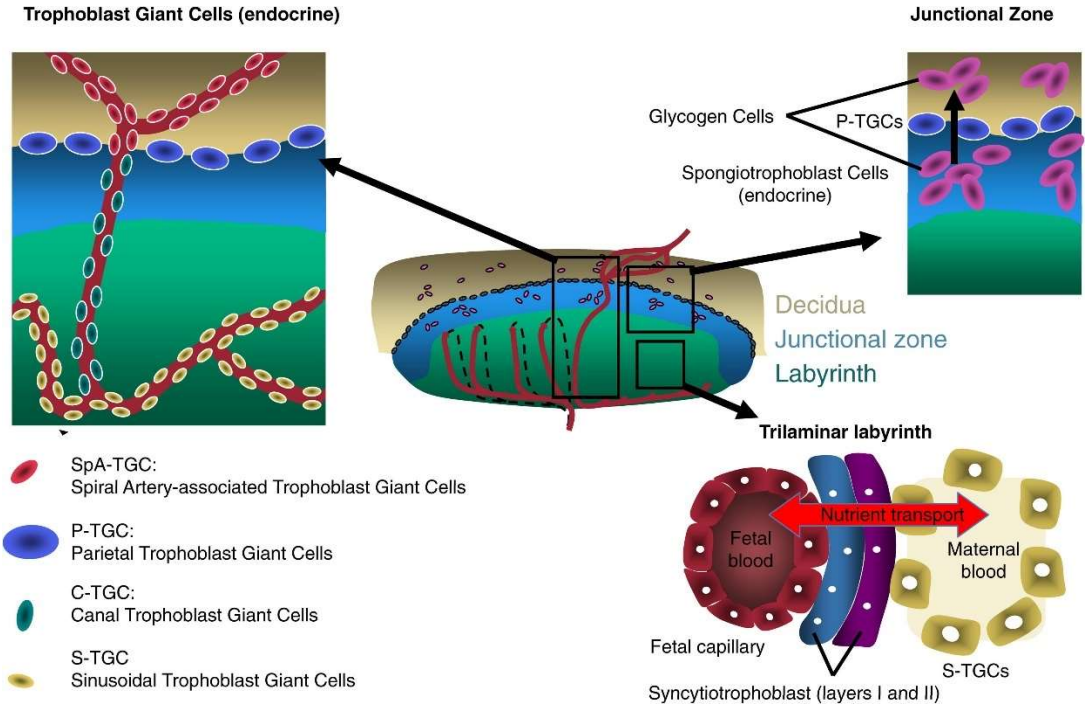


**Figure 4.1. Compartments and cell types in the mouse placenta.** Taken from John and Hemberger (2012).

The placenta has also been suggested to be an essential locus for the action of imprinted genes (John, 2017). Imprinted genes are expressed from one parental allele only as a result of epigenetic marks laid down during gametogenesis (Surani, 1998). The parental conflict hypothesis posits that imprinted genes evolved as a result of viviparity in mammals and the coincident conflict between the maternal and paternal genomes (Moore & Haig, 1991). Imprinted genes are highly expressed in the placenta and are involved in regulating placental endocrine lineages in a manner consistent with the conflict hypothesis (John, 2017). Specifically, maternally-expressed genes (e.g., *Phlda2*) restrict the development of endocrine lineages (Tunster, Creeth, & John, 2016), whereas paternally expressed genes (e.g., *Peg3* and *Igf2*) promote endocrine lineage expansion (Esquiliano, Guo, Liang, Dikkes, & Lopez, 2009; Tunster, Boqué-Sastre, et al., 2018). Interestingly, placental-specific knockout of *Igf2* is sufficient to cause IUGR and neurobehavioural changes in adulthood (Mikaelsson, Constância, Dent, Wilkinson, & Humby, 2013), implicating

perturbations to the balance between placental supply and foetal demand in prenatal programming.

H3K4 methylation has been postulated to influence both the establishment and maintenance of the epigenetic marks that are responsible for monoallelic imprinted gene expression (Kelsey & Feil, 2013; Sanli & Feil, 2015). Imprint acquisition occurs in the germline and involves the addition of DNA methylation at imprinting control regions (ICRs), leading to parent-of-origin specific differentially methylated regions (DMRs) (Barlow, 2011). This is dependent upon the action of the *de novo* DNA methyltransferase *DNMT3A* and its accessory protein *DNMT3L* (Bourc'his, Xu, Lin, Bollman, & Bestor, 2001; Hata, Okano, Lei, & Li, 2002). H3K4 methylation at ICRs prevents the DNMT3A/DNMT3L complex from binding to its target sequence (Henckel, Chebli, Kota, Arnaud, & Feil, 2012; Jia, Jurkowska, Zhang, Jeltsch, & Cheng, 2007; Ooi et al., 2007). Moreover, removal of H3K4 methylation by *KDM1B* is required for imprint acquisition in oocytes (Ciccone et al., 2009).

Following imprint acquisition, DMRs at ICRs are maintained by *DNMT1* during preimplantation development (Hirasawa et al., 2008), despite widespread demethylation in the genome of the developing zygote (Reik, Dean, & Walter, 2001). *DNMT1* is also required for correct expression of imprinted genes in the embryo (Li, Beard, & Jaenisch, 1993) but is not involved in monoallelic expression of some imprinted genes in the placenta (Caspary, Cleary, Baker, Guan, & Tilghman, 1998; Lewis et al., 2004; Umlauf et al., 2004). Instead, imprint maintenance of these genes appears to involve histone modifications. Whether this extends to all imprinted genes in the placenta is unclear at present. Nevertheless, H3K4 dimethylation has been demonstrated to mark maternally-expressed genes in imprinting centre 2 (Lewis et al., 2004; Umlauf et al., 2004). Since *Setd1a* encodes a H3K4 methyltransferase subunit (Shilatifard, 2012), it is possible that it could influence placental function indirectly by affecting imprinted gene expression, either due to aberrant H3K4 methylation during imprint establishment or imprint maintenance.

The aim of this chapter was to conduct preliminary investigations into the role of *Setd1a* in the placenta. This was assessed by measuring placental weights, an indicator of placental efficiency (Fowden, Sferruzzi-Perri, Coan, Constancia, & Burton, 2009), and gene expression of placental lineage markers and three imprinted genes known to regulate placental endocrine function. Associated effects of placental changes on foetal and postnatal growth were also examined.

## 4.2. Methods

### *4.2.1. Timed-matings, dissections, and assessment of embryonic and placental weights*

Timed-matings were conducted as described in Chapter 2.4.1. Placental and foetal wet weights were recorded at E13.5 for 5 litters (N = 46; Table 4.1). A foetal:placental weight ratio was calculated by dividing foetal wet weight by placental wet weight. Whole placentas and a foetal tissue biopsy were snap frozen using dry ice and stored at -80 °C until required. Genotyping was conducted using DNA extracted from the tissue biopsy to identify *Setd1a*$^{+/-}$ mice (Chapter 2.2.2) and determine embryonic sex (Chapter 2.2.3).

**Table 4.1.** Sample characteristics for assessment of placental and foetal weights.

| | **KO** | **WT** | **Total** |
|---|---|---|---|
| Male | 11 | 13 | 24 |
| Female | 8 | 14 | 22 |
| **Total** | **19** | **27** | **46** |

### *4.2.2. Placental gene expression RT-qPCR*

RNA was extracted from placentas (N = 16, balanced for sex and genotype) and assessed for purity and concentration as described in Chapter 2.4.2. cDNA synthesis was performed as described in Chapter 2.4.3, diluted 1:100 in nuclease-free water and stored at -20 °C until required.

Intron-spanning primers (annealing temperature = 60 °C) were designed for markers of the spongiotrophoblast (*Prl8a8* and *Prl3b1*), glycogen cells (*Prl7b1* and *Pcdh12*), TGCs (*Prl2c* and *Ctsq*), labyrinth zone (*Flk1* and *Dlx3*), syncytiotrophoblast-I (*Syna*) and syncytiotrophoblast-II (*Synb* and *Gcm1*), 3 imprinted genes (*Phlda2, Peg3, and Igf2*), and two housekeeping genes (*β-Actin* and *Gapdh*; Table 4.2). Samples were run in triplicate on two separate runs and data were averaged across both runs. A nuclease-free water no-template control was included on each run. The contents of each 9.5 µL reaction comprised 2 uL cDNA and 7.5 µL RT-qPCR mastermix (Table 4.3). Reactions were performed using a Quantstudio 5 PCR Machine with the following cycling conditions; i) 95 °C for 3 minutes, ii) 95 °C for 20 seconds, iii) 60 °C for 20 seconds, iv) 72 °C for 20 seconds, v) 75 °C for 20 seconds, vi) repeat ii-v 34 times. Ct values were calculated using an Rn threshold of 1.5 x $10^4$ for all reactions.

Data were prepared for analysis using the $2^{-\Delta\Delta CT}$ method (Chapter 2.4.4) and statistical analysis was performed on ΔCt values for each gene.

**Table 4.2.** Primer sequences and product sizes for RT-qPCR of placental gene expression.

| Primer target | Forward primer | Reverse primer | Product size (bp) |
|---|---|---|---|
| *Prl8a8* | CCTGCATGTATGGCAGAAAA | CCCTTATTTGGGGGATTTGT | 244 |
| *Prl3b1* | AGCAGCCTTCTGGTGTTGTC | TGTGACACCACAATCACACG | 197 |
| *Prl7b1* | CAGCACATCAATAGCCTTGC | TTGGTGATTTGAGTGGCAAA | 162 |
| *Pcdh12* | ACTCTCCTCCTGTCCAGCAA | CTGCTCTCAGCTGCCTTCTT | 173 |
| *Prl2c* | TCCAGAAAACAAGGAACAAGC | TGTCTGTGGCTTTGGAGATG | 161 |
| *Ctsq* | TGGAAACGTGCACTTGGTAG | GTGGGATCAGTTTGCCTGTT | 196 |
| *Flk1* | GGCGGTGGTGACAGTATCTT | GTCACTGACAGAGGCGATGA | 183 |
| *Dlx3* | CGTTTCCAGAAAGCCCAGTA | ACTGTTGTTGGGGCTGTGTT | 169 |
| *Syna* | CAGGGACACAAAGACCCCTA | ACCAGAGGAGTTGAGGCAGA | 180 |
| *Synb* | CTGGCACTTCATTCCCATTT | TGGCTGTAGGCTCTCAGGTT | 163 |
| *Gcm1* | AGCCTGTGTTGAGCAGACCT | TGTCGTCCGAGCTGTAGATG | 173 |
| *Phlda2* | TCAGCGCTCTGAGTCTGAAA | CAGCAAGCACGGGAATATCT | 188 |
| *Peg3* | AAAACTCACCACTCCGTTGG | GTCTCGAGGCTCCACATCTC | 190 |
| *Igf2* | GTCGATGTTGGTGCTTCTCA | AAGCAGCACTCTTCCACGAT | 195 |
| *β-Actin* | CCTGTATGCCTCTGGTCGTA | CCATCTCCTGCTCGAAGTCT | 260 |
| *Gapdh* | CACAGTCAAGGCCGAGAATG | TCTCGTGGTTCACACCCATC | 242 |

**Table 4.3.** Placental gene expression RT-qPCR reaction mix.

| Reagent | Amount (µL) |
|---|---|
| Nuclease-free water | 6.25 |
| Buffer | 1.0 |
| dNTPs | 0.2 |
| Primer mix (25 µM forward and reverse) | 0.4 |
| DreamTaq™ Hot Start DNA polymerase (ThermoFisher, UK) | 0.065 |
| DyNAmo HS SYBR Green (ThermoFisher, UK) | 0.08 |

### *4.2.3. Postnatal growth*

Animals (N = 84; Table 4.4) were weighed at maternal separation (P28) and then every seventh day thereafter until P70. A subsample of these animals was used for the initial behavioural characterisation (Chapter 5). Thus, growth curves were assessed after maternal separation to eliminate potential effects of early-life stress induced by repeated handling on behaviour in adulthood.

**Table 4.4.** Sample characteristics for assessment of postnatal growth curves.

| | KO | WT | Total |
|---|---|---|---|
| Male | 18 | 23 | 41 |
| Female | 18 | 25 | 43 |
| **Total** | **36** | **48** | **84** |

*4.2.4. Data analysis*

All data were analysed using a 2 x 2 between-subjects ANOVA with sex (male and female) and genotype (WT and KO), followed by Bonferroni-corrected post-hoc tests. One male KO was removed from the RT-qPCR experiment due to no signal being detected for all genes tested. The additional within-subjects factor age (7 levels) was included for analysis of postnatal weight data.

## 4.3. Results

*4.3.1. E13.5 foetal and placental weight*

Foetal weight of *Setd1a*$^{+/-}$ mice at E13.5 was not significantly different from WT ($F$(1, 42) = 0.42, $p$ = .84; Figure 4.2A). There was no significant effect of sex ($F$(1, 42) = 1.93, $p$ = .17) or interaction between sex and genotype ($F$(1, 42) = 1.57, $p$ = .22). Placental weights of *Setd1a*$^{+/-}$ mice were on average 8.9 % lighter than WTs ($F$(1, 42) = 8.36, $p$ = .006; Figure 4.2B). In addition, placenta of male mice were significantly heavier than females ($F$(1, 42) = 4.46, $p$ = .04) but there was no significant interaction between genotype and sex ($F$(1, 42) = 0.68, $p$ = .41). There was no significant effect of genotype ($F$(1, 42) = 2.80, $p$ = .10; Figure 4.2C) or sex $F$(1, 42) = 0.82, $p$ = .78) and no significant genotype x sex interaction ($F$(1, 42) = 0.21, $p$ = .65) for foetal:placental ratio.

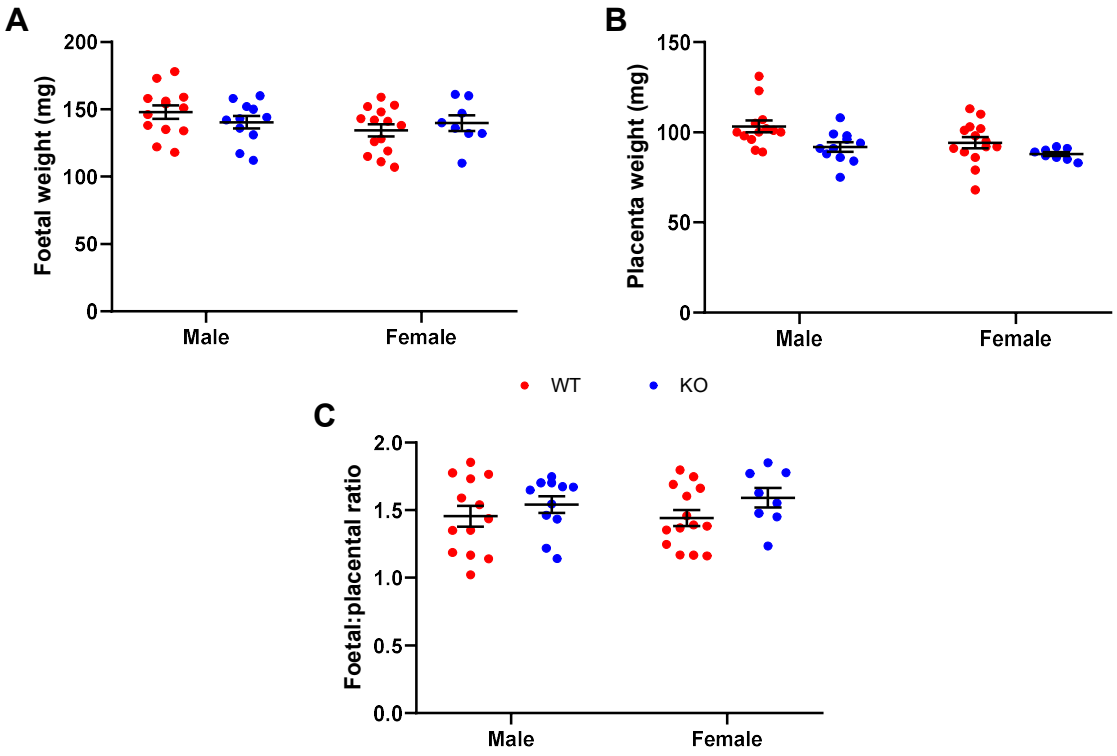


**Figure 4.2. Effects of *Setd1a* haploinsufficiency on placental and foetal weights at E13.5.** Mean (+/- SEM) **A)** foetal weight, **B)** placental weight, and **C)** foetal:placental ratio, presented separately for males and females.

*4.3.2. Placental gene expression*

Effects of *Setd1a* haploinsufficiency on placental gene expression are summarised in Table 4.5. Analysis of the placental lineage markers (Figure 4.3A) revealed that the spongiotrophoblast marker *Prl8a8* was significantly down-regulated in placenta of *Setd1a*$^{+/-}$ males ($p$ = .01) but not females ($p$ = .30). In addition, expression of the TGC marker *Ctsq* was also down-regulated in placenta of *Setd1a*$^{+/-}$ males ($p$ = .01) but not females ($p$ = .72). No other placental lineage markers were differentially expressed in placentas of *Setd1a*$^{+/-}$ mice (all $p \geq .14$). Analysis of the imprinted genes (Figure 4.3B) revealed that *Peg3* expression was significantly reduced in male *Setd1a*$^{+/-}$ placenta ($p$ = .02) but not in females ($p$ = .48). There was no significant change in expression of *Phlda2* ($p$ = .09) or *Igf2* ($p$ = .18).

**Table 4.5.** Results of statistical analysis of RT-qPCR assessing effects of *Setd1a* haploinsufficiency on placental gene expression.

| Marker | Gene | Main effect genotype | Main effect sex | Genotype x sex |
|---|---|---|---|---|
| Spongiotrophoblast | *Prl8a8* | $F(1,11) = 2.12$, $p = .17$ | $F(1,11) = 4.62$, $p = .06$ | $F(1,11) = 8.57$, $\mathbf{p = .01}$ |
| | *Prl3b1* | $F(1,11) = 0.03$, $p = .87$ | $F(1,11) = 0.06$, $p = .81$ | $F(1,11) = 2.48$, $p = .14$ |
| Glycogen cells | *Prl7b1* | $F(1,11) = 0.003$, $p = .95$ | $F(1,11) = 2.53$, $p = .14$ | $F(1,11) = 0.52$, $p = .49$ |
| | *Pcdh12* | $F(1,11) = 0.04$, $p = .84$ | $F(1,11) = 2.51$, $p = .14$ | $F(1,11) = 0.54$, $p = .48$ |
| TGCs | *Prl2c* | $F(1,11) = 0.15$, $p = .71$ | $F(1,11) = 1.08$, $p = .32$ | $F(1,11) = 1.56$, $p = .24$ |
| | *Ctsq* | $F(1,11) = 6.46$, $\mathbf{p = .03}$ | $F(1,11) = 0.89$, $p = .37$ | $F(1,11) = 4.20$, $p = .07$ |
| Labyrinth | *Flk1* | $F(1,11) = 1.34$, $p = .27$ | $F(1,11) = 0.06$, $p = .82$ | $F(1,11) = 0.31$, $p = .59$ |
| | *Dlx3* | $F(1,11) = 0.36$, $p = .56$ | $F(1,11) = 0.001$, $p = .98$ | $F(1,11) = 0.03$, $p = .87$ |
| Syncytiotrophoblast-I | *Syna* | $F(1,11) = 1.04$, $p = .33$ | $F(1,11) = 0.19$, $p = .68$ | $F(1,11) = 0.22$, $p = .65$ |
| Syncytiotrophoblast-II | *Synb* | $F(1,11) = 0.46$, $p = .51$ | $F(1,11) = 0.69$, $p = .42$ | $F(1,11) = 0.42$, $p = .53$ |
| | *Gcm1* | $F(1,11) = 0.68$, $p = .43$ | $F(1,11) = 0.001$, $p = .97$ | $F(1,11) = 0.26$, $p = .62$ |
| Imprinted genes | *Phlda2* | $F(1,11) = 3.38$, $p = .09$ | $F(1,11) = 2.39$, $p = .15$ | $F(1,11) = 0.87$, $p = .37$ |
| | *Peg3* | $F(1,11) = 6.19$, $\mathbf{p = .03}$ | $F(1,11) = 1.16$, $p = .31$ | $F(1,11) = 2.20$, $p = .17$ |
| | *Igf2* | $F(1,11) = 2.01$, $p = .18$ | $F(1,11) = 1.01$, $p = .34$ | $F(1,11) = 0.80$, $p = .39$ |

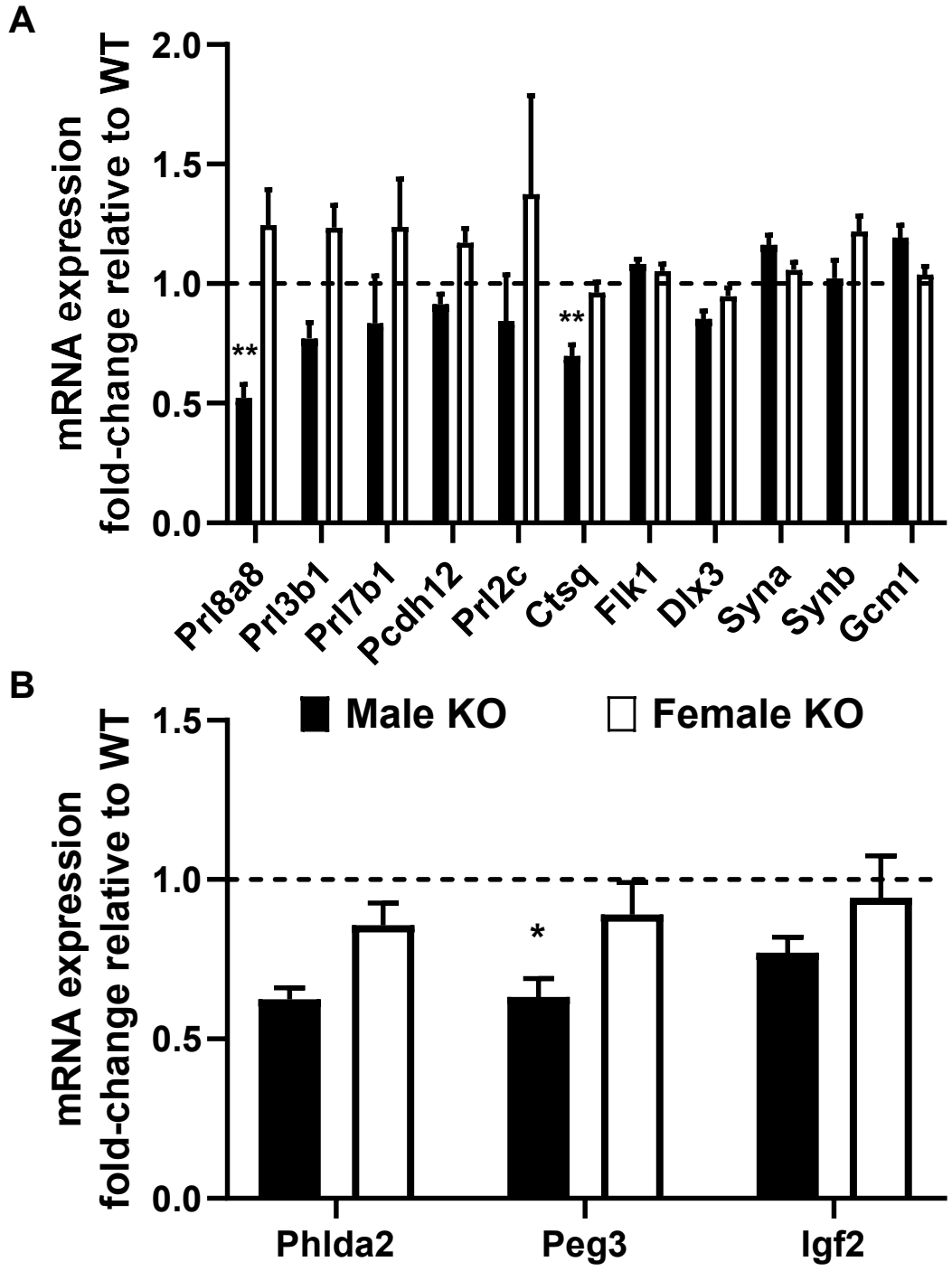


**Figure 4.3. Effects of *Setd1a* haploinsufficiency on placental gene expression.** Mean (+/- SEM) fold-change expression (calculated separately for males and females) relative to WT for **A)** placental lineage markers and **B)** imprinted genes. Dotted line represents WT expression levels; ** $p < .01$; * $p < .05$.

*4.3.3. General viability*

The median litter size across 18 litters was 7 (SD = 3.0). Genotype distributions did not deviate from Mendelian ratios ($X^2(1, N = 84) = 1.71$, $p > .05$), suggesting that *Setd1a* haploinsufficiency did not cause embryonic lethality. All animals appeared in good general health and low pre-weaning mortality was observed (2.3 %).

*4.3.4. Postnatal growth curves*

Assessment of body weight from the point at which pups were separated from dams (P28) until P70 revealed that overall, there was no significant effect of genotype ($F(1, 80) = 1.71$, $p = .20$). However, a significant interaction was observed between age and sex ($F(2.26, 180.93) = 63.79$, $p < .001$) and age and genotype ($F(2.26, 180.93) = 11.43$, $p < .001$). Post-hoc tests revealed that male *Setd1a*$^{+/-}$ mice were significantly lighter than their WT littermates at maternal separation (P28; $p = .005$, Figure 4.4A) and this effect was sustained one week later at P35 ($p < .001$). By P42, male *Setd1a*$^{+/-}$ and WT mice were of equivalent body weight ($p = .06$), indicating that catch-up growth had occurred. By contrast, in females, no significant effect of genotype was observed at any of the timepoints tested (all $p \geq .20$; Figure 4.4B). Similar findings were observed when analysing the percentage increase in body weight from P28 (Table 4.6). Specifically, body weights of *Setd1a*$^{+/-}$ male (but not female) increased by significantly more than their WT littermates from P42 onwards, the age at which there was no longer a genotype effect on body weight.

**Table 4.6.** Mean (SD) percentage increase in body weight from P28 at P35-P70 in *Setd1a*$^{+/-}$ and WT mice and Bonferroni corrected *p* values for effects of genotype, presented separately for males and females.

| | **Male** | | | **Female** | | |
|---|---|---|---|---|---|---|
| **Age** | **WT** | **KO** | ***p*** | **WT** | **KO** | ***p*** |
| Body weight change at P35 (%) | 35.9 (10.0) | 44.3 (11.6) | .21 | 31.8 (9.3) | 33.0 (9.9) | .69 |
| Body weight change at P42 (%) | 51.4 (12.2) | 66.9 (21.7) | **.005** | 41.1 (17.2) | 48.8 (16.9) | .15 |
| Body weight change at P49 (%) | 62.2 (14.4) | 82.1 (25.5) | **.002** | 48.9 (17.9) | 58.6 (20.0) | .11 |
| Body weight change at P56 (%) | 67.8 (16.1) | 89.7 (26.9) | **.001** | 50.7 (17.5) | 62.7 (21.2) | .06 |
| Body weight change at P63 (%) | 71.0 (16.4) | 94.4 (31.0) | **.001** | 56.0 (19.5) | 67.0 (23.0) | .12 |
| Body weight change at P70 (%) | 76.4 (17.4) | 101.3 (30.7) | **.001** | 61.0 (19.4) | 72.0 (24.2) | .12 |

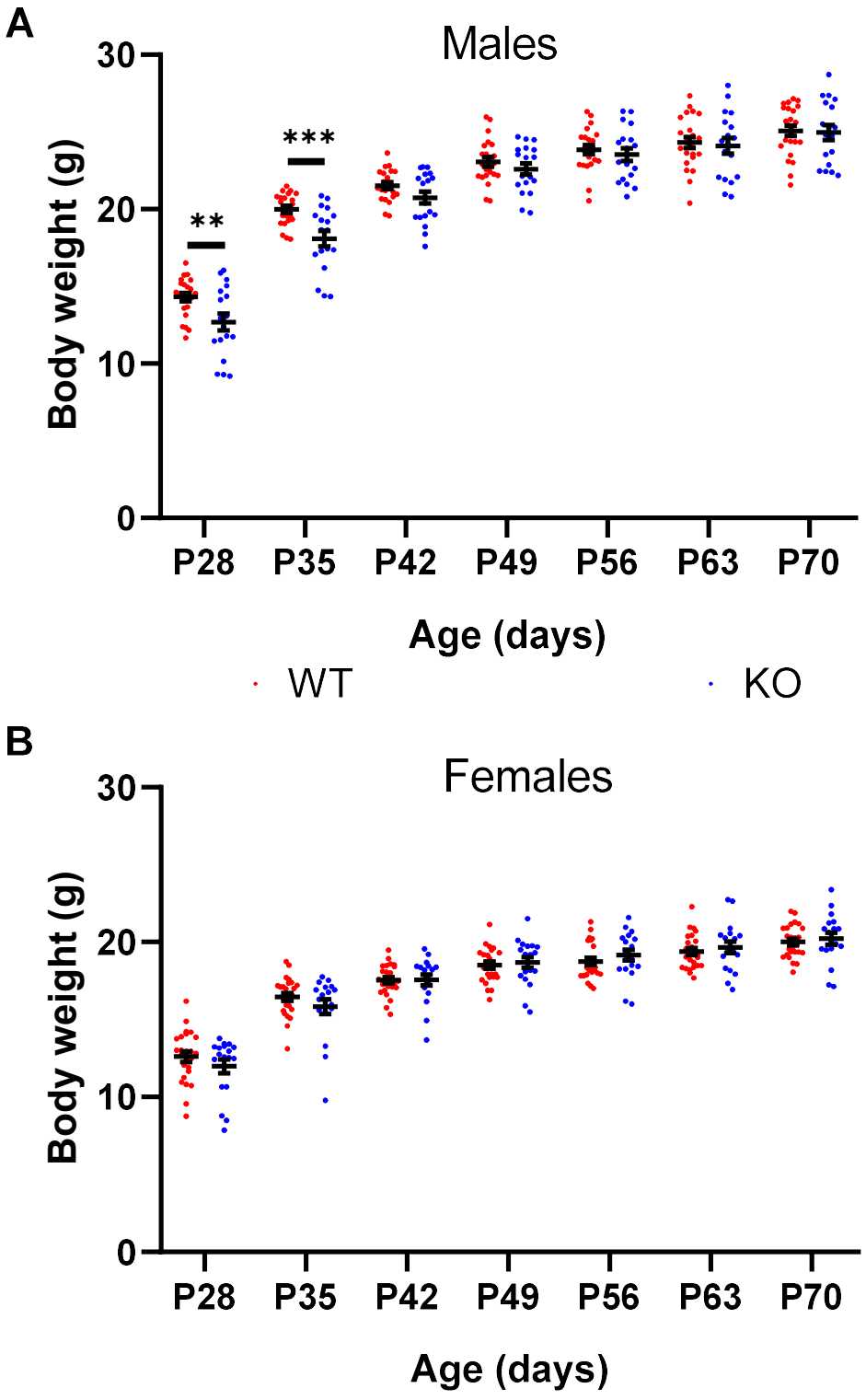


**Figure 4.4. Effect of *Setd1a* haploinsufficiency on postnatal growth curves.** Mean (+/- SEM) body weight of *Setd1a*$^{+/-}$ mice and their WT littermates measured at maternal separation (P28) and every 7 days thereafter until P70 in **A)** males and **B)** females; *** $p < .001$, ** $p < .01$.

### 4.4. Discussion

This chapter investigated the effects of *Setd1a* haploinsufficiency on measures of placental function and foetal and postnatal growth. Findings revealed that placental weight was reduced in *Setd1a*$^{+/-}$ embryos from WT dams. This was accompanied by sexually dimorphic changes in placental gene expression, with males showing reduced expression of two placental lineage markers (*Prl8a8* and *Ctsq*) and imprinted genes known to play a role in regulating placental endocrine lineages (although only *Peg3* was statistically significant). No differences were observed in foetal weight at E13.5. However, sexually dimorphic effects of *Setd1a* loss of function on postnatal growth were observed, with a reduction in body weight at P28 followed by catch-up growth by P42 in males but not females.

The present findings provide initial evidence for a role for *Setd1a* in the placenta. The weight of placentas from *Setd1a*$^{+/-}$ mice were 8.9 % lighter than placenta from WTs. A similar magnitude of reduction has been reported following prenatal nutritional challenges that have functional consequences for placental efficiency (Sferruzzi-Perri & Camm, 2016). However, foetal:placenta ratio was not significantly affected, possibly suggesting that *Setd1a* haploinsufficiency exerts subtle effects on placental function. Future work should examine the effects of *Setd1a* haploinsufficiency on placental function (e.g., placental transport and endocrine signalling) to elucidate potential placental programming mechanisms that could influence prenatal brain development.

Examination of placental gene expression revealed that foetal sex modulated the effects of *Setd1a* loss of function. Specifically, reduced expression of *Prl8a8* was observed in male *Setd1a*$^{+/-}$ placenta. This placental lactogen hormone is exclusively expressed in the spongiotrophoblast (Simmons et al., 2008), which may suggest a reduced contribution of this lineage. Consistent with this, expression of the spongiotrophoblast marker *Prl3b1* was also reduced, albeit non-significantly. The TGC marker *Ctsq* was downregulated in male *Setd1a*$^{+/-}$ placenta but there was no effect on *Prl2c* expression. *Prl2c* is ubiquitously expressed in all TGC subtypes (Simmons et al., 2008), whereas *Ctsq* is exclusively expressed in sinusoidal and channel TGCs (Gasperowicz et al., 2013; Simmons et al., 2007). This may indicate a relatively specific reduction of these TGC subtypes in male *Setd1a*$^{+/-}$ placenta. These findings should be confirmed histologically to rule out the possibility that these effects are due to changes in gene expression in the absence of morphological changes.

Placental expression of the imprinted gene *Peg3* was also down-regulated in male, but not female, *Setd1a*$^{+/-}$ mice. Loss of *Peg3* has been shown to result in a smaller spongiotrophoblast and reduced expression of spongiotrophoblast-expressed placental hormones (Tunster et al., 2018). This raises the possibility that the effects of *Setd1a* could be mediated through reduced *Peg3* expression. However, *Ctsq* is not affected by *Peg3* KO (Tunster et al., 2018), potentially suggesting a direct effect of *Setd1a* on placental function. However, reduced *Ctsq* expression could also be mediated by effects on imprinted genes not tested in the current experiment. For example, loss of imprinting centre 2 has been shown to cause a 50 % reduction in *Ctsq* expression (Tunster, Van de Pette, Creeth, Lefebvre, & John, 2018).

Interestingly, two other imprinted genes (*Phlda2* and *Igf2*) were also downregulated in male placenta but did not reach criteria for significance. This may suggest that *Setd1a* haploinsufficiency causes a general dysregulation of imprinting in male placenta. Further work is needed to investigate the effect of *Setd1a* loss of function on a wider repertoire of imprinted genes. More generally, the role of H3K4 methylation in mediating the correct expression of imprinted genes in the placenta is not well understood. Bidirectional interactions have been described between histone methylation and DNA methylation (Cedar & Bergman, 2009), making it unclear whether H3K4 methylation on the expressed allele plays a causal role in facilitating mono-allelic expression or is simply a marker of gene expression. Therefore, the mechanism underlying the effects of *Setd1a* loss of function on placental imprinted gene expression should be investigated in more detail.

While there was no difference in foetal weight at E13.5, the sexually dimorphic effects on placental gene expression were mirrored by male-specific reduced body weight in *Setd1a*$^{+/-}$ mice between P28-P42. The lack of effect on foetal weight was surprising given evidence that a smaller spongiotrophoblast is linked with IUGR (Woods et al., 2018). In addition, loss of *Ctsq* has also been linked with IUGR (Outhwaite, McGuire, & Simmons, 2015), an effect that is thought to be due to loss of placental hormones expressed in sinusoidal-TGCs (Simmons et al., 2008). It is possible that the effects of *Setd1a* loss of function on body weight emerge later in prenatal development as the effects of placental insufficiency accumulate, leading to low birth weight. Indeed, similar findings have been reported for *Igf2* and *Peg3*, with reduced placental weight at around mid-gestation but no effect on foetal weight until later in gestation (Constância et al., 2002; Li et al., 1999; Tunster et al., 2018). An alternative explanation is that these effects arise postnatally in the pre-weaning period. This could occur as a consequence of foetal programming via the placenta, direct effects

on pup development, or abnormal interactions with the mother (e.g., by affecting pup ultrasonic vocalisations, which is known to influence maternal behaviour (Hashimoto, Saito, Furudate, & Takahashi, 2001)).

The sexually dimorphic effects of *Setd1a* loss of function on placental gene expression and postnatal growth described in this chapter suggest that compensatory mechanisms in female placenta may be able to buffer the effects of *Setd1a* haploinsufficiency. This is consistent with several previous studies showing that increased susceptibility of males to prenatal insults is associated with sex-specific changes in placental function (Clifton, 2010; Kalisch-Smith, Simmons, Dickinson, & Moritz, 2017; Rosenfeld, 2015). Sex differences are also reported for schizophrenia liability, with higher incidence rates (Aleman, Kahn, & Selten, 2003; McGrath et al., 2008), earlier onset (Ochoa, Usall, Cobo, Labad, & Kulkarni, 2012), and poorer prognosis (Grossman, Harrow, Rosen, Faull, & Strauss, 2008) in males. Interestingly, common variants for schizophrenia that are differentially expressed in the placenta after early-life complications are also more highly expressed in male than female placenta (Ursini et al., 2018). It has been suggested that the male bias in liability for neurodevelopmental disorders may be due, in part, to sex differences in placental expression of X-linked genes involved in histone methylation (Singh, Singh, & Schneider, 2019). No data is currently available on whether sex affects the penetrance of *Setd1a* loss of function in humans (Singh et al., 2016). However, the results reported here highlight that sex modulates the effects of *Setd1a* haploinsufficiency in the placenta with potentially important consequences for understanding sex differences in pathogenesis.

In conclusion, this chapter provides evidence for sexually dimorphic effects of *Setd1a* loss of function on placental gene expression with concomitant effects on postnatal growth. Future work should investigate the effects of *Setd1a* haploinsufficiency on placental functioning to establish potential mechanisms that could contribute to abnormal prenatal brain development.

# Chapter 5: Behavioural consequences of *Setd1a* haploinsufficiency in a constitutive knockout mouse

## 5.1 Introduction

### *5.1.1. Aims*

The aim of this chapter was to conduct an extensive characterisation of behavioural phenotypes arising from *Setd1a* haploinsufficiency. The rationale for this work was two-fold. First, behavioural tests were chosen that assay several schizophrenia-relevant endophenotypes. Second, it was important to establish whether there were any potential confounding behavioural alterations (e.g., motoric problems) that needed to be considered when interpreting apparent cognitive phenotypes.

### *5.1.2. Anxiety*

It is well documented that the prevalence of anxiety symptoms is higher in patients with schizophrenia compared to the general population (Karpov et al., 2016). Indeed, many patients meet diagnostic criteria for a range of comorbid anxiety disorders, including obsessive compulsive disorder, social phobia, generalised anxiety disorder, panic disorder, and post-traumatic stress disorder (Achim et al., 2011; Braga, Reynolds, & Siris, 2013; Buckley, Miller, Lehrer, & Castle, 2009). Cross-sectional studies have shown that anxiety symptoms correlate with severity of hallucinations and delusions (Hartley, Barrowclough, & Haddock, 2013). This may suggest that the increased prevalence of anxiety disorders observed in schizophrenia is a consequence of distress associated with the positive symptoms of schizophrenia. Alternatively, elevated anxiety levels may be a marker of general liability to psychopathology. Indeed, anxiety symptoms precede schizophrenia diagnosis in up to 50 % of cases (Pokos & Castle, 2006). However, while several studies have shown that anxiety disorders are common in individuals at high clinical risk for schizophrenia, the presence of an anxiety disorder does not predict transition to schizophrenia (Addington et al., 2017; McAusland et al., 2017). Although the precise relationship between anxiety and schizophrenia is poorly understood, it is clear that anxiety is an important aspect of psychopathology.

The elevated-plus maze (EPM) and open field test (OFT) are widely used unconditioned behavioural tests for measuring anxiety-related behaviour in rodents (Belzung & Griebel, 2001). These tests rely on the conflict between a rodents' natural tendency to explore novel environments and an aversion to open, unprotected spaces (Sartori, Landgraf, & Singewald, 2011). Anxiety-related behaviour is

indexed/quantified by measuring the propensity to explore the aversive regions of the arena (i.e., the open arms of the EPM and the central region of the OFT), although additional 'ethobiological' measures can also be considered, such as defecation, stretch-attend postures, and head dips (Harro, 2018). The construct and predictive validity of these tests is based on evidence that anxiolytic drugs, confirmed as such in people, increase the amount of exploration of the aversive areas, whereas avoidance behaviour is induced upon administration of anxiogenic substances (Carobrez & Bertoglio, 2005; Cryan & Holmes, 2005; Prut & Belzung, 2003). There is some evidence that different tests measure distinct aspects of anxiety-related behaviour (Ramos, 2008), which highlights the importance of convergent findings from multiple tasks.

### *5.1.3. Locomotor activity*

Locomotor hyperactivity in rodent models of schizophrenia has been suggested to model 'positive-like' symptoms of the disorder (Jones, Watson, & Fone, 2011; Van Den Buuse, 2010). This is based on evidence that recapitulating the neurochemical changes observed in schizophrenia using *in vivo* model systems results in a hyperactive phenotype. The dopamine hypothesis of schizophrenia posits that elevated subcortical dopaminergic neurotransmission contributes to positive symptoms (Davis et al., 1991; Howes & Kapur, 2009). Evidence in rodents shows that basal activity levels are increased following administration of drugs that increase mesolimbic dopaminergic neurotransmission, such as cocaine (Uhl, Hall, & Sora, 2002) and amphetamine (Salahpour et al., 2008). Moreover, increased extracellular dopamine as a result of knockout of the dopamine transporter also leads to hyperactivity (Gainetdinov, Jones, & Caron, 1999; Zhuang et al., 2002).

Recent evidence suggests that hyperdopaminergic function may be downstream of the primary schizophrenia pathophysiology, with NMDA receptor hypofunction also being implicated (Grace, 2016; Howes, McCutcheon, & Stone, 2015). Administration of NMDA receptor antagonists, such as phencyclidine (PCP) (Mouri, Noda, Enomoto, & Nabeshima, 2007), ketamine (Chan, Chiu, Sou, & Chen, 2008; Wilson et al., 2007), and MK-801 (Irifune, Shimizu, Nomoto, & Fukuda, 1995; Nilsson, Carlsson, & Carlsson, 1997) also result in a hyperactive phenotype in rodents. Studies in humans have shown that sub-anaesthetic doses of these drugs induce psychotic-like symptoms in healthy controls (Krystal et al., 1994; Lahti et al., 2001). These findings support the proposition that locomotor hyperactivity can be used as an assay, operationally, of positive-like symptoms of schizophrenia in rodent models.

Another aspect of locomotor activity that can be assessed is habituation to a novel environment, whereby a decline in exploration occurs after prolonged exposure as the animal becomes familiar with the environment. Habituation is regarded as an elementary form of learning (Rankin et al., 2009) and is dependent on hippocampal function (Daenen, Van der Heyden, Kruse, Wolterink, & Van Ree, 2001; Daenen, Wolterink, Gerrits, & Van Ree, 2002). It can occur both within a session, as the animal learns about the environment, and between consecutive sessions, which relies on memory of the previous session (Leussis & Bolivar, 2006). Memory impairments are common in schizophrenia (Fioravanti, Bianchi, & Cinti, 2012) and many *Setd1a* loss of function carriers also present with learning disabilities (Singh et al., 2016). On this basis, habituation of locomotor activity was assessed during three test sessions to investigate basic learning impairments in *Setd1a*$^{+/-}$ mice.

*5.1.4. Motoric function abnormalities*

A wide variety of motor symptoms have been reported in schizophrenia patients, including catatonia, neurological soft signs (e.g., impaired motor coordination and sequencing), involuntary movements, and psychomotor slowing (Hirjak, Meyer-Lindenberg, Kubera, Thomann, & Wolf, 2018; Walther & Strik, 2012). Widespread pathology in the motor system has been observed in schizophrenia, implicating morphological and neurochemical alterations in primary and supplementary motor cortices, cerebellum, and basal ganglia (Abboud, Noronha, & Diwadkar, 2017). Motor symptoms are present in antipsychotic naïve patients (Cortese et al., 2005; Peralta, Campos, De Jalón, & Cuesta, 2010), individuals at high clinical risk for schizophrenia (Callaway, Perkins, Woods, Liu, & Addington, 2014; Kindler et al., 2016), and unaffected relatives (Chan, Xu, Heinrichs, Yu, & Gong, 2010). These findings suggest that motor abnormalities are not simply a side-effect of medication and likely form part of the core pathophysiology of schizophrenia.

The Rotarod performance test is the most widely used test for measuring motor system dysfunction in rodents (Brooks & Dunnett, 2009) and is sensitive to abnormalities arising from lesions to the cerebellum (Caston, Jones, & Stelz, 1995; Lalonde, Filali, Bensoula, & Lestienne, 1996) and nigrostriatal pathway (Heuer, Smith, Lelos, Lane, & Dunnett, 2012; Monville, Torres, & Dunnett, 2006). In this test, mice are placed on a rotating rod and must walk on the rod at the correct pace to maintain balance and avoid falling. The speed of rotation can either be fixed or accelerate over the trial. It is generally recommended that motor coordination be assessed at a range of fixed speeds to avoid confounding effects of fatigue that may

occur at longer latencies during accelerating trials (Monville et al., 2006). In addition, motor learning can be assessed by measuring the effect of repeated training on accelerating trials (Buitrago, Schulz, Dichgans, & Luft, 2004; Scholz, Niibori, Frankland, & Lerch, 2015).

*5.1.5. Sensorimotor gating*

Sensorimotor gating refers to the filtering and transmission of sensory information to the motor system and as such is often characterised as a form of low-level attentional functioning (Powell, Weber, & Geyer, 2012). In humans, sensorimotor gating is usually measured using electromyography to determine the degree to which a non-startling auditory prestimulus inhibits the magnitude of the eyeblink response elicited by a closely following, and louder, auditory stimulus (Braff, Grillon, & Geyer, 1992). Reduced prepulse inhibition (PPI) of the startle response has been reliably observed in schizophrenia patients (Swerdlow, Braff, & Geyer, 2016; Swerdlow et al., 2018; Swerdlow, Weber, Qu, Light, & Braff, 2008) and is also reported in prodromal schizophrenia (Quednow et al., 2008) and unaffected relatives (Cadenhead, Swerdlow, Shafer, Diaz, & Braff, 2000), though PPI deficits are relatively non-specific being found across multiple psychopathologies (Swerdlow et al., 2016). Consistent with its role in filtering out irrelevant stimuli, deficient PPI correlates with symptoms of thought disorder (Perry & Braff, 1994) and distractibility (Karper et al., 1996). PPI is a cross-species phenomena, making it a viable endophenotype for *in vivo* modelling of neuropsychiatric disorders (Powell, Zhou, & Geyer, 2009).

The neural circuitry of sensorimotor gating has been studied extensively in rodents (Swerdlow, Geyer, & Braff, 2001). The caudal pontine reticular nucleus plays a central role in mediating the acoustic startle response (ASR), receiving inputs from the primary auditory system and projecting to spinal motor neurons to generate a motor response (Koch, 1999). PPI of the ASR is mediated by a cortico-striato-pallido-thalamic circuit, which influences the startle response through projections from the ventral pallidum to the caudal pontine reticular nucleus via the pedunculopontine nucleus (Swerdlow et al., 2016). Forebrain structures that project to the nucleus accumbens, such as the prefrontal cortex, hippocampus, and basolateral amygdala, are involved in regulating the properties of PPI (Swerdlow et al., 2001). Pharmacological studies have shown that PPI deficits can be induced in rodents using dopaminergic or 5-HT2 receptor agonists and NMDA receptor antagonists (Geyer, Krebs-Thomson, Braff, & Swerdlow, 2001), consistent, arguably, with neurochemical abnormalities in schizophrenia.

### *5.1.6. Learning and memory*

Cognitive impairments are a core aspect of schizophrenia psychopathology impacting on several domains of memory function (Fatouros-Bergman, Cervenka, Flyckt, Edman, & Farde, 2014; Fioravanti et al., 2012), particularly episodic memory (Schaefer, Giangrande, Weinberger, & Dickinson, 2013). *Setd1a* LoF is associated with learning difficulties in patients with schizophrenia and developmental delay in children with a range of neurodevelopmental disorders (Singh et al., 2016). *Setd1a* (*KMT2F*) is one of a family of KMT2 genes involved in H3K4 methylation (Shilatifard, 2012). Knockout of *KMT2A* (Gupta et al., 2010; Kerimoglu et al., 2017) and *KMT2B* (Kerimoglu et al., 2013; Kerimoglu et al., 2017) are both associated with memory impairments, suggesting an important role for H3K4 methylation in memory formation. Consistent with this, *KMT2A* and *KMT2B* are involved in regulating the breadth of H3K4 trimethylation at learning-associated genes in the CA1 region of the hippocampus, leading to increased expression during memory formation (Collins et al., 2019). Moreover, *KMT2A* is essential for increased H3K4 trimethylation in the hippocampus and anterior cingulate cortex following memory reactivation (Webb et al., 2017), suggesting a role for H3K4 methylation in memory retrieval. These findings suggest that *Setd1a* haploinsufficiency might lead to similar learning and memory deficits by disrupting H3K4 methylation.

The novel object recognition (NOR) memory test is the most widely used test of declarative memory in rodents (Grayson et al., 2015; Leger et al., 2013). In this task, rodents are exposed to two identical objects during encoding. Recognition memory is tested after a retention interval by replacing one of the objects with a novel object and measuring the amount of time spent exploring each of the objects. Intact recognition memory is indicated by increased exploration of the novel object relative to the familiar object. Performance on this task relies on hippocampal (Clark, Zola, & Squire, 2000) and perirhinal cortex (Aggleton, Albasser, Aggleton, Poirier, & Pearce, 2010) function. One advantage of this test is that it is a one-trial test of memory performance that does not require extensive training, avoiding potential confounds of differential sensitivity to positive or negative reinforcement (Antunes & Biala, 2012). It is also possible to manipulate the interval between encoding and test in order to assay memory retention at short and long delays.

### *5.1.7. Summary*

In this chapter, constitutive *Setd1a*$^{+/-}$ knockout mice and their wild type littermates were subjected to an extensive behavioural characterisation to examine

schizophrenia-relevant phenotypes; anxiety-related behaviour, locomotor activity, motor coordination, sensorimotor gating, and NOR memory.

## 5.2. Methods

### *5.2.1. Behavioural testing*

77 adult mice (39 male and 38 female) were included in behavioural experiments (Table 5.1). Behavioural testing started when animals were 8 weeks old and was conducted as described in Chapter 2.3. All mice completed the experiments in the following order: EPM, OFT, locomotor activity, sensorimotor gating, rotarod test, and NOR.

**Table 5.1.** Genotype and sex information for *Setd1a*$^{+/-}$ mice included in behavioural experiments.

| | **KO** | **WT** | **Total** |
|---|---|---|---|
| Male | 18 | 21 | 39 |
| Female | 18 | 20 | 38 |
| **Total** | **36** | **41** | **77** |

### *5.2.2. Data analysis*

Multivariate ANOVAs were used to analyse data from the EPM and OFT. The four dependent variables included in each analysis were: distance moved, proportion of time spent in anxiogenic regions, latency of first entry into anxiogenic regions (log transformed to remove positive skew), and number of entries into anxiogenic regions.

Locomotor activity data were analysed by a mixed ANOVA with day (3 levels) and quartile (4 levels) as within-subjects factors and genotype and sex as between-subjects factors. Greenhouse-Geisser corrected results are reported due to violations of sphericity, indicated by a significant Mauchly's test.

Weight-adjusted ASR data were analysed using a mixed ANOVA with pulse amplitude (80 dB, 90 dB, 100 dB, 110 dB, and 120 dB) as a within-subjects factor and genotype and sex as between-subjects factors. PPI data were analysed using a mixed ANOVA with prepulse amplitude (4 dB, 8 dB, and 16 dB) as a within-subjects factor and genotype and sex as between-subjects factors. Greenhouse-Geisser corrected results are reported where violations of sphericity occurred. Bonferroni corrected post-hoc tests were used to compare the effect of genotype on PPI at the different prepulse intensities, separately.

To assess motor learning in the rotarod performance test, the latency to fall data from the five accelerating runs were analysed by mixed ANOVA with run (5 levels) as a within-subjects factor and genotype and sex as between-subjects factors. Motor coordination was assessed by calculating the average latency to fall at each fixed speed for each mouse. These data were analysed using a mixed ANOVA with speed (10 levels) as a within-subjects factor and genotype and sex as between-subjects factors. Greenhouse-Geisser corrected results are reported due to violations of sphericity.

NOR performance was assessed by calculating a discrimination ratio as the proportion of time the animal spent exploring the novel object relative to total time spent exploring either object (sum of novel and familiar). Data from one male WT mouse was missing due to a technical issue during the test session. Data were analysed using a mixed ANOVA with delay (30 minutes vs. 24 hours) as a within-subjects factor and genotype and sex as between-subjects factors.

## 5.3 Results

### *5.3.1. Elevated plus maze*

MANOVA revealed a significant multivariate effect of genotype on indices of anxiety-related behaviour in the EPM ($F(4, 70) = 2.52$, $p = .049$; Wilk's $\lambda = 0.87$). Follow-up analysis revealed a non-significant trend for *Setd1a*$^{+/-}$ mice taking longer than their WT littermates to enter one of the open arms ($p = .057$; Figure 5.1D). There were no significant effects of genotype on distance moved ($p = .99$; Figure 5.1A), the proportion of time spent on the open arms ($p = .75$; Figure 5.1C) or the number of entries into the open arms ($p = .20$; Figure 5.1B). There was no significant multivariate effect of sex ($F(4, 70) = 1.39$, $p = .25$; Wilk's $\lambda = 0.93$) and no interaction between genotype and sex ($F(4, 70) = 1.33$, $p = .27$; Wilk's $\lambda = 0.93$).

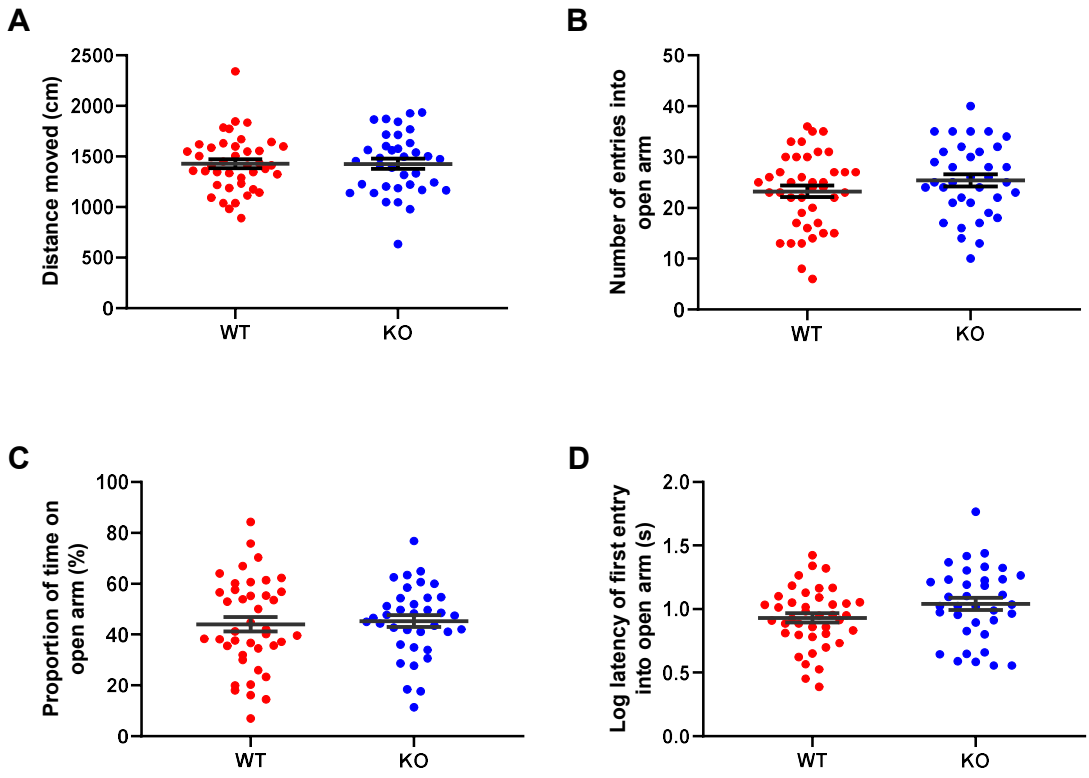


**Figure 5.1. Effect of *Setd1a* haploinsufficiency on anxiety-related behaviour in the EPM.** Mean (+/- SEM) **A)** distance moved, **B)** number of open arm entries, **C)** proportion of time on open arms, and **D)** log latency of first entry into an open arm.

*5.3.2. Open field test*

MANOVA revealed a significant multivariate effect of genotype on indices of anxiety-related behaviour in the OFT ($F(4, 70) = 3.43$, $p = .01$; Wilk's $\lambda = 0.84$). Follow-up analysis revealed that *Setd1a*$^{+/-}$ mice made significantly fewer entries into the inner zone ($p = .04$; Figure 5.2B) and spent significantly less time in this region ($p = .02$; Figure 5.2C) than their WT littermates. There were no significant effects of genotype on distance moved ($p = .11$; Figure 5.2A) or log latency of first entry into the inner zone ($p = .18$; Figure 5.2D). There was no significant multivariate effect of sex ($F(4, 70) = 1.31$, $p = .27$; Wilk's $\lambda = 0.93$) and no interaction between genotype and sex ($F(4, 70) = 0.13$, $p = .97$; Wilk's $\lambda = 0.99$).

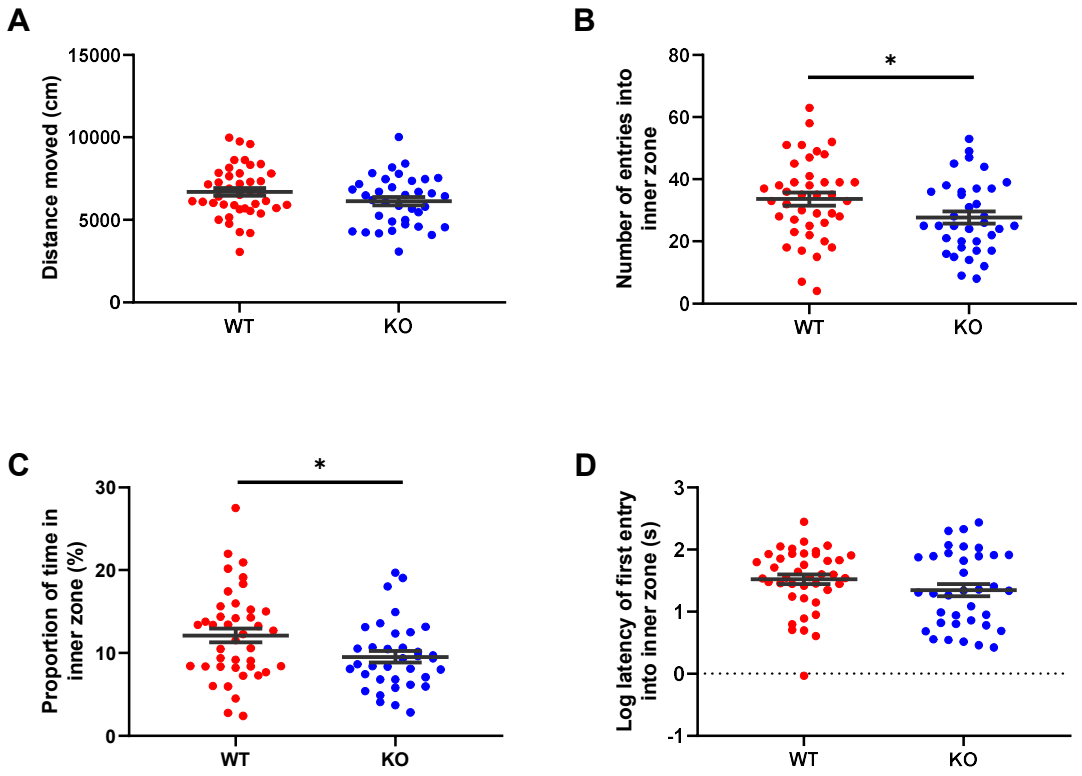


**Figure 5.2. Effect of *Setd1a* haploinsufficiency on anxiety-related behaviour in the OFT.** Mean (+/- SEM) **A)** distance moved, **B)** number of inner zone entries, **C)** proportion of time in inner zone, and **D)** log latency of first entry into inner zone; * $p <$ .05.

*5.3.3. Locomotor activity*

There was no significant main effect of genotype on locomotor activity levels ($F(1, 73) = 0.46$, $p = .50$). There was also no significant main effect of sex ($F(1, 73) = 0.04$, $p = .84$) and no significant interaction between sex and genotype ($F(1, 73) = 2.45$, $p = .12$). A significant main effect of day was observed ($F(1.69, 123.09) = 28.63$, $p < .001$; Figure 5.3A) and there was no significant interaction between day and genotype ($F(1.69, 123.09) = 0.18$, $p = .80$). This indicates that activity levels decreased by a similar amount in WT and *Setd1a*$^{+/-}$ mice across test days, suggesting normal habituation to a novel environment. Consistent with this, there was a significant main effect of quartile ($F(1.74, 127.04) = 183.14$, $p < .001$; Figure 5.3B) and no significant interaction between quartile and genotype ($F(1.74, 127.04) = 1.41$, $p = .25$). This shows that activity levels of WT and *Setd1a*$^{+/-}$ mice declined to the same degree during a session as they became more familiar with the environment.

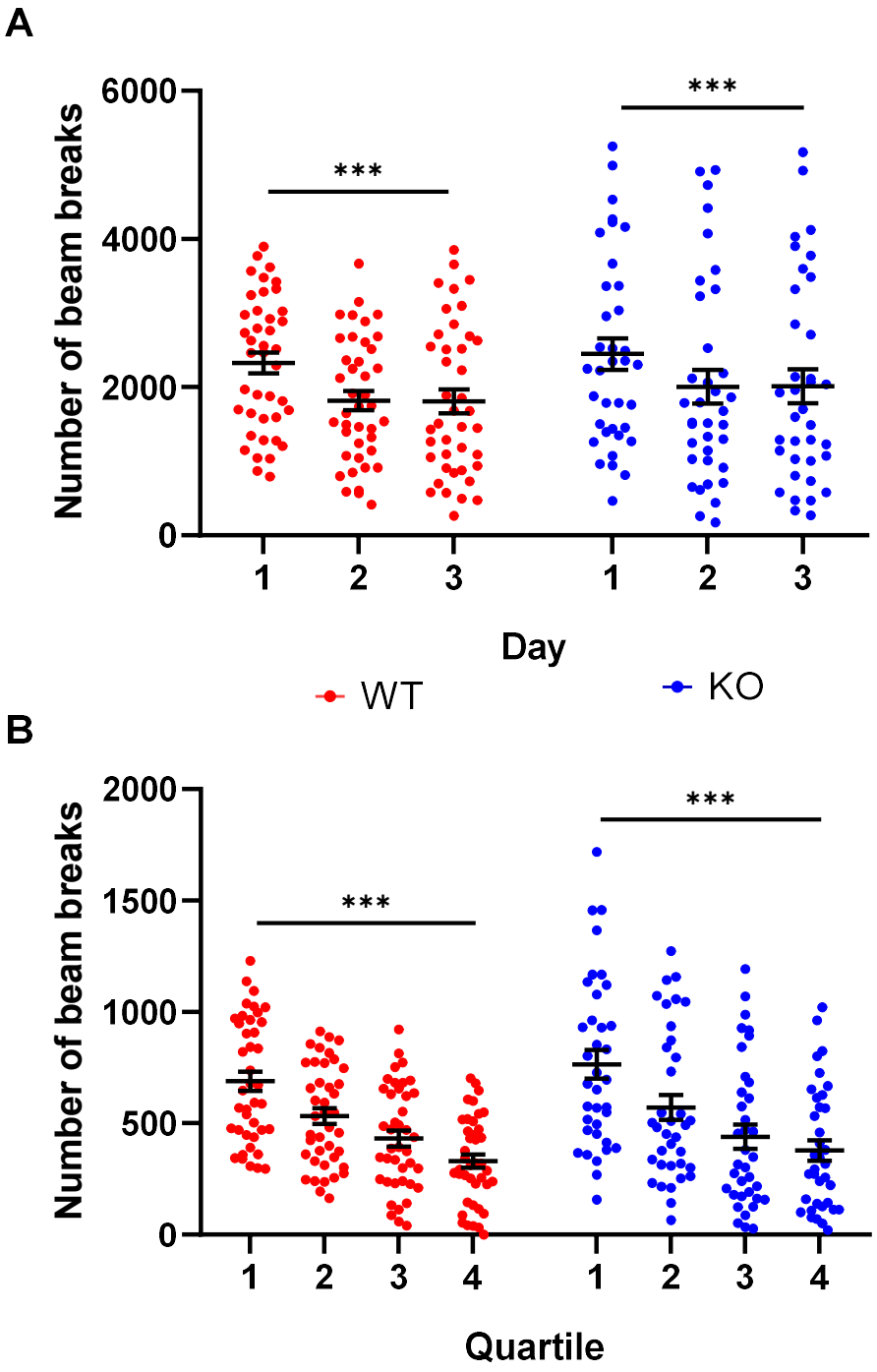


**Figure 5.3. Effect of *Setd1a* haploinsufficiency on locomotor activity levels.** Mean (+/- SEM) beam breaks **A)** for each day, summed across a whole session and **B)** for each quartile, pooled across sessions; *** $p < .001$.

*5.3.4. Sensorimotor gating*

Analysis of the weight-adjusted ASR data (Figure 5.4) revealed a significant main effect of pulse ($F(1.84, 134.58) = 293.21$, $p < .001$), indicating an increased magnitude

of startle response at higher pulse intensities. There was a significant main effect of genotype ($F(1, 73) = 8.44$, $p = .005$), which was qualified by a significant interaction between genotype and pulse intensity ($F(1.84, 134.58) = 8.15$, $p = .001$). Post-hoc tests revealed that startle magnitude was significantly higher in *Setd1a*$^{+/-}$ than WT mice at 110 dB ($p = .04$) and 120 dB ($p = .001$) but not at 80 dB ($p = .07$), 90 dB ($p = .55$) or 100 dB ($p = .12$) The main effect of sex was not significant ($F(1, 73) = 0.02$, $p = .88$) and there was no significant interaction between sex and genotype ($F(1, 73) = 0.11$, $p = .74$), showing that *Setd1a*$^{+/-}$ mice exhibited a greater startle response than WTs irrespective of sex.

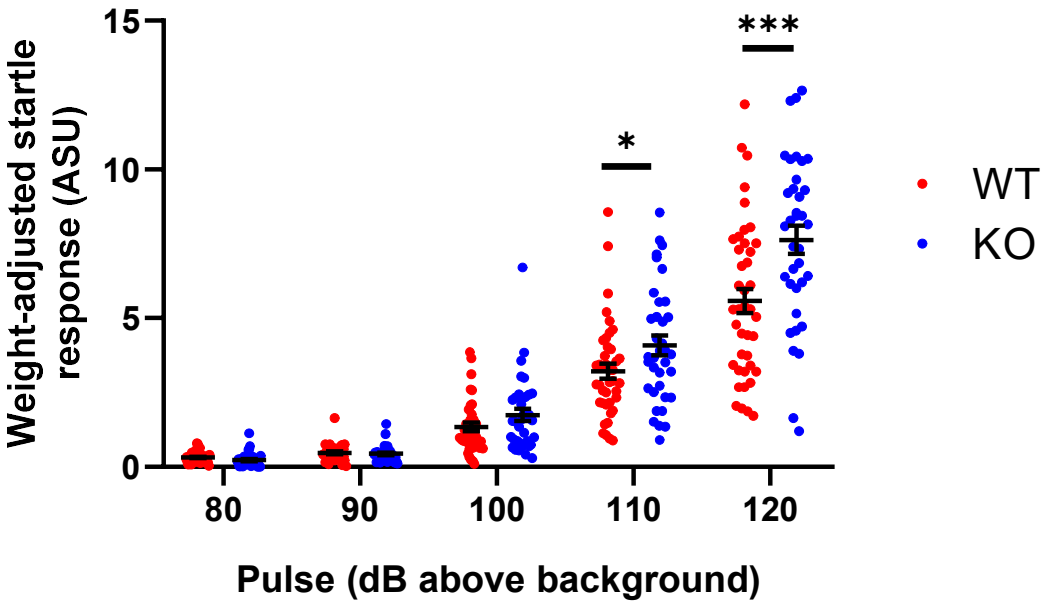


**Figure 5.4. Effect of *Setd1a* haploinsufficiency on ASR.** Mean (+/- SEM) weight-adjusted ASR at 80-120 dB (above background); *** $p < .001$; * $p < .05$.

Analysis of the PPI data (Figure 5.5) revealed a significant main effect of prepulse ($F(1.64, 119.57) = 264.22$, $p < .001$), indicating greater PPI with increasing prepulse intensity. There was also a significant main effect of genotype ($F(1, 73) = 19.01$, $p < .001$) and this was qualified by a significant interaction between genotype and prepulse ($F(1.64, 119.57) = 8.37$, $p = .001$). Post-hoc testing revealed that PPI was significantly reduced in *Setd1a*$^{+/-}$ mice at 8 dB ($p < .001$) and 16 dB ($p < .001$) but not at 4 dB ($p = .26$). There was no significant main effect of sex ($F(1, 73) = 1.40$, $p = .24$) and no interaction between sex and genotype ($F(1, 73) = 1.84$, $p = .18$).

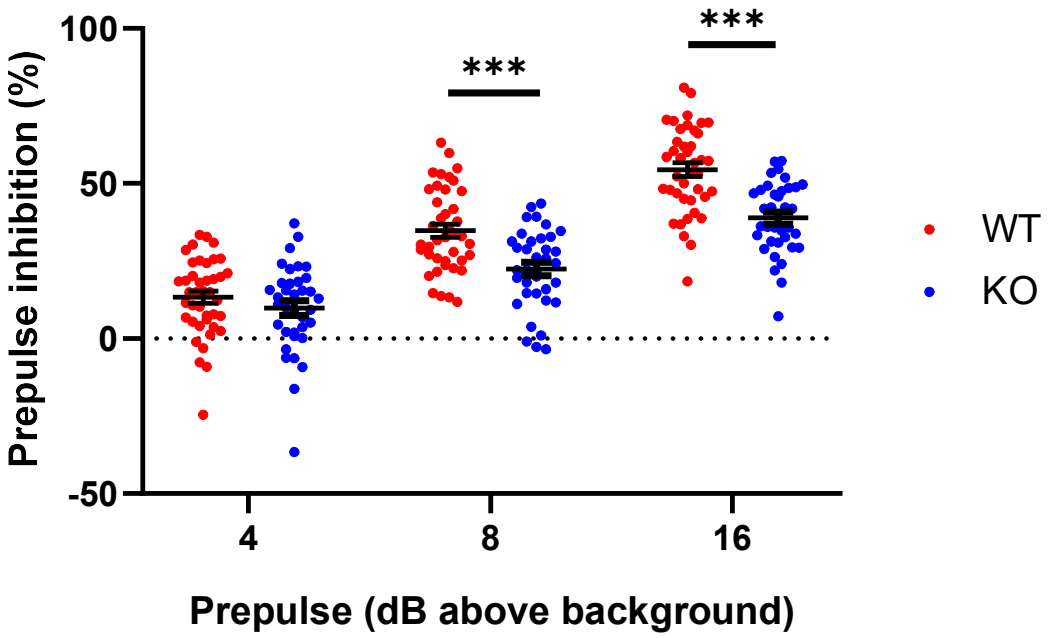


**Figure 5.5. Effect of *Setd1a* haploinsufficiency on PPI of the ASR.** Mean (+/- SEM) PPI by a 4, 8, and 16 dB (above background) prepulse; *** $p < .001$.

*5.3.5. Rotarod performance test*

Analysis of the latency to fall on accelerating trials (Figure 5.6A) revealed a significant main effect of trial ($F(2.97, 217.0)$, = 16.99, $p < .001$), indicating that latency to fall increased with training. There was no significant effect of genotype ($F(1, 73) = 2.70$, $p = .11$) and no significant interaction between genotype and trial ($F(2.97, 217.0)$, = 0.50, $p = .68$), suggesting that motor learning was not affected in *Setd1a*$^{+/-}$ mice. No significant sex differences were observed ($F(1, 73) = 0.33$, $p = .57$) and there was no significant interaction between sex and genotype ($F(1, 73) = 0.001$, $p = .98$).

Analysis of the latency to fall on fixed speed trials (Figure 5.6B) revealed that the latency to fall was significantly shorter at higher speeds ($F(5.62, 410.06) = 131.64$, $p < .001$). There was no significant effect of genotype ($F(1, 73) = 2.38$, $p = .13$), indicating that motor coordination was equivalent between *Setd1a*$^{+/-}$ and WT mice. No significant sex differences were observed ($F(1,73) = 8.25 \times 10^{-8}$, $p = .99$) and there was no significant interaction between sex and genotype ($F(1, 73) = 0.57$, $p = .45$).

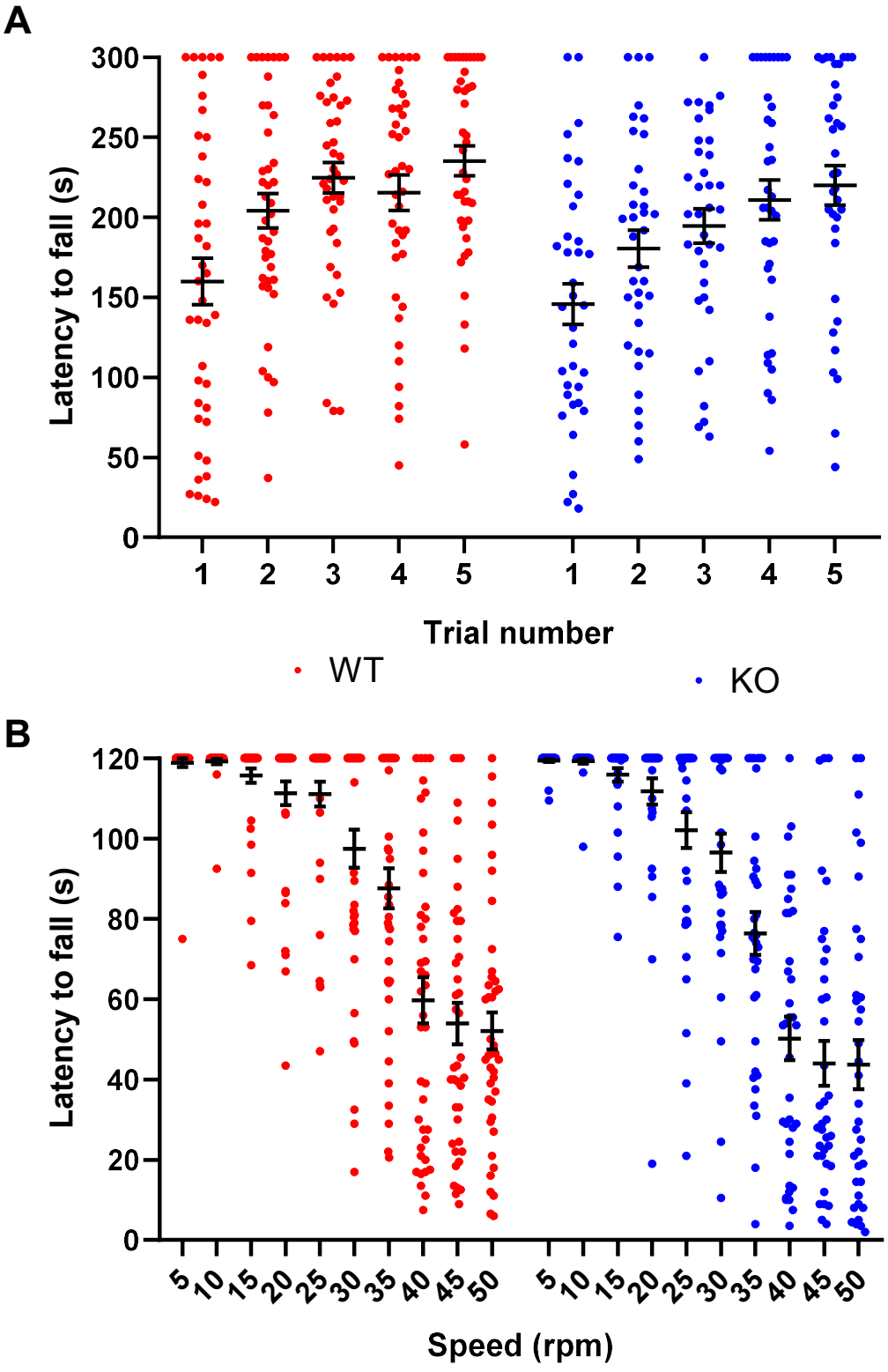


**Figure 5.6. Effect of *Setd1a* haploinsufficiency on motoric function in the Rotarod test.** Mean (+/- SEM) latency to fall **A)** on accelerating trials (5-50 rpm at 0.15 rpm/s) and **B)** at fixed speeds increasing in 5 rpm increments from 5-50 rpm.

*5.3.6. Novel object recognition*

Analysis of the acquisition time data revealed no significant effect of genotype on the time taken to achieve 40 seconds of object exploration ($F(1, 72) = 0.09$, $p = .76$) (Table 5.2). Raw exploration times at test are also shown in Table 5.2. Discrimination ratios were significantly higher at the 30 minute than 24 hour retention interval ($F(1, 72) = 19.61$, $p < .001$). There was no significant effect of genotype ($F(1, 72) = 0.05$, $p = .82$) and no significant interaction between genotype and delay ($F(1, 72) = 1.68$, $p = .20$), indicating that short- and long-term object recognition memory was intact in *Setd1a*$^{+/-}$ mice. There was also no significant effect of sex ($F(1, 72) = 0.32$, $p = .57$) and no interaction between sex and genotype ($F(1, 72) = 0.45$, $p = .51$).

**Table 5.2.** Mean (SD) acquisition time and object exploration at test for the 30 minute and 24 hour retention intervals.

| | 30 mins | | 24 hours | |
|---|---|---|---|---|
| **Dependent variable** | **WT** | **KO** | **WT** | **KO** |
| Acquisition time (mins) | 6.9 (3.8) | 7.3 (4.2) | 7.1 (4.0) | 6.9 (4.1) |
| Novel object exploration time (s) | 19.2 (9.0) | 20.1 (11.0) | 8.1 (5.2) | 8.0 (5.4) |
| Familiar object exploration time (s) | 10.9 (8.7) | 9.5 (6.8) | 5.7 (4.0) | 6.1 (3.6) |

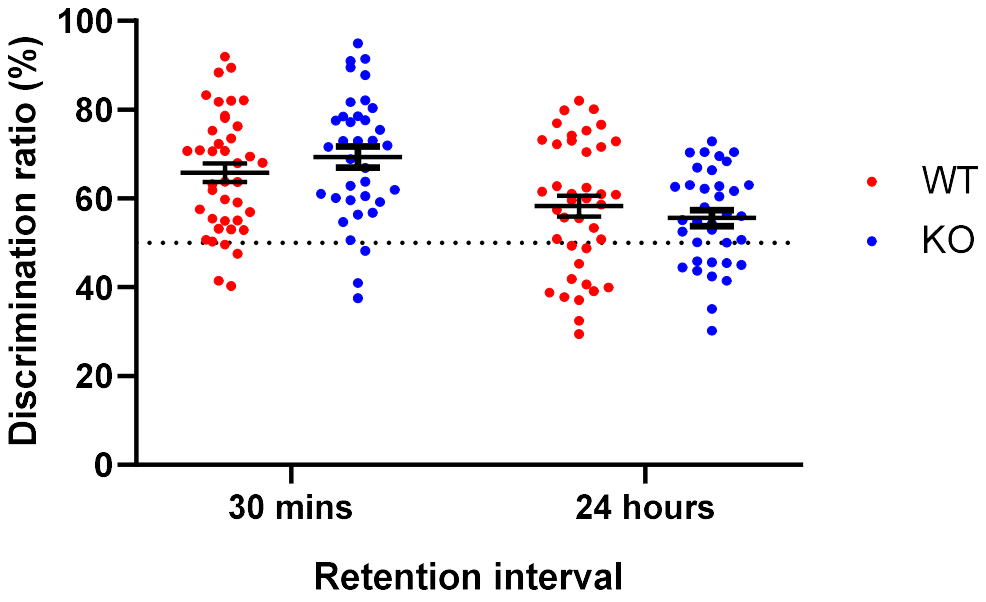


**Figure 5.7. Effect of *Setd1a* haploinsufficiency on object recognition memory.** Mean (+/- SEM) discrimination ratios (%) in the NOR test after a 30 minute and 24 hour retention interval. Dotted line shows chance performance.

## 5.4. Discussion

In this chapter, behavioural consequences of constitutive *Setd1a* haploinsufficiency were examined. Findings revealed abnormal sensorimotor gating (increased ASR and reduced PPI) and mixed evidence for increased anxiety (increased anxiety in the OFT but no significant differences in the EPM). Conversely, locomotor activity, motor coordination, and object recognition memory were not affected by *Setd1a* loss of function. These results demonstrate that *Setd1a* haploinsufficiency leads to highly specific behavioural impairments in sensorimotor gating and anxiety without affecting general aspects of motoric function, habituation to a novel environment, or object recognition memory.

At the time of conducting these experiments, there was no literature available on behavioural consequences of *Setd1a* haploinsufficiency. Subsequently, one study has shown that *Setd1a* loss of function results in working memory impairments (Mukai et al., 2019). The present findings extend our understanding of the functional consequences of *Setd1a* haploinsufficiency to reveal that sensorimotor gating and emotional reactivity are also affected. Consistent with the present results, Mukai et al. (2019) also showed normal locomotor activity levels and intact object recognition memory performance in heterozygous *Setd1a* mice. However, they report no difference in anxiety-related behaviour in the OFT, whereas the present results suggest that *Setd1a* loss of function leads to increased anxiety. A possible explanation for these divergent results is that the duration of the open field test used by Mukai et al. (2019) was considerably longer (60 minute trial) than the findings reported here (10 minute trial). It is likely that subtle anxiety phenotypes may have been masked by the longer session as the animals would have habituated to the arena after prolonged exposure.

The reduced PPI observed in *Setd1a*$^{+/-}$ mice is reminiscent of pervasive PPI deficits observed in schizophrenia patients (Swerdlow et al., 2018). PPI deficits can be induced by dopaminergic or 5-HT2 receptor agonists and NMDA receptor antagonists in rodents (Geyer et al., 2001). This suggests that there are several mechanisms that could be responsible for the current findings. PPI deficits can be reversed with a variety of antipsychotics and this approach is often used as a screening tool for putative antipsychotics (Swerdlow et al., 2008). By comparing the effects of typical and atypical antipsychotics with different pharmacological profiles, this would shed light on underlying neurochemical changes in *Setd1a*$^{+/-}$ mice (see Chapter 6). It would also be interesting to explore whether other types of gating are impaired due to *Setd1a* haploinsufficiency. For example, latent inhibition is also impaired in

schizophrenia patients, which is thought to reflect cognitive gating mechanisms (Swerdlow, Braff, Hartston, Perry, & Geyer, 1996).

The present findings suggest that *Setd1a* haploinsufficiency is associated with an increased anxiety phenotype. Specifically, *Setd1a*$^{+/-}$ mice spent less time in the central region of the open field and exhibited a greater ASR, another index of increased anxiety (Grillon, 2008). However, there was only weak evidence for increased anxiety in the EPM, with a non-significant trend for *Setd1a*$^{+/-}$ mice to take longer to enter the open arms than WTs. It is interesting to note that the average amount of time spent on the open arm was approximately 40 %. This is substantially higher than expected: other data from our laboratory from a similar hybrid C57BL/6J x C57BL/6NTac strain shows that WT animals usually spend only 30 % of the time on the open arms (T. Humby, personal communication). This suggests that the EPM task may not have been particularly aversive, which could explain why no differences in anxiety were observed. It has also been suggested that different tests of anxiety assay distinct, albeit overlapping, aspects of anxiety (Ramos, 2008). Consistent with this, factor analysis has shown that data from the EPM and OFT load onto different factors (Trullas & Skolnick, 1993). Future work could further characterise the anxiety phenotype of *Setd1a*$^{+/-}$ mice using other tests of anxiety (e.g., elevated zero maze and light-dark box).

In our hands, there was no evidence for basic learning and memory impairments in *Setd1a*$^{+/-}$ mice. This was surprising given the link between *Setd1a* loss of function and learning disabilities (Singh et al., 2016) and the role of H3K4 methylation in memory formation (Collins, Greer, Coleman, & Sweatt, 2019). It is important to note that memory is multi-faceted; the present findings indicate normal novelty-based memory (intact object recognition and habituation of locomotor activity in a novel environment) and procedural memory (equivalent motor learning on the Rotarod). However, it remains to be tested whether other forms of memory, such as associative memory, are affected by *Setd1a* haploinsufficiency. This could be investigated using the object-in-place task, which requires encoding of the relationship between objects and their location in the environment (Dix & Aggleton, 1999).

In summary, the findings of this chapter show that constitutive haploinsufficiency of *Setd1a* causes impaired sensorimotor gating and a subtle anxiety phenotype, with spared motoric function and basic learning and memory. The results of this initial behavioural characterisation demonstrate functional consequences of *Setd1a* loss of function on behaviour that are of relevance to schizophrenia. These findings serve as

a foundation for further work into additional behavioural consequences of *Setd1a* loss of function and investigation of neurobiological mechanisms underlying behavioural phenotypes.

## Chapter 6: Pharmacological modulation of sensorimotor gating deficits in *Setd1a*$^{+/-}$ mice using antipsychotics

### 6.1. Introduction

In this chapter, the effects of established antipsychotics on aberrant sensorimotor gating in *Setd1a*$^{+/-}$ mice were examined. The primary aim of this work was to test whether deficient prepulse inhibition (PPI) can be restored by antipsychotic treatment. In addition, the effects of two antipsychotics with different pharmacological profiles (haloperidol and risperidone) were compared to investigate underlying neurochemical changes.

Deficient PPI is a robust endophenotype in schizophrenia (Swerdlow et al., 2018). Such deficits are influenced by antipsychotic medication, with patients currently taking antipsychotic medication showing higher levels of PPI than unmedicated patients, an effect that is more pronounced for atypical antipsychotics (Kumari, Soni, & Sharma, 2002; Leumann, Feldon, Vollenweider, & Ludewig, 2002; Oranje, Van Oel, Gispen-De Wied, Verbaten, & Kahn, 2002; Quednow et al., 2008). However, due to the cross-sectional nature of these studies, it is possible that other confounding factors, such as heterogeneity in treatment history and severity of symptoms, may contribute to these effects. A few randomised controlled trials have been conducted but these have yielded mixed results and are difficult to interpret due to the lack of a placebo control group (Mackeprang, Kristiansen, & Glenthoj, 2002; Quednow et al., 2006; Wynn et al., 2007). Longitudinal studies have shown that several months treatment with the atypical antipsychotics risperidone or quetiapine leads to an increased level of PPI in schizophrenia patients relative to baseline (Aggernaes et al., 2010; Martinez-Gras et al., 2009). PPI is also enhanced by the atypical antipsychotics clozapine and quetiapine in individuals who normally show low levels of PPI in the absence of a psychiatric diagnosis (Swerdlow, Talledo, Sutherland, Nagy, & Shoemaker, 2006; Vollenweider, Barro, Csomor, & Feldon, 2006).

Many studies have shown that PPI deficits in rodent models of schizophrenia can be reversed by treatment with antipsychotics (for reviews, see: Geyer, Krebs-Thomson, Braff, & Swerdlow, 2001; Swerdlow, Weber, Qu, Light, & Braff, 2008). This metric is often used in preclinical studies as a screening tool for novel antipsychotics, based on initial work demonstrating that the clinical potency of antipsychotic medication is strongly correlated with their ability to reverse apomorphine-induced PPI deficits in rats (Swerdlow, Braff, Taaid, & Geyer, 1994). There is some evidence to support a dissociation between the efficacy of typical and atypical antipsychotics in rescuing

PPI deficits induced by different pharmacological treatments. In general, both typical and atypical antipsychotics improve PPI deficits in D2 agonist models, whereas atypical antipsychotics tend to be more effective than typical antipsychotics in reversing PPI deficits in 5-HT receptor agonist and NMDAR antagonist models (Geyer et al., 2001).

It is important to note that the division of antipsychotics into typical and atypical has been suggested to reflect their historical development rather than a pharmacological distinction (Cunningham Owens & Johnstone, 2018). D2 receptor blockade is common to all antipsychotics and is thought to be responsible for therapeutic effects (Creese et al., 1976; Kapur & Remington, 2001). This may also explain the ability of both typical and atypical antipsychotics to improve PPI deficits induced by D2 agonists. Consistent with this, the ability to reverse apomorphine-induced PPI deficits correlates with D2 receptor affinity (Yamada, Harano, Annoh, Nakamura, & Tanaka, 1999). Despite a large degree of heterogeneity in the pharmacological action of atypical antipsychotics (Miyamoto, Duncan, Marx, & Lieberman, 2005), some have argued that a higher relative affinity for 5-HT2A versus D2 receptors defines 'atypicality' (Meltzer & Massey, 2011), which may explain the superiority of atypical antipsychotics in reversing PPI deficits induced by NMDAR antagonists and 5-HT2 receptor agonists.

In addition to causing NMDA receptor hypofunction, administration of the non-competitive NMDA antagonists PCP (Hernandez, Auerbach, & Hoebel, 1988; Lillrank, O'Connor, Oja, & Ungerstedt, 1994; Martin, Carlsson, & Hjorth, 1998) and dizocilpine (Dall'Olio, Gaggi, Bonfante, & Gandolfi, 1999; Yan, Reith, Jobe, & Dailey, 1997) have been shown to cause serotonergic hyperactivity. Conversely, serotonin has been reported to influence glutamate release in the prefrontal cortex via its action at the 5-HT2A receptor (Aghajanian & Marek, 1997). Attenuation of PCP-induced PPI deficits by antipsychotics correlates with their affinity for 5-HT2A receptors (Yamada et al., 1999). Similar effects have been reported for PCP-induced hyperlocomotion, with antipsychotics that show a greater affinity for 5-HT2A relative to D2 receptors being more effective at normalising activity levels (Meltzer & Massey, 2011). In addition, dizocilpine-induced PPI deficits are rescued by the selective 5-HT2A antagonist M100907 (Varty, Bakshi, & Geyer, 1999) and selective 5-HT2A receptor antagonists block the PPI-reducing effect of the 5-HT2 receptor agonists DOI (Sipes & Geyer, 1997) and LSD (Halberstadt & Geyer, 2010; Ouagazzal, Grottick, Moreau, & Higgins, 2001). These findings illustrate the role of 5-HT2A receptor function in moderating PPI disruptions caused by NMDAR-antagonists and 5-HT2 receptor agonists.

The aim of this chapter was to assess whether deficient PPI in *Setd1a*$^{+/-}$ mice (Chapter 5.3.4) can be influenced, possibly rescued, by haloperidol or risperidone. Haloperidol is predominantly D2 selective, with a much higher affinity for D2 (Ki = 1.4 nM) than 5-HT2A (Ki = 25 nM) receptors, whereas risperidone has a higher affinity for 5-HT2A (Ki = 0.16 nM) than D2 (Ki = 3.3 nM) receptors (Figure 6.1) (Kusumi, Boku, & Takahashi, 2015). Previous work in rodent models has shown that PPI deficits induced by D2 receptor agonists are reversed by both haloperidol and risperidone, whereas NMDAR antagonist induced deficits are generally insensitive to haloperidol but can be reversed by risperidone (Geyer et al., 2001; Swerdlow et al., 2008). Effects in 5-HT2 receptor agonist models are less well studied but there is some evidence that haloperidol is not able to rescue DOI- (Padich, McCloskey, & Kehne, 1996; Varty & Higgins, 1995) or LSD-induced PPI deficits (Ouagazzal et al., 2001), whereas risperidone enhances deficient PPI in DOI treated animals (Varty & Higgins, 1995).

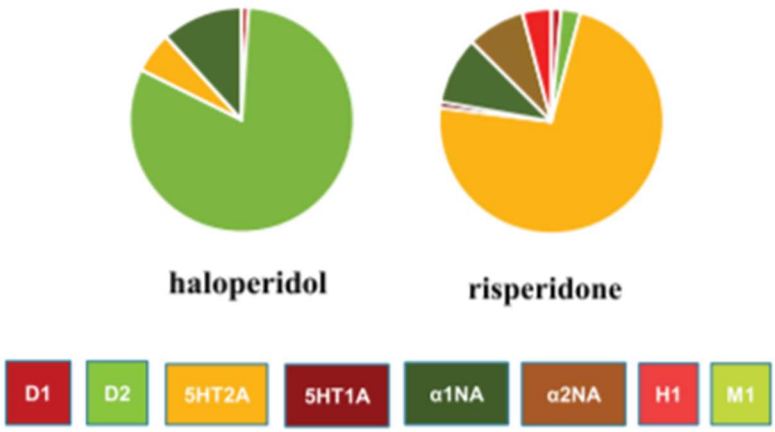


**Figure 6.1. Receptor binding profiles of haloperidol and risperidone.** Adapted from Cunningham Owens & Johnstone (2018).

This work was conducted in three parts; first, two pilot studies were conducted to establish the feasibility of a within-subjects drug challenge by investigating stability of ASR and PPI over repeated sessions (Pilot study 1) and an appropriate dose range of each drug was identified (Pilot study 2). Second, the basic effects of *Setd1a* loss of function on increased ASR and decreased PPI described in Chapter 5.3.4 were replicated. Finally, the effects of haloperidol and risperidone on sensorimotor gating impairments in *Setd1a*$^{+/-}$ mice were compared. The rationale for this was two-fold; i) assess whether PPI deficits can be rescued by antipsychotics and ii) probe underlying neurochemical mechanisms. Considering the evidence reviewed above, it was hypothesised that if PPI deficits were rescued by both haloperidol and risperidone then this may indicate dopaminergic dysfunction. Conversely, if risperidone but not

haloperidol was effective in reversing PPI deficits then this may indicate the involvement of other neurotransmitter systems (e.g., glutamatergic or serotonergic).

## 6.2. Methods

### *6.2.1. Subjects*

#### *6.2.1.1 Pilot work*

Two pilot studies were conducted with male mice (3 months old at the start of testing) on a similar genetic background (C57BL/6J) to the *Setd1a*$^{+/-}$ mice. 6 mice were included in Pilot study 1 to investigate the stability of ASR and PPI over repeated test sessions. In Pilot study 2, 34 mice were divided into two groups to identify an appropriate dose range of haloperidol (N = 17) and risperidone (N = 17) to use in the main experiment.

#### *6.2.1.2 Main experiment*

56 adult mice (26 male and 30 female) were tested in the main experiment (3 months old at the start of testing). First, all mice completed a pre-test session to replicate the basic effects. Then, mice were divided into two approximately equal groups (balanced for sex and genotype) and allocated to either the haloperidol or risperidone condition (see Table 6.1).

**Table 6.1.** Sample characteristics for mice included in the main experiment and their allocation to drug condition.

| | **Haloperidol** | | **Risperidone** | | |
|---|---|---|---|---|---|
| | KO | WT | KO | WT | Total |
| Male | 5 | 8 | 5 | 8 | 26 |
| Female | 7 | 9 | 6 | 8 | 30 |
| **Total** | **12** | **17** | **11** | **16** | **56** |

### *6.2.2 Apparatus and materials*

#### *6.2.2.1 Testing apparatus*

The apparatus for measuring ASR and PPI are described in Chapter 2.3.4. Briefly, SR-Lab (San Diego Instruments, USA) sound attenuating chambers were used to present acoustic stimuli. Animals were placed in a clear Perspex tube (35 mm diameter) mounted on a plinth and the whole-body startle response was detected

using a piezoelectric sensor attached to the plinth. The average startle response (Vavg) was recorded in arbitrary startle units using SR-Lab software over the 65 ms period following stimulus onset.

*6.2.2.2 Drugs*

Each drug solution was prepared by dissolving either 1 mg haloperidol (Sigma, UK) or risperidone (Sigma, UK) in 2.5 µL 1M glacial acetic acid. This was transferred to an appropriate volume of 0.9 % saline (see Table 6.2), such that an equal volume (100 µL per g of body weight) of drug were administered for all dosages. A 0.025 % (v/v) glacial acetic acid in 0.9 % saline solution was used as vehicle. pH of all solutions were adjusted to 6.0 using 1 M sodium hydroxide.

**Table 6.2.** Dilutions for the different dosages of drug solutions.

| Dosage (mg/kg) | Volume 0.9 % saline (mL) |
|---|---|
| 1.0 | 10 |
| 0.5 | 20 |
| 0.1 | 100 |

*6.2.3 Design*

*6.2.3.1 Test protocol*

In all experiments, ASR and PPI were assessed using a modified version of the protocol described in Chapter 2.3.4 using an identical trial structure. A 70 dB white noise background was presented throughout. Each session started with a 5 minute habituation period. Six 120 dB pulse alone trials were presented on consecutive trials, followed by an additional 7 pulse alone trials interspersed with 12 prepulse trials (8 dB or 16 dB above background, 6 trials of each). Two no stimulus trials were presented at the beginning and end of the session. In the pre-test session, an additional range of pulse alone trials (80 – 120 dB in 10 dB increments, 3 trials of each) were presented at the end of the session, as in the previous experiment.

*6.2.3.2 Testing procedure*

In Pilot study 1, there were 8 sessions spaced 3-4 days apart performed under basal conditions. In Pilot study 2, each group completed a within-subjects dose-response experiment (vehicle, 0.1 mg/kg, 0.5 mg/kg and 1.0 mg/kg) for either haloperidol or risperidone. Order of dosage was counterbalanced and there were 7 days washout between each session.

In the main experiment, mice first completed a pre-test session to replicate the previous findings of elevated ASR and reduced PPI in *Setd1a*$^{+/-}$ mice (Chapter 5.3.4). Each group then completed 3 further sessions of either haloperidol or risperidone (vehicle, 0.5 mg/kg or 1.0 mg/kg) spaced 7 days apart. This dose range was chosen based on the results of Pilot study 2 (section 6.3.2). Dose order was counterbalanced across runs for vehicle and 0.5 mg/kg and all mice received the highest dose of each drug in the final session.

All drugs were administered by intraperitoneal (IP) injection 30 minutes before the start of the session. The degree of sedation was rated on a scale from 1 (no sedation) to 5 (completely sedated) immediately prior to behavioural testing. Any animal scoring above 3 was excluded, which led to the removal of one animal at the 1 mg/kg dose of risperidone in Pilot study 2.

### *6.2.4. Data analysis*

ASR data were weight-adjusted by dividing the average ASR by body weight. PPI was calculated as the percentage reduction in startle amplitude between prepulse and pulse alone trials (excluding the first 3 pulse-alone trials). Data were analysed using ANOVA, described below.

- Pilot study 1: repeated measures ANOVA with session (8 levels) (ASR) and prepulse (8 & 16 dB) (PPI)
- Pilot study 2: repeated measures ANOVA with dose (vehicle, 0.1 mg/kg, 0.5 mg/kg, and 1.0 mg/kg) (ASR) and prepulse (8 & 16 dB) (PPI)
- Pre-test: mixed ANOVAs with between-subjects factors genotype and sex and within-subjects factor pulse (5 levels) (ASR) or prepulse (8 & 16 dB) (PPI)
- Main experiment: mixed ANOVA with between-subjects factors genotype and sex and within-subjects factor dose (vehicle, 0.5 mg/kg, 1.0 mg/kg) (ASR) and prepulse (8 & 16 dB) (PPI)

Bonferroni corrected post-hoc tests were used to follow up main effects of dose. Where a significant 3-way interaction between dose, genotype, and sex was observed, simple main effects were examined using separate ANOVAs for each sex, followed by Bonferroni corrected post-hoc tests.

## 6.3. Results

### *6.3.1. Pilot work*

#### *6.3.1.1. Pilot study 1*

The aim of this study was to assess the stability of basal ASR and PPI in WT mice over repeated testing. There was no significant change in ASR ($F(7, 35) = 1.96$, $p = .09$; Figure 6.2A) or PPI ($F(7, 35) = 2.22$, $p = .06$; Figure 6.2B) measured across 8 separate sessions spaced 3-4 days apart. These data show that these measures were robust over repeated test sessions.

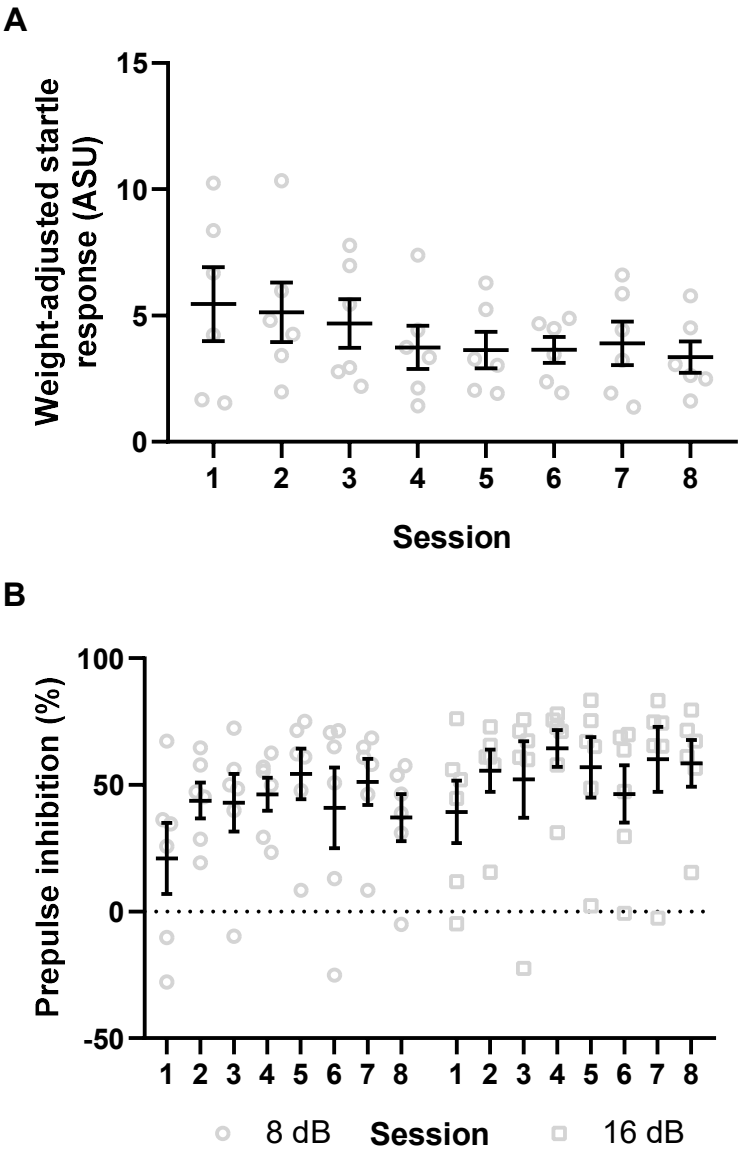


**Figure 6.2. Robustness of sensorimotor gating measures over 8 test sessions.** Mean (+/- SEM) **A)** ASR at 120 dB above background and **B)** PPI of ASR by an 8 and 16 dB above background prepulse.

*6.3.1.2. Pilot study 2*

The aim of this study was to test effects of haloperidol and risperidone in WT mice to identify an appropriate dose range for the main experiment. For haloperidol, there was no significant main effect of dose on magnitude of the ASR ($F(3, 48) = 1.43$, $p = .25$; Figure 6.3A). However, a significant main effect of dose was observed for PPI ($F(3, 48) = 4.11$, $p = .01$; Figure 6.3B). Post-hoc tests revealed that PPI was significantly greater than vehicle at 1.0 mg/kg ($p = .04$) but not at 0.5 mg/kg ($p = .18$) or 0.1 mg/kg ($p = .99$).

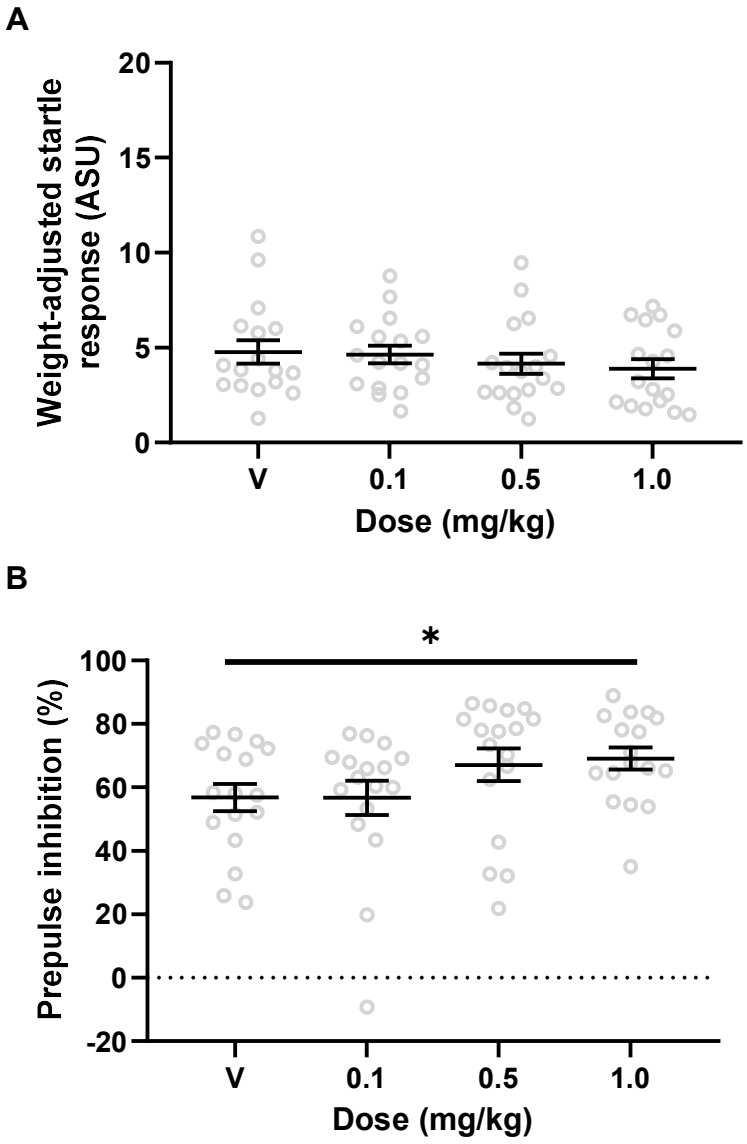


**Figure 6.3. Effects of haloperidol on sensorimotor gating in WT mice.** Mean (+/- SEM) **A)** ASR at 120 dB above background and **B)** PPI of the ASR, pooled across 8 and 16 dB above background prepulses. Data are presented following IP administration of vehicle, 0.1, 0.5 and 1.0 mg/kg haloperidol; * $p < .05$.

A significant main effect of risperidone dose was observed for ASR ($F(3, 45) = 6.42$, $p = .001$; Figure 6.4A). Post-hoc tests revealed a significantly reduced startle response at 1.0 mg/kg ($p = .03$) but not at 0.5 mg/kg ($p = .10$) or 0.1 mg/kg ($p = .99$). There was no significant main effect of dose on PPI ($F(1.70, 25.51) = 2.12$, $p = .15$; Figure 6.4B).

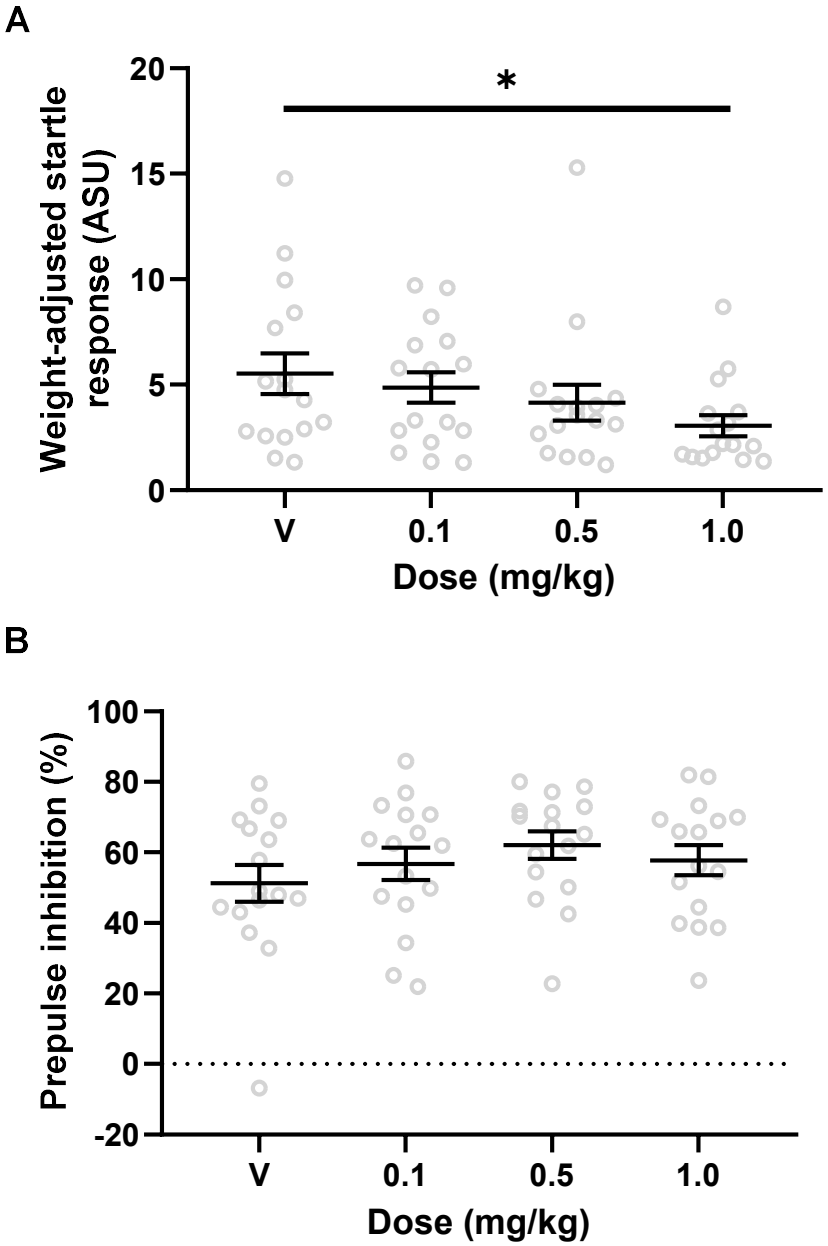


**Figure 6.4. Effects of risperidone on sensorimotor gating in WT mice.** Mean (+/- SEM) **A)** ASR at 120 dB above background and **B)** PPI of the ASR, pooled across 8 and 16 dB above background prepulses. Data are presented following IP administration of vehicle, 0.1, 0.5 and 1.0 mg/kg risperidone; * $p < .05$.

The results of Pilot study 2 showed that 0.5 mg/kg was the highest dose of haloperidol and risperidone tested that did not have significant effects on basal sensorimotor gating in WT mice. Thus, in the main experiment, all mice were tested at this dosage in the first instance to explore drug effects on sensorimotor gating in *Setd1a*$^{+/-}$ mice in the absence of non-specific effects.

### *6.3.2. Main experiment*

#### *6.3.2.1. Pre-test session*

This experiment investigated whether the sensorimotor gating deficits reported in Chapter 5.3.4 could be replicated in an independent sample of *Setd1a*$^{+/-}$ mice and their WT littermates. Consistent with the previous results, a significant main effect of genotype on ASR ($F(1, 52) = 16.36$, $p < .001$; Figure 6.5) was observed. There was also a significant interaction between genotype and pulse ($F(1.77, 91.88) = 10.46$, $p < .001$). Post hoc tests revealed that startle magnitude was significantly greater in *Setd1a*$^{+/-}$ mice at 100 dB ($p = .003$), 110 dB ($p = .004$), and 120 dB ($p < .001$) but not at 80 dB ($p = .75$) or 90 dB ($p = .88$). There was a non-significant trend for greater startle magnitude in males ($F(1, 52) = 3.89$, $p = .05$) but no significant interaction between sex and genotype was observed ($F(1, 52) = 2.10$, $p = .15$).

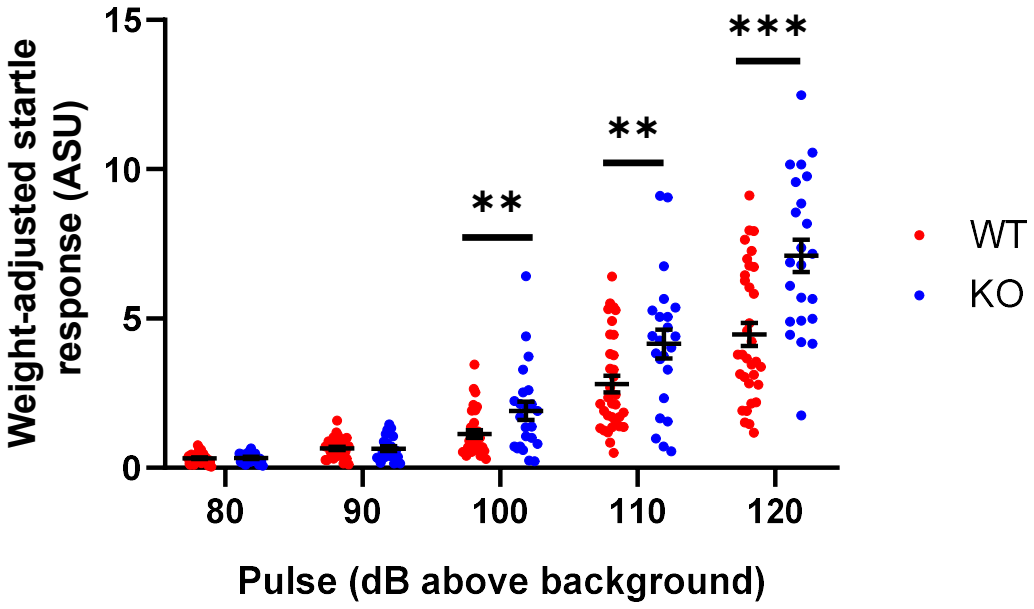


**Figure 6.5. Replication of increased ASR in *Setd1a*$^{+/-}$ mice.** Mean (+/- SEM) ASR at 80-120 dB (above background) in 10 dB increments; *** $p < .001$, ** $p < .01$.

The effects of *Setd1a* haploinsufficiency on PPI were also replicated in this experiment; a significant reduction in PPI was observed in *Setd1a*$^{+/-}$ mice ($F(1, 52) = 19.79$, $p < .001$; Figure 6.6). There was no significant main effect of sex ($F(1, 52) = 0.42$, $p = .52$) or interaction between sex and genotype ($F(1, 52) = 2.37$, $p = .13$).

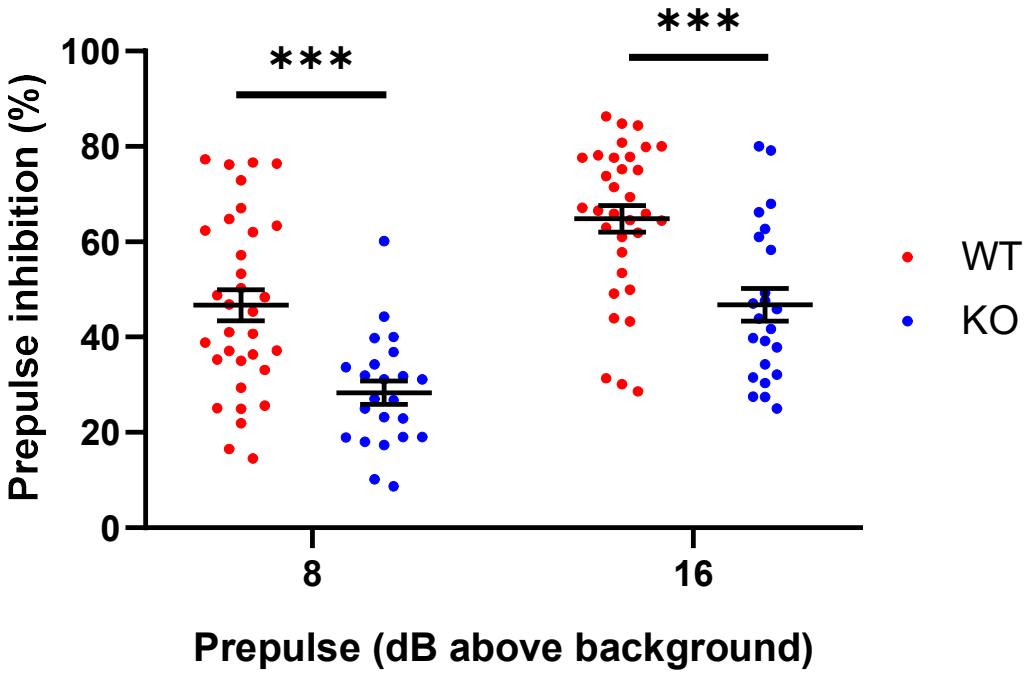


**Figure 6.6. Replication of decreased PPI in *Setd1a*$^{+/-}$ mice.** Mean (+/- SEM) PPI of the ASR at 120 dB (above background) by an 8 and 16 dB (above background) prepulse; *** $p < .001$.

*6.3.2.2. Drug challenge*

*6.3.2.2.1 Haloperidol*

Analysis of the ASR data revealed that *Setd1a*$^{+/-}$ mice showed an elevated startle response ($F(1, 25) = 14.01$, $p = .001$; Figure 6.7). This effect was maintained at all doses tested (genotype x dose interaction: $F(2, 50) = 1.72$, $p = .19$). The main effect of dose was not significant ($F(2, 50) = 3.17$, $p = .05$). There was no significant effect of sex ($F(1, 25) = 3.83$, $p = .06$) and no significant sex x genotype interaction ($F(1, 25) = 0.02$, $p = .90$). There was also no significant 3 way interaction between dose, sex and genotype ($F(2, 50) = 1.22$, $p = .29$), suggesting equivalent drug effects across genotypes in both sexes.

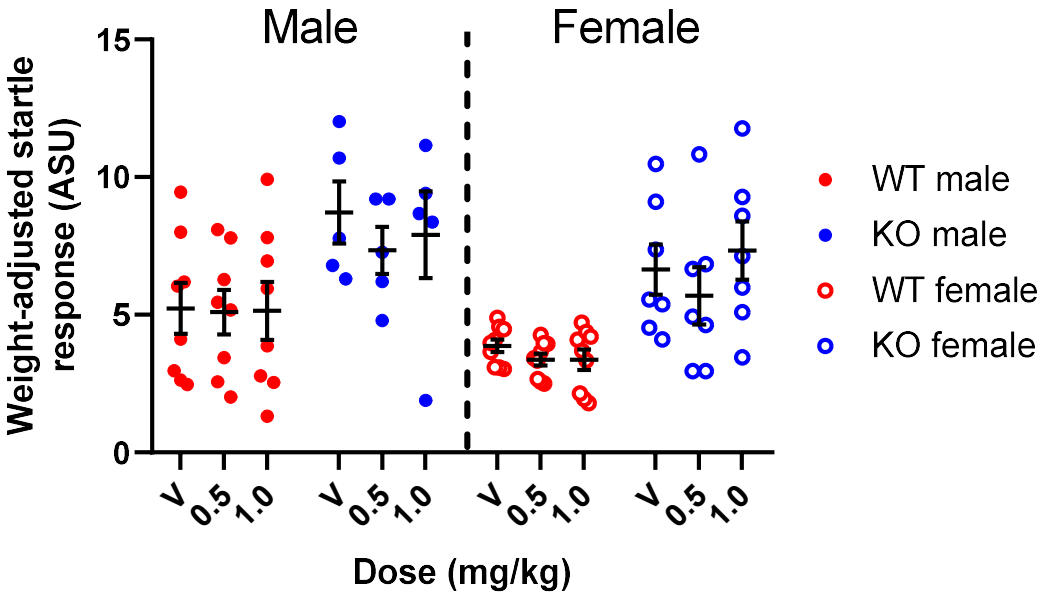


**Figure 6.7. Effect of haloperidol on ASR in *Setd1a*$^{+/-}$ and WT mice.** Mean (+/- SEM) ASR at 120 dB (above background) following IP administration of vehicle, 0.5 or 1.0 mg/kg haloperidol, presented separately for males and females.

Analysis of the PPI data revealed a significant main effect of genotype ($F(1, 25) = 21.92$, $p < .001$; Figure 6.8). However, this effect was qualified by a significant interaction between genotype and sex ($F(1, 25) = 9.16$, $p = .01$). Post hoc tests revealed that the effect of genotype was significant in females ($p < .001$) but not in males ($p = .28$). In addition, WT females showed greater PPI than WT males ($p = .02$) but there was no significant sex difference in *Setd1a*$^{+/-}$ mice ($p = .08$). The main effect of dose was not significant ($F(2, 50) = 3.08$, $p = .06$) but indicated a trend for a dose-related increase in PPI. There was also no significant interaction between dose and genotype ($F(2, 50) = 0.02$, $p = .98$) or between dose, genotype and sex ($F(2, 50) = 1.20$, $p = .31$), indicating that the non-significant enhancement of PPI occurred in all groups and did not reflect a reversal of PPI deficits in *Setd1a*$^{+/-}$ mice by haloperidol.

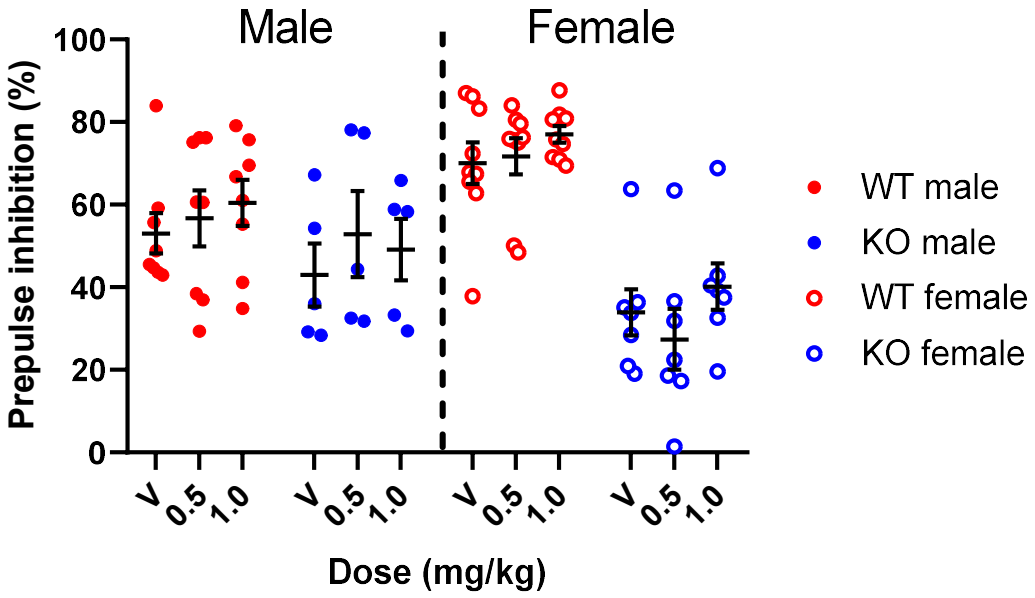


**Figure 6.8. Effect of haloperidol on PPI in *Setd1a*$^{+/-}$ and WT mice.** Mean (+/- SEM) PPI of the ASR at 120 dB (above background) pooled across 8 and 16 (dB above background) prepulses following IP administration of vehicle, 0.5 or 1.0 mg/kg haloperidol, presented separately for males and females.

*6.3.2.2.2 Risperidone*

Analysis of the weight-adjusted ASR data revealed that startle magnitude was significantly higher in *Setd1a*$^{+/-}$ mice ($F(1, 23) = 63.38$, $p < .001$; Figure 6.9). There was no significant effect of sex ($F(1, 23) = 2.82$, $p = .11$) and no significant sex x genotype interaction ($F(1, 23) = 1.41$, $p = .25$). A significant main effect of dose was observed ($F(2, 46) = 25.25$, $p < .001$) but this effect was qualified by a significant three-way interaction with sex and genotype ($F(2, 46) = 5.51$, $p = .01$). In males, simple main effects analyses revealed that the main effect of dose ($F(2, 22) = 7.32$, $p = .004$) was qualified by a significant dose x genotype interaction ($F(2, 22) = 6.26$, $p = .01$). Post-hoc tests showed that startle magnitude was dose dependently reduced in WT males (relative to vehicle: $p = .05$ at 0.5 mg/kg and $p = .01$ at 1.0 mg/kg) but not in *Setd1a*$^{+/-}$ males (relative to vehicle: $p = .62$ at 0.5 mg/kg and $p = .42$ at 1.0 mg/kg). Conversely, in females there was a significant main effect of dose ($F(2, 24) = 23.10$, $p < .001$) but no significant dose x genotype interaction ($F(2, 24) = 1.32$ $p = .29$), indicating an equivalent risperidone-induced reduction in startle magnitude in female WT and *Setd1a*$^{+/-}$ mice (relative to vehicle: $p = .002$ at 0.5 mg/kg and $p < .001$ at 1.0 mg/kg). These findings suggest an insensitivity to risperidone in *Setd1a*$^{+/-}$ males but not females.

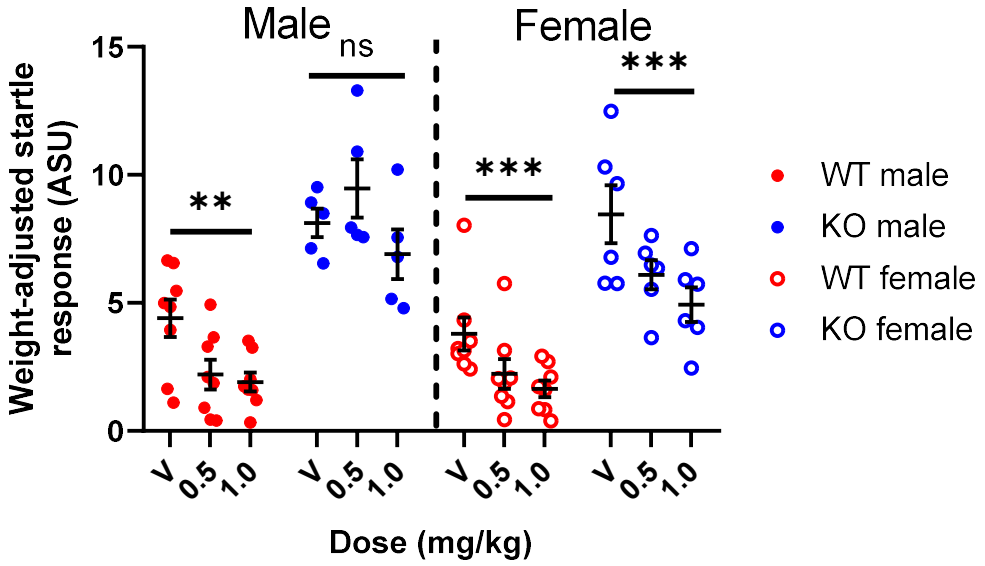


**Figure 6.9. Effect of risperidone on ASR in *Setd1a*$^{+/-}$ and WT mice.** Mean (+/- SEM) ASR at 120 dB (above background) following IP administration of vehicle, 0.5 or 1.0 mg/kg risperidone, presented separately for males and females; *** $p < .001$, ** $p < .01$.

Analysis of the PPI data revealed that *Setd1a*$^{+/-}$ mice showed significantly less PPI than WTs ($F(1, 23) = 6.36$, $p = .02$ Figure 6.10). There was no main effect of sex ($F(1, 23) = 0.13$, $p = .73$) and the effect of genotype was consistent for males and females (sex x genotype: $F(1, 23) = 0.24$, $p = .63$). The main effect of dose was not significant ($F(2, 46) = 2.71$, $p = .08$) and there was no significant interaction between dose and genotype ($F(2, 46) = 1.38$, $p = .26$). Although the genotype effect in females appeared to be normalised at 1.0 mg/kg (Figure 6.10), there was no significant 3-way interaction between dose, genotype and sex ($F(2, 46) = 0.50$, $p = .61$). In addition, a paired samples *t*-test performed on data from female *Setd1a*$^{+/-}$ mice revealed that PPI at 1.0 mg/kg was not significantly different from vehicle ($t(5) = 1.56$, $p = .18$). Thus, this apparent normalisation is probably due to greater variability in this group at the high dose. These results show that risperidone did not reverse PPI deficits in *Setd1a*$^{+/-}$ mice.

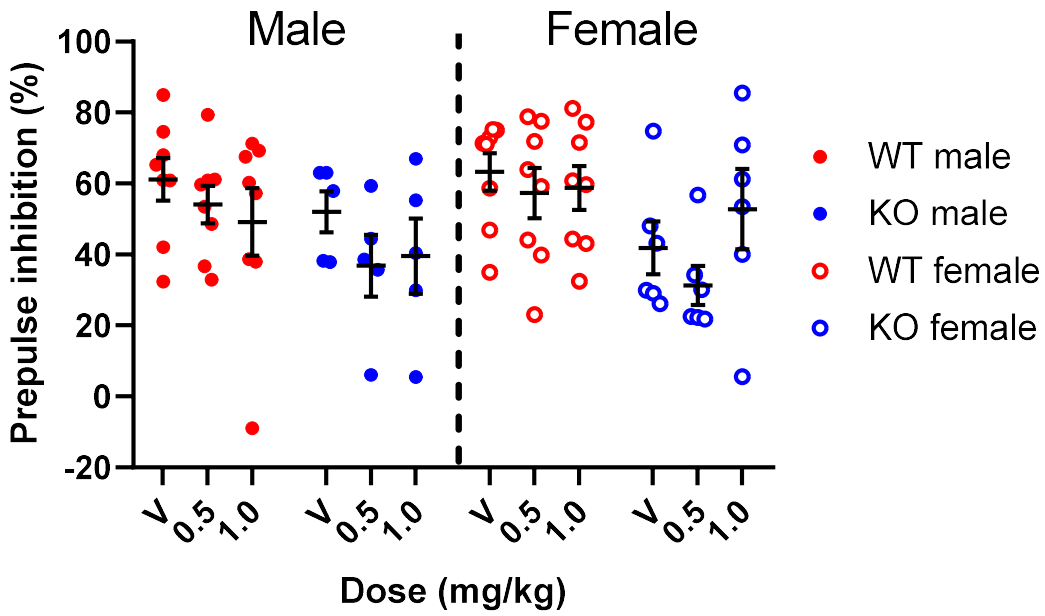


**Figure 6.10. Effect of risperidone on PPI in *Setd1a*$^{+/-}$ and WT mice.** Mean (+/- SEM) PPI of the ASR at 120 dB (above background) pooled across 8 and 16 (dB above background) prepulses following IP administration of vehicle, 0.5 or 1.0 mg/kg risperidone, presented separately for males and females.

### 6.4. Discussion

This chapter examined whether PPI deficits in *Setd1a*$^{+/-}$ mice are reversed by haloperidol or risperidone. First, the effects of *Setd1a* haploinsufficiency on sensorimotor gating (i.e., increased startle magnitude and reduced PPI) described in Chapter 5.3.4 were replicated in a separate cohort under basal conditions. However, genotype effects on PPI were more pronounced in females than males in the drug challenge experiment. Neither haloperidol nor risperidone were able to rescue PPI deficits at dosages that had effects on WT sensorimotor gating in pilot work. Unexpectedly, a sexually dimorphic effect of risperidone on startle magnitude was observed, whereby *Setd1a*$^{+/-}$ males (but not females) showed an insensitivity to the startle-reducing effect of the drug.

Both haloperidol and risperidone have previously been shown to reverse PPI deficits in several rodent models of schizophrenia (Geyer et al., 2001; Swerdlow et al., 2008). Therefore, the inability to enhance PPI in *Setd1a*$^{+/-}$ mice is not due to a general insensitivity of PPI to these drugs. Rather, it suggests that the neurobiological changes that cause deficient PPI in *Setd1a*$^{+/-}$ mice are not appropriately targeted by haloperidol or risperidone. It is possible that a particular combination of receptor

binding and/or targeting additional receptor types may be necessary. For example, it would be interesting to test the efficacy of olanzapine, quetiapine, or clozapine. These atypical antipsychotics have mixed receptor-binding profiles with varying affinities for additional receptors (i.e., muscarinic acetylcholine M1 and histaminergic H1 receptors) that are not bound by haloperidol or risperidone at therapeutic doses (Miyamoto et al., 2005). In addition, putative antipsychotics could be tested in the *Setd1a*$^{+/-}$ model. For example, co-agonists of the glycine site on the NMDA receptor, such as glycine (Le Pen et al., 2003) and D-serine (Kanahara et al., 2008), and the DAO inhibitor sodium benzoate (Matsuura, Fujita, Iyo, & Hashimoto, 2015) have been reported to reverse PPI deficits in other rodent models of schizophrenia. Interestingly, a recent study has shown that inhibition of the histone demethylase LSD1 with either tranylcypromine (TCP) or ORY-1001 rescues the effects of *Setd1a* haploinsufficiency on aberrant axon-branching *in vitro* and working memory deficits *in vivo* (Mukai et al., 2019). Future work should test whether LSD1 inhibition is also effective for improving sensorimotor gating impairments in *Setd1a*$^{+/-}$ mice.

Despite the inability of haloperidol or risperidone to modify PPI deficits in *Setd1a*$^{+/-}$ mice, an interesting dissociation was observed in their effects on the startle response. Specifically, the magnitude of startle response was dose-dependently reduced by risperidone in all groups except for *Setd1a*$^{+/-}$ males. Conversely, all groups responded equally to haloperidol. Since risperidone binds preferentially to 5-HT2A receptors (Miyamoto et al., 2005), this finding may suggest that, in males, *Setd1a* haploinsufficiency causes abnormal 5-HT2A receptor functioning. Indeed, reduced expression of 5-HT2A receptors has been reported in schizophrenia patients (Burnet et al., 1996; Harrison, 1999c). However, risperidone also has moderate to high affinity for several other receptors (i.e., D2, D3, 5-HT2C, 5-HT7, and alpha-1 and alpha-2 adrenergic receptors), and D2 receptor occupancy is increased at higher doses (Kusumi et al., 2015). Thus, further work is needed to determine the extent to which this effect is caused by 5-HT2A receptor dysfunction, such as examining 5-HT2A receptor gene expression levels in the brain and testing propensity for head-twitch responses following administration of 2,5-Dimethoxy-4-iodoamphetamine (DOI), which is known to depend on 5-HT2A receptor activation (Willins & Meltzer, 1997). Nevertheless, it is interesting to note that sexually dimorphic effects of *Setd1a* loss of function on placental gene expression were also observed in males but not females (see Chapter 4).

Although PPI deficits in *Setd1a*$^{+/-}$ mice were replicated in the pre-test session, the genotype effect on PPI was not sustained in males allocated to the haloperidol drug

challenge. This is likely due to reduced statistical power in combination with the fact that male WTs showed a low level of PPI. Indeed, PPI in WT males was significantly lower than WT females, whereas *Setd1a*$^{+/-}$ males showed a similar level of PPI to *Setd1a*$^{+/-}$ females. Therefore, the “low-gating” WT males may have masked a genotype effect in males in the haloperidol group. An alternative possibility is that the effects of *Setd1a* haploinsufficiency on PPI are stronger in females. Interestingly, evidence from humans suggests that PPI is more impaired in females with schizophrenia than males (Swerdlow et al., 2014). While this cannot be ruled out, it is unlikely to be the case here since no significant sex differences in the effect of *Setd1a* on PPI were observed at baseline or in a larger sample (Chapter 5.3.4).

In conclusion, PPI deficits in *Setd1a*$^{+/-}$ mice were not rescued by haloperidol or risperidone, two established antipsychotics that have both been used successfully in previous preclinical studies. Further work is needed to assess the efficacy of other established and putative antipsychotic compounds. Unexpectedly, male (but not female) *Setd1a*$^{+/-}$ mice showed an insensitivity to the inhibitory effects of risperidone on the ASR. This indicates sexually dimorphic effects of *Setd1a* haploinsufficiency on brain function, potentially implicating abnormal 5-HT2A receptor functioning.

## Chapter 7: Isolating the contribution of *Setd1a* haploinsufficiency in the nervous system to behavioural phenotypes using a conditional *Setd1a* KO mouse model

### 7.1. Introduction

The aim of this chapter was to generate and characterise a conditional knockout mouse model of *Setd1a* haploinsufficiency confined to the (central and peripheral) nervous system. This work was conducted to examine the extent to which behavioural consequences of *Setd1a* loss of function have their origin in effects solely on the nervous system.

Conditional mutagenesis involves spatially and/or temporally restricted genetic modification (Gavériaux-Ruff & Kieffer, 2007). This approach enables investigation of the nervous system function of genes that are widely expressed in several tissues, whereby constitutive inactivation is associated with deficits arising in multiple systems (Deussing, 2013). Constitutive *Setd1a* haploinsufficiency has been reported to cause immune and metabolic phenotypes by the IMPC, including decreased leukocyte and B cell number, increased $CD8^+$ T cell number, decreased circulating (HDL and LDL) cholesterol levels, decreased total body fat, and decreased circulating alkaline phosphatase and alanine transaminase levels. It is possible that these phenotypes could exert effects on behaviour that are independent of the nervous system role of *Setd1a*. Therefore, it is necessary to constrain *Setd1a* loss of function to the nervous system to isolate the biological mechanisms underlying behavioural phenotypes.

The Cre/LoxP system is the most widely used tool for creating conditional knockout mouse models (Lewandoski, 2001). Cre recombinase is an enzyme that catalyses DNA recombination between two LoxP sites (Heldt, 2009). A Cre driver line that expresses Cre recombinase under the control of a promoter known to be expressed in the target cell types is crossed with a line in which the critical exon of the gene of interest is 'floxed' (i.e., flanked by LoxP sites). This results in excision or inversion of the floxed exon only in cells that express Cre recombinase, leading to tissue-specific disruption of gene function.

Several Cre lines are available that drive recombination in the nervous system, many of which result in brain region or cell-type specific recombination (Morozov, Kellendonk, Simpson, & Tronche, 2003). Nestin-Cre mice were chosen to create the *Setd1a* conditional knockout line because this driver results in widespread loss of function in neuronal and glial progenitors throughout the developing brain. These mice express Cre recombinase in neural stem cells under the control of the rat Nestin

promoter and nervous system-specific enhancer (Tronche et al., 1999). Recombination occurs from E11.5, which coincides with the peak *Setd1a* expression levels reported in Chapter 3. Therefore, effects of *Setd1a* loss of function on neurodevelopmental processes that have downstream effects on later brain function should be recapitulated in this model.

Findings from Chapter 5 revealed that constitutive *Setd1a* haploinsufficiency causes increased anxiety in the open field test (OFT) and altered sensorimotor gating (elevated acoustic startle response (ASR) and reduced prepulse inhibition (PPI)), with normal locomotor activity levels, motoric function, and object recognition memory. The aim of this chapter was to explore the extent to which these behavioural effects are caused by *Setd1a* loss of function in the nervous system. To this end, conditional KO mice were subjected to an identical behavioural testing pipeline to enable comparison with results from the constitutive KO model.

## 7.2. Methods

### *7.2.1. Generation of the model*

Heterozygous *Setd1a* floxed mice were crossed with a hemizygous B6.Cg-Tg(Nes-cre)1Kln/J line (referred to as 'Nes-Cre'), purchased from The Jackson Laboratory. This generated mixed litters comprising conditional KO (referred to as ‘cKO’) mice and three littermate control groups (WT, Nes-cre and floxed). These were included in all experiments to assess potential confounding effects of other constructs involved in generating the cKO mouse line (i.e., Cre transgene and LoxP sites).

To establish that *Setd1a* knockdown was achieved in the cKO model, *Setd1a* mRNA and SETD1A protein levels were assessed in whole brain tissue using RT-qPCR (N = 5 per group) and Western blot (N = 4 per group), respectively. To demonstrate that *Setd1a* knockdown was specific to the nervous system, a PCR for the deleted *Setd1a* allele (see Chapter 2.2.2) was performed on DNA extracted from several brain regions (frontal cortex, hippocampus, striatum, midbrain, and cerebellum) and other non-nervous system tissue (testis, kidney, liver, heart, lung, pancreas, thymus, large intestine, muscle, and spleen) in adulthood (approximately 7 months old).

### *7.2.2. Animals*

77 adult mice (45 male and 32 female) were included in behavioural experiments (Table 7.1). Behavioural testing started when the animals were 8 weeks old and was conducted in the order described in Chapter 2.3 (i.e., EPM, OFT, locomotor activity, sensorimotor gating, rotarod, and novel object recognition).

**Table 7.1.** Genotype and sex information for mice included in behavioural experiments.

| | cKO | WT | Nes-Cre | Floxed | Total |
|---|---|---|---|---|---|
| Male | 15 | 11 | 11 | 8 | 45 |
| Female | 7 | 7 | 10 | 8 | 32 |
| **Total** | **22** | **18** | **21** | **16** | **77** |

*7.2.3. Data analysis*

RT-qPCR and Western blot data were prepared for analysis as described in Chapter 2. ΔCT values (RT-qPCR) and normalised fluorescence (Western blot) were analysed using a one-way ANOVA with genotype as the between-subjects factor, followed by Dunnett post-hoc tests to compare all groups with WT.

Multivariate ANOVAs were used to analyse data from the EPM and OFT. One female WT mouse was identified as a multivariate outlier in the OFT (Mahalanobis distance $p < .001$) and was excluded from the analysis. The four dependent variables included in each analysis were: distance moved, proportion of time spent in anxiogenic regions, latency of first entry into anxiogenic regions (log transformed to remove positive skew), and number of entries into anxiogenic regions. Where a significant multivariate result was observed, separate between-subjects ANOVAs were conducted for each dependent variable. Dunnett post-hoc tests were conducted for significant main effects of genotype to identify which genotypes were significantly different from WT.

Locomotor activity data were analysed by a mixed ANOVA with day (3 levels) and quartile (4 levels) as within-subjects factors and genotype and sex as between-subjects factors. Greenhouse-Geisser corrected results are reported due to violations of sphericity, indicated by a significant Mauchly's test. Significant interactions were followed up with simple main effects analyses and Bonferroni corrected post-hoc tests.

Weight-adjusted ASR data were analysed using a mixed ANOVA with pulse amplitude (80 dB, 90 dB, 100 dB, 110 dB, and 120 dB) as a within-subjects factor and genotype and sex as between-subjects factors. PPI data were analysed using a mixed ANOVA with prepulse amplitude (4 dB, 8 dB, and 16 dB) as a within-subjects factor and genotype and sex as between-subjects factors. Greenhouse-Geisser corrected results are reported where violations of sphericity occurred.

To assess motor learning in the Rotarod performance test, the latency to fall data from the five accelerating runs were analysed with a mixed ANOVA with run (5 levels) as a within-subjects factor and genotype and sex as between-subjects factors. Motor coordination was assessed by calculating the average latency to fall at each fixed speed for each mouse. These data were analysed using a mixed ANOVA with speed (10 levels) as a within-subjects factor and genotype and sex as between-subjects factors. Greenhouse-Geisser corrected results are reported due to violations of sphericity. Bonferroni-corrected pairwise comparisons were conducted to examine significant interactions.

Data from the NOR test were analysed using a mixed ANOVA with delay (30 minutes vs. 24 hours) as a within-subjects factor and genotype and sex as between-subjects factors.

## 7.3. Results

### *7.3.1. Model validation*

A significant main effect of genotype on *Setd1a* mRNA expression in E13.5 brain tissue was observed ($F(3, 16) = 3.78$, $p = .03$; Figure 7.1A). Dunnett's post-hoc tests showed that expression levels of *Setd1a* were reduced by approximately 30 % in cKO brain relative to WT ($p = .04$). As expected, *Setd1a* expression levels in Nes-cre and floxed groups were similar to WT (both $p > .99$), suggesting intact *Setd1a* expression in these control groups. Analysis of the Western blot data showed that while the main effect of genotype was not statistically significant ($F(3, 12) = 1.03$, $p = .41$), a 30 % reduction was also observed for *Setd1a* protein levels in cKO mice (Figure 7.1B). This demonstrates that *Setd1a* expression levels were reduced in E13.5 brain tissue. However, the magnitude of reduction achieved was less than the 50 % reduction that would be predicted to occur due to haploinsufficiency.

Figure 7.1C shows an example PCR for the deleted *Setd1a* allele performed on several brain regions and other non-nervous system tissues. As was expected, the deleted allele (174 bp) was only present in brain tissue. Only the floxed allele (259 bp) was observed in all other non-nervous system tissues. This shows that *Setd1a* haploinsufficiency was specific to the nervous system. However, the floxed allele was also observed in all brain regions, indicating the presence of residual non-recombined floxed allele in some cells.

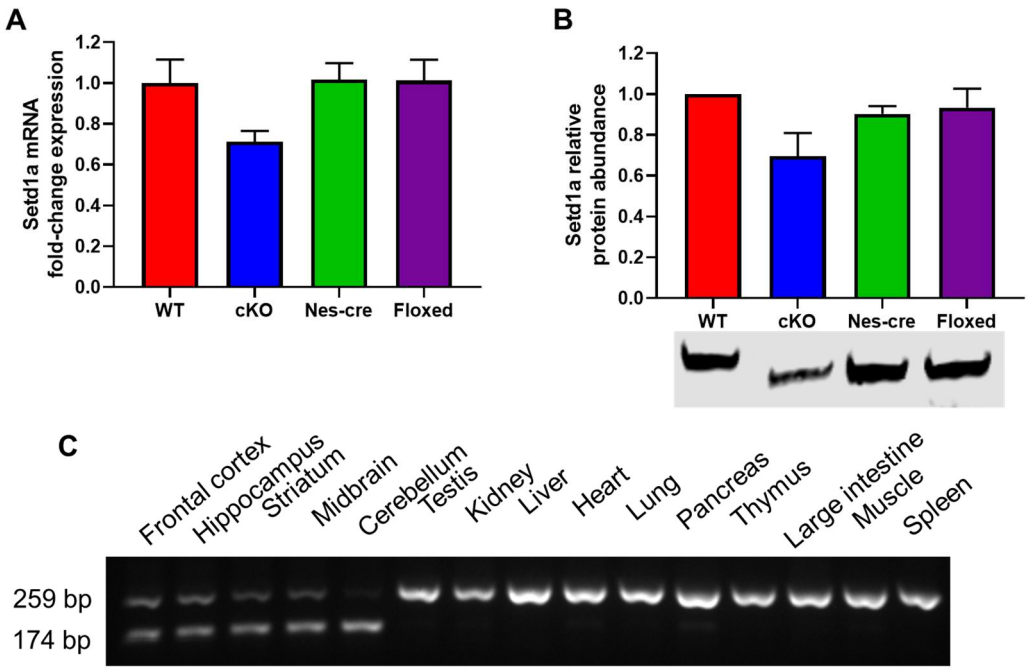


**Figure 7.1. Confirmation of brain-specific knockdown of *Setd1a* in the cKO model.** Mean (+/- SEM) fold-change in expression of **A)** *Setd1a* mRNA and **B)** SETD1A protein abundance relative to WT. **C)** Example PCR for the deleted (174 bp) and floxed (259 bp) alleles in brain and non-nervous system tissue.

*7.3.2. Elevated plus maze*

There was no significant multivariate effect of genotype on indices of anxiety-related behaviour ($F(12, 174.91) = 1.36$, $p = .19$; Wilk's $\lambda = 0.79$; Figure 7.2). A significant multivariate main effect of sex was observed ($F(4, 66) = 3.21$, $p = .02$; Wilk's $\lambda = 0.84$; Table 7.2). Follow-up analysis revealed that males took significantly longer than females to enter one of the open arms ($F(1, 69) = 11.10$, $p = .001$). There were no significant sex differences observed for distance moved ($p = .23$), proportion of time spent on the open arm ($p = .27$), or number of entries into the open arm ($p = .11$). There was also no significant interaction between genotype and sex ($F(12, 174.91) = 0.94$, $p = .51$; Wilk's $\lambda = 0.85$).

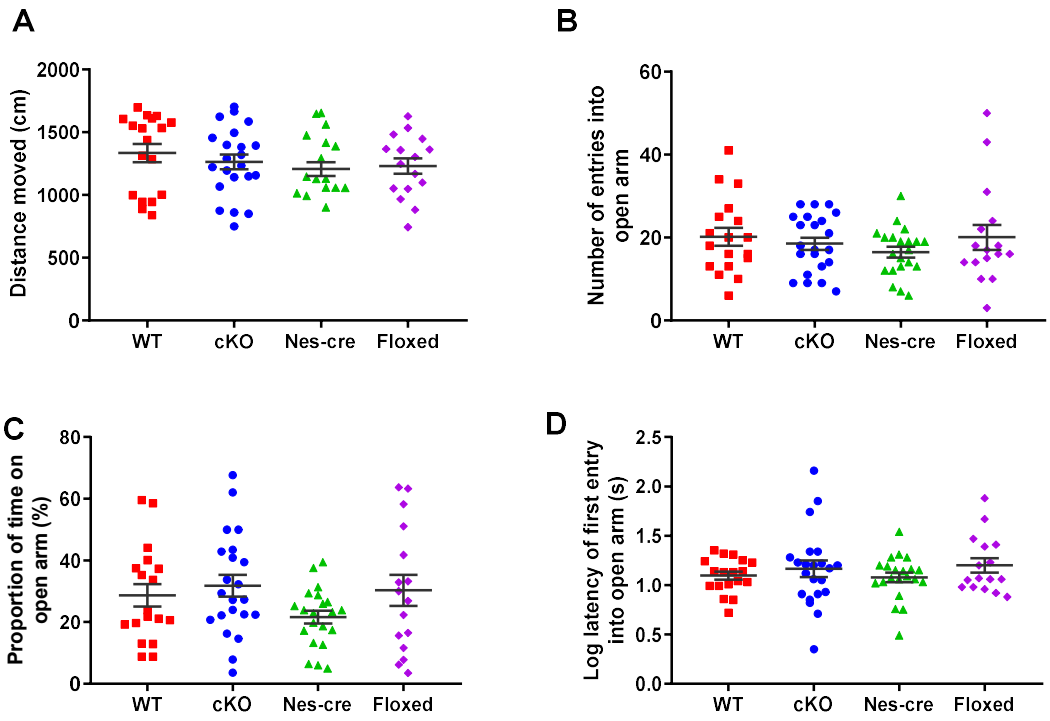


**Figure 7.2. Effects of conditional knockdown of *Setd1a* on anxiety-related behaviour in the EPM.** Mean (+/- SEM) **A)** distance moved, **B)** number of open arm entries, **C)** proportion of time on open arms, and **D)** log latency of first entry into an open arm.

**Table 7.2.** Mean (SD) indices of anxiety-related behaviour in the EPM in males and females pooled across genotypes.

| Dependent variable | Males | Females |
|---|---|---|
| Distance moved (cm) | 1232.6 (287.3) | 1304.5 (253.1) |
| Number of entries into open arms | 17.5 (7.5) | 20.3 (9.5) |
| Proportion of time spent on open arms (%) | 26.8 (16.2) | 30.1 (15.3) |
| Log latency of first entry into open arm | 1.2 (0.3) | 1.0 (0.2) |

*7.3.3. Open field test*

There was a significant multivariate main effect of genotype on anxiety-related behaviour in the OFT ($F(12, 172.27) = 2.15$, $p = .01$; Wilk's $\lambda = 0.68$). Follow-up ANOVAs revealed a significant main effect of genotype for distance travelled ($F(3,68) = 4.21$, $p = .01$; Figure 7.3A), number of entries into the inner zone ($F(3,68) = 5.64$, $p = .002$; Figure 7.3B), proportion of time spent in the inner zone ($F(3,68) = 4.46$, $p = .01$; Figure 7.3C), and log latency of first entry into the inner zone ($F(3,68) = 3.60$, $p$

= .02; Figure 7.3D). Dunnett post-hoc tests revealed *Setd1a* cKO mice displayed increased anxiety-related behaviour relative to WTs, indicated by a significant reduction in distance moved ($p$ = .046), making significantly fewer entries into the inner zone ($p$ = .046), and spending significantly less time in the inner zone ($p$ = .04). However, there was no significant difference in log latency of first entry into the inner zone ($p$ = .48). In addition, Nes-Cre mice showed a similar pattern of elevated anxiety related behaviour, evidenced by a significant reduction in overall distance travelled ($p$ = .02), significantly fewer entries into the inner zone ($p$ = .01), a significantly lower proportion of time in the inner zone ($p$ = .01) and a significantly longer latency of first entry into the inner zone ($p$ = .03). There were no significant differences between WT and floxed animals for any of the measures of anxiety (all $p$ > .09).

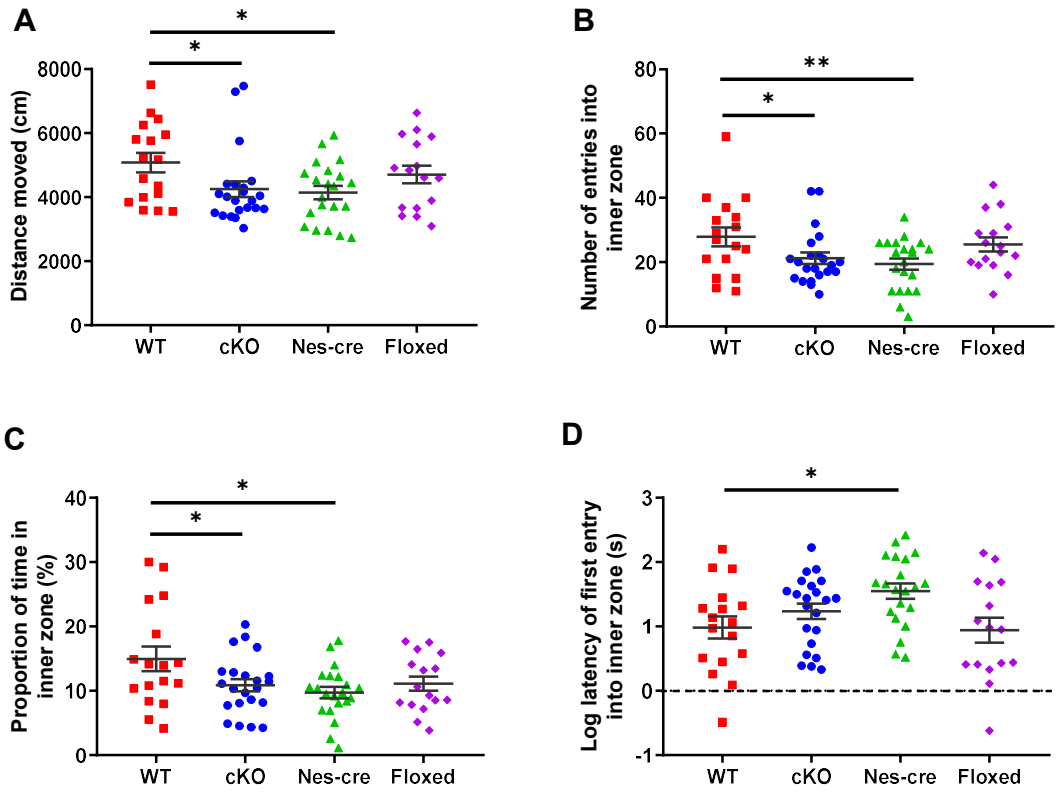


**Figure 7.3. Effects of conditional knockdown of *Setd1a* on anxiety-related behaviour in the OFT.** Mean (+/- SEM) **A)** distance moved, **B)** number of inner zone entries, **C)** proportion of time in inner zone, **D)** and log latency of first entry into inner zone; **$p \leq .01$, * $p < .05$.

There was also a significant multivariate main effect of sex on anxiety-related behaviour in the OFT ($F(4, 65) = 3.38$, $p$ = .01; Wilk's λ = 0.83; Table 7.3). Follow-up testing revealed that males travelled significantly less distance ($F(1, 68) = 6.46$, $p$ =

.013), made significantly fewer entries ($F$(1, 68) = 12.91, $p$ = .001) and spent significantly less time ($F$(1, 68) = 7.99, $p$ = .01) in the inner zone relative to females. However, there was no significant sex difference in log latency of first entry into the inner zone ($F$(1, 68) = 0.02, $p$ = .90). In addition, there was no significant multivariate interaction between sex and genotype ($F$(12, 172.27) = 1.04, $p$ = .16; Wilk's λ = 0.83).

**Table 7.3.** Mean (SD) indices of anxiety-related behaviour in the OFT in males and females, pooled across genotypes.

| Dependent variable | Males | Females |
|---|---|---|
| Distance moved (cm) | 4270.3 (1017.6) | 4839.0 (1263.4) |
| Number of entries into inner zone | 20.6 (7.6) | 26.9 (11.5) |
| Proportion of time spent in inner zone (%) | 10.3 (5.3) | 13.3 (5.6) |
| Log latency of first entry into inner zone | 1.2 (0.7) | 1.2 (0.6) |

*7.3.4. Locomotor activity*

There was no significant effect of genotype on number of beam breaks ($F$(3, 69) = 1.08, $p$ = .36), suggesting that overall activity levels were equivalent across groups (Figure 7.4). Activity levels of females were significantly greater than males ($F$(1, 69) = 13.90, $p$ < .001; Table 7.4). However, there was no significant interaction between sex and genotype ($F$(3, 69) = 1.85, $p$ = .15).

**Table 7.4.** Mean (SD) total beam breaks for each day in males and females, pooled across genotypes.

| Number of beam breaks | Males | Females |
|---|---|---|
| Day 1 | 1952.6 (813.3) | 2716.2 (1298.0) |
| Day 2 | 1506.9 (852.2) | 2467.0 (1587.7) |
| Day 3 | 1281.4 (811.2) | 2404.7 (1627.9) |

A significant main effect of day was observed ($F$(1.81, 125.13) = 27.68, $p$ < .001), which was qualified by a significant interaction between day and genotype ($F$(5.44, 125.13) = 2.91, $p$ = .01; Figure 7.4A). Simple main effects analyses revealed a significant effect of day for WTs ($F$(2, 68) = 15.56, $p$ < .001) and floxed mice ($F$(2, 68) = 6.91, $p$ = .002), indicating the expected reduction in activity levels across the test days as the animals habituated to the testing environment. However, there was no significant effect of day for *Setd1a* cKOs ($F$(2, 68) = 1.56, $p$ = .22) or Nes-Cre mice

($F(2, 68) = 1.91$, $p = .16$), suggesting that these groups did not habituate to the testing environment across consecutive test days.

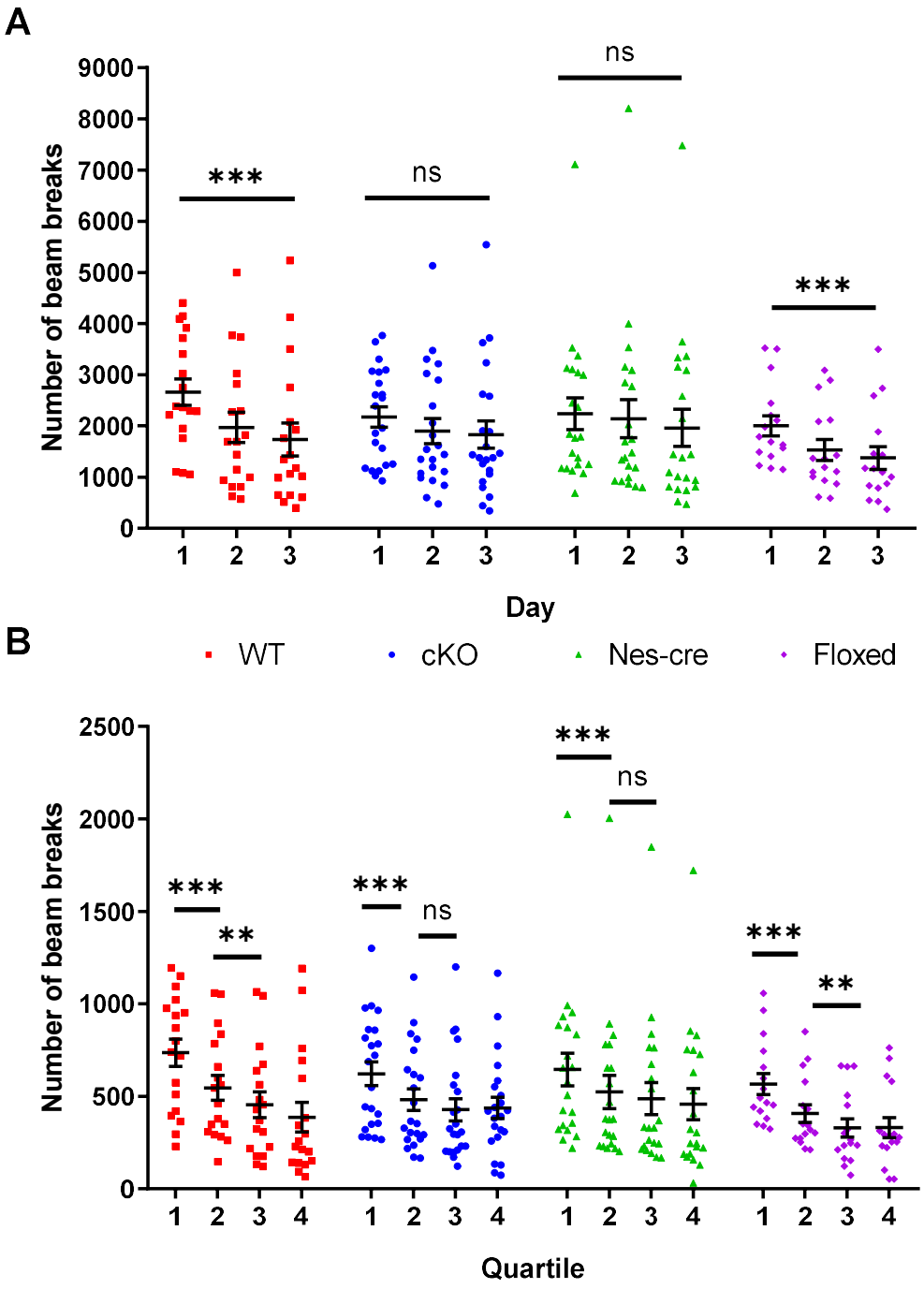


**Figure 7.4. Effects of conditional knockdown of *Setd1a* on locomotor activity levels.** Mean (+/- SEM) beam breaks **A)** for each day, summed across a whole session and **B)** for each quartile, pooled across sessions; *** $p < .001$, ** $p < .01$.

A significant main effect of quartile was observed ($F(2.01, 138.42) = 92.56$, $p < .001$), which was also qualified by a significant interaction with genotype ($F(6.02, 138.42) =$

2.41, $p$ = .03; Figure 7.4B). Simple main effects analyses revealed a significant effect of quartile for all four groups (all $p$ < .001). Post-hoc pairwise comparisons revealed that all four groups made significantly fewer beam breaks in the second quartile relative to the first quartile (all $p$ < .001). However, while there was a significant reduction in activity levels between the second and third quartile for WTs ($p$ = .002) and floxed mice ($p$ = .009), no significant difference was observed in *Setd1a* cKOs ($p$ = .44) or Nes-Cre mice ($p$ = .57). No further significant decline in activity levels between the third and fourth quartile was observed in any of the groups (all $p$ > .36). This suggests that habituation of activity levels within a test session was also blunted in *Setd1a* cKO and Nes-Cre mice.

### *7.3.5. Sensorimotor gating*

Analysis of the weight-adjusted ASR data revealed a significant main effect of pulse amplitude ($F$(1.54, 106.02) = 186.68, $p$ < .001; Figure 7.5), indicating that startle magnitude was greater on trials with a louder pulse stimulus. However, there was no significant effect of genotype ($F$(3, 69) = 0.61, $p$ = .61). There was also no significant effect of sex ($F$(1, 69) = 1.28, $p$ = .26) or interaction between sex and genotype ($F$(3, 69) = 1.24, $p$ = .30).

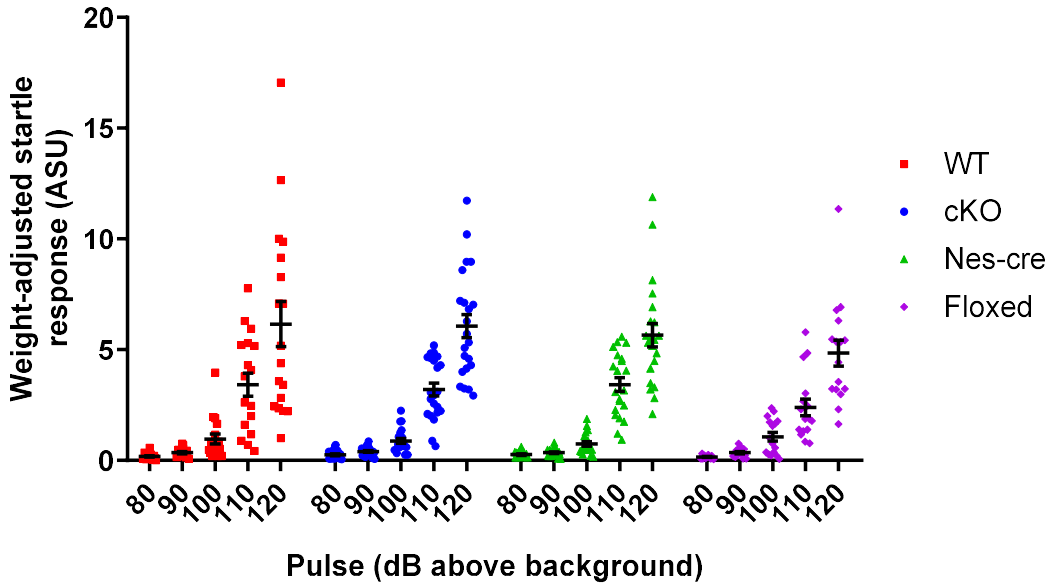


**Figure 7.5. Effect of conditional knockdown of *Setd1a* on ASR.** Mean (+/- SEM) weight-adjusted ASR at 80-120 dB (above background).

Analysis of the PPI data revealed that louder prepulse stimuli elicited significantly greater PPI ($F$(2, 138) = 278.37, p < .001; Figure 7.5B). However, there was no

significant main effect of genotype on the magnitude of PPI ($F(3, 69) = 2.25$, $p = .09$). There was no significant main effect of sex ($F(1, 69) = 1.24$, $p = .27$) or interaction between sex and genotype ($F(3, 69) = 0.38$, $p = .77$).

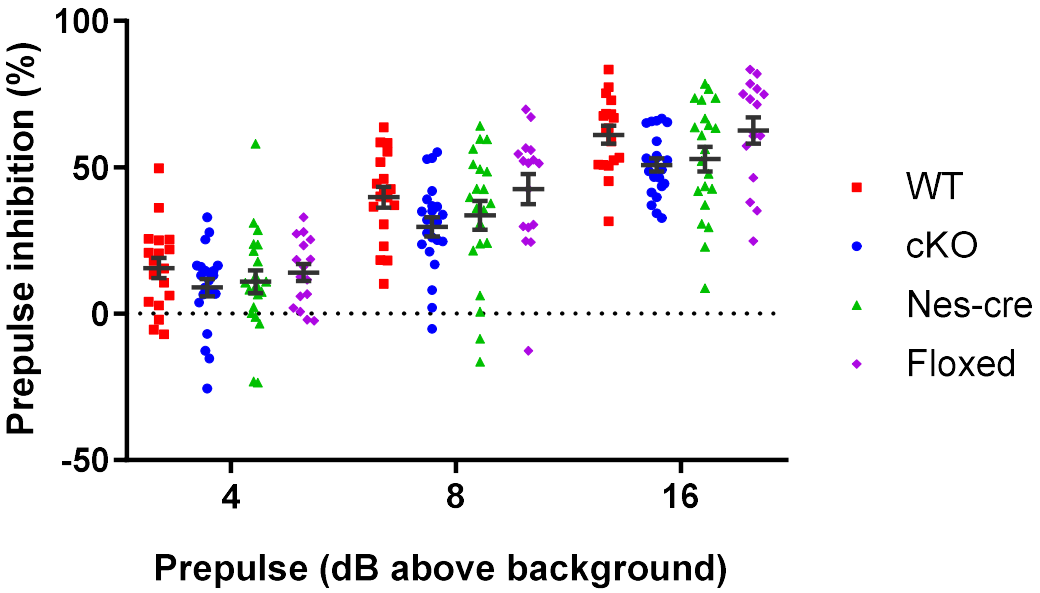


**Figure 7.6. Effect of conditional knockdown of *Setd1a* on PPI of the ASR.** Mean (+/- SEM) PPI by a 4, 8, and 16 dB (above background) prepulse.

*7.3.6. Rotarod performance test*

Analysis of the latency to fall on accelerating trials revealed a significant main effect of run ($F(3.09, 213.3) = 24.42$, $p < .001$; Figure 7.7A), indicating that the latency to fall was significantly increased by training. There was no significant main effect of genotype ($F(3, 69) = 1.23$, $p = .31$) or sex ($F(1, 69) = 0.10$, $p = .75$). A significant interaction was observed between genotype and sex ($F(3, 69) = 3.13$, $p = .03$). Post-hoc tests revealed that no genotype pairwise comparisons within each sex were significantly different from WT (all $p > .41$). However, across trials, the latency to fall was significantly longer in female cKOs (mean = 155.7, SEM = 12.80) compared with male cKOs (mean = 211.43, SEM = 18.71; $p = .02$). No significant sex differences were observed for the other genotypes (data not shown; all $p > .10$). Importantly, there were no significant interactions between run and genotype ($F(9.27, 213.31) = 0.74$, $p = .68$), run and sex ($F(3.09, 213.31) = 0.99$, $p = .40$), and no three-way interaction between run, sex, and genotype ($F(9.27, 213.31) = 0.70$, $p = .71$) indicating equivalent motor learning across groups.

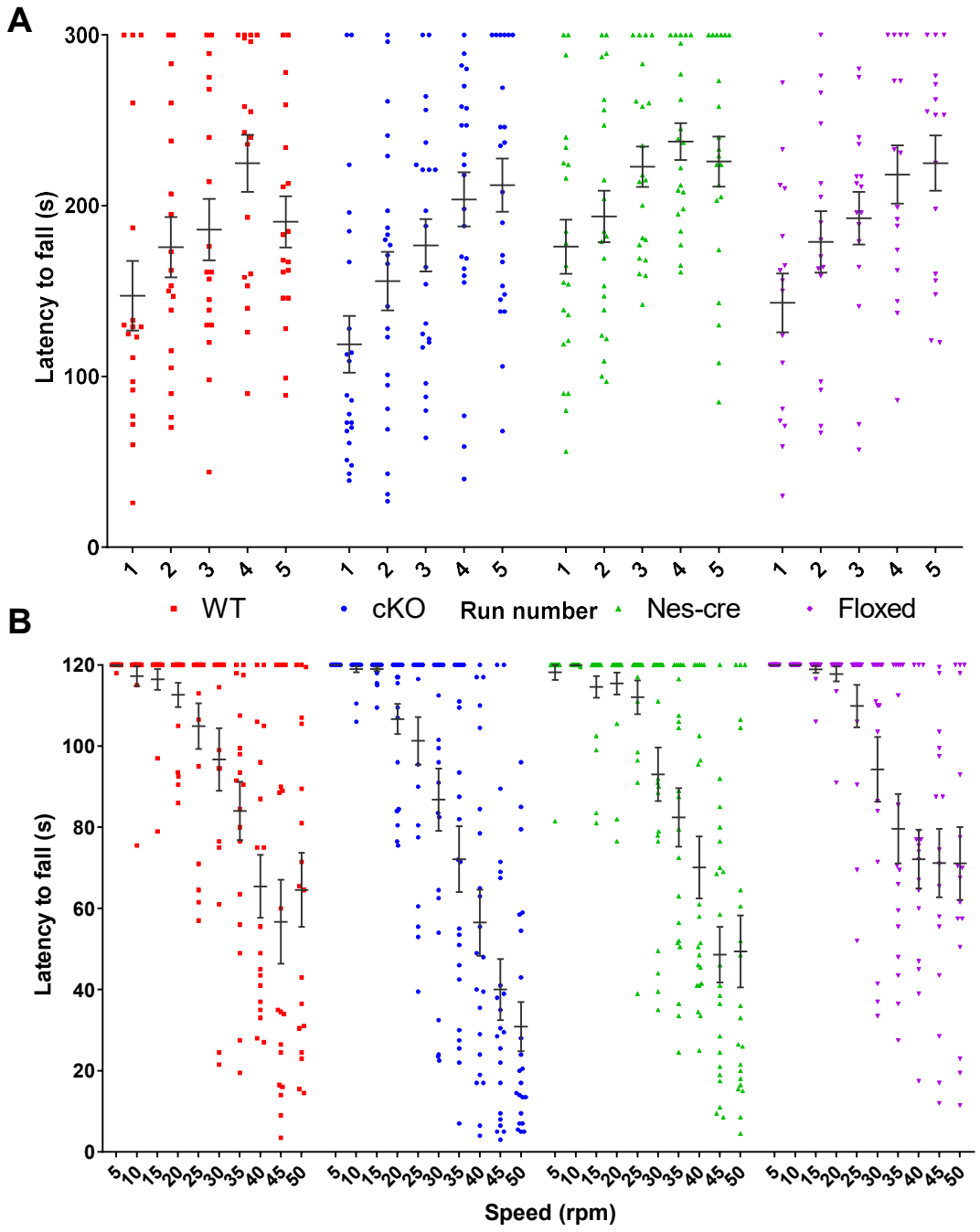


**Figure 7.7. Effect of conditional *Setd1a* knockdown on motoric function in the Rotarod test.** Mean (+/- SEM) latency to fall **A)** on accelerating trials (5-50 rpm at 0.15 rpm/s) and **B)** at fixed speeds increasing in 5 rpm increments from 5-50 rpm.

Analysis of the latency to fall on fixed-speed trials revealed latency to fall was significantly shorter at higher speeds ($F(4.12, 284.23) = 110.82$, $p < .001$; Figure 7.7B). There was no significant main effect of genotype ($F(3, 69) = 1.38$, $p = .26$) or sex ($F(1, 69) = 0.001$, $p = .97$). However, a significant three-way interaction between speed, sex, and genotype was observed ($F(12.36, 284.23) = 1.86$, $p = .04$). Post-hoc analysis revealed that no genotype pairwise comparisons within each sex were

significantly different from WT (all $p > .13$), indicating equivalent motor coordination across genotypes. Sex differences were observed at some speeds but no consistent pattern was observed across genotypes (Table 7.5).

**Table 7.5.** Mean (SD) latency to fall (s) on fixed-speed Rotarod trials for each genotype, stratified by sex.

| | **WT** | | **cKO** | | **Nes-cre** | | **Floxed** | |
|---|---|---|---|---|---|---|---|---|
| | Male | Female | Male | Female | Male | Female | Male | Female |
| Latency to fall at 5 rpm (s) | 119.82 (0.60) | 120.0 (0.00) | 120.0 (0.00) | 120.0 (0.00) | **120.0 (0.00)** | **116.20 (12.17)** | 120.0 (0.00) | 120.0 (0.00) |
| Latency to fall at 10 rpm (s) | 115.95 (13.41) | 119.29 (1.89) | 118.43 (4.22) | 120.0 (0.00) | 120.0 (0.00) | 119.95 (0.16) | 120.0 (0.00) | 120.0 (0.00) |
| Latency to fall at 15 rpm (s) | 117.91 (6.93) | 114.14 (15.49) | 118.53 (3.01) | 120.0 (0.00) | 111.55 (15.40) | 117.90 (6.64) | 120.0 (0.00) | 117.81 (4.92) |
| Latency to fall at 20 rpm (s) | 112.41 (13.02) | 113.00 (13.15) | **102.07 (18.47)** | **116.57 (9.07)** | 114.72 (13.40) | 116.20 (12.02) | 115.56 (10.18) | 120.00 (0.00) |
| Latency to fall at 25 rpm (s) | 109.63 (23.07) | 97.50 (24.77) | **92.57 (29.59)** | **120.0 (0.00)** | 107.86 (25.17) | 116.65 (6.99) | 107.81 (24.80) | 111.94 (17.83) |
| Latency to fall at 30 rpm (s) | **84.32 (36.76)** | **116.21 (7.86)** | **75.20 (37.30)** | **111.71 (14.98)** | 93.50 (32.73) | 92.55 (28.71) | 107.94 (30.28) | 80.63 (28.97) |
| Latency to fall at 35 rpm (s) | 78.45 (34.72) | 92.79 (22.23) | 63.97 (39.53) | 89.64 (30.21) | 82.68 (30.92) | 82.15 (36.99) | **102.75 (30.34)** | **56.56 (19.00)** |
| Latency to fall at 40 rpm (s) | 62.68 (36.22) | 69.79 (28.69) | 53.10 (42.81) | 63.86 (27.12) | 64.68 (33.58) | 76.05 (37.50) | 86.94 (28.77) | 57.38 (21.96) |
| Latency to fall at 45 rpm (s) | 58.64 (45.53) | 53.71 (44.72) | 42.50 (41.07) | 34.71 (19.40) | 48.45 (35.15) | 48.80 (28.94) | 81.38 (25.04) | 60.94 (39.69) |
| Latency to fall at 50 rpm (s) | 62.41 (42.41) | 68.00 (34.75) | 29.43 (26.87) | 34.00 (33.66) | 59.32 (52.96) | 38.50 (16.80) | **89.56 (26.55)** | **52.63 (35.72)** |

Emboldened cells show significant sex difference (Bonferroni-corrected $p < .05$).

*7.3.7. Novel object recognition*

Analysis of the acquisition data revealed no effect of genotype on the time taken to achieve 40 seconds of object exploration ($F(3, 69) = 0.72$, $p = .54$; Table 7.6). Table 7.6 also shows raw object exploration times at test. Analysis of the discrimination ratios revealed a significant main effect of delay ($F(1, 69) = 4.57$, $p = .04$; Figure 7.8), indicating better object recognition memory at 30 minutes compared to 24 hours. There was no significant effect of genotype ($F(3, 69) = 0.92$, $p = .44$) and no significant interaction between genotype and delay ($F(3, 69) = 0.20$, $p = .89$). There was also no significant effect of sex ($F(1, 69) = 0.05$, $p = .82$) and no significant interaction between sex and genotype ($F(3, 69) = 0.22$, $p = .88$).

**Table 7.6.** Mean (SD) acquisition time and object exploration at test for the 30 minute and 24 hour retention intervals.

| | **30 mins** | | | | **24 hours** | | | |
|---|---|---|---|---|---|---|---|---|
| **Dependent variable** | WT | cKO | Nes-cre | Floxed | WT | cKO | Nes-cre | Floxed |
| Acquisition time (mins) | 8.89 (3.87) | 7.50 (3.71) | 9.64 (4.40) | 8.38 (3.58) | 7.06 (2.94) | 8.30 (3.83) | 8.86 (3.75) | 8.13 (3.45) |
| Novel object exploration time (s) | 20.58 (9.99) | 17.18 (9.32) | 14.65 (7.87) | 18.40 (9.91) | 6.53 (3.84) | 8.81 (4.97) | 9.41 (5.50) | 7.97 (4.86) |
| Familiar object exploration time (s) | 9.31 (2.12) | 8.71 (3.38) | 7.60 (4.58) | 9.62 (5.99) | 4.08 (2.52) | 6.75 (3.17) | 5.70 (2.92) | 6.08 (3.61) |

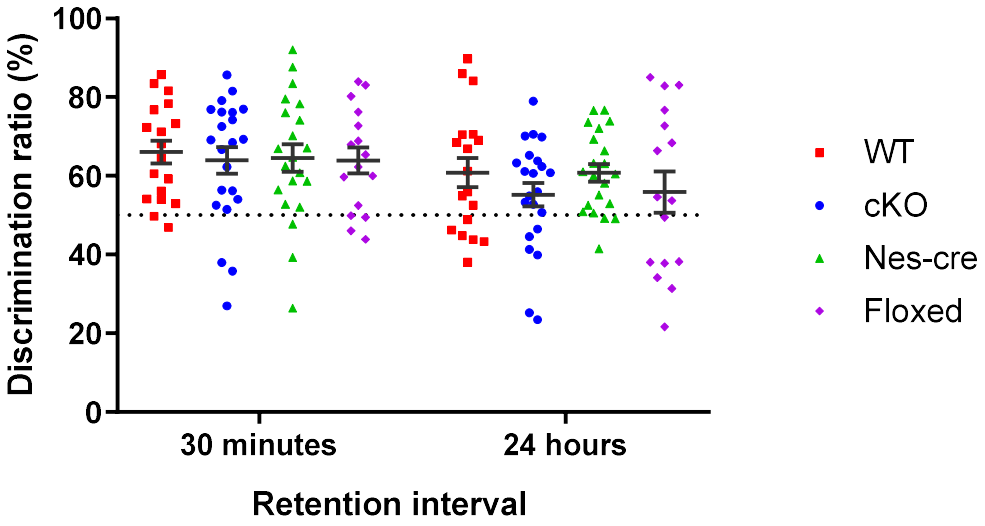


**Figure 7.8. Effect of conditional *Setd1a* knockdown on object recognition memory.** Mean (+/- SEM) discrimination ratios (%) after a 30 minute and 24 hour retention interval. Dotted line shows chance performance.

### 7.4. Discussion

This chapter investigated the extent to which increased anxiety-related behaviour in the OFT and aberrant sensorimotor gating (increased ASR and reduced PPI) identified in constitutive *Setd1a* KO mice is due to effects of *Setd1a* loss of function in the nervous system. Consistent with the results reported in Chapter 6, mice with conditional *Setd1a* loss of function constrained to the nervous system under a Nestin-Cre promoter showed; i) an increased anxiety phenotype in the OFT despite no difference in anxiety-related behaviour in the EPM, ii) normal motor coordination and motor learning, and iii) intact object recognition memory. In contrast to the constitutive KO, there were no significant effects on ASR or PPI. In addition, an impairment in habituation of activity levels in a novel environment was observed in conditional KOs, a finding that was not observed in constitutive KOs.

It is important to note that Nestin-Cre control mice also showed evidence of increased anxiety in the OFT and impaired habituation of activity levels in a novel environment. Since the conditional KO mice also carry the Nestin-Cre transgene, it is possible that this transgene may have exerted confounding effects on behaviour in the conditional KO mice. Although this possibility cannot be conclusively eliminated, this is unlikely to be the case for the anxiety phenotype because convergent findings are observed in the constitutive KO line that does not carry a Cre transgene. In contrast, impaired habituation was not observed in the constitutive KO mice, which may suggest that the habituation impairments observed in conditional KO mice are attributable to the

Nestin-Cre transgene. Future studies could investigate whether the observed effects are due to *Setd1a* loss of function using alternative Cre drivers, such as the BAF53b-cre line which results in neuron-specific recombination (Zhan et al., 2015).

The present findings underline the importance of including a Cre control group for behavioural phenotyping of conditional KO mice using the Cre/LoxP system (Harno, Cottrell, & White, 2013). A previous study has reported that Nestin-Cre mice display a mild increase in anxiety-related behaviour on the EPM but not in the OFT (Giusti et al., 2014). It is possible that differences in the experimental set-up and background strain may explain the differing results of the present experiments, whereby increased anxiety was observed in the OFT but not the EPM. Nevertheless, the present findings are consistent with a subtle anxiety phenotype in Nestin-Cre mice that should be considered when interpreting behavioural experiments using this Cre driver. Moreover, the observation of impaired habituation to a novel environment in Nestin-Cre mice in the present experiments may contribute to previously reported deficits in contextual-conditioning of fear (Giusti et al., 2014) and could suggest some mild spatial learning impairments. These behavioural alterations may be, in part, due to excitotoxic effects of Cre recombinase (Naiche & Papaioannou, 2007) leading to compromised neurodevelopment (Forni et al., 2006) and/or the presence of human growth hormone minigene in the Nestin-Cre transgene (Declercq et al., 2015).

In contrast to constitutive *Setd1a* KO mice, conditional KO mice did not show evidence of an increased ASR and the effects on PPI were not statistically significant. There are several explanations for these discrepant findings. First, the absence of significant effects on PPI may be due to a lack of statistical power due to the inclusion of additional control groups. Consistent with this, relative to WTs, conditional KO mice showed a non-significant reduction in PPI at all prepulse amplitudes. Another possibility is that *Setd1a* expression levels were not sufficiently reduced in the conditional KO model. In the constitutive KO, the deleted *Setd1a* allele is inherited, causing a 50 % reduction in *Setd1a* expression from conception. In the conditional KO, recombination of the floxed allele commences at E11.5 (Tronche et al., 1999), which means that neurodevelopmental processes prior to this will not be affected by *Setd1a* loss of function. In addition, only a 30 % reduction in *Setd1a* expression was observed in E13.5 brain tissue. This is less than would be expected to occur as a result of haploinsufficiency and may be because recombination using a Nestin-Cre driver has been reported to only occur in post-mitotic neurons (Liang, Hippenmeyer, & Ghashghaei, 2012). Another possibility is that the effects of *Setd1a* loss of function on sensorimotor gating are not directly mediated by effects in the brain; rather, they

could be indirect consequences of effects in other tissues that contribute to neurodevelopment and/or adult brain function (see General Discussion).

In this chapter, a conditional KO mouse model of *Setd1a* has been generated and subjected to an extensive behavioural characterisation to investigate behavioural consequences of *Setd1a* haploinsufficiency in the nervous system. Consistent with results of the constitutive KO described in Chapter 5, conditional KO mice displayed elevated anxiety-related behaviour in the OFT and no differences in motoric function or object recognition memory. In contrast to the constitutive KO, no significant effects on sensorimotor gating were observed in the conditional KO. In addition, confounding effects of Cre recombinase on behaviour were identified (i.e., increased anxiety in the OFT and reduced habituation in a novel environment). This highlights the importance of adequately designed experiments in conditional KO studies to prevent erroneous interpretation.

# Chapter 8: General Discussion

## 8.1. Overview

Translating genetic findings into mechanistic insights regarding neuropsychiatric disorder pathogenesis remains a major challenge for neuroscience. Exome sequencing studies are beginning to identify highly damaging loss of function (LoF) variants in protein-coding genes that are promising candidates for disease modelling. In particular, LoF variants in the *Setd1a* gene were the first rare variants to be identified for schizophrenia (Singh et al., 2016; Takata et al., 2014). This thesis aimed to investigate the functional consequences of *Setd1a* haploinsufficiency using a mouse model to recapitulate the predicted effects of LoF variants on gene function in human carriers. The primary aims and key findings from each experimental chapter are summarised in Table 8.1.

## 8.2. *Setd1a* haploinsufficiency causes neuropsychiatric endophenotypes that cannot be rescued by antipsychotic treatments

In depth behavioural phenotyping of the constitutive *Setd1a*$^{+/-}$ model (Chapter 5) revealed behavioural effects that resemble specific endophenotypes of schizophrenia and neurodevelopmental disorders, rather than a general impairment of functioning. Specifically, *Setd1a*$^{+/-}$ mice displayed increased anxiety-related behaviour in the OFT but not in the EPM. The reasons for these inconsistent findings are unclear but may be because the EPM was not as aversive as the OFT, reflected by high levels of open arm exploration in the EPM. Nevertheless, *Setd1a*$^{+/-}$ mice also displayed an exaggerated ASR, providing to an extent convergent evidence for an increased anxiety phenotype. Moreover, PPI of the ASR was markedly reduced in *Setd1a*$^{+/-}$ mice, a robust endophenotype of schizophrenia and neurodevelopmental disorders (Swerdlow et al., 2006; Swerdlow et al., 2018). There were no effects of *Setd1a* haploinsufficiency on locomotor activity levels, motoric functioning, or object recognition memory. These findings provide the first evidence that *Setd1a* haploinsufficiency causes heightened emotional reactivity and abnormal sensorimotor gating in a model system.

The effects of *Setd1a* haploinsufficiency on sensorimotor gating were replicated in a separate cohort (Chapter 6) and could not be rescued by haloperidol (primarily selective for the D2 receptor) or risperidone (high 5-HT2A receptor affinity). Both antipsychotics have previously been shown to improve PPI deficits in pharmacological and transgenic models (Geyer et al., 2001; Swerdlow et al., 2008). These findings demonstrate that the neurobiological mechanisms of deficient PPI in

*Setd1a*$^{+/-}$ mice are not corrected by haloperidol or risperidone. Further work is needed to establish the pathophysiological mechanisms underlying the effects of *Setd1a* haploinsufficiency on sensorimotor gating impairments. This would inform future pharmacological studies investigating the effects of other validated antipsychotics with different pharmacological profiles (e.g., clozapine, quetiapine, and olanzapine) and putative antipsychotics, such as DAO inhibitors which have the potential to normalise NMDA receptor function (Verrall et al., 2010). Another possibility includes treatment with histone demethylase inhibitors (TCP and ORY-1001) that have recently been shown to improve working memory deficits in *Setd1a*$^{+/-}$ mice (Mukai et al., 2019).

**Table 8.1.** Primary aims and key findings from each experimental chapter, associated limitations, and suggestions for future work.

| Aims | Key findings | Limitations | Future work |
|---|---|---|---|
| Assess transcriptomic effects of *Setd1a* haploinsufficiency in the developing mouse brain | • Peak *Setd1a* expression in embryonic brain<br>• Modest changes in gene expression: 267 differentially expressed genes with fold changes -0.67 – 1.19<br>• Significantly enriched for mitochondrion and nominal enrichment for cilium<br>• No enrichment for schizophrenia common variant association | • Whole brain may have masked subtle region- and cell-type specific effects<br>• Lack of power to detect sexually dimorphic effects | • Assess enrichment for CNVs associated with schizophrenia and neurodevelopmental disorders<br>• Single-cell RNA-seq to assess cell-type specific effects across development |
| Investigate effects of *Setd1a* loss of function on placental phenotypes and growth curves | • 8.9 % reduction in placental weight but no effect on foetal weight at E13.5<br>• Sexually dimorphic changes in placental gene expression in males but not females<br>• Reduced body weight at maternal separation (P28) in males but not females | • No histological assessment of placental morphological changes<br>• Lack of assessment of foetal weight later in gestation, birth weight, and early postnatal growth | • Developmental assessment of pup and placental weights<br>• Histology to confirm morphological changes<br>• Assessment of placental transport and endocrine functions |

| Aims | Key findings | Limitations | Future work |
|---|---|---|---|
| Perform behavioural characterisation of *Setd1a*$^{+/-}$ mice | • Increased anxiety in OFT but not EPM<br>• Increased ASR and decreased PPI<br>• No effects on locomotor activity, motoric function, or novel object recognition | • Inconsistent findings from EPM and OFT<br>• Limited assessment of cognitive function | • Assess other measures of anxiety (e.g., elevated zero maze and light-dark box)<br>• Cognitive testing of associative memory and attentional processing (e.g., 5-choice serial reaction time task) |
| Rescue PPI impairments in *Setd1a*$^{+/-}$ mice using antipsychotics and investigate neurochemical changes | • Neither haloperidol nor risperidone rescued deficient PPI<br>• Males (but not females) showed insensitivity to startle-inhibiting effects of risperidone, suggesting 5-HT2A receptor dysfunction | • Lack of genotype effect in males allocated to haloperidol challenge, possibly due to small sample size | • Replicate findings in larger sample<br>• Assess expression of 5-HT2A receptor in the brain<br>• Test effects of other validated and putative antipsychotics |
| Isolate contribution of effects of *Setd1a* LoF in the nervous system to behavioural phenotypes using a conditional KO | • Increased anxiety in OFT but not EPM<br>• No effect on ASR and non-significant reduction in PPI<br>• Impaired habituation to a novel environment | • Confounding effects of Nestin-cre<br>• Only 30 % reduction in *Setd1a* dosage at E13.5 | • Inducible and/or brain-region specific conditional knockout |

## 8.3. Potential mechanisms underlying pathogenic effects of *Setd1a* haploinsufficiency

### *8.3.1. Disrupted transcriptome of the developing brain*

H3K4 methylation is essential for transcriptional regulation during neurodevelopment (Roidl & Hacker, 2014). Previous studies have shown that *Setd1a* plays an important role in regulating embryonic neurogenesis (Bledau et al., 2014; Li & Jiao, 2017; Qiao et al., 2018). On this basis, *Setd1a* LoF could perturb neurodevelopment with downstream consequences for adult brain function. Consistent with this, intellectual disability is common in *Setd1a* LoF carriers (Singh et al., 2016), potentially indicating a general effect on neurodevelopmental robustness, although an increased burden of LoF variants is also observed in individuals with schizophrenia who do not have intellectual disability (Singh et al., 2017).

Despite the aforementioned evidence implicating a role for *Setd1a* in the developing brain, pathway analysis of transcriptomic changes occurring in E13.5 *Setd1a*$^{+/-}$ brain did not strongly implicate effects on neurodevelopment (Chapter 3). There was nominally significant enrichment for cilium-related annotations but the only GO term to survive correction for multiple testing was the mitochondrion. This finding is consistent with previous studies (Cameron et al., 2019; Hoshii et al., 2018) and mitochondrial dysfunction has been implicated in schizophrenia pathogenesis (Ben-Shachar, 2017; Flippo & Strack, 2017; Rajasekaran et al., 2015). Nevertheless, the extent to which this reflects a primary cause or downstream consequence of *Setd1a* haploinsufficiency remains to be tested. One possibility is that this enrichment is a surrogate marker of increased cellular stress during neurodevelopment but the precise biological mechanisms and associated functional consequences for the developing brain are unclear.

Gene-set enrichment analysis revealed that the genes that were differentially expressed in *Setd1a*$^{+/-}$ E13.5 brain were not enriched for schizophrenia common variant association. This was surprising given previous work showing enrichment in a human cell line (Cameron et al., 2019). Other work has shown that although *Setd1a* target genes identified by Chip-seq are enriched for schizophrenia common variants, only 10 % of these genes are differentially expressed in adult mouse prefrontal cortex (Mukai et al., 2019). Common variants for schizophrenia are dynamically expressed during neurodevelopment, with high expression in foetal brain (Birnbaum et al., 2015; Clifton et al., 2019; Jaffe et al., 2018). Moreover, functional genomics approaches strongly implicate convergence of common variant risk on foetal brain development

(de la Torre-Ubieta et al., 2018; Hannon et al., 2016; Li et al., 2018; O'Brien et al., 2018; Pidsley et al., 2014; Won et al., 2016) and an enrichment for particular brain cell-types (Skene et al., 2018). Further work is needed to investigate the degree of molecular convergence between *Setd1a* haploinsufficiency and other genetic variants for schizophrenia and neurodevelopmental disorders at different stages of development and consideration of potential cell-type and brain region specific effects.

### *8.3.2. Prenatal programming by the placenta: preliminary evidence for sexually dimorphic effects of Setd1a haploinsufficiency*

Several lines of evidence converge on the placenta as contributing to neuropsychiatric disorder pathogenesis (Bronson & Bale, 2016; Jansson & Powell, 2007; Sandovici et al., 2012). In particular, common variant genetic risk for schizophrenia is, in part, mediated by effects on the placenta (Ursini et al., 2018). These findings raise the possibility that rare variants, such as *Setd1a*, may also exert pathogenic effects via the placenta (Chapter 4). Consistent with this hypothesis, placentas of *Setd1a*$^{+/-}$ mice were found to be 8.9 % lighter than WT placentas at E13.5. This reduction in placental weight is suggestive of placental insufficiency during prenatal development. Prenatal programming by placental dysfunction has been shown to have long-lasting effects on offspring neurobehavioural outcomes (Mikaelsson et al., 2013). Further work is needed to investigate the effects of *Setd1a* haploinsufficiency on placental function (e.g., nutrient transfer and endocrine signalling) to determine mechanisms by which it may influence prenatal brain development.

Notably, the effects of *Setd1a* haploinsufficiency on placental gene expression were moderated by foetal sex. That is, expression of markers of the spongiotrophoblast (*Prl8a8* and to a lesser extent *Prl3b1*) (Simmons et al., 2008) were reduced in *Setd1a*$^{+/-}$ male but not female placenta. Moreover, male *Setd1a*$^{+/-}$ placenta showed reduced expression of *Ctsq*, a marker of (channel and sinusoidal) TGCs lining the maternal vasculature (Gasperowicz et al., 2013; Simmons et al., 2007). These findings may indicate morphological changes in the spongiotrophoblast and TGC lineages in male *Setd1a*$^{+/-}$ placenta, with effects on endocrine signalling and placental transfer, respectively. Similarly, *Setd1a* haploinsufficiency was also associated with reduced expression of the imprinted gene *Peg3* (and non-significant reductions in *Phlda2* and *Igf2*) in male but not female placenta. These findings are the first demonstration of effects of *Setd1a* on placental expression of imprinted genes, which are known to play essential roles in placental function (John, 2017). More generally,

they provide novel insights into potential sexually dimorphic mechanisms by which *Setd1a* LoF increases risk for psychopathology. This notion is consistent with recent evidence implicating sex differences in genetic pathways underlying schizophrenia risk (Tiihonen et al., 2019).

**Table 8.2.** Summary of sexually dimorphic effects of *Setd1a* haploinsufficiency.

| Measures | Males | Females |
|---|---|---|
| Placental *Prl8a8* expression | ↓ | ↔ |
| Placental *Ctsq* expression | ↓ | ↔ |
| Placental *Peg3* expression | ↓ | ↔ |
| Postnatal weight | ↓ | ↔ |
| Effect of risperidone on ASR | ↓ | ↔ |

Sexual dimorphism was also observed in the effects of *Setd1a* haploinsufficiency in postnatal life (Table 8.2). Specifically, while no differences were observed in foetal weight at E13.5, male (but not female) *Setd1a*$^{+/-}$ mice were significantly smaller at maternal separation (Chapter 4). Although there are several potential explanations for this finding (including placental programming, direct effects on pup development, and effects on maternal interactions), all are consistent with sexually dimorphic effects of *Setd1a* haploinsufficiency. Moreover, the effects of risperidone on the ASR dissociated between *Setd1a*$^{+/-}$ males and females, whereby males showed insensitivity to its startle-inhibiting effects (Chapter 6), potentially indicating 5-HT2A receptor dysfunction. This hypothesis is consistent with observations of decreased 5-HT2A receptor expression in post-mortem brains of schizophrenia patients (Burnet et al., 1996; Eastwood et al., 2001; Harrison, 1999c). It is also worth mentioning that the placenta expresses several 5-HT receptor subtypes and is a source of serotonin influencing prenatal brain development (Bonnin et al., 2011). Although the effects of *Setd1a* expression on 5-HT2A receptor dysfunction in the brain require confirmation, it may also be informative in future work to assess the effects of *Setd1a* haploinsufficiency on the placental serotonin system.

### *8.3.3. Nervous system specific mechanisms*

To explore the contribution of nervous system specific effects of *Setd1a* haploinsufficiency to behavioural phenotypes, a heterozygous conditional KO was created using a Nestin-Cre driver (Chapter 7). While the constitutive KO model more closely resembles the consequences of LoF mutations in human carriers, the

conditional KO was used as an experimental tool to examine the direct effects of *Setd1a* haploinsufficiency on the brain. This was necessary to eliminate potentially confounding effects of *Setd1a* haploinsufficiency on metabolic and immune phenotypes previously reported by the IMPC and effects on the placenta described earlier (section 8.4.2). Some convergence was observed in the behavioural effects of nervous system specific *Setd1a* LoF (Table 8.3). Consistent with the constitutive LoF model, increased anxiety was observed in the OFT but not the EPM and there were no effects on motoric function or object recognition memory. Conversely, the increased ASR observed in the constitutive LoF model was not recapitulated by conditional *Setd1a* knockdown. Although the conditional LoF model exhibited reduced PPI, this effect was not statistically significant. Moreover, the conditional LoF model had an additional impairment in habituation of locomotor activity, which was likely due to the confounding effect of Cre recombinase. Similarly, the Nestin-Cre control group also displayed increased anxiety in the OFT and (non-significantly) impaired PPI, which complicates interpretation of these results.

**Table 8.3.** Summary of behavioural phenotypes in the constitutive and conditional heterozygous *Setd1a* knockout models.

| Behaviour | Test | Constitutive KO | Conditional KO |
|---|---|---|---|
| Anxiety-related behaviour | EPM | ↔ | ↔ |
| | OFT | ↑ | ↑* |
| Motoric function | Basal locomotor activity levels | ↔ | ↔ |
| | Rotarod | ↔ | ↔ |
| Sensorimotor gating | ASR | ↑ | ↔ |
| | PPI | ↓ | NS ↓* |
| Learning and memory | Habituation of activity levels | ↔ | ↓* |
| | NOR | ↔ | ↔ |

*Confounded by Nestin-Cre control group

The convergent findings between the constitutive and conditional models regarding increased anxiety and decreased PPI (albeit non-significant in the conditional model) suggest that these findings are likely due to effects of *Setd1a* LoF in the nervous system. Nevertheless, the confounding effect of Nestin-Cre should be highlighted as an important caveat to this interpretation. Moreover, the effect on PPI was not statistically significant in the conditional model, which may be attributable to a lack of statistical power or because only a 30 % reduction in *Setd1a* dosage was achieved

in this model. Conversely, the dissociation in effects on ASR, which was increased in the constitutive model whereas no effect was observed in the conditional model, suggest that this effect may be due to *Setd1a* LoF in other systems with indirect effects on the brain. One possibility includes perturbed brain development via the placenta. In addition, constitutive *Setd1a* LoF causes reduced circulating LDL cholesterol, a major component of myelin, potentially leading to white matter abnormalities which are known to be widespread in schizophrenia and other neurodevelopmental disorders (Fields, 2008). Increased $CD8^+$ T cell number and decreased leukocyte and B cell number have also been reported in *Setd1a*$^{+/-}$ mice, which may be relevant given recent evidence supporting a role for the immune system in schizophrenia pathogenesis (Carter, Bullmore, & Harrison, 2014; Network and Pathway Analysis Subgroup of Psychiatric Genomics Consortium, 2015; Sekar et al., 2016). Although speculative, it is biologically plausible that these peripheral effects of *Setd1a* could play a role in pathogenic mechanisms since constitutive LoF occurs in human carriers.

The Nestin-Cre driver used to generate the heterozygous conditional *Setd1a* knockout results in recombination from E11.5 in the mouse brain (Tronche et al., 1999). Therefore, the observed effects on behaviour could either be attributable to effects on neurodevelopment and/or adult brain function. Indeed, reinstatement of *Setd1a* expression in adult *Setd1a*$^{+/-}$ mice results in a partial reversal of working memory deficits (Mukai et al., 2019). This suggests that the residual impairment may be attributable to neurodevelopmental effects of *Setd1a* LoF. It would be informative to explore whether similar findings are observed for heightened emotional reactivity and impairments of sensorimotor gating, as this would shed light on underlying pathogenic mechanisms.

### *8.3.4. Summary*

The findings presented in this thesis implicate diverse mechanisms that could underlie neuropsychiatric endophenotypes associated with *Setd1a* haploinsufficiency, ranging from effects on the placenta to transcriptomic changes in the developing brain and 5-HT2A receptor dysfunction in the adult brain. While the precise contributions of these effects to the emergence of psychopathology remains unclear, they serve as a starting point for further investigations to be undertaken in the context of the working model outlined in Figure 8.1.

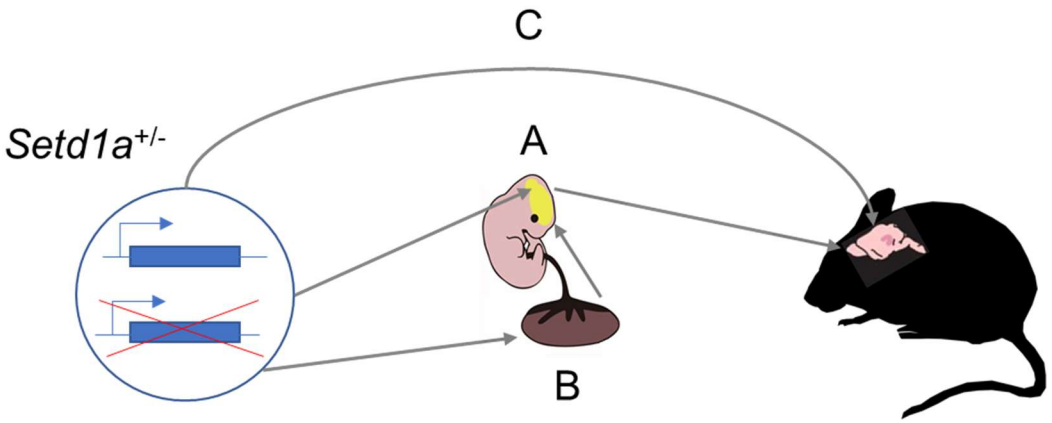


**Figure 8.1. Working model of pathogenic mechanisms underlying effects of *Setd1a* haploinsufficiency. A)** *Setd1a* LoF has direct effects on brain development via transcriptional dysregulation during neurodevelopment with downstream consequences for adult brain function. **B)** Indirect effects on brain development due to effects on placental function, potentially leading to sexually dimorphic placental programming of neurobehavioural outcomes. **C)** *Setd1a* haploinsufficiency disrupts adult brain function due to aberrant H3K4 methylation, which contributes to synaptic plasticity and learning and memory.

### 8.4. Limitations

Specific limitations have been acknowledged and discussed throughout this thesis and are summarised in Table 8.1. More generally, a potential limitation of the work presented herein is that the models used were intercrosses of two C57BL/6 substrains. This was necessary because founder animals harbouring the floxed *Setd1a* allele were generated in C57BL/6NTac mouse ESCs by EUCOMM, whereas commercially available Cre driver lines were produced on the C57BL/6J substrain. Phenotypic and genomic differences have been reported between these two substrains, albeit to a considerably lesser degree than between mice from entirely different strains (Simon et al., 2013; Vanden Berghe et al., 2015). To address this, littermate controls were used in all experiments to ensure that the relative contribution of each genetic background was equal in *Setd1a* knockouts and controls. However, residual heterozygosity at other loci may have introduced additional variability. Despite this, robust genotype effects were observed for several phenotypes. Another potential concern is the possibility of passenger mutations flanking the *Setd1a* gene that are co-inherited with the knockout allele. The closest identified variant to *Setd1a* is approximately 500 kb upstream (occurring in the *Zp2* gene, which is not known to have neurobehavioural effects) and all other variants are at least 1.5 Mb from *Setd1a*

(Vanden Berghe, 2015; Simon, 2013). While the probability of passenger mutations over this genomic distance is unlikely, it may be necessary to conduct sequencing in order to conclusively rule out this possibility.

It is important to note that the main aim of this thesis was to investigate the functional consequences of *Setd1a* haploinsufficiency to identify pathogenic mechanisms that might contribute to the association between *Setd1a* LoF and risk for psychopathology. This haploinsufficiency models the predicted effects of the heterozygous LoF mutations on gene function observed in human carriers (Singh et al., 2016). Nevertheless, a potential limitation of this approach is that the model used does not reflect the precise risk variant(s) observed in people (i.e., exon 4 is deleted in the mouse model, leading to haploinsufficiency via nonsense-mediated decay, whereas LoF mutations in human carriers are distributed throughout the *SETD1A* gene). It has been proposed that such 'humanised' genetic mouse models provide greater construct validity for interrogating pathogenic mechanisms of genetic risk for neuropsychiatric disorders (Harrison et al., 2012). Considering this, it would be interesting in future work to generate a model of the recurrent two-base pair deletion at the exon 16 splice acceptor site, which was observed in 7 out of 16 carriers by Singh et al. (2016).

### 8.5. Future directions

The findings of this thesis provide several avenues for future experiments aimed at investigating pathogenic mechanisms associated with *Setd1a* haploinsufficiency (summarised in Table 8.1). The working model outlined in Figure 8.1 has been proposed as a preliminary framework for conducting further studies that is by no means exhaustive and can be refined as additional pathogenic mechanisms and associated neurobehavioural effects are identified. In the first instance, further behavioural testing of the *Setd1a*$^{+/-}$ model is necessary to explore as yet unidentified effects of *Setd1a* haploinsufficiency on other neuropsychiatric endophenotypes, such as cognitive function (e.g., 5-choice serial reaction time task, associative learning) and hedonics (e.g., lick cluster analysis, progressive ratio task). Such studies would serve as the basis for investigating whether dissociable pathogenic mechanisms contribute to distinct endophenotypes using conditional knockout approaches that target *Setd1a* LoF to particular cell types at specific stages of development. The details of this work would be informed by further interrogation of the direct effects of *Setd1a* LoF in the developing brain (e.g., single-cell RNA-seq across development, Figure 8.1A) and the effects of *Setd1a* LoF on placental function (e.g., placental

transport and endocrine signalling, Figure 8.1B). Moreover, an inducible knockout system could be used to dissociate the effects of *Setd1a* LoF on adult brain function (Figure 8.1C) from downstream effects of perturbed neurodevelopment. Together, these studies would provide a comprehensive understanding of the causal roles of pathogenic mechanisms associated with *Setd1a* haploinsufficiency.

### 8.6. Concluding remarks

Recent advances in understanding the genetic architecture of schizophrenia and related neurodevelopmental disorders are providing opportunities to investigate pathophysiology with the hope that this may one day lead to more effective treatments. Using a model system to recapitulate *Setd1a* haploinsufficiency, the first highly damaging LoF variant to be identified for schizophrenia, this thesis has provided novel insights into its role in pathogenesis that warrant further investigation to delineate the pathophysiological contributions of *Setd1a* LoF in the developing brain, placenta, and adult brain function.

**Bibliography**

Abboud, R., Noronha, C., & Diwadkar, V. A. (2017). Motor system dysfunction in the schizophrenia diathesis: Neural systems to neurotransmitters. *European Psychiatry*, *44*, 125–133. doi: 10.1016/j.eurpsy.2017.04.004

Abi-Dargham, A., & Horga, G. (2016). The search for imaging biomarkers in psychiatric disorders. *Nature Medicine*, *22*(11), 1248–1255. doi: 10.1038/nm.4190

Abi-Dargham, A., van de Giessen, E., Slifstein, M., Kegeles, L. S., & Laruelle, M. (2009). Baseline and Amphetamine-Stimulated Dopamine Activity Are Related in Drug-Naïve Schizophrenic Subjects. *Biological Psychiatry*, *65*(12), 1091–1093. doi: 10.1016/j.biopsych.2008.12.007

Abi-Dargham, A. (2007). Alterations of Serotonin Transmission in Schizophrenia. *International Review of Neurobiology*, *78*, 133–164. doi: 10.1016/S0074-7742(06)78005-9

Achim, A. M., Maziade, M., Raymond, É., Olivier, D., Mérette, C., & Roy, M. A. (2011). How prevalent are anxiety disorders in schizophrenia? a meta-analysis and critical review on a significant association. *Schizophrenia Bulletin*, *37*(4), 811–821. doi: 10.1093/schbul/sbp148

Addington, J., Piskulic, D., Liu, L., Lockwood, J., Cadenhead, K. S., Cannon, T. D., … Woods, S. W. (2017). Comorbid diagnoses for youth at clinical high risk of psychosis. *Schizophrenia Research*, *190*, 90–95. doi: 10.1016/j.schres.2017.03.043

Aggernaes, B., Glenthoj, B. Y., Ebdrup, B. H., Rasmussen, H., Lublin, H., & Oranje, B. (2010). Sensorimotor gating and habituation in antipsychotic-naive, first-episode schizophrenia patients before and after 6 months' treatment with quetiapine. *The International Journal of Neuropsychopharmacology*, *13*(10), 1383–1395. doi: 10.1017/S1461145710000787

Aggleton, J. P., Albasser, M. M., Aggleton, D. J., Poirier, G. L., & Pearce, J. M. (2010). Lesions of the Rat Perirhinal Cortex Spare the Acquisition of a Complex Configural Visual Discrimination Yet Impair Object Recognition. *Behavioral Neuroscience*, *124*(1), 55–68. doi: 10.1037/a0018320

Aghajanian, G. K., & Marek, G. J. (1997). Serotonin induces excitatory postsynaptic potentials in apical dendrites of neocortical pyramidal cells. *Neuropharmacology*,

*36*(4–5), 589–599. doi: 10.1016/s0028-3908(97)00051-8

Akbarian, S., Kim, J. J., Potkin, S. G., Hagman, J. O., Tafazzoli, A., Bunney, W. E., & Jones, E. G. (1995). Gene Expression for Glutamic Acid Decarboxylase Is Reduced Without Loss of Neurons in Prefrontal Cortex of Schizophrenics. *Archives of General Psychiatry*, *52*(4), 258. doi: 10.1001/archpsyc.1995.03950160008002

Al-Diwani, A., Handel, A., Townsend, L., Pollak, T., Leite, M. I., Harrison, P. J., … Irani, S. R. (2019). The psychopathology of NMDAR-antibody encephalitis in adults: a systematic review and phenotypic analysis of individual patient data. *The Lancet Psychiatry*, *6*(3), 235–246. doi: 10.1016/S2215-0366(19)30001-X

Aleman, A., Kahn, R. S., & Selten, J.-P. (2003). Sex Differences in the Risk of Schizophrenia. *Archives of General Psychiatry*, *60*(6), 565–571. doi: 10.1001/archpsyc.60.6.565

American Psychiatric Association. (2013). *Diagnostic and Statistical Manual of Mental Disorders - fifth edition: DSM-5*. Arlington, VA.

Andrews, S. (2010). FastQC A Quality Control tool for High Throughput Sequence Data. Retrieved from https://www.bioinformatics.babraham.ac.uk/projects/fastqc/

Antunes, M., & Biala, G. (2012). The novel object recognition memory: Neurobiology, test procedure, and its modifications. *Cognitive Processing*, *13*(2), 93–110. doi: 10.1007/s10339-011-0430-z

Arango, C., & Carpenter, W. T. (2011). The Schizophrenia Construct: Symptomatic Presentation. In D. R. Weinberger & P. J. Harrison (Eds.), *Schizophrenia* (3rd ed., pp. 9–23). Oxford: Wiley-Blackwell doi: 10.1002/9781444327298.ch2

Bannister, A. J., & Kouzarides, T. (2011). Regulation of chromatin by histone modifications. *Cell Research*, *21*(3), 381–395. doi: 10.1038/cr.2011.22

Barlow, D. P. (2011). Genomic Imprinting: A Mammalian Epigenetic Discovery Model. *Annual Review of Genetics*, *45*(1), 379–403. doi: 10.1146/annurev-genet-110410-132459

Barski, A., Cuddapah, S., Cui, K., Roh, T.-Y., Schones, D. E., Wang, Z., … Zhao, K. (2007). High-Resolution Profiling of Histone Methylations in the Human Genome. *Cell*, *129*(4), 823–837. doi: 10.1016/j.cell.2007.05.009

Belzung, C., & Griebel, G. (2001). Measuring normal and pathological anxiety-like behaviour in mice: A review. *Behavioural Brain Research*, *125*(1–2), 141–149. doi: 10.1016/S0166-4328(01)00291-1

Ben-Shachar, D. (2017). Mitochondrial multifaceted dysfunction in schizophrenia; complex I as a possible pathological target. *Schizophrenia Research*, *187*, 3–10. doi: 10.1016/J.SCHRES.2016.10.022

Benes, F. M., Vincent, S. ., Marie, A., & Khan, Y. (1996). Up-regulation of GABAA receptor binding on neurons of the prefrontal cortex in schizophrenic subjects. *Neuroscience*, *75*(4), 1021–1031. doi: 10.1016/0306-4522(96)00328-4

Benes, F. M., Vincent, S. L., Alsterberg, G., Bird, E. D., & SanGiovanni, J. P. (1992). Increased GABAA receptor binding in superficial layers of cingulate cortex in schizophrenics. *The Journal of Neuroscience*, *12*(3), 924–929. doi: 10.1523/JNEUROSCI.12-03-00924.1992

Bergen, S. E., Ploner, A., Howrigan, D., CNV Analysis Group and the Schizophrenia Working Group of the Psychiatric Genomics Consortium, O'Donovan, M. C., Smoller, J. W., … Kendler, K. S. (2019). Joint Contributions of Rare Copy Number Variants and Common SNPs to Risk for Schizophrenia. *American Journal of Psychiatry*, *176*(1), 29–35. doi: 10.1176/appi.ajp.2018.17040467

Bernstein, B. E., Mikkelsen, T. S., Xie, X., Kamal, M., Huebert, D. J., Cuff, J., … Lander, E. S. (2006). A Bivalent Chromatin Structure Marks Key Developmental Genes in Embryonic Stem Cells. *Cell*, *125*(2), 315–326. doi: 10.1016/j.cell.2006.02.041

Bhattacharyya, S., Lin, J., & Linzer, D. I. H. (2002). Reactivation of a Hematopoietic Endocrine Program of Pregnancy Contributes to Recovery from Thrombocytopenia. *Molecular Endocrinology*, *16*(6), 1386–1393. doi: 10.1210/mend.16.6.0847

Birnbaum, R., Jaffe, A. E., Chen, Q., Hyde, T. M., Kleinman, J. E., & Weinberger, D. R. (2015). Investigation of the Prenatal Expression Patterns of 108 Schizophrenia-Associated Genetic Loci. *Biological Psychiatry*, *77*(11), e43–e51. doi: 10.1016/j.biopsych.2014.10.008

Birnbaum, R., & Weinberger, D. R. (2017). Genetic insights into the neurodevelopmental origins of schizophrenia. *Nature Reviews Neuroscience*, *18*(12), 727–740. doi: 10.1038/nrn.2017.125

Bledau, A. S., Schmidt, K., Neumann, K., Hill, U., Ciotta, G., Gupta, A., … Anastassiadis, K. (2014). The H3K4 methyltransferase Setd1a is first required at the epiblast stage, whereas Setd1b becomes essential after gastrulation. *Development*, *141*(5), 1022–1035. doi: 10.1242/dev.098152

Bolger, A. M., Lohse, M., & Usadel, B. (2014). Trimmomatic: a flexible trimmer for Illumina sequence data. *Bioinformatics*, *30*(15), 2114–2120. doi: 10.1093/bioinformatics/btu170

Bonnin, A., Goeden, N., Chen, K., Wilson, M. L., King, J., Shih, J. C., … Levitt, P. (2011). A transient placental source of serotonin for the fetal forebrain. *Nature*, *472*(7343), 347–350. doi: 10.1038/nature09972

Bourc'his, D., Xu, G. L., Lin, C. S., Bollman, B., & Bestor, T. H. (2001). Dnmt3L and the Establishment of Maternal Genomic Imprints. *Science*, *294*(5551), 2536–2539. doi: 10.1126/science.1065848

Bowie, C. R., Reichenberg, A., Patterson, T. L., Heaton, R. K., & Harvey, P. D. (2006). Determinants of Real-World Functional Performance in Schizophrenia Subjects: Correlations With Cognition, Functional Capacity, and Symptoms. *American Journal of Psychiatry*, *163*(3), 418–425. doi: 10.1176/appi.ajp.163.3.418

Braff, D. L., Grillon, C., & Geyer, M. A. (1992). Gating and Habituation of the Startle Reflex in Schizophrenic Patients. *Archives of General Psychiatry*, *49*(3), 206–215. doi: 10.1001/archpsyc.1992.01820030038005

Braga, R. J., Reynolds, G. P., & Siris, S. G. (2013). Anxiety comorbidity in schizophrenia. *Psychiatry Research*, *35*(2), 383–402. doi: 10.1016/j.psychres.2013.07.030

Brainstorm Consortium, Anttila, V., Bulik-Sullivan, B., Finucane, H. K., Walters, R. K., Bras, J., … Murray, R. (2018). Analysis of shared heritability in common disorders of the brain. *Science*, *360*(6395), eaap8757. doi: 10.1126/science.aap8757

Bray, N. J. (2008). Gene expression in the etiology of schizophrenia. *Schizophrenia Bulletin*, *34*(3), 412–418. doi: 10.1093/schbul/sbn013

Bray, N. J., Buckland, P. R., Hall, H., Owen, M. J., & O'Donovan, M. C. (2004). The serotonin-2A receptor gene locus does not contain common polymorphism affecting mRNA levels in adult brain. *Molecular Psychiatry*, *9*(1), 109–114. doi: 10.1038/sj.mp.4001366

Bray, N. J., & Hill, M. J. (2016). Translating Genetic Risk Loci Into Molecular Risk Mechanisms for Schizophrenia. *Schizophrenia Bulletin*, *42*(1), 5–8. doi: 10.1093/schbul/sbv156

Bray, N. J., & O'Donovan, M. C. (2018). The genetics of neuropsychiatric disorders. *Brain and Neuroscience Advances*, *2*, 1–6. doi: 10.1177/2398212818799271

Breier, A., Su, T. P., Saunders, R., Carson, R. E., Kolachana, B. S., de Bartolomeis, A., … Pickar, D. (1997). Schizophrenia is associated with elevated amphetamine-induced synaptic dopamine concentrations: evidence from a novel positron emission tomography method. *Proceedings of the National Academy of Sciences of the United States of America*, *94*(6), 2569–2574. doi: 10.1073/pnas.94.6.2569

Bronson, S. L., & Bale, T. L. (2016). The Placenta as a Mediator of Stress Effects on Neurodevelopmental Reprogramming. *Neuropsychopharmacology*, *41*(1), 207–218. doi: 10.1038/npp.2015.231

Brooks, S. P., & Dunnett, S. B. (2009). Tests to assess motor phenotype in mice: A user's guide. *Nature Reviews Neuroscience*, *10*(7), 519–529. doi: 10.1038/nrn2652

Brown, A. S., & Derkits, E. J. (2010). Prenatal Infection and Schizophrenia: A Review of Epidemiologic and Translational Studies. *American Journal of Psychiatry*, *167*(3), 261–280. doi: 10.1176/appi.ajp.2009.09030361

Brown, A. S., & Susser, E. S. (2008). Prenatal Nutritional Deficiency and Risk of Adult Schizophrenia. *Schizophrenia Bulletin*, *34*(6), 1054–1063. doi: 10.1093/schbul/sbn096

Buchanan, R. W., Freedman, R., Javitt, D. C., Abi-Dargham, A., & Lieberman, J. A. (2007). Recent Advances in the Development of Novel Pharmacological Agents for the Treatment of Cognitive Impairments in Schizophrenia. *Schizophrenia Bulletin*, *33*(5), 1120–1130. doi: 10.1093/schbul/sbm083

Buckley, P. F., Miller, B. J., Lehrer, D. S., & Castle, D. J. (2009). Psychiatric comorbidities and schizophrenia. *Schizophrenia Bulletin*, *210*(1), 1–7. doi: 10.1093/schbul/sbn135

Buitrago, M. M., Schulz, J. B., Dichgans, J., & Luft, A. R. (2004). Short and long-term motor skill learning in an accelerated rotarod training paradigm. *Neurobiology of Learning and Memory*, *81*(3), 211–216. doi: 10.1016/j.nlm.2004.01.001

Burnet, P. W. J., Eastwood, S. L., Bristow, G. C., Godlewska, B. R., Sikka, P., Walker, M., & Harrison, P. J. (2008b). D-Amino acid oxidase activity and expression are increased in schizophrenia. *Molecular Psychiatry*, *13*(7), 658–660. doi: 10.1038/mp.2008.47

Burnet, P. W. J., Eastwood, S. L., & Harrison, P. J. (1996). 5-HT1A and 5-HT2A receptor mRNAs and binding site densities are differentially altered in schizophrenia. *Neuropsychopharmacology*, *15*(5), 442–455. doi: 10.1016/S0893-133X(96)00053-X

Burnet, P. W. J., Hutchinson, L., von Hesling, M., Gilbert, E.-J., Brandon, N. J., Rutter, A. R., … Harrison, P. J. (2008a). Expression of D-serine and glycine transporters in the prefrontal cortex and cerebellum in schizophrenia. *Schizophrenia Research*, *102*(1–3), 283–294. doi: 10.1016/j.schres.2008.02.009

Cadenhead, K. S., Swerdlow, N. R., Shafer, K. M., Diaz, M., & Braff, D. L. (2000). Modulation of the startle response and startle laterality in relatives of schizophrenic patients and in subjects with schizotypal personality disorder: Evidence of inhibitory deficits. *American Journal of Psychiatry*, *157*(10), 1660–1668. doi: 10.1176/appi.ajp.157.10.1660

Callaway, D. A., Perkins, D. O., Woods, S. W., Liu, L., & Addington, J. (2014). Movement abnormalities predict transitioning to psychosis in individuals at clinical high risk for psychosis. *Schizophrenia Research*, *159*(2–3), 263–266. doi: 10.1016/j.schres.2014.09.031

Cameron, D., Blake, D. J., Bray, N. J., & Hill, M. J. (2019). Transcriptional Changes following Cellular Knockdown of the Schizophrenia Risk Gene SETD1A Are Enriched for Common Variant Association with the Disorder. *Molecular Neuropsychiatry*, *5*(2), 109–114. doi: 10.1159/000497181

Cannon, M., Jones, P. B., & Murray, R. M. (2002). Obstetric Complications and Schizophrenia: Historical and Meta-Analytic Review. *American Journal of Psychiatry*, *159*(7), 1080–1092. doi: 10.1176/appi.ajp.159.7.1080

Carobrez, A. P., & Bertoglio, L. J. (2005). Ethological and temporal analyses of anxiety-like behavior: The elevated plus-maze model 20 years on. *Neuroscience and Biobehavioral Reviews*, *29*(8), 1193–1205. doi: 10.1016/j.neubiorev.2005.04.017

Carter, C. S., Bullmore, E. T., & Harrison, P. (2014). Is there a flame in the brain in

psychosis? *Biological Psychiatry*, *75*(4), 258–259. doi: 10.1016/j.biopsych.2013.10.023

Caspary, T., Cleary, M. A., Baker, C. C., Guan, X. J., & Tilghman, S. M. (1998). Multiple mechanisms regulate imprinting of the mouse distal chromosome 7 gene cluster. *Molecular and Cellular Biology*, *18*(6), 3466–3474. doi: 10.1128/mcb.18.6.3466

Caston, J., Jones, N., & Stelz, T. (1995). Role of preoperative and postoperative sensorimotor training on restoration of the equilibrium behavior in adult mice following cerebellectomy. *Neurobiology of Learning and Memory*, *64*(3), 195–202. doi: 10.1006/nlme.1995.0002

Cedar, H., & Bergman, Y. (2009). Linking DNA methylation and histone modification: patterns and paradigms. *Nature Reviews Genetics*, *10*(5), 295–304. doi: 10.1038/nrg2540

Chan, M. H., Chiu, P. H., Sou, J. H., & Chen, H. H. (2008). Attenuation of ketamine-evoked behavioral responses by mGluR5 positive modulators in mice. *Psychopharmacology*, *198*(1), 141–148. doi: 10.1007/s00213-008-1103-1

Chan, R. C. K., Xu, T., Heinrichs, R. W., Yu, Y., & Gong, Q. yong. (2010). Neurological soft signs in non-psychotic first-degree relatives of patients with schizophrenia: A systematic review and meta-analysis. *Neuroscience and Biobehavioral Reviews*, *34*(6), 889–896. doi: 10.1016/j.neubiorev.2009.11.012

Chesney, E., Goodwin, G. M., & Fazel, S. (2014). Risks of all-cause and suicide mortality in mental disorders: a meta-review. *World Psychiatry*, *13*(2), 153–160. doi: 10.1002/wps.20128

Cheung, I., Shulha, H. P., Jiang, Y., Matevossian, A., Wang, J., Weng, Z., & Akbarian, S. (2010). Developmental regulation and individual differences of neuronal H3K4me3 epigenomes in the prefrontal cortex. *Proceedings of the National Academy of Sciences of the United States of America*, *107*(19), 8824–8829. doi: 10.1073/pnas.1001702107

Cho, S.-E., Na, K.-S., Cho, S.-J., & Kang, S. G. (2016). Low d-serine levels in schizophrenia: A systematic review and meta-analysis. *Neuroscience Letters*, *634*, 42–51. doi: 10.1016/j.neulet.2016.10.006

Ciccone, D. N., Su, H., Hevi, S., Gay, F., Lei, H., Bajko, J., … Chen, T. (2009). KDM1B is a histone H3K4 demethylase required to establish maternal genomic imprints.

*Nature*, *461*(7262), 415–418. doi: 10.1038/nature08315

Clark, R. E., Zola, S. M., & Squire, L. R. (2000). Impaired recognition memory in rats after damage to the hippocampus. *The Journal of Neuroscience*, *20*(23), 8853–8860. doi: 10.1523/JNEUROSCI.20-23-08853.2000

Clifton, N. E., Hannon, E., Harwood, J. C., Di Florio, A., Thomas, K. L., Holmans, P. A., … Hall, J. (2019). Dynamic expression of genes associated with schizophrenia and bipolar disorder across development. *Translational Psychiatry*, *9*(1), 74. doi: 10.1038/s41398-019-0405-x

Clifton, V. L. (2010). Review: Sex and the Human Placenta: Mediating Differential Strategies of Fetal Growth and Survival. *Placenta*, *31*, S33–S39. doi: 10.1016/j.placenta.2009.11.010

Clouaire, T., Webb, S., Skene, P., Illingworth, R., Kerr, A., Andrews, R., … Bird, A. (2012). Cfp1 integrates both CpG content and gene activity for accurate H3K4me3 deposition in embryonic stem cells. *Genes & Development*, *26*(15), 1714–1728. doi: 10.1101/gad.194209.112

Coan, P. M., Conroy, N., Burton, G. J., & Ferguson-Smith, A. C. (2006). Origin and characteristics of glycogen cells in the developing murine placenta. *Developmental Dynamics*, *235*(12), 3280–3294. doi: 10.1002/dvdy.20981

Cohen, S. M., Tsien, R. W., Goff, D. C., & Halassa, M. M. (2015). The impact of NMDA receptor hypofunction on GABAergic neurons in the pathophysiology of schizophrenia. *Schizophrenia Research*, *167*(1–3), 98–107. doi: 10.1016/j.schres.2014.12.026

Coleman, J. L. J., Brennan, K., Ngo, T., Balaji, P., Graham, R. M., & Smith, N. J. (2015). Rapid Knockout and Reporter Mouse Line Generation and Breeding Colony Establishment Using EUCOMM Conditional-Ready Embryonic Stem Cells: A Case Study. *Frontiers in Endocrinology*, *6*, 105. doi: 10.3389/fendo.2015.00105

Collins, B. E., Greer, C. B., Coleman, B. C., & Sweatt, J. D. (2019). Histone H3 lysine K4 methylation and its role in learning and memory. *Epigenetics & Chromatin*, *12*(7). doi: 10.1186/s13072-018-0251-8

Collins, B. E., Sweatt, J. D., & Greer, C. B. (2019). Broad domains of histone 3 lysine 4 trimethylation are associated with transcriptional activation in CA1 neurons of the hippocampus during memory formation. *Neurobiology of Learning and*

*Memory*, *161*, 149–157. doi: 10.1016/j.nlm.2019.04.009

Constância, M., Hemberger, M., Hughes, J., Dean, W., Ferguson-Smith, A., Fundele, R., … Reik, W. (2002). Placental-specific IGF-II is a major modulator of placental and fetal growth. *Nature*, *417*(6892), 945–948. doi: 10.1038/nature00819

Cortese, L., Caligiuri, M. P., Malla, A. K., Manchanda, R., Takhar, J., & Haricharan, R. (2005). Relationship of neuromotor disturbances to psychosis symptoms in first-episode neuroleptic-naïve schizophrenia patients. *Schizophrenia Research*, *75*(1), 65–75. doi: 10.1016/j.schres.2004.08.003

Coutinho, E., Harrison, P., & Vincent, A. (2014). Do neuronal autoantibodies cause psychosis? A neuroimmunological perspective. *Biological Psychiatry*, *75*(4), 269–275. doi: 10.1016/j.biopsych.2013.07.040

Cox, B., Kotlyar, M., Evangelou, A. I., Ignatchenko, V., Ignatchenko, A., Whiteley, K., … Kislinger, T. (2009). Comparative systems biology of human and mouse as a tool to guide the modeling of human placental pathology. *Molecular Systems Biology*, *5*(279). doi: 10.1038/msb.2009.37

Creese, I., Burt, D., & Snyder, S. (1976). Dopamine receptor binding predicts clinical and pharmacological potencies of antischizophrenic drugs. *Science*, *192*(4238), 481–483. doi: 10.1126/science.3854

Cross-Disorder Group of the Psychiatric Genomics Consortium, Lee, S. H., Ripke, S., Neale, B. M., Faraone, S. V, Purcell, S. M., … International Inflammatory Bowel Disease Genetics Consortium (IIBDGC). (2013). Genetic relationship between five psychiatric disorders estimated from genome-wide SNPs. *Nature Genetics*, *45*(9), 984–994. doi: 10.1038/ng.2711

Cryan, J. F., & Holmes, A. (2005). Model organisms: The ascent of mouse: Advances in modelling human depression and anxiety. *Nature Reviews Drug Discovery*, *4*(9), 775–790. doi: 10.1038/nrd1825

Cunningham Owens, D., & Johnstone, E. C. (2018). The development of antipsychotic drugs. *Brain and Neuroscience Advances*, *2*, 1–6. doi: 10.1177/2398212818817498

Curtis, D. (2016). Pathway analysis of whole exome sequence data provides further support for the involvement of histone modification in the aetiology of schizophrenia. *Psychiatric Genetics*, *26*(5), 223–227. doi: 10.1097/YPG.0000000000000132

Curtis, D., Coelewij, L., Liu, S.-H., Humphrey, J., & Mott, R. (2018). Weighted Burden Analysis of Exome-Sequenced Case-Control Sample Implicates Synaptic Genes in Schizophrenia Aetiology. *Behavior Genetics*, *48*(3), 198–208. doi: 10.1007/s10519-018-9893-3

Cuthbert, B. N. (2015). Research Domain Criteria: toward future psychiatric nosologies. *Dialogues in Clinical Neuroscience*, *17*(1), 89–97. doi: 10.1016/j.ajp.2013.12.007

Daenen, E. W. P. M., Van der Heyden, J. A., Kruse, C. G., Wolterink, G., & Van Ree, J. M. (2001). Adaptation and habituation to an open field and responses to various stressful events in animals with neonatal lesions in the amygdala or ventral hippocampus. *Brain Research*, *918*(1–2), 153–165. doi: 10.1016/S0006-8993(01)02987-0

Daenen, E. W. P. M., Wolterink, G., Gerrits, M. A. F. M., & Van Ree, J. M. (2002). Amygdala or ventral hippocampal lesions at two early stages of life differentially affect open field behaviour later in life; an animal model of neurodevelopmental psychopathological disorders. *Behavioural Brain Research*, *131*(1–2), 67–78. doi: 10.1016/S0166-4328(01)00350-3

Dall'Olio, R., Gaggi, R., Bonfante, V., & Gandolfi, O. (1999). The non-competitive NMDA receptor blocker dizocilpine potentiates serotonergic function. *Behavioural Pharmacology*, *10*(1), 63–71.

Davis, K. L., Kahn, R. S., Ko, G., & Davidson, M. (1991). Dopamine in schizophrenia: a review and reconceptualization. *American Journal of Psychiatry*, *148*(11), 1474–1486. doi: 10.1176/ajp.148.11.1474

de la Torre-Ubieta, L., Stein, J. L., Won, H., Opland, C. K., Liang, D., Lu, D., & Geschwind, D. H. (2018). The Dynamic Landscape of Open Chromatin during Human Cortical Neurogenesis. *Cell*, *172*(1–2), 289-304.e18. doi: 10.1016/j.cell.2017.12.014

de Leeuw, C. A., Mooij, J. M., Heskes, T., & Posthuma, D. (2015). MAGMA: Generalized Gene-Set Analysis of GWAS Data. *PLOS Computational Biology*, *11*(4), e1004219. doi: 10.1371/journal.pcbi.1004219

Declercq, J., Brouwers, B., Pruniau, V. P. E. G., Stijnen, P., de Faudeur, G., Tuand, K., … Creemers, J. W. M. (2015). Metabolic and Behavioural Phenotypes in Nestin-Cre Mice Are Caused by Hypothalamic Expression of Human Growth

Hormone. *PLOS ONE*, *10*(8), e0135502. doi: 10.1371/journal.pone.0135502

Demjaha, A., Lappin, J. M., Stahl, D., Patel, M. X., MacCabe, J. H., Howes, O. D., … Murray, R. M. (2017). Antipsychotic treatment resistance in first-episode psychosis: prevalence, subtypes and predictors. *Psychological Medicine*, *47*(11), 1981–1989. doi: 10.1017/S0033291717000435

Deussing, J. M. (2013). Targeted mutagenesis tools for modelling psychiatric disorders. *Cell and Tissue Research*, *354*(1), 9–25. doi: 10.1007/s00441-013-1708-5

Dincer, A., Gavin, D. P., Xu, K., Zhang, B., Dudley, J. T., Schadt, E. E., & Akbarian, S. (2015). Deciphering H3K4me3 broad domains associated with gene-regulatory networks and conserved epigenomic landscapes in the human brain. *Translational Psychiatry*, *5*(11), e679. doi: 10.1038/tp.2015.169

Dix, S. L., & Aggleton, J. P. (1999). Extending the spontaneous preference test of recognition: Evidence of object-location and object-context recognition. *Behavioural Brain Research*, *99*(2), 191–200. doi: 10.1016/S0166-4328(98)00079-5

Dobin, A., Davis, C. A., Schlesinger, F., Drenkow, J., Zaleski, C., Jha, S., … Gingeras, T. R. (2013). STAR: ultrafast universal RNA-seq aligner. *Bioinformatics*, *29*(1), 15–21. doi: 10.1093/bioinformatics/bts635

Dong, D., Wang, Y., Chang, X., Luo, C., & Yao, D. (2018). Dysfunction of Large-Scale Brain Networks in Schizophrenia: A Meta-analysis of Resting-State Functional Connectivity. *Schizophrenia Bulletin*, *44*(1), 168–181. doi: 10.1093/schbul/sbx034

Eastwood, S. L., Burnet, P. W. J., Gittins, R., Baker, K., & Harrison, P. J. (2001). Expression of serotonin 5-HT2A receptors in the human cerebellum and alterations in schizophrenia. *Synapse*, *42*(2), 104–114. doi: 10.1002/syn.1106

Egerton, A., Modinos, G., Ferrera, D., & McGuire, P. (2017). Neuroimaging studies of GABA in schizophrenia: a systematic review with meta-analysis. *Translational Psychiatry*, *7*(6), e1147. doi: 10.1038/tp.2017.124

Eising, E., Carrion-Castillo, A., Vino, A., Strand, E. A., Jakielski, K. J., Scerri, T. S., … Fisher, S. E. (2019). A set of regulatory genes co-expressed in embryonic human brain is implicated in disrupted speech development. *Molecular Psychiatry*, *24*(7), 1065–1078. doi: 10.1038/s41380-018-0020-x

Ernst, J., Kheradpour, P., Mikkelsen, T. S., Shoresh, N., Ward, L. D., Epstein, C. B., … Bernstein, B. E. (2011). Mapping and analysis of chromatin state dynamics in nine human cell types. *Nature*, *473*(7345), 43–49. doi: 10.1038/nature09906

Esquiliano, D. R., Guo, W., Liang, L., Dikkes, P., & Lopez, M. F. (2009). Placental Glycogen Stores are Increased in Mice with H19 Null Mutations but not in those with Insulin or IGF Type 1 Receptor Mutations. *Placenta*, *30*(8), 693–699. doi: 10.1016/j.placenta.2009.05.004

Fang, L., Zhang, J., Zhang, H., Yang, X., Jin, X., Zhang, L., … Wong, J. (2016). H3K4 Methyltransferase Set1a Is A Key Oct4 Coactivator Essential for Generation of Oct4 Positive Inner Cell Mass. *Stem Cells*, *34*(3), 565–580. doi: 10.1002/stem.2250

Farrell, M. S., Werge, T., Sklar, P., Owen, M. J., Ophoff, R. A., O'Donovan, M. C., … Sullivan, P. F. (2015). Evaluating historical candidate genes for schizophrenia. *Molecular Psychiatry*, *20*(5), 555–562. doi: 10.1038/mp.2015.16

Fatouros-Bergman, H., Cervenka, S., Flyckt, L., Edman, G., & Farde, L. (2014). Meta-analysis of cognitive performance in drug-naïve patients with schizophrenia. *Schizophrenia Research*, *158*(1–3), 156–162. doi: 10.1016/j.schres.2014.06.034

Fields, R. D. (2008). White matter in learning, cognition and psychiatric disorders. *Trends in Neurosciences*, *31*(7), 361–370. doi: 10.1016/j.tins.2008.04.001

Finlay, B., & Darlington, R. (1995). Linked regularities in the development and evolution of mammalian brains. *Science*, *268*(5217), 1578–1584. doi: 10.1126/science.7777856

Fioravanti, M., Bianchi, V., & Cinti, M. E. (2012). Cognitive deficits in schizophrenia: An updated metanalysis of the scientific evidence. *BMC Psychiatry*, *12*(64). doi: 10.1186/1471-244X-12-64

Flippo, K. H., & Strack, S. (2017). An emerging role for mitochondrial dynamics in schizophrenia. *Schizophrenia Research*, *187*, 26–32. doi: 10.1016/J.SCHRES.2017.05.003

Folsom, D. P., Hawthorne, W., Lindamer, L., Gilmer, T., Bailey, A., Golshan, S., … Jeste, D. V. (2005). Prevalence and Risk Factors for Homelessness and Utilization of Mental Health Services Among 10,340 Patients With Serious Mental Illness in a Large Public Mental Health System. *American Journal of*

*Psychiatry*, *162*(2), 370–376. doi: 10.1176/appi.ajp.162.2.370

Fone, K. C. F., & Porkess, M. V. (2008). Behavioural and neurochemical effects of post-weaning social isolation in rodents—Relevance to developmental neuropsychiatric disorders. *Neuroscience & Biobehavioral Reviews*, *32*(6), 1087–1102. doi: 10.1016/j.neubiorev.2008.03.003

Forni, P. E., Scuoppo, C., Imayoshi, I., Taulli, R., Dastrù, W., Sala, V., … Ponzetto, C. (2006). High Levels of Cre Expression in Neuronal Progenitors Cause Defects in Brain Development Leading to Microencephaly and Hydrocephaly. *Journal of Neuroscience*, *26*, 9593–9602. doi: 10.1523/JNEUROSCI.2815-06.2006

Fowden, A. L., Sferruzzi-Perri, A. N., Coan, P. M., Constancia, M., & Burton, G. J. (2009). Placental efficiency and adaptation: endocrine regulation. *The Journal of Physiology*, *587*(14), 3459–3472. doi: 10.1113/jphysiol.2009.173013

Frankle, W. G., Cho, R. Y., Prasad, K. M., Mason, N. S., Paris, J., Himes, M. L., … Narendran, R. (2015). In Vivo Measurement of GABA Transmission in Healthy Subjects and Schizophrenia Patients. *American Journal of Psychiatry*, *172*(11), 1148–1159. doi: 10.1176/appi.ajp.2015.14081031

Friston, K., Brown, H. R., Siemerkus, J., & Stephan, K. E. (2016). The dysconnection hypothesis (2016). *Schizophrenia Research*, *176*(2–3), 83–94. doi: 10.1016/j.schres.2016.07.014

Fröhner, J. H., Teckentrup, V., Smolka, M. N., & Kroemer, N. B. (2019). Addressing the reliability fallacy in fMRI: Similar group effects may arise from unreliable individual effects. *NeuroImage*, *195*, 174–189. doi: 10.1016/J.NEUROIMAGE.2019.03.053

Fromer, M., Pocklington, A. J., Kavanagh, D. H., Williams, H. J., Dwyer, S., Gormley, P., … O'Donovan, M. C. (2014). De novo mutations in schizophrenia implicate synaptic networks. *Nature*, *506*(7487), 179–184. doi: 10.1038/nature12929

Fusar-Poli, P., Borgwardt, S., Crescini, A., Deste, G., Kempton, M. J., Lawrie, S., … Sacchetti, E. (2011). Neuroanatomy of vulnerability to psychosis: A voxel-based meta-analysis. *Neuroscience & Biobehavioral Reviews*, *35*(5), 1175–1185. doi: 10.1016/j.neubiorev.2010.12.005

Fusar-Poli, P., & Meyer-Lindenberg, A. (2013). Striatal presynaptic dopamine in schizophrenia, part II: meta-analysis of [(18)F/(11)C]-DOPA PET studies. *Schizophrenia Bulletin*, *39*(1), 33–42. doi: 10.1093/schbul/sbr180

Fusar-Poli, P., & Meyer-Lindenberg, A. (2016). Forty years of structural imaging in psychosis: promises and truth. *Acta Psychiatrica Scandinavica*, *134*(3), 207–224. doi: 10.1111/acps.12619

Fusar-Poli, P., Smieskova, R., Kempton, M. J., Ho, B. C., Andreasen, N. C., & Borgwardt, S. (2013). Progressive brain changes in schizophrenia related to antipsychotic treatment? A meta-analysis of longitudinal MRI studies. *Neuroscience & Biobehavioral Reviews*, *37*(8), 1680–1691. doi: 10.1016/j.neubiorev.2013.06.001

Gabory, A., Ferry, L., Fajardy, I., Jouneau, L., Gothié, J.-D., Vigé, A., … Junien, C. (2012). Maternal Diets Trigger Sex-Specific Divergent Trajectories of Gene Expression and Epigenetic Systems in Mouse Placenta. *PLoS ONE*, *7*(11), e47986. doi: 10.1371/journal.pone.0047986

Gainetdinov, R. R., Jones, S. R., & Caron, M. G. (1999). Functional hyperdopaminergia in dopamine transporter knock-out mice. *Biological Psychiatry*, *46*(3), 303–311. doi: 10.1016/S0006-3223(99)00122-5

Gasperowicz, M., Surmann-Schmitt, C., Hamada, Y., Otto, F., & Cross, J. C. (2013). The transcriptional co-repressor TLE3 regulates development of trophoblast giant cells lining maternal blood spaces in the mouse placenta. *Developmental Biology*, *382*(1), 1–14. doi: 10.1016/j.ydbio.2013.08.005

Gavériaux-Ruff, C., & Kieffer, B. L. (2007). Conditional gene targeting in the mouse nervous system: Insights into brain function and diseases. *Pharmacology & Therapeutics*, *113*(3), 619–634. doi: 10.1016/j.pharmthera.2006.12.003

Geddes, J., Freemantle, N., Harrison, P., & Bebbington, P. (2000). Atypical antipsychotics in the treatment of schizophrenia: systematic overview and meta-regression analysis. *BMJ*, *321*(7273), 1371–1376. doi: 10.1136/bmj.321.7273.1371

Genovese, G., Fromer, M., Stahl, E. A., Ruderfer, D. M., Chambert, K., Landén, M., … McCarroll, S. A. (2016). Increased burden of ultra-rare protein-altering variants among 4,877 individuals with schizophrenia. *Nature Neuroscience*, *19*(11), 1433–1441. doi: 10.1038/nn.4402

Georgiades, P., Ferguson-Smith, A. C., & Burton, G. J. (2002). Comparative Developmental Anatomy of the Murine and Human Definitive Placentae. *Placenta*, *23*(1), 3–19. doi: 10.1053/plac.2001.0738

Geyer, M. A., Krebs-Thomson, K., Braff, D. L., & Swerdlow, N. R. (2001). Pharmacological studies of prepulse inhibition models of sensorimotor gating deficits in schizophrenia: a decade in review. *Psychopharmacology*, *156*(2–3), 117–154. doi: 10.1007/s002130100811

Geyer, M. A., & Vollenweider, F. X. (2008). Serotonin research: contributions to understanding psychoses. *Trends in Pharmacological Sciences*, *29*(9), 445–453. doi: 10.1016/j.tips.2008.06.006

Girdhar, K., Hoffman, G. E., Jiang, Y., Brown, L., Kundakovic, M., Hauberg, M. E., … Akbarian, S. (2018). Cell-specific histone modification maps in the human frontal lobe link schizophrenia risk to the neuronal epigenome. *Nature Neuroscience*, *21*(8), 1126–1136. doi: 10.1038/s41593-018-0187-0

Giusti, S. A., Vercelli, C. A., Vogl, A. M., Kolarz, A. W., Pino, N. S., Deussing, J. M., & Refojo, D. (2014). Behavioral phenotyping of Nestin-Cre mice: Implications for genetic mouse models of psychiatric disorders. *Journal of Psychiatric Research*, *55*, 87–95. doi: 10.1016/j.jpsychires.2014.04.002

González-Maeso, J., & Sealfon, S. C. (2009). Psychedelics and schizophrenia. *Trends in Neurosciences*, *32*(4), 225–232. doi: 10.1016/j.tins.2008.12.005

Grace, A. A. (2016). Dysregulation of the dopamine system in the pathophysiology of schizophrenia and depression. *Nature Reviews Neuroscience*, *17*(8), 524–532. doi: 10.1038/nrn.2016.57

Grayson, B., Leger, M., Piercy, C., Adamson, L., Harte, M., & Neill, J. C. (2015). Assessment of disease-related cognitive impairments using the novel object recognition (NOR) task in rodents. *Behavioural Brain Research*, *285*, 176–193. doi: 10.1016/j.bbr.2014.10.025

Green, E. K., Rees, E., Walters, J. T. R., Smith, K.-G., Forty, L., Grozeva, D., … Kirov, G. (2016). Copy number variation in bipolar disorder. *Molecular Psychiatry*, *21*(1), 89–93. doi: 10.1038/mp.2014.174

Grillon, C. (2008). Models and mechanisms of anxiety: Evidence from startle studies. *Psychopharmacology*, *199*(3), 421–437. doi: 10.1007/s00213-007-1019-1

Grossman, L. S., Harrow, M., Rosen, C., Faull, R., & Strauss, G. P. (2008). Sex differences in schizophrenia and other psychotic disorders: a 20-year longitudinal study of psychosis and recovery. *Comprehensive Psychiatry*, *49*(6), 523–529. doi: 10.1016/j.comppsych.2008.03.004

Guemez-Gamboa, A., Coufal, N. G., & Gleeson, J. G. (2014). Primary Cilia in the Developing and Mature Brain. *Neuron*, *82*(3), 511–521. doi: 10.1016/j.neuron.2014.04.024

Gupta, S., Kim, S. Y., Artis, S., Molfese, D. L., Schumacher, A., Sweatt, J. D., … Lubin, F. D. (2010). Histone Methylation Regulates Memory Formation. *Journal of Neuroscience*, *30*(10), 3589–3599. doi: 10.1523/JNEUROSCI.3732-09.2010

Halberstadt, A. L., & Geyer, M. A. (2010). LSD but not lisuride disrupts prepulse inhibition in rats by activating the 5-HT(2A) receptor. *Psychopharmacology*, *208*(2), 179–189. doi: 10.1007/s00213-009-1718-x

Halberstadt, A. L., & Geyer, M. A. (2011). Multiple receptors contribute to the behavioral effects of indoleamine hallucinogens. *Neuropharmacology*, *61*(3), 364–381. doi: 10.1016/j.neuropharm.2011.01.017

Hall, J., Trent, S., Thomas, K. L., O'Donovan, M. C., & Owen, M. J. (2015). Genetic Risk for Schizophrenia: Convergence on Synaptic Pathways Involved in Plasticity. *Biological Psychiatry*, *77*(1), 52–58. doi: 10.1016/j.biopsych.2014.07.011

Hannon, E., Spiers, H., Viana, J., Pidsley, R., Burrage, J., Murphy, T. M., … Mill, J. (2016). Methylation QTLs in the developing brain and their enrichment in schizophrenia risk loci. *Nature Neuroscience*, *19*(1), 48–54. doi: 10.1038/nn.4182

Harno, E., Cottrell, E. C., & White, A. (2013). Metabolic pitfalls of CNS cre-based technology. *Cell Metabolism*, *18*(1), 21–28. doi: 10.1016/j.cmet.2013.05.019

Harrison, P. J. (1999a). The neuropathology of schizophrenia. A critical review of the data and their interpretation. *Brain*, *122*(4), 593–624. doi: 10.1093/brain/122.4.593

Harrison, P. J. (1999b). The neuropathological effects of antipsychotic drugs. *Schizophrenia Research*, *40*(2), 87–99. doi: 10.1016/S0920-9964(99)00065-1

Harrison, P. J. (1999c). Neurochemical alterations in schizophrenia affecting the putative receptor targets of atypical antipsychotics. Focus on dopamine (D1, D3, D4) and 5-HT2a receptors. *The British Journal of Psychiatry*, *174*(suppl. 38), 12–22.

Harrison, P. J. (2004). The hippocampus in schizophrenia: A review of the

neuropathological evidence and its pathophysiological implications. *Psychopharmacology*, *174*(1), 151–162. doi: 10.1007/s00213-003-1761-y

Harrison, P. J. (2008). Neuropathology of schizophrenia. *Psychiatry*, *7*(10), 421–424. doi: 10.1016/J.MPPSY.2008.07.013

Harrison, P. J. (2015a). The current and potential impact of genetics and genomics on neuropsychopharmacology. *European Neuropsychopharmacology*, *25*(5), 671–681. doi: 10.1016/j.euroneuro.2013.02.005

Harrison, P. J. (2015b). Recent genetic findings in schizophrenia and their therapeutic relevance. *Journal of Psychopharmacology*, *29*(2), 85–96. doi: 10.1177/0269881114553647

Harrison, P. J. (2018). D-Amino Acid Oxidase Inhibition: A New Glutamate Twist for Clozapine Augmentation in Schizophrenia? *Biological Psychiatry*, *84*(6), 396–398. doi: 10.1016/j.biopsych.2018.06.001

Harrison, P. J., Freemantle, N., & Geddes, J. R. (2003). Meta-analysis of brain weight in schizophrenia. *Schizophrenia Research*, *64*(1), 25–34. doi: 10.1016/S0920-9964(02)00502-9

Harrison, P. J., & Owen, M. J. (2003). Genes for schizophrenia? Recent findings and their pathophysiological implications. *Lancet*, *361*(9355), 417–419. doi: 10.1016/S0140-6736(03)12379-3

Harrison, P. J., Pritchett, D., Stumpenhorst, K., Betts, J. F., Nissen, W., Schweimer, J., … Tunbridge, E. M. (2012). Genetic mouse models relevant to schizophrenia: Taking stock and looking forward. *Neuropharmacology*, *62*(3), 1164–1167. doi: 10.1016/j.neuropharm.2011.08.009

Harrison, P. J., & Weinberger, D. R. (2005). Schizophrenia genes, gene expression, and neuropathology: On the matter of their convergence. *Molecular Psychiatry*, *10*(1), 40–68. doi: 10.1038/sj.mp.4001558

Harro, J. (2018). Animals, anxiety, and anxiety disorders: How to measure anxiety in rodents and why. *Behavioural Brain Research*, *352*, 81–93. doi: 10.1016/j.bbr.2017.10.016

Hartley, S., Barrowclough, C., & Haddock, G. (2013). Anxiety and depression in psychosis: A systematic review of associations with positive psychotic symptoms. *Acta Psychiatrica Scandinavica*, *128*(5), 327–346. doi:

10.1111/acps.12080

Hashimoto, H., Saito, T. R., Furudate, S., & Takahashi, K. W. (2001). Prolactin Levels and Maternal Behavior Induced by Ultrasonic Vocalizations of the Rat Pup. *Experimental Animals*, *50*(4), 307–312. doi: 10.1538/expanim.50.307

Hashimoto, T., Volk, D. W., Eggan, S. M., Mirnics, K., Pierri, J. N., Sun, Z., … Lewis, D. A. (2003). Gene expression deficits in a subclass of GABA neurons in the prefrontal cortex of subjects with schizophrenia. *The Journal of Neuroscience*, *23*(15), 6315–6326. doi: 10.1523/JNEUROSCI.23-15-06315.2003

Hata, K., Okano, M., Lei, H., & Li, E. (2002). Dnmt3L cooperates with the Dnmt3 family of de novo DNA methyltransferases to establish maternal imprints in mice. *Development*, *129*(8), 1983–1993.

Heckers, S., & Konradi, C. (2015). GABAergic mechanisms of hippocampal hyperactivity in schizophrenia. *Schizophrenia Research*, *167*(1–3), 4–11. doi: 10.1016/j.schres.2014.09.041

Heintzman, N. D., Hon, G. C., Hawkins, R. D., Kheradpour, P., Stark, A., Harp, L. F., … Ren, B. (2009). Histone modifications at human enhancers reflect global cell-type-specific gene expression. *Nature*, *459*(7243), 108–112. doi: 10.1038/nature07829

Heintzman, N. D., Stuart, R. K., Hon, G., Fu, Y., Ching, C. W., Hawkins, R. D., … Ren, B. (2007). Distinct and predictive chromatin signatures of transcriptional promoters and enhancers in the human genome. *Nature Genetics*, *39*(3), 311–318. doi: 10.1038/ng1966

Heldt, S. (2009). The use of lentiviral vectors combined with Cre/loxP to investigate the function of genes in complex behaviors. *Frontiers in Molecular Neuroscience*, *2*(22). doi: 10.3389/neuro.02.022.2009

Henckel, A., Chebli, K., Kota, S. K., Arnaud, P., & Feil, R. (2012). Transcription and histone methylation changes correlate with imprint acquisition in male germ cells. *The EMBO Journal*, *31*(3), 606–615. doi: 10.1038/emboj.2011.425

Hernandez, L., Auerbach, S., & Hoebel, B. G. (1988). Phencyclidine (PCP) injected in the nucleus accumbens increases extracellular dopamine and serotonin as measured by microdialysis. *Life Sciences*, *42*(18), 1713–1723. doi: 10.1016/0024-3205(88)90037-9

Heuer, A., Smith, G. A., Lelos, M. J., Lane, E. L., & Dunnett, S. B. (2012). Unilateral nigrostriatal 6-hydroxydopamine lesions in mice I: Motor impairments identify extent of dopamine depletion at three different lesion sites. *Behavioural Brain Research*, *228*(1), 30–43. doi: 10.1016/j.bbr.2011.11.027

Hirasawa, R., Chiba, H., Kaneda, M., Tajima, S., Li, E., Jaenisch, R., & Sasaki, H. (2008). Maternal and zygotic Dnmt1 are necessary and sufficient for the maintenance of DNA methylation imprints during preimplantation development. *Genes & Development*, *22*(12), 1607–1616. doi: 10.1101/gad.1667008

Hirjak, D., Meyer-Lindenberg, A., Kubera, K. M., Thomann, P. A., & Wolf, R. C. (2018). Motor dysfunction as research domain in the period preceding manifest schizophrenia: A systematic review. *Neuroscience & Biobehavioral Reviews*, *87*, 87–105. doi: 10.1016/j.neubiorev.2018.01.011

Hjorthøj, C., Stürup, A. E., McGrath, J. J., & Nordentoft, M. (2017). Years of potential life lost and life expectancy in schizophrenia: a systematic review and meta-analysis. *The Lancet Psychiatry*, *4*(4), 295–301. doi: 10.1016/S2215-0366(17)30078-0

Homayoun, H., & Moghaddam, B. (2007). NMDA Receptor Hypofunction Produces Opposite Effects on Prefrontal Cortex Interneurons and Pyramidal Neurons. *Journal of Neuroscience*, *27*(43), 11496–11500. doi: 10.1523/JNEUROSCI.2213-07.2007

Hoshii, T., Cifani, P., Feng, Z., Huang, C.-H., Koche, R., Chen, C.-W., … Armstrong, S. A. (2018). A Non-catalytic Function of SETD1A Regulates Cyclin K and the DNA Damage Response. *Cell*, *172*(5), 1007-1021.e17. doi: 10.1016/j.cell.2018.01.032

Howe, F. S., Fischl, H., Murray, S. C., & Mellor, J. (2017). Is H3K4me3 instructive for transcription activation? *BioEssays*, *39*(1), e201600095. doi: 10.1002/bies.201600095

Howes, O. D., Kambeitz, J., Kim, E., Stahl, D., Slifstein, M., Abi-Dargham, A., & Kapur, S. (2012). The Nature of Dopamine Dysfunction in Schizophrenia and What This Means for Treatment. *Archives of General Psychiatry*, *69*(8), 776–786. doi: 10.1001/archgenpsychiatry.2012.169

Howes, O. D., & Kapur, S. (2009). The dopamine hypothesis of schizophrenia: Version III - The final common pathway. *Schizophrenia Bulletin*, *35*(3), 549–562.

doi: 10.1093/schbul/sbp006

Howes, O. D., McCutcheon, R., & Stone, J. (2015). Glutamate and dopamine in schizophrenia: An update for the 21st century. *Journal of Psychopharmacology*, *29*(2), 97–115. doi: 10.1177/0269881114563634

Huang, D. W., Sherman, B. T., & Lempicki, R. A. (2009). Systematic and integrative analysis of large gene lists using DAVID bioinformatics resources. *Nature Protocols*, *4*(1), 44–57. doi: 10.1038/nprot.2008.211

Huang, H.-S., & Akbarian, S. (2007). GAD1 mRNA Expression and DNA Methylation in Prefrontal Cortex of Subjects with Schizophrenia. *PLoS ONE*, *2*(8), e809. doi: 10.1371/journal.pone.0000809

Huang, H.-S., Matevossian, A., Whittle, C., Kim, S. Y., Schumacher, A., Baker, S. P., & Akbarian, S. (2007). Prefrontal Dysfunction in Schizophrenia Involves Mixed-Lineage Leukemia 1-Regulated Histone Methylation at GABAergic Gene Promoters. *Journal of Neuroscience*, *27*(42), 11254–11262. doi: 10.1523/JNEUROSCI.3272-07.2007

Huhn, M., Nikolakopoulou, A., Schneider-Thoma, J., Krause, M., Samara, M., Peter, N., … Leucht, S. (2019). Comparative efficacy and tolerability of 32 oral antipsychotics for the acute treatment of adults with multi-episode schizophrenia: a systematic review and network meta-analysis. *The Lancet*, *394*(10202), 939–951. doi: 10.1016/S0140-6736(19)31135-3

Hyun, K., Jeon, J., Park, K., & Kim, J. (2017). Writing, erasing and reading histone lysine methylations. *Experimental & Molecular Medicine*, *49*(4), e324. doi: 10.1038/emm.2017.11

International Schizophrenia Consortium, Purcell, S. M., Wray, N. R., Stone, J. L., Visscher, P. M., O'Donovan, M. C., … Sklar, P. (2009). Common polygenic variation contributes to risk of schizophrenia and bipolar disorder. *Nature*, *460*(7256), 748–752. doi: 10.1038/nature08185

Irifune, M., Shimizu, T., Nomoto, M., & Fukuda, T. (1995). Involvement of N-methyl-D-aspartate (NMDA) receptors in noncompetitive NMDA receptor antagonist-induced hyperlocomotion in mice. *Pharmacology, Biochemistry and Behavior*, *51*(2–3), 291–296. doi: 10.1016/0091-3057(94)00379-W

Jääskeläinen, E., Juola, P., Hirvonen, N., McGrath, J. J., Saha, S., Isohanni, M., … Miettunen, J. (2013). A Systematic Review and Meta-Analysis of Recovery in

Schizophrenia. *Schizophrenia Bulletin*, *39*(6), 1296–1306. doi: 10.1093/schbul/sbs130

Jaffe, A. E., Straub, R. E., Shin, J. H., Tao, R., Gao, Y., Collado-Torres, L., … Weinberger, D. R. (2018). Developmental and genetic regulation of the human cortex transcriptome illuminate schizophrenia pathogenesis. *Nature Neuroscience*, *21*(8), 1117–1125. doi: 10.1038/s41593-018-0197-y

Jakovcevski, M., Ruan, H., Shen, E. Y., Dincer, A., Javidfar, B., Ma, Q., … Akbarian, S. (2015). Neuronal Kmt2a/Mll1 Histone Methyltransferase Is Essential for Prefrontal Synaptic Plasticity and Working Memory. *Journal of Neuroscience*, *35*(13), 5097–5108. doi: 10.1523/JNEUROSCI.3004-14.2015

Jansson, T., & Powell, T. L. (2007). Role of the placenta in fetal programming: underlying mechanisms and potential interventional approaches. *Clinical Science*, *113*(1), 1–13. doi: 10.1042/CS20060339

Jauhar, S., McCutcheon, R., Borgan, F., Veronese, M., Nour, M., Pepper, F., … Howes, O. D. (2018). The relationship between cortical glutamate and striatal dopamine in first-episode psychosis: a cross-sectional multimodal PET and magnetic resonance spectroscopy imaging study. *The Lancet Psychiatry*, *5*(10), 816–823. doi: 10.1016/S2215-0366(18)30268-2

Jézéquel, J., Johansson, E. M., Leboyer, M., & Groc, L. (2018). Pathogenicity of Antibodies against NMDA Receptor: Molecular Insights into Autoimmune Psychosis. *Trends in Neurosciences*, *41*(8), 502–511. doi: 10.1016/j.tins.2018.05.002

Jia, D., Jurkowska, R. Z., Zhang, X., Jeltsch, A., & Cheng, X. (2007). Structure of Dnmt3a bound to Dnmt3L suggests a model for de novo DNA methylation. *Nature*, *449*(7159), 248–251. doi: 10.1038/nature06146

John, R. M. (2017). Imprinted genes and the regulation of placental endocrine function: Pregnancy and beyond. *Placenta*, *56*, 86–90. doi: 10.1016/j.placenta.2017.01.099

John, R. M., & Hemberger, M. (2012). A placenta for life. *Reproductive BioMedicine Online*, *25*(1), 5–11. doi: 10.1016/j.rbmo.2012.03.018

Jones, C. A., Watson, D. J. G., & Fone, K. C. F. (2011). Animal models of schizophrenia. *British Journal of Pharmacology*, *164*(4), 1162–1194. doi: 10.1111/j.1476-5381.2011.01386.x

Jongsma, H. E., Turner, C., Kirkbride, J. B., & Jones, P. B. (2019). International incidence of psychotic disorders, 2002–17: a systematic review and meta-analysis. *The Lancet Public Health*, *4*(5), e229–e244. doi: 10.1016/S2468-2667(19)30056-8

Kalisch-Smith, J. I., Simmons, D. G., Dickinson, H., & Moritz, K. M. (2017). Review: Sexual dimorphism in the formation, function and adaptation of the placenta. *Placenta*, *54*, 10–16. doi: 10.1016/j.placenta.2016.12.008

Kambeitz, J., Abi-Dargham, A., Kapur, S., & Howes, O. D. (2014). Alterations in cortical and extrastriatal subcortical dopamine function in schizophrenia: systematic review and meta-analysis of imaging studies. *British Journal of Psychiatry*, *204*(6), 420–429. doi: 10.1192/bjp.bp.113.132308

Kanahara, N., Shimizu, E., Ohgake, S., Fujita, Y., Kohno, M., Hashimoto, T., … Iyo, M. (2008). Glycine and d-serine, but not d-cycloserine, attenuate prepulse inhibition deficits induced by NMDA receptor antagonist MK-801. *Psychopharmacology*, *198*(3), 363–374. doi: 10.1007/s00213-008-1151-6

Kapur, S., & Remington, G. (2001). Dopamine D2 receptors and their role in atypical antipsychotic action: still necessary and may even be sufficient. *Biological Psychiatry*, *50*(11), 873–883. doi: 10.1016/S0006-3223(01)01251-3

Karper, L. P., Freeman, G. K., Grillon, C., Morgan, C. A., Charney, D. S., & Krystal, J. H. (1996). Preliminary evidence of an association between sensorimotor gating and distractibility in psychosis. *The Journal of Neuropsychiatry and Clinical Neurosciences*, *8*(1), 60–66. doi: 10.1176/jnp.8.1.60

Karpov, B., Joffe, G., Aaltonen, K., Suvisaari, J., Baryshnikov, I., Näätänen, P., … Isometsä, E. (2016). Anxiety symptoms in a major mood and schizophrenia spectrum disorders. *European Psychiatry*, *37*, 1–7. doi: 10.1016/j.eurpsy.2016.04.007

Kelly, S., Jahanshad, N., Zalesky, A., Kochunov, P., Agartz, I., Alloza, C., … Donohoe, G. (2018). Widespread white matter microstructural differences in schizophrenia across 4322 individuals: results from the ENIGMA Schizophrenia DTI Working Group. *Molecular Psychiatry*, *23*(5), 1261–1269. doi: 10.1038/mp.2017.170

Kelsey, G., & Feil, R. (2013). New insights into establishment and maintenance of DNA methylation imprints in mammals. *Philosophical Transactions of the Royal*

*Society B: Biological Sciences*, *368*(1609). doi: 10.1098/rstb.2011.0336

Kendall, K. M., Bracher-Smith, M., Fitzpatrick, H., Lynham, A., Rees, E., Escott-Price, V., … Kirov, G. (2019a). Cognitive performance and functional outcomes of carriers of pathogenic copy number variants: analysis of the UK Biobank. *The British Journal of Psychiatry*, *214*(5), 297–304. doi: 10.1192/bjp.2018.301

Kendall, K. M., Rees, E., Bracher-Smith, M., Legge, S., Riglin, L., Zammit, S., … Walters, J. T. R. (2019b). Association of Rare Copy Number Variants With Risk of Depression. *JAMA Psychiatry*, *76*(8), 818–825. doi: 10.1001/jamapsychiatry.2019.0566

Kerimoglu, C., Agis-Balboa, R. C., Kranz, A., Stilling, R., Bahari-Javan, S., Benito-Garagorri, E., … Fischer, A. (2013). Histone-Methyltransferase MLL2 (KMT2B) Is Required for Memory Formation in Mice. *Journal of Neuroscience*, *33*(8), 3452–3464. doi: 10.1523/JNEUROSCI.3356-12.2013

Kerimoglu, C., Sakib, M. S., Jain, G., Benito, E., Burkhardt, S., Capece, V., … Fischer, A. (2017). KMT2A and KMT2B Mediate Memory Function by Affecting Distinct Genomic Regions. *Cell Reports*, *20*(3), 538–548. doi: 10.1016/j.celrep.2017.06.072

Khandaker, G. M., Zimbron, J., Lewis, G., & Jones, P. B. (2013). Prenatal maternal infection, neurodevelopment and adult schizophrenia: a systematic review of population-based studies. *Psychological Medicine*, *43*(2), 239–257. doi: 10.1017/S0033291712000736

Khashan, A. S., Abel, K. M., McNamee, R., Pedersen, M. G., Webb, R. T., Baker, P. N., … Mortensen, P. B. (2008). Higher Risk of Offspring Schizophrenia Following Antenatal Maternal Exposure to Severe Adverse Life Events. *Archives of General Psychiatry*, *65*(2), 146–152. doi: 10.1001/archgenpsychiatry.2007.20

Kim, K.-Y., Tanaka, Y., Su, J., Cakir, B., Xiang, Y., Patterson, B., … Park, I.-H. (2018). Uhrf1 regulates active transcriptional marks at bivalent domains in pluripotent stem cells through Setd1a. *Nature Communications*, *9*(1), 2583. doi: 10.1038/s41467-018-04818-0

Kim, T. H., Barrera, L. O., Zheng, M., Qu, C., Singer, M. A., Richmond, T. A., … Ren, B. (2005). A high-resolution map of active promoters in the human genome. *Nature*, *436*(7052), 876–880. doi: 10.1038/nature03877

Kindler, J., Schultze-Lutter, F., Michel, C., Martz-Irngartinger, A., Linder, C., Schmidt,

S. J., … Walther, S. (2016). Abnormal involuntary movements are linked to psychosis-risk in children and adolescents: Results of a population-based study. *Schizophrenia Research*, *174*(1–3), 58–64. doi: 10.1016/j.schres.2016.04.032

Kirkbride, J. B., Keyes, K. M., & Susser, E. (2018). City Living and Psychotic Disorders—Implications of Global Heterogeneity for Theory Development. *JAMA Psychiatry*, *75*(12), 1211–1212. doi: 10.1001/jamapsychiatry.2018.2640

Kirov, G. K. (2015). CNVs in neuropsychiatric disorders. *Human Molecular Genetics*, *24*(R1), R45–R49. doi: 10.1093/hmg/ddv253

Kirov, G. K., Pocklington, A. J., Holmans, P., Ivanov, D., Ikeda, M., Ruderfer, D., … Owen, M. J. (2012). De novo CNV analysis implicates specific abnormalities of postsynaptic signalling complexes in the pathogenesis of schizophrenia. *Molecular Psychiatry*, *17*(2), 142–153. doi: 10.1038/mp.2011.154

Kirov, G. K., Rees, E., Walters, J. T. R., Escott-Price, V., Georgieva, L., Richards, A. L., … Owen, M. J. (2014). The Penetrance of Copy Number Variations for Schizophrenia and Developmental Delay. *Biological Psychiatry*, *75*(5), 378–385. doi: 10.1016/j.biopsych.2013.07.022

Klauser, P., Baker, S. T., Cropley, V. L., Bousman, C., Fornito, A., Cocchi, L., … Zalesky, A. (2016). White Matter Disruptions in Schizophrenia Are Spatially Widespread and Topologically Converge on Brain Network Hubs. *Schizophrenia Bulletin*, *43*(2), 425–435. doi: 10.1093/schbul/sbw100

Koch, M. (1999). The neurobiology of startle. *Progress in Neurobiology*, *59*(2), 107–128. doi: 10.1016/S0301-0082(98)00098-7

Kornberg, R. D., & Lorch, Y. (1999). Twenty-five years of the nucleosome, fundamental particle of the eukaryote chromosome. *Cell*, *98*(3), 285–294. doi: 10.1016/s0092-8674(00)81958-3

Kouzarides, T. (2007). Chromatin Modifications and Their Function. *Cell*, *128*(4), 693–705. doi: 10.1016/j.cell.2007.02.005

Krause, M., Zhu, Y., Huhn, M., Schneider-Thoma, J., Bighelli, I., Nikolakopoulou, A., & Leucht, S. (2018). Antipsychotic drugs for patients with schizophrenia and predominant or prominent negative symptoms: a systematic review and meta-analysis. *European Archives of Psychiatry and Clinical Neuroscience*, *268*(7), 625–639. doi: 10.1007/s00406-018-0869-3

Krystal, J. H., Karper, L. P., Seibyl, J. P., Freeman, G. K., Delaney, R., Bremner, J. D., … Charney, D. S. (1994). Subanesthetic Effects of the Noncompetitive NMDA Antagonist, Ketamine, in Humans: Psychotomimetic, Perceptual, Cognitive, and Neuroendocrine Responses. *Archives of General Psychiatry*, *51*(3), 199–214. doi: 10.1001/archpsyc.1994.03950030035004

Kumari, V., Soni, W., & Sharma, T. (2002). Prepulse inhibition of the startle response in risperidone-treated patients: comparison with typical antipsychotics. *Schizophrenia Research*, *55*(1–2), 139–146. doi: 10.1016/S0920-9964(01)00276-6

Kusumi, I., Boku, S., & Takahashi, Y. (2015). Psychopharmacology of atypical antipsychotic drugs: From the receptor binding profile to neuroprotection and neurogenesis. *Psychiatry and Clinical Neurosciences*, *69*(5), 243–258. doi: 10.1111/pcn.12242

Lahti, A. C., Weiler, M. A., Michaelidis, T., Parwani, A., & Tamminga, C. A. (2001). Effects of ketamine in normal and schizophrenic volunteers. *Neuropsychopharmacology*, *25*(4), 455–467. doi: 10.1016/S0893-133X(01)00243-3

Lally, J., Ajnakina, O., Di Forti, M., Trotta, A., Demjaha, A., Kolliakou, A., … Murray, R. M. (2016). Two distinct patterns of treatment resistance: clinical predictors of treatment resistance in first-episode schizophrenia spectrum psychoses. *Psychological Medicine*, *46*(15), 3231–3240. doi: 10.1017/S0033291716002014

Lally, J., Ajnakina, O., Stubbs, B., Cullinane, M., Murphy, K. C., Gaughran, F., & Murray, R. M. (2017). Remission and recovery from first-episode psychosis in adults: systematic review and meta-analysis of long-term outcome studies. *British Journal of Psychiatry*, *211*(6), 350–358. doi: 10.1192/bjp.bp.117.201475

Lalonde, R., Filali, M., Bensoula, A. N., & Lestienne, F. (1996). Sensorimotor learning in three cerebellar mutant mice. *Neurobiology of Learning and Memory*, *65*(2), 113–120. doi: 10.1006/nlme.1996.0013

Lane, H.-Y., Lin, C.-H., Green, M. F., Hellemann, G., Huang, C.-C., Chen, P.-W., … Tsai, G. E. (2013). Add-on treatment of benzoate for schizophrenia: a randomized, double-blind, placebo-controlled trial of D-amino acid oxidase inhibitor. *JAMA Psychiatry*, *70*(12), 1267–1275. doi: 10.1001/jamapsychiatry.2013.2159

Laruelle, M., Abi-Dargham, A., van Dyck, C. H., Gil, R., D'Souza, C. D., Erdos, J., … Innis, R. B. (1996). Single photon emission computerized tomography imaging of amphetamine-induced dopamine release in drug-free schizophrenic subjects. *Proceedings of the National Academy of Sciences*, *93*(17), 9235–9240. doi: 10.1073/pnas.93.17.9235

Laursen, T. M., Nordentoft, M., & Mortensen, P. B. (2014). Excess Early Mortality in Schizophrenia. *Annual Review of Clinical Psychology*, *10*(1), 425–448. doi: 10.1146/annurev-clinpsy-032813-153657

Le Pen, G., Kew, J., Alberati, D., Borroni, E., Heitz, M.-P., & Moreau, J.-L. (2003). Prepulse inhibition deficits of the startle reflex in neonatal ventral hippocampal–lesioned rats: reversal by glycine and a glycine transporter inhibitor. *Biological Psychiatry*, *54*(11), 1162–1170. doi: 10.1016/S0006-3223(03)00374-3

Lee, G., & Zhou, Y. (2019). NMDAR Hypofunction Animal Models of Schizophrenia. *Frontiers in Molecular Neuroscience*, *12*, 185. doi: 10.3389/fnmol.2019.00185

Lee, J.-H., & Skalnik, D. G. (2005). CpG-binding Protein (CXXC Finger Protein 1) Is a Component of the Mammalian Set1 Histone H3-Lys4 Methyltransferase Complex, the Analogue of the Yeast Set1/COMPASS Complex. *Journal of Biological Chemistry*, *280*(50), 41725–41731. doi: 10.1074/jbc.M508312200

Lee, J.-H., & Skalnik, D. G. (2008). Wdr82 Is a C-Terminal Domain-Binding Protein That Recruits the Setd1A Histone H3-Lys4 Methyltransferase Complex to Transcription Start Sites of Transcribed Human Genes. *Molecular and Cellular Biology*, *28*(2), 609–618. doi: 10.1128/MCB.01356-07

Leger, M., Quiedeville, A., Bouet, V., Haelewyn, B., Boulouard, M., Schumann-Bard, P., & Freret, T. (2013). Object recognition test in mice. *Nature Protocols*, *8*(12), 2531–2537. doi: 10.1038/nprot2013155

Lennox, B. R., Palmer-Cooper, E. C., Pollak, T., Hainsworth, J., Marks, J., Jacobson, L., … PPiP study team. (2017). Prevalence and clinical characteristics of serum neuronal cell surface antibodies in first-episode psychosis: a case-control study. *The Lancet Psychiatry*, *4*(1), 42–48. doi: 10.1016/S2215-0366(16)30375-3

Leucht, S., Cipriani, A., Spineli, L., Mavridis, D., Örey, D., Richter, F., … Davis, J. M. (2013). Comparative efficacy and tolerability of 15 antipsychotic drugs in schizophrenia: a multiple-treatments meta-analysis. *The Lancet*, *382*(9896), 951–962. doi: 10.1016/S0140-6736(13)60733-3

Leumann, L., Feldon, J., Vollenweider, F. X., & Ludewig, K. (2002). Effects of typical and atypical antipsychotics on prepulse inhibition and latent inhibition in chronic schizophrenia. *Biological Psychiatry*, *52*(7), 729–739. doi: 10.1016/S0006-3223(02)01344-6

Leussis, M. P., & Bolivar, V. J. (2006). Habituation in rodents: A review of behavior, neurobiology, and genetics. *Neuroscience and Biobehavioral Reviews*, *30*(7), 1045–1064. doi: 10.1016/j.neubiorev.2006.03.006

Lewandoski, M. (2001). Conditional control of gene expression in the mouse. *Nature Reviews Genetics*, *2*(10), 743–755. doi: 10.1038/35093537\n35093537

Lewandowski, K. E., Cohen, B. M., & Öngur, D. (2011). Evolution of neuropsychological dysfunction during the course of schizophrenia and bipolar disorder. *Psychological Medicine*, *41*(2), 225–241. doi: 10.1017/S0033291710001042

Lewis, A., Mitsuya, K., Umlauf, D., Smith, P., Dean, W., Walter, J., … Reik, W. (2004). Imprinting on distal chromosome 7 in the placenta involves repressive histone methylation independent of DNA methylation. *Nature Genetics*, *36*(12), 1291–1295. doi: 10.1038/ng1468

Lewis, D. A., Hashimoto, T., & Volk, D. W. (2005). Cortical inhibitory neurons and schizophrenia. *Nature Reviews Neuroscience*, *6*(4), 312–324. doi: 10.1038/nrn1648

Li, E., Beard, C., & Jaenisch, R. (1993). Role for DNA methylation in genomic imprinting. *Nature*, *366*(6453), 362–365. doi: 10.1038/366362a0

Li, L., Keverne, E. B., Aparicio, S. A., Ishino, F., Barton, S. C., & Surani, M. A. (1999). Regulation of maternal behavior and offspring growth by paternally expressed Peg3. *Science*, *284*(5412), 330–333. doi: 10.1126/science.284.5412.330

Li, M., Santpere, G., Kawasawa, Y. I., Evgrafov, O. V., Gulden, F. O., Pochareddy, S., … Sestan, N. (2018). Integrative functional genomic analysis of human brain development and neuropsychiatric risks. *Science*, *362*(6420), eaat7615. doi: 10.1126/SCIENCE.AAT7615

Li, S., Hu, N., Zhang, W., Tao, B., Dai, J., Gong, Y., … Lui, S. (2019). Dysconnectivity of Multiple Brain Networks in Schizophrenia: A Meta-Analysis of Resting-State Functional Connectivity. *Frontiers in Psychiatry*, *10*, 482. doi: 10.3389/fpsyt.2019.00482

Li, Y., & Jiao, J. (2017). Histone chaperone HIRA regulates neural progenitor cell proliferation and neurogenesis via β-catenin. *Journal of Cell Biology*, *216*(7), 1975–1992. doi: 10.1083/jcb.201610014

Liang, H., Hippenmeyer, S., & Ghashghaei, H. T. (2012). A Nestin-cre transgenic mouse is insufficient for recombination in early embryonic neural progenitors. *Biology Open*, *1*(12), 1200–1203. doi: 10.1242/BIO.20122287

Liao, Y., Smyth, G. K., & Shi, W. (2014). featureCounts: an efficient general purpose program for assigning sequence reads to genomic features. *Bioinformatics*, *30*(7), 923–930. doi: 10.1093/bioinformatics/btt656

Lieberman, J. A., Perkins, D., Belger, A., Chakos, M., Jarskog, F., Boteva, K., & Gilmore, J. (2001). The early stages of schizophrenia: speculations on pathogenesis, pathophysiology, and therapeutic approaches. *Biological Psychiatry*, *50*(11), 884–897. doi: 10.1016/S0006-3223(01)01303-8

Lillrank, S. M., O'Connor, W. T., Oja, S. S., & Ungerstedt, U. (1994). Systemic phencyclidine administration is associated with increased dopamine, GABA, and 5-HIAA levels in the dorsolateral striatum of conscious rats: an in vivo microdialysis study. *Journal of Neural Transmission*, *95*(2), 145–155. doi: 10.1007/BF01276433

Lin, C.-H., Lin, C.-H., Chang, Y.-C., Huang, Y.-J., Chen, P.-W., Yang, H.-T., & Lane, H.-Y. (2018). Sodium Benzoate, a D-Amino Acid Oxidase Inhibitor, Added to Clozapine for the Treatment of Schizophrenia: A Randomized, Double-Blind, Placebo-Controlled Trial. *Biological Psychiatry*, *84*(6), 422–432. doi: 10.1016/j.biopsych.2017.12.006

Loonstra, A., Vooijs, M., Beverloo, H. B., Allak, B. A., van Drunen, E., Kanaar, R., … Jonkers, J. (2001). Growth inhibition and DNA damage induced by Cre recombinase in mammalian cells. *Proceedings of the National Academy of Sciences of the United States of America*, *98*(16), 9209–9214. doi: 10.1073/pnas.161269798

Love, M. I., Huber, W., & Anders, S. (2014). Moderated estimation of fold change and dispersion for RNA-seq data with DESeq2. *Genome Biology*, *15*(12), 550. doi: 10.1186/s13059-014-0550-8

Luger, K., Mäder, A. W., Richmond, R. K., Sargent, D. F., & Richmond, T. J. (1997). Crystal structure of the nucleosome core particle at 2.8 Å resolution. *Nature*,

*389*(6648), 251–260. doi: 10.1038/38444

Mackeprang, T., Kristiansen, K. T., & Glenthoj, B. Y. (2002). Effects of antipsychotics on prepulse inhibition of the startle response in drug-naïve schizophrenic patients. *Biological Psychiatry*, *52*(9), 863–873. doi: 10.1016/S0006-3223(02)01409-9

Maher, B. (2008). Personal genomes: The case of the missing heritability. *Nature*, *456*(7218), 18–21. doi: 10.1038/456018a

Malhotra, D., & Sebat, J. (2012). CNVs: Harbingers of a Rare Variant Revolution in Psychiatric Genetics. *Cell*, *148*(6), 1223–1241. doi: 10.1016/j.cell.2012.02.039

Mangalore, R., & Knapp, M. (2007). Cost of schizophrenia in England. *The Journal of Mental Health Policy and Economics*, *10*(1), 23–41.

Marco, E. M., Llorente, R., López-Gallardo, M., Mela, V., Llorente-Berzal, Á., Prada, C., & Viveros, M.-P. (2015). The maternal deprivation animal model revisited. *Neuroscience & Biobehavioral Reviews*, *51*, 151–163. doi: 10.1016/j.neubiorev.2015.01.015

Marley, A., & von Zastrow, M. (2012). A Simple Cell-Based Assay Reveals That Diverse Neuropsychiatric Risk Genes Converge on Primary Cilia. *PLoS ONE*, *7*(10), e46647. doi: 10.1371/journal.pone.0046647

Marshall, C. R., Howrigan, D. P., Merico, D., Thiruvahindrapuram, B., Wu, W., Greer, D. S., … CNV and Schizophrenia Working Groups of the Psychiatric Genomics Consortium. (2017). Contribution of copy number variants to schizophrenia from a genome-wide study of 41,321 subjects. *Nature Genetics*, *49*(1), 27–35. doi: 10.1038/ng.3725

Martin, P., Carlsson, M. L., & Hjorth, S. (1998). Systemic PCP treatment elevates brain extracellular 5-HT. *NeuroReport*, *9*(13), 2985–2988. doi: 10.1097/00001756-199809140-00012

Martinez-Gras, I., Rubio, G., del Manzano, B. A., Rodriguez-Jimenez, R., Garcia-Sanchez, F., Bagney, A., … Borrell, J. (2009). The relationship between prepulse inhibition and general psychopathology in patients with schizophrenia treated with long-acting risperidone. *Schizophrenia Research*, *115*(2–3), 215–221. doi: 10.1016/j.schres.2009.09.035

Marwaha, S., & Johnson, S. (2004). Schizophrenia and employment. *Social*

*Psychiatry and Psychiatric Epidemiology*, *39*(5), 337–349. doi: 10.1007/s00127-004-0762-4

Matsuura, A., Fujita, Y., Iyo, M., & Hashimoto, K. (2015). Effects of sodium benzoate on pre-pulse inhibition deficits and hyperlocomotion in mice after administration of phencyclidine. *Acta Neuropsychiatrica*, *27*(3), 159–167. doi: 10.1017/neu.2015.1

McAusland, L., Buchy, L., Cadenhead, K. S., Cannon, T. D., Cornblatt, B. A., Heinssen, R., … Addington, J. (2017). Anxiety in youth at clinical high risk for psychosis. *Early Intervention in Psychiatry*, *11*(6), 480–487. doi: 10.1111/eip.12274

McCutcheon, R. A., Abi-Dargham, A., & Howes, O. D. (2019). Schizophrenia, Dopamine and the Striatum: From Biology to Symptoms. *Trends in Neurosciences*, *42*(3), 205–220. doi: 10.1016/j.tins.2018.12.004

McCutcheon, R. A., Beck, K., Jauhar, S., & Howes, O. D. (2018). Defining the Locus of Dopaminergic Dysfunction in Schizophrenia: A Meta-analysis and Test of the Mesolimbic Hypothesis. *Schizophrenia Bulletin*, *44*(6), 1301–1311. doi: 10.1093/schbul/sbx180

McGrath, J. J., McLaughlin, K. A., Saha, S., Aguilar-Gaxiola, S., Al-Hamzawi, A., Alonso, J., … Kessler, R. C. (2017). The association between childhood adversities and subsequent first onset of psychotic experiences: a cross-national analysis of 23 998 respondents from 17 countries. *Psychological Medicine*, *47*(7), 1230–1245. doi: 10.1017/S0033291716003263

McGrath, J. J., Saha, S., Chant, D., & Welham, J. (2008). Schizophrenia: A Concise Overview of Incidence, Prevalence, and Mortality. *Epidemiologic Reviews*, *30*(1), 67–76. doi: 10.1093/epirev/mxn001

McGuire, P., Howes, O., Stone, J., & Fusar-Poli, P. (2008). Functional neuroimaging in schizophrenia: diagnosis and drug discovery. *Trends in Pharmacological Sciences*, *29*(2), 91–98. doi: 10.1016/j.tips.2007.11.005

Meldrum, B. S. (2000). Glutamate as a Neurotransmitter in the Brain: Review of Physiology and Pathology. *The Journal of Nutrition*, *130*(4), 1007S-1015S. doi: 10.1093/jn/130.4.1007S

Meltzer, H. Y. (1997). Treatment-Resistant Schizophrenia - The Role of Clozapine. *Current Medical Research and Opinion*, *14*(1), 1–20. doi:

10.1185/03007999709113338

Meltzer, H. Y., & Massey, B. (2011). The role of serotonin receptors in the action of atypical antipsychotic drugs. *Current Opinion in Pharmacology*, *11*(1), 59–67. doi: 10.1016/j.coph.2011.02.007

Meltzer, H. Y., & Stahl, S. M. (1976). The Dopamine Hypothesis of Schizophrenia: A Review. *Schizophrenia Bulletin*, *2*(1), 19–76. doi: 10.1093/schbul/2.1.19

Merritt, K., Egerton, A., Kempton, M. J., Taylor, M. J., & McGuire, P. K. (2016). Nature of Glutamate Alterations in Schizophrenia. *JAMA Psychiatry*, *73*(7), 665–674. doi: 10.1001/jamapsychiatry.2016.0442

Meyer, U., & Feldon, J. (2010). Epidemiology-driven neurodevelopmental animal models of schizophrenia. *Progress in Neurobiology*, *90*(3), 285–326. doi: 10.1016/j.pneurobio.2009.10.018

Mikaelsson, M. A., Constância, M., Dent, C. L., Wilkinson, L. S., & Humby, T. (2013). Placental programming of anxiety in adulthood revealed by Igf2-null models. *Nature Communications*, *4*(1), 2311. doi: 10.1038/ncomms3311

Mikkelsen, T. S., Ku, M., Jaffe, D. B., Issac, B., Lieberman, E., Giannoukos, G., … Bernstein, B. E. (2007). Genome-wide maps of chromatin state in pluripotent and lineage-committed cells. *Nature*, *448*(7153), 553–560. doi: 10.1038/nature06008

Millan, M. J., Andrieux, A., Bartzokis, G., Cadenhead, K., Dazzan, P., Fusar-Poli, P., … Weinberger, D. (2016). Altering the course of schizophrenia: progress and perspectives. *Nature Reviews Drug Discovery*, *15*(7), 485–515. doi: 10.1038/nrd.2016.28

Miller, T., Krogan, N. J., Dover, J., Erdjument-Bromage, H., Tempst, P., Johnston, M., … Shilatifard, A. (2001). COMPASS: A complex of proteins associated with a trithorax-related SET domain protein. *Proceedings of the National Academy of Sciences*, *98*(23), 12902–12907. doi: 10.1073/pnas.231473398

Miyamoto, S., Duncan, G. E., Marx, C. E., & Lieberman, J. A. (2005). Treatments for schizophrenia: a critical review of pharmacology and mechanisms of action of antipsychotic drugs. *Molecular Psychiatry*, *10*(1), 79–104. doi: 10.1038/sj.mp.4001556

Moberget, T., Doan, N. T., Alnæs, D., Kaufmann, T., Córdova-Palomera, A.,

Lagerberg, T. V, … Westlye, L. T. (2018). Cerebellar volume and cerebellocerebral structural covariance in schizophrenia: a multisite mega-analysis of 983 patients and 1349 healthy controls. *Molecular Psychiatry*, *23*(6), 1512–1520. doi: 10.1038/mp.2017.106

Moncrieff, J., & Leo, J. (2010). A systematic review of the effects of antipsychotic drugs on brain volume. *Psychological Medicine*, *40*(9), 1409–1422. doi: 10.1017/S0033291709992297

Monville, C., Torres, E. M., & Dunnett, S. B. (2006). Comparison of incremental and accelerating protocols of the rotarod test for the assessment of motor deficits in the 6-OHDA model. *Journal of Neuroscience Methods*, *158*(2), 219–223. doi: 10.1016/j.jneumeth.2006.06.001

Moore, T., & Haig, D. (1991). Genomic imprinting in mammalian development: a parental tug-of-war. *Trends in Genetics*, *7*(2), 45–49. doi: 10.1016/0168-9525(91)90230-N

Morozov, A., Kellendonk, C., Simpson, E., & Tronche, F. (2003). Using conditional mutagenesis to study the brain. *Biological Psychiatry*, *54*(11), 1125–1133. doi: 10.1016/S0006-3223(03)00467-0

Mouri, A., Noda, Y., Enomoto, T., & Nabeshima, T. (2007). Phencyclidine animal models of schizophrenia: Approaches from abnormality of glutamatergic neurotransmission and neurodevelopment. *Neurochemistry International*, *51*(2–4), 173–184. doi: 10.1016/j.neuint.2007.06.019

Mukai, J., Cannavo, E., Sun, Z., Crabtree, G., Diamantopoulou, A., Thakur, P., … Gogos, J. (2019). Recapitulation and reversal of schizophrenia-related phenotypes in Setd1a-deficient mice. *BioRxiv*. doi: 10.1101/529701

Müller, H., Liu, B., Croy, B. A., Head, J. R., Hunt, J. S., Dai, G., & Soares, M. J. (1999). Uterine Natural Killer Cells Are Targets for a Trophoblast Cell-Specific Cytokine, Prolactin-Like Protein A. *Endocrinology*, *140*(6), 2711–2720. doi: 10.1210/endo.140.6.6828

Murray, R. M., & Lewis, S. W. (1987). Is schizophrenia a neurodevelopmental disorder? *British Medical Journal*, *295*(6600), 681–682. doi: 10.1136/bmj.295.6600.681

Mustonen, A., Niemelä, S., Nordström, T., Murray, G. K., Mäki, P., Jääskeläinen, E., & Miettunen, J. (2018). Adolescent cannabis use, baseline prodromal symptoms

and the risk of psychosis. *The British Journal of Psychiatry*, *212*(4), 227–233. doi: 10.1192/bjp.2017.52

Naiche, L. A., & Papaioannou, V. E. (2007). Cre activity causes widespread apoptosis and lethal anemia during embryonic development. *Genesis*, *45*, 768–775. doi: 10.1002/dvg.20353

Nakao, K., Jeevakumar, V., Jiang, S. Z., Fujita, Y., Diaz, N. B., Pretell Annan, C. A., … Nakazawa, K. (2019). Schizophrenia-Like Dopamine Release Abnormalities in a Mouse Model of NMDA Receptor Hypofunction. *Schizophrenia Bulletin*, *45*(1), 138–147. doi: 10.1093/schbul/sby003

Network and Pathway Analysis Subgroup of Psychiatric Genomics Consortium. (2015). Psychiatric genome-wide association study analyses implicate neuronal, immune and histone pathways. *Nature Neuroscience*, *18*(2), 199–209. doi: 10.1038/nn.3922

Nielsen, P. R., Mortensen, P. B., Dalman, C., Henriksen, T. B., Pedersen, M. G., Pedersen, C. B., & Agerbo, E. (2013). Fetal Growth and Schizophrenia: A Nested Case-Control and Case-Sibling Study. *Schizophrenia Bulletin*, *39*(6), 1337–1342. doi: 10.1093/schbul/sbs148

Nilsson, M., Carlsson, A., & Carlsson, M. L. (1997). Glycine and D-serine decrease MK-801-induced hyperactivity in mice. *Journal of Neural Transmission*, *104*(11–12), 1195–1205. doi: 10.1007/BF01294720

Noma, K. -i., Allis, C. D., & Grewal, S. I. (2001). Transitions in Distinct Histone H3 Methylation Patterns at the Heterochromatin Domain Boundaries. *Science*, *293*(5532), 1150–1155. doi: 10.1126/science.1064150

O'Brien, H. E., Hannon, E., Hill, M. J., Toste, C. C., Robertson, M. J., Morgan, J. E., … Bray, N. J. (2018). Expression quantitative trait loci in the developing human brain and their enrichment in neuropsychiatric disorders. *Genome Biology*, *19*(1), 194. doi: 10.1186/s13059-018-1567-1

O'Donovan, M. C., & Owen, M. J. (2016). The implications of the shared genetics of psychiatric disorders. *Nature Medicine*, *22*(11), 1214–1219. doi: 10.1038/nm.4196

Ochoa, S., Usall, J., Cobo, J., Labad, X., & Kulkarni, J. (2012). Gender Differences in Schizophrenia and First-Episode Psychosis: A Comprehensive Literature Review. *Schizophrenia Research and Treatment*, *2012*, 1–9. doi:

10.1155/2012/916198

Olney, J. W., & Farber, N. B. (1995). Glutamate Receptor Dysfunction and Schizophrenia. *Archives of General Psychiatry*, *52*(12), 998–1007. doi: 10.1001/archpsyc.1995.03950240016004

Ooi, S. K. T., Qiu, C., Bernstein, E., Li, K., Jia, D., Yang, Z., … Bestor, T. H. (2007). DNMT3L connects unmethylated lysine 4 of histone H3 to de novo methylation of DNA. *Nature*, *448*(7154), 714–717. doi: 10.1038/nature05987

Oranje, B., Van Oel, C. J., Gispen-De Wied, C. C., Verbaten, M. N., & Kahn, R. S. (2002). Effects of typical and atypical antipsychotics on the prepulse inhibition of the startle reflex in patients with schizophrenia. *Journal of Clinical Psychopharmacology*, *22*(4), 359–365. doi: 10.1097/00004714-200208000-00005

Ouagazzal, A., Grottick, A. J., Moreau, J., & Higgins, G. A. (2001). Effect of LSD on Prepulse Inhibition and Spontaneous Behavior in the Rat A Pharmacological Analysis and Comparison between Two Rat Strains. *Neuropsychopharmacology*, *25*(4), 565–575. doi: 10.1016/S0893-133X(01)00282-2

Outhwaite, J. E., McGuire, V., & Simmons, D. G. (2015). Genetic ablation of placental sinusoidal trophoblast giant cells causes fetal growth restriction and embryonic lethality. *Placenta*, *36*(8), 951–955. doi: 10.1016/j.placenta.2015.05.013

Owen, M. J. (2014). New Approaches to Psychiatric Diagnostic Classification. *Neuron*, *84*(3), 564–571. doi: 10.1016/j.neuron.2014.10.028

Owen, M. J., & O'Donovan, M. C. (2017). Schizophrenia and the neurodevelopmental continuum: evidence from genomics. *World Psychiatry*, *16*(3), 227–235. doi: 10.1002/wps.20440

Owen, M. J., O'Donovan, M. C., Thapar, A., & Craddock, N. (2011). Neurodevelopmental hypothesis of schizophrenia. *British Journal of Psychiatry*, *198*(3), 173–175. doi: 10.1192/bjp.bp.110.084384

Owen, M. J., Sawa, A., & Mortensen, P. B. (2016). Schizophrenia. *The Lancet*, *388*(10039), 86–97. doi: 10.1016/S0140-6736(15)01121-6

Padich, R. A., McCloskey, T. C., & Kehne, J. H. (1996). 5-HT modulation of auditory and visual sensorimotor gating: II. Effects of the 5-HT2A antagonist MDL

100,907 on disruption of sound and light prepulse inhibition produced by 5-HT agonists in Wistar rats. *Psychopharmacology*, *124*(1–2), 107–116. doi: 10.1007/bf02245610

Papouin, T., Ladépêche, L., Ruel, J., Sacchi, S., Labasque, M., Hanini, M., … Oliet, S. H. R. (2012). Synaptic and extrasynaptic NMDA receptors are gated by different endogenous coagonists. *Cell*, *150*(3), 633–646. doi: 10.1016/j.cell.2012.06.029

Pardiñas, A. F., Holmans, P., Pocklington, A. J., Escott-Price, V., Ripke, S., Carrera, N., … Walters, J. T. R. (2018). Common schizophrenia alleles are enriched in mutation-intolerant genes and in regions under strong background selection. *Nature Genetics*, *50*(3), 381–389. doi: 10.1038/s41588-018-0059-2

Paridaen, J. T., & Huttner, W. B. (2014). Neurogenesis during development of the vertebrate central nervous system. *EMBO Reports*, *15*(4), 351–364. doi: 10.1002/embr.201438447

Pathmanandavel, K., Starling, J., Merheb, V., Ramanathan, S., Sinmaz, N., Dale, R. C., & Brilot, F. (2015). Antibodies to surface dopamine-2 receptor and N-methyl-D-aspartate receptor in the first episode of acute psychosis in children. *Biological Psychiatry*, *77*(6), 537–547. doi: 10.1016/j.biopsych.2014.07.014

Peralta, V., Campos, M. S., De Jalón, E. G., & Cuesta, M. J. (2010). Motor behavior abnormalities in drug-naïve patients with schizophrenia spectrum disorders. *Movement Disorders*, *25*(8), 1068–1076. doi: 10.1002/mds.23050

Perez-Garcia, V., Fineberg, E., Wilson, R., Murray, A., Mazzeo, C. I., Tudor, C., … Hemberger, M. (2018). Placentation defects are highly prevalent in embryonic lethal mouse mutants. *Nature*, *555*(7697), 463–468. doi: 10.1038/nature26002

Perry, W., & Braff, D. L. (1994). Information-processing deficits and thought disorder in schizophrenia. *American Journal of Psychiatry*, *151*(3), 363–367. doi: 10.1176/ajp.151.3.363

Pham, C. T. N., MacIvor, D. M., Hug, B. A., Heusel, J. W., & Ley, T. J. (1996). Long-range disruption of gene expression by a selectable marker cassette. *Proceedings of the National Academy of Sciences*, *93*(23), 13090–13095. doi: 10.1073/pnas.93.23.13090

Pidsley, R., Viana, J., Hannon, E., Spiers, H., Troakes, C., Al-saraj, S., … Mill, J. (2014). Methylomic profiling of human brain tissue supports a

neurodevelopmental origin for schizophrenia. *Genome Biology*, *15*(10), 483. doi: 10.1186/s13059-014-0483-2

Plana-Ripoll, O., Pedersen, C. B., & McGrath, J. J. (2018). Urbanicity and Risk of Schizophrenia—New Studies and Old Hypotheses. *JAMA Psychiatry*, *75*(7), 687–688. doi: 10.1001/jamapsychiatry.2018.0551

Pocklington, A. J., Rees, E., Walters, J. T. R., Han, J., Kavanagh, D. H., Chambert, K. D., … Owen, M. J. (2015). Novel Findings from CNVs Implicate Inhibitory and Excitatory Signaling Complexes in Schizophrenia. *Neuron*, *86*(5), 1203–1214. doi: 10.1016/j.neuron.2015.04.022

Pokos, V., & Castle, D. (2006). Prevalence of Comorbid Anxiety Disorders in Schizophrenia Spectrum Disorders: A Literature Review. *Current Psychiatry Reviews*, *2*(3), 285–307. doi: 10.2174/157340006778018193

Powell, S. B., Weber, M., & Geyer, M. A. (2012). Genetic models of sensorimotor gating: Relevance to neuropsychiatric disorders. *Current Topics in Behavioral Neurosciences*, *12*, 251–318. doi: 10.1007/7854_2011_195

Powell, S. B., Zhou, X., & Geyer, M. A. (2009). Prepulse inhibition and genetic mouse models of schizophrenia. *Behavioural Brain Research*, *204*(2), 282–294. doi: 10.1016/j.bbr.2009.04.021

Power, R. A., Verweij, K. J. H., Zuhair, M., Montgomery, G. W., Henders, A. K., Heath, A. C., … Martin, N. G. (2014). Genetic predisposition to schizophrenia associated with increased use of cannabis. *Molecular Psychiatry*, *19*(11), 1201–1204. doi: 10.1038/mp.2014.51

Prut, L., & Belzung, C. (2003). The open field as a paradigm to measure the effects of drugs on anxiety-like behaviors: A review. *European Journal of Pharmacology*, *463*(1), 3–33. doi: 10.1016/S0014-2999(03)01272-X

PsychENCODE Consortium. (2018). Revealing the brain's molecular architecture. *Science*, *362*(6420), 1262–1263. doi: 10.1126/science.362.6420.1262

Purcell, S. M., Moran, J. L., Fromer, M., Ruderfer, D., Solovieff, N., Roussos, P., … Sklar, P. (2014). A polygenic burden of rare disruptive mutations in schizophrenia. *Nature*, *506*(7487), 185–190. doi: 10.1038/nature12975

Qiao, H., Li, Y., Feng, C., Duo, S., Ji, F., & Jiao, J. (2018). Nap1l1 Controls Embryonic Neural Progenitor Cell Proliferation and Differentiation in the Developing Brain.

*Cell Reports*, *22*(9), 2279–2293. doi: 10.1016/j.celrep.2018.02.019

Quednow, B. B., Frommann, I., Berning, J., Kühn, K. U., Maier, W., & Wagner, M. (2008). Impaired Sensorimotor Gating of the Acoustic Startle Response in the Prodrome of Schizophrenia. *Biological Psychiatry*, *64*(9), 766–773. doi: 10.1016/j.biopsych.2008.04.019

Quednow, B. B., Wagner, M., Westheide, J., Beckmann, K., Bliesener, N., Maier, W., & Kühn, K.-U. (2006). Sensorimotor Gating and Habituation of the Startle Response in Schizophrenic Patients Randomly Treated With Amisulpride or Olanzapine. *Biological Psychiatry*, *59*(6), 536–545. doi: 10.1016/j.biopsych.2005.07.012

Rabinowitz, J., Levine, S. Z., Garibaldi, G., Bugarski-Kirola, D., Berardo, C. G., & Kapur, S. (2012). Negative symptoms have greater impact on functioning than positive symptoms in schizophrenia: Analysis of CATIE data. *Schizophrenia Research*, *137*(1–3), 147–150. doi: 10.1016/j.schres.2012.01.015

Rai, A., & Cross, J. C. (2014). Development of the hemochorial maternal vascular spaces in the placenta through endothelial and vasculogenic mimicry. *Developmental Biology*, *387*(2), 131–141. doi: 10.1016/j.ydbio.2014.01.015

Rajasekaran, A., Venkatasubramanian, G., Berk, M., & Debnath, M. (2015). Mitochondrial dysfunction in schizophrenia: Pathways, mechanisms and implications. *Neuroscience & Biobehavioral Reviews*, *48*, 10–21. doi: 10.1016/J.NEUBIOREV.2014.11.005

Ramos, A. (2008). Animal models of anxiety: do I need multiple tests? *Trends in Pharmacological Sciences*, *29*(10), 493–498. doi: 10.1016/j.tips.2008.07.005

Rankin, C. H., Abrams, T., Barry, R. J., Bhatnagar, S., Clayton, D. F., Colombo, J., … Thompson, R. F. (2009). Habituation revisited: An updated and revised description of the behavioral characteristics of habituation. *Neurobiology of Learning and Memory*, *92*(2), 135–138. doi: 10.1016/j.nlm.2008.09.012

Rees, E., Carrera, N., Morgan, J., Hambridge, K., Escott-Price, V., Pocklington, A. J., … Luykx, J. J. (2019). Targeted Sequencing of 10,198 Samples Confirms Abnormalities in Neuronal Activity and Implicates Voltage-Gated Sodium Channels in Schizophrenia Pathogenesis. *Biological Psychiatry*, *85*(7), 554–562. doi: 10.1016/j.biopsych.2018.08.022

Rees, E., Kendall, K., Pardiñas, A. F., Legge, S. E., Pocklington, A., Escott-Price, V.,

… Kirov, G. (2016). Analysis of Intellectual Disability Copy Number Variants for Association With Schizophrenia. *JAMA Psychiatry*, *73*(9), 963–969. doi: 10.1001/jamapsychiatry.2016.1831

Rees, E., Walters, J. T. R., Georgieva, L., Isles, A. R., Chambert, K. D., Richards, A. L., … Kirov, G. (2014a). Analysis of copy number variations at 15 schizophrenia-associated loci. *British Journal of Psychiatry*, *204*(2), 108–114. doi: 10.1192/bjp.bp.113.131052

Rees, E., Walters, J. T. R., Chambert, K. D., O'Dushlaine, C., Szatkiewicz, J., Richards, A. L., … Kirov, G. (2014b). CNV analysis in a large schizophrenia sample implicates deletions at 16p12.1 and SLC1A1 and duplications at 1p36.33 and CGNL1. *Human Molecular Genetics*, *23*(6), 1669–1676. doi: 10.1093/hmg/ddt540

Reichel, J. M., Bedenk, B. T., Gassen, N. C., Hafner, K., Bura, S. A., Almeida-Correa, S., … Wotjak, C. T. (2016). Beware of your Cre-Ation: lacZ expression impairs neuronal integrity and hippocampus-dependent memory. *Hippocampus*, *26*(10), 1250–1264. doi: 10.1002/hipo.22601

Reik, W., Dean, W., & Walter, J. (2001). Epigenetic Reprogramming in Mammalian Development. *Science*, *293*(5532), 1089–1093. doi: 10.1126/science.1063443

Renard, J., Rushlow, W. J., & Laviolette, S. R. (2016). What Can Rats Tell Us about Adolescent Cannabis Exposure? Insights from Preclinical Research. *The Canadian Journal of Psychiatry*, *61*(6), 328–334. doi: 10.1177/0706743716645288

Ripke, S., O'Dushlaine, C., Chambert, K., Moran, J. L., Kähler, A. K., Akterin, S., … Sullivan, P. F. (2013). Genome-wide association analysis identifies 13 new risk loci for schizophrenia. *Nature Genetics*, *45*(10), 1150–1159. doi: 10.1038/ng.2742

Roidl, D., & Hacker, C. (2014). Histone methylation during neural development. *Cell and Tissue Research*, *356*(3), 539–552. doi: 10.1007/s00441-014-1842-8

Rosenfeld, C. S. (2015). Sex-Specific Placental Responses in Fetal Development. *Endocrinology*, *156*(10), 3422–3434. doi: 10.1210/en.2015-1227

Ruthenburg, A. J., Allis, C. D., & Wysocka, J. (2007). Methylation of Lysine 4 on Histone H3: Intricacy of Writing and Reading a Single Epigenetic Mark. *Molecular Cell*, *25*(1), 15–30. doi: 10.1016/j.molcel.2006.12.014

Salahpour, A., Ramsey, A. J., Medvedev, I. O., Kile, B., Sotnikova, T. D., Holmstrand, E., … Caron, M. G. (2008). Increased amphetamine-induced hyperactivity and reward in mice overexpressing the dopamine transporter. *Proceedings of the National Academy of Sciences*, *105*(11), 4405–4410. doi: 10.1073/pnas.0707646105

Samartzis, L., Dima, D., Fusar-Poli, P., & Kyriakopoulos, M. (2014). White Matter Alterations in Early Stages of Schizophrenia: A Systematic Review of Diffusion Tensor Imaging Studies. *Journal of Neuroimaging*, *24*(2), 101–110. doi: 10.1111/j.1552-6569.2012.00779.x

Sandovici, I., Hoelle, K., Angiolini, E., & Constância, M. (2012). Placental adaptations to the maternal–fetal environment: implications for fetal growth and developmental programming. *Reproductive BioMedicine Online*, *25*(1), 68–89. doi: 10.1016/j.rbmo.2012.03.017

Sanli, I., & Feil, R. (2015). Chromatin mechanisms in the developmental control of imprinted gene expression. *The International Journal of Biochemistry & Cell Biology*, *67*, 139–147. doi: 10.1016/j.biocel.2015.04.004

Sartori, S. B., Landgraf, R., & Singewald, N. (2011). The clinical implications of mouse models of enhanced anxiety. *Future Neurology*, *6*(4), 531–571. doi: 10.2217/fnl.11.34

Schaefer, J., Giangrande, E., Weinberger, D. R., & Dickinson, D. (2013). The global cognitive impairment in schizophrenia: Consistent over decades and around the world. *Schizophrenia Research*, *150*(1), 42–50. doi: 10.1016/j.schres.2013.07.009

Schizophrenia Working Group of the Psychiatric Genomics Consortium, Ripke, S., Neale, B. M., Corvin, A., Walters, J. T. R., Farh, K.-H., … O'Donovan, M. C. (2014). Biological insights from 108 schizophrenia-associated genetic loci. *Nature*, *511*(7510), 421–427. doi: 10.1038/nature13595

Scholz, J., Niibori, Y., Frankland, P. W., & Lerch, J. P. (2015). Rotarod training in mice is associated with changes in brain structure observable with multimodal MRI. *NeuroImage*, *107*, 182–189. doi: 10.1016/j.neuroimage.2014.12.003

Scott, J. G., Gillis, D., Ryan, A. E., Hargovan, H., Gundarpi, N., McKeon, G., … Blum, S. (2018). The prevalence and treatment outcomes of antineuronal antibody-positive patients admitted with first episode of psychosis. *BJPsych Open*, *4*(2),

69–74. doi: 10.1192/bjo.2018.8

Sebat, J., Lakshmi, B., Troge, J., Alexander, J., Young, J., Lundin, P., … Wigler, M. (2004). Large-Scale Copy Number Polymorphism in the Human Genome. *Science*, *305*(5683), 525–528. doi: 10.1126/science.1098918

Seeman, P., Lee, T., Chau-Wong, M., & Wong, K. (1976). Antipsychotic drug doses and neuroleptic/dopamine receptors. *Nature*, *261*(5562), 717–719. doi: 10.1038/261717a0

Sekar, A., Bialas, A. R., De Rivera, H., Davis, A., Hammond, T. R., Kamitaki, N., … McCarroll, S. A. (2016). Schizophrenia risk from complex variation of complement component 4. *Nature*, *530*(7589), 177–183. doi: 10.1038/nature16549

Selten, J.-P., van der Ven, E., Rutten, B. P. F., & Cantor-Graae, E. (2013). The Social Defeat Hypothesis of Schizophrenia: An Update. *Schizophrenia Bulletin*, *39*(6), 1180–1186. doi: 10.1093/schbul/sbt134

Selten, J.-P., van der Ven, E., & Termorshuizen, F. (2019). Migration and psychosis: a meta-analysis of incidence studies. *Psychological Medicine*, 1–11. doi: 10.1017/S0033291719000035

Selvaraj, S., Arnone, D., Cappai, A., & Howes, O. (2014). Alterations in the serotonin system in schizophrenia: A systematic review and meta-analysis of postmortem and molecular imaging studies. *Neuroscience & Biobehavioral Reviews*, *45*, 233–245. doi: 10.1016/j.neubiorev.2014.06.005

Sferruzzi-Perri, A. N., & Camm, E. J. (2016). The Programming Power of the Placenta. *Frontiers in Physiology*, *7*, 33. doi: 10.3389/fphys.2016.00033

Shah, C., Zhang, W., Xiao, Y., Yao, L., Zhao, Y., Gao, X., … Lui, S. (2017). Common pattern of gray-matter abnormalities in drug-naive and medicated first-episode schizophrenia: a multimodal meta-analysis. *Psychological Medicine*, *47*(3), 401–413. doi: 10.1017/S0033291716002683

Shen, E. Y., Jiang, Y., Javidfar, B., Kassim, B., Loh, Y.-H. E., Ma, Q., … Akbarian, S. (2016). Neuronal Deletion of Kmt2a/Mll1 Histone Methyltransferase in Ventral Striatum is Associated with Defective Spike-Timing-Dependent Striatal Synaptic Plasticity, Altered Response to Dopaminergic Drugs, and Increased Anxiety. *Neuropsychopharmacology*, *41*(13), 3103–3113. doi: 10.1038/npp.2016.144

Shen, E. Y., Shulha, H., Weng, Z., & Akbarian, S. (2014). Regulation of histone H3K4 methylation in brain development and disease. *Philosophical Transactions of the Royal Society B: Biological Sciences*, *369*(1652), 20130514. doi: 10.1098/rstb.2013.0514

Shilatifard, A. (2008). Molecular implementation and physiological roles for histone H3 lysine 4 (H3K4) methylation. *Current Opinion in Cell Biology*, *20*(3), 341–348. doi: 10.1016/j.ceb.2008.03.019

Shilatifard, A. (2012). The COMPASS Family of Histone H3K4 Methylases: Mechanisms of Regulation in Development and Disease Pathogenesis. *Annual Review of Biochemistry*, *81*(1), 65–95. doi: 10.1146/annurev-biochem-051710-134100

Shulha, H. P., Cheung, I., Guo, Y., Akbarian, S., & Weng, Z. (2013). Coordinated Cell Type–Specific Epigenetic Remodeling in Prefrontal Cortex Begins before Birth and Continues into Early Adulthood. *PLoS Genetics*, *9*(4), e1003433. doi: 10.1371/journal.pgen.1003433

Silbereis, J. C., Pochareddy, S., Zhu, Y., Li, M., & Sestan, N. (2016). The Cellular and Molecular Landscapes of the Developing Human Central Nervous System. *Neuron*, *89*(2), 248–268. doi: 10.1016/j.neuron.2015.12.008

Simmons, D. G., Fortier, A. L., & Cross, J. C. (2007). Diverse subtypes and developmental origins of trophoblast giant cells in the mouse placenta. *Developmental Biology*, *304*(2), 567–578. doi: 10.1016/j.ydbio.2007.01.009

Simmons, D. G., Rawn, S. M., Davies, A., Hughes, M., & Cross, J. C. (2008). Spatial and temporal expression of the 23 murine Prolactin/Placental Lactogen-related genes is not associated with their position in the locus. *BMC Genomics*, *9*(1), 352. doi: 10.1186/1471-2164-9-352

Simon, M. M., Greenaway, S., White, J. K., Fuchs, H., Gailus-Durner, V., Wells, S., … Brown, S. D. M. (2013). A comparative phenotypic and genomic analysis of C57BL/6J and C57BL/6N mouse strains. *Genome Biology*, *14*(7), R82. doi: 10.1186/gb-2013-14-7-r82

Singh, G., Singh, V., & Schneider, J. S. (2019). Post-translational histone modifications and their interaction with sex influence normal brain development and elaboration of neuropsychiatric disorders. *Biochimica et Biophysica Acta (BBA) - Molecular Basis of Disease*, *1865*(8), 1968–1981. doi:

10.1016/j.bbadis.2018.10.016

Singh, T., Kurki, M. I., Curtis, D., Purcell, S. M., Crooks, L., McRae, J., … Barrett, J. C. (2016). Rare loss-of-function variants in SETD1A are associated with schizophrenia and developmental disorders. *Nature Neuroscience*, *19*(4), 571–577. doi: 10.1038/nn.4267

Singh, T., Walters, J. T. R., Johnstone, M., Curtis, D., Suvisaari, J., Torniainen, M., … Barrett, J. C. (2017). The contribution of rare variants to risk of schizophrenia in individuals with and without intellectual disability. *Nature Genetics*, *49*(8), 1167–1173. doi: 10.1038/ng.3903

Sipes, T. E., & Geyer, M. A. (1997). DOI disrupts prepulse inhibition of startle in rats via 5-HT2A receptors in the ventral pallidum. *Brain Research*, *761*(1), 97–104. doi: 10.1016/S0006-8993(97)00316-8

Skarnes, W. C., Rosen, B., West, A. P., Koutsourakis, M., Bushell, W., Iyer, V., … Bradley, A. (2011). A conditional knockout resource for the genome-wide study of mouse gene function. *Nature*, *474*(7351), 337–342. doi: 10.1038/nature10163

Skene, N. G., Bryois, J., Bakken, T. E., Breen, G., Crowley, J. J., Gaspar, H. A., … Hjerling-Leffler, J. (2018). Genetic identification of brain cell types underlying schizophrenia. *Nature Genetics*, *50*(6), 825–833. doi: 10.1038/s41588-018-0129-5

Slifstein, M., van de Giessen, E., Van Snellenberg, J., Thompson, J. L., Narendran, R., Gil, R., … Abi-Dargham, A. (2015). Deficits in Prefrontal Cortical and Extrastriatal Dopamine Release in Schizophrenia. *JAMA Psychiatry*, *72*(4), 316–324. doi: 10.1001/jamapsychiatry.2014.2414

Spencer, L., Abate, D., Abate, K. H., Abay, S. M., Abbafati, C., Abbasi, N., … Murray, C. J. L. (2018). Global, regional, and national incidence, prevalence, and years lived with disability for 354 diseases and injuries for 195 countries and territories, 1990-2017: a systematic analysis for the Global Burden of Disease Study 2017. *The Lancet*, *392*(10159), 1789–1858. doi: 10.1016/S0140-6736(18)32279-7

Stadler, F., Kolb, G., Rubusch, L., Baker, S. P., Jones, E. G., & Akbarian, S. (2005). Histone methylation at gene promoters is associated with developmental regulation and region-specific expression of ionotropic and metabotropic glutamate receptors in human brain. *Journal of Neurochemistry*, *94*(2), 324–336. doi: 10.1111/j.1471-4159.2005.03190.x

Steen, R. G., Mull, C., Mcclure, R., Hamer, R. M., & Lieberman, J. A. (2006). Brain volume in first-episode schizophrenia. *British Journal of Psychiatry*, *188*(6), 510–518. doi: 10.1192/bjp.188.6.510

Steiner, J., Walter, M., Glanz, W., Sarnyai, Z., Bernstein, H.-G., Vielhaber, S., … Stoecker, W. (2013). Increased prevalence of diverse N-methyl-D-aspartate glutamate receptor antibodies in patients with an initial diagnosis of schizophrenia: specific relevance of IgG NR1a antibodies for distinction from N-methyl-D-aspartate glutamate receptor encephalitis. *JAMA Psychiatry*, *70*(3), 271–278. doi: 10.1001/2013.jamapsychiatry.86

Stone, J. M., Howes, O. D., Egerton, A., Kambeitz, J., Allen, P., Lythgoe, D. J., … McGuire, P. (2010). Altered Relationship Between Hippocampal Glutamate Levels and Striatal Dopamine Function in Subjects at Ultra High Risk of Psychosis. *Biological Psychiatry*, *68*(7), 599–602. doi: 10.1016/j.biopsych.2010.05.034

Strahl, B. D., & Allis, C. D. (2000). The language of covalent histone modifications. *Nature*, *403*(6765), 41–45. doi: 10.1038/47412

Sullivan, E. L., Riper, K. M., Lockard, R., & Valleau, J. C. (2015). Maternal high-fat diet programming of the neuroendocrine system and behavior. *Hormones and Behavior*, *76*, 153–161. doi: 10.1016/j.yhbeh.2015.04.008

Sullivan, P. F., Agrawal, A., Bulik, C. M., Andreassen, O. A., Børglum, A. D., Breen, G., … Psychiatric Genomics Consortium. (2018). Psychiatric Genomics: An Update and an Agenda. *American Journal of Psychiatry*, *175*(1), 15–27. doi: 10.1176/appi.ajp.2017.17030283

Sullivan, P. F., & Geschwind, D. H. (2019). Defining the Genetic, Genomic, Cellular, and Diagnostic Architectures of Psychiatric Disorders. *Cell*, *177*(1), 162–183. doi: 10.1016/j.cell.2019.01.015

Sullivan, P. F., Kendler, K. S., & Neale, M. C. (2003). Schizophrenia as a Complex Trait. *Archives of General Psychiatry*, *60*(12), 1187–1192. doi: 10.1001/archpsyc.60.12.1187

Surani, M. A. (1998). Imprinting and the Initiation of Gene Silencing in the Germ Line. *Cell*, *93*(3), 309–312. doi: 10.1016/S0092-8674(00)81156-3

Swerdlow, N. R., Braff, D. L., & Geyer, M. A. (2016). Sensorimotor gating of the startle reflex: What we said 25 years ago, what has happened since then, and what

comes next. *Journal of Psychopharmacology*, *30*(11), 1072–1081. doi: 10.1177/0269881116661075

Swerdlow, N. R., Braff, D. L., Hartston, H., Perry, W., & Geyer, M. A. (1996). Latent inhibition in schizophrenia. *Schizophrenia Research*, *20*(1–2), 91–103. doi: 10.1016/0920-9964(95)00097-6

Swerdlow, N. R., Braff, D. L., Taaid, N., & Geyer, M. A. (1994). Assessing the Validity of an Animal Model of Deficient Sensorimotor Gating in Schizophrenic Patients. *Archives of General Psychiatry*, *51*(2), 139. doi: 10.1001/archpsyc.1994.03950020063007

Swerdlow, N. R., Geyer, M. A., & Braff, D. L. (2001). Neural circuit regulation of prepulse inhibition of startle in the rat: current knowledge and future challenges. *Psychopharmacology*, *156*(2–3), 194–215. doi: 10.1007/s002130100799

Swerdlow, N. R., Light, G. A., Sprock, J., Calkins, M. E., Green, M. F., Greenwood, T. A., … Braff, D. L. (2014). Deficient prepulse inhibition in schizophrenia detected by the multi-site COGS. *Schizophrenia Research*, *152*(2–3), 503–512. doi: 10.1016/j.schres.2013.12.004

Swerdlow, N. R., Light, G. A., Thomas, M. L., Sprock, J., Calkins, M. E., Green, M. F., … Braff, D. L. (2018). Deficient prepulse inhibition in schizophrenia in a multi-site cohort: Internal replication and extension. *Schizophrenia Research*, *198*, 6–15. doi: 10.1016/j.schres.2017.05.013

Swerdlow, N. R., Talledo, J., Sutherland, A. N., Nagy, D., & Shoemaker, J. M. (2006). Antipsychotic Effects on Prepulse Inhibition in Normal 'Low Gating' Humans and Rats. *Neuropsychopharmacology*, *31*(9), 2011–2021. doi: 10.1038/sj.npp.1301043

Swerdlow, N. R., Weber, M., Qu, Y., Light, G. A., & Braff, D. L. (2008). Realistic expectations of prepulse inhibition in translational models for schizophrenia research. *Psychopharmacology*, *199*(3), 331–388. doi: 10.1007/s00213-008-1072-4

Sze, C. C., Cao, K., Collings, C. K., Marshall, S. A., Rendleman, E. J., Ozark, P. A., … Shilatifard, A. (2017). Histone H3K4 methylation-dependent and -independent functions of Set1A/COMPASS in embryonic stem cell self-renewal and differentiation. *Genes & Development*, *31*(17), 1732–1737. doi: 10.1101/gad.303768.117

Takata, A., Xu, B., Ionita-Laza, I., Roos, J. L., Gogos, J. A., & Karayiorgou, M. (2014). Loss-of-Function Variants in Schizophrenia Risk and SETD1A as a Candidate Susceptibility Gene. *Neuron*, *82*(4), 773–780. doi: 10.1016/j.neuron.2014.04.043

Tansey, K. E., Rees, E., Linden, D. E., Ripke, S., Chambert, K. D., Moran, J. L., … O'Donovan, M. C. (2016). Common alleles contribute to schizophrenia in CNV carriers. *Molecular Psychiatry*, *21*(8), 1085–1089. doi: 10.1038/mp.2015.143

Tate, C. M., Lee, J.-H., & Skalnik, D. G. (2010). CXXC finger protein 1 restricts the Setd1A histone H3K4 methyltransferase complex to euchromatin. *FEBS Journal*, *277*(1), 210–223. doi: 10.1111/j.1742-4658.2009.07475.x

Thyagarajan, B., Guimarães, M. J., Groth, A. C., & Calos, M. P. (2000). Mammalian genomes contain active recombinase recognition sites. *Gene*, *244*(1–2), 47–54. doi: 10.1016/S0378-1119(00)00008-1

Tiihonen, J., Koskuvi, M., Storvik, M., Hyötyläinen, I., Gao, Y., Puttonen, K. A., … Koistinaho, J. (2019). Sex-specific transcriptional and proteomic signatures in schizophrenia. *Nature Communications*, *10*(1), 3933. doi: 10.1038/s41467-019-11797-3

Toste, C. C., Duarte, R. R. R., Jeffries, A. R., Selvackadunco, S., Troakes, C., O'Donovan, M. C., … Bray, N. J. (2019). No Effect of Genome-Wide Significant Schizophrenia Risk Variation at the DRD2 Locus on the Allelic Expression of DRD2 in Postmortem Striatum. *Molecular Neuropsychiatry*, 1–6. doi: 10.1159/000501022

Tronche, F., Kellendonk, C., Kretz, O., Gass, P., Anlag, K., Orban, P. C., … Schütz, G. (1999). Disruption of the glucocorticoid receptor gene in the nervous system results in reduced anxiety. *Nature Genetics*, *23*(1), 99–103. doi: 10.1038/12703

Trullas, R., & Skolnick, P. (1993). Differences in fear motivated behaviors among inbred mouse strains. *Psychopharmacology*, *111*(3), 323–331. doi: 10.1007/BF02244948

Tunster, S. J., Boqué-Sastre, R., McNamara, G. I., Hunter, S. M., Creeth, H. D. J., & John, R. M. (2018). Peg3 Deficiency Results in Sexually Dimorphic Losses and Gains in the Normal Repertoire of Placental Hormones. *Frontiers in Cell and Developmental Biology*, *6*, 123. doi: 10.3389/fcell.2018.00123

Tunster, S. J., Creeth, H. D. J., & John, R. M. (2016). The imprinted Phlda2 gene

modulates a major endocrine compartment of the placenta to regulate placental demands for maternal resources. *Developmental Biology*, *409*(1), 251–260. doi: 10.1016/j.ydbio.2015.10.015

Tunster, S. J., Van de Pette, M., Creeth, H. D. J., Lefebvre, L., & John, R. M. (2018). Fetal growth restriction in a genetic model of sporadic Beckwith–Wiedemann syndrome. *Disease Models & Mechanisms*, *11*(11), dmm035832. doi: 10.1242/dmm.035832

Uhl, G. R., Hall, F. S., & Sora, I. (2002). Cocaine, reward, movement and monoamine transporters. *Molecular Psychiatry*, *7*(1), 21–26. doi: 10.1038/sj/mp/4001964

Umlauf, D., Goto, Y., Cao, R., Cerqueira, F., Wagschal, A., Zhang, Y., & Feil, R. (2004). Imprinting along the Kcnq1 domain on mouse chromosome 7 involves repressive histone methylation and recruitment of Polycomb group complexes. *Nature Genetics*, *36*(12), 1296–1300. doi: 10.1038/ng1467

Ursini, G., Punzi, G., Chen, Q., Marenco, S., Robinson, J. F., Porcelli, A., … Weinberger, D. R. (2018). Convergence of placenta biology and genetic risk for schizophrenia. *Nature Medicine*, *24*(6), 792–801. doi: 10.1038/s41591-018-0021-y

Vallianatos, C. N., & Iwase, S. (2015). Disrupted intricacy of histone H3K4 methylation in neurodevelopmental disorders. *Epigenomics*, *7*(3), 503–519. doi: 10.2217/epi.15.1

Van Den Buuse, M. (2010). Modeling the positive symptoms of schizophrenia in genetically modified mice: Pharmacology and methodology aspects. *Schizophrenia Bulletin*, *36*(2), 246–270. doi: 10.1093/schbul/sbp132

van der Merwe, C., Passchier, R., Mufford, M., Ramesar, R., Dalvie, S., & Stein, D. J. (2019). Polygenic risk for schizophrenia and associated brain structural changes: A systematic review. *Comprehensive Psychiatry*, *88*, 77–82. doi: 10.1016/j.comppsych.2018.11.014

van Erp, T. G. M., Hibar, D. P., Rasmussen, J. M., Glahn, D. C., Pearlson, G. D., Andreassen, O. A., … Turner, J. A. (2016). Subcortical brain volume abnormalities in 2028 individuals with schizophrenia and 2540 healthy controls via the ENIGMA consortium. *Molecular Psychiatry*, *21*(4), 547–553. doi: 10.1038/mp.2015.63

van Erp, T. G. M., Walton, E., Hibar, D. P., Schmaal, L., Jiang, W., Glahn, D. C., …

Orhan, F. (2018). Cortical Brain Abnormalities in 4474 Individuals With Schizophrenia and 5098 Control Subjects via the Enhancing Neuro Imaging Genetics Through Meta Analysis (ENIGMA) Consortium. *Biological Psychiatry*, *84*(9), 644–654. doi: 10.1016/j.biopsych.2018.04.023

van Os, J., Kenis, G., & Rutten, B. P. F. (2010). The environment and schizophrenia. *Nature*, *468*(7321), 203–212. doi: 10.1038/nature09563

van Os, J., Rutten, B. P., Myin-Germeys, I., Delespaul, P., Viechtbauer, W., van Zelst, C., … Mirjanic, T. (2014). Identifying Gene-Environment Interactions in Schizophrenia: Contemporary Challenges for Integrated, Large-scale Investigations. *Schizophrenia Bulletin*, *40*(4), 729–736. doi: 10.1093/schbul/sbu069

van Os, J., & Selten, J.-P. (1998). Prenatal exposure to maternal stress and subsequent schizophrenia. *British Journal of Psychiatry*, *172*(4), 324–326. doi: 10.1192/bjp.172.4.324

Vanden Berghe, T., Hulpiau, P., Martens, L., Vandenbroucke, R. E., Van Wonterghem, E., Perry, S. W., … Vandenabeele, P. (2015). Passenger Mutations Confound Interpretation of All Genetically Modified Congenic Mice. *Immunity*, *43*(1), 200–209. doi: 10.1016/j.immuni.2015.06.011

Varese, F., Smeets, F., Drukker, M., Lieverse, R., Lataster, T., Viechtbauer, W., … Bentall, R. P. (2012). Childhood Adversities Increase the Risk of Psychosis: A Meta-analysis of Patient-Control, Prospective- and Cross-sectional Cohort Studies. *Schizophrenia Bulletin*, *38*(4), 661–671. doi: 10.1093/schbul/sbs050

Varty, G. B., Bakshi, V. P., & Geyer, M. A. (1999). M100907, a Serotonin 5-HT2A Receptor Antagonist and Putative Antipsychotic, Blocks Dizocilpine-Induced Prepulse Inhibition Deficits in Sprague–Dawley and Wistar Rats. *Neuropsychopharmacology*, *20*(4), 311–321. doi: 10.1016/S0893-133X(98)00072-4

Varty, G. B., & Higgins, G. A. (1995). Examination of drug-induced and isolation-induced disruptions of prepulse inhibition as models to screen antipsychotic drugs. *Psychopharmacology*, *122*(1), 15–26. doi: 10.1007/bf02246437

Vassos, E., Pedersen, C. B., Murray, R. M., Collier, D. A., & Lewis, C. M. (2012). Meta-Analysis of the Association of Urbanicity With Schizophrenia. *Schizophrenia Bulletin*, *38*(6), 1118–1123. doi: 10.1093/schbul/sbs096

Vermeulen, M., Mulder, K. W., Denissov, S., Pijnappel, W. W. M. P., van Schaik, F. M. A., Varier, R. A., … Timmers, H. T. M. (2007). Selective Anchoring of TFIID to Nucleosomes by Trimethylation of Histone H3 Lysine 4. *Cell*, *131*(1), 58–69. doi: 10.1016/j.cell.2007.08.016

Verrall, L., Burnet, P. W. J., Betts, J. F., & Harrison, P. J. (2010). The neurobiology of D-amino acid oxidase and its involvement in schizophrenia. *Molecular Psychiatry*, *15*(2), 122–137. doi: 10.1038/mp.2009.99

Volk, D. W., Austin, M. C., Pierri, J. N., Sampson, A. R., & Lewis, D. A. (2000). Decreased Glutamic Acid Decarboxylase67 Messenger RNA Expression in a Subset of Prefrontal Cortical γ-Aminobutyric Acid Neurons in Subjects With Schizophrenia. *Archives of General Psychiatry*, *57*(3), 237–245. doi: 10.1001/archpsyc.57.3.237

Vollenweider, F. X., Barro, M., Csomor, P. A., & Feldon, J. (2006). Clozapine Enhances Prepulse Inhibition in Healthy Humans with Low But Not with High Prepulse Inhibition Levels. *Biological Psychiatry*, *60*(6), 597–603. doi: 10.1016/j.biopsych.2006.03.058

Walther, S., & Strik, W. (2012). Motor symptoms and schizophrenia. *Neuropsychobiology*, *66*(2), 77–92. doi: 10.1159/000339456

Wang, D., Liu, S., Warrell, J., Won, H., Shi, X., Navarro, F. C. P., … Gerstein, M. B. (2018). Comprehensive functional genomic resource and integrative model for the human brain. *Science*, *362*(6420), eaat8464. doi: 10.1126/science.aat8464

Warland, A., Kendall, K. M., Rees, E., Kirov, G., & Caseras, X. (2019). Schizophrenia-associated genomic copy number variants and subcortical brain volumes in the UK Biobank. *Molecular Psychiatry*. doi: 10.1038/s41380-019-0355-y

Watson, E. D., & Cross, J. C. (2005). Development of Structures and Transport Functions in the Mouse Placenta. *Physiology*, *20*(3), 180–193. doi: 10.1152/physiol.00001.2005

Webb, W. M., Sanchez, R. G., Perez, G., Butler, A. A., Hauser, R. M., Rich, M. C., … Lubin, F. D. (2017). Dynamic association of epigenetic H3K4me3 and DNA 5hmC marks in the dorsal hippocampus and anterior cingulate cortex following reactivation of a fear memory. *Neurobiology of Learning and Memory*, *142*, 66–78. doi: 10.1016/j.nlm.2017.02.010

Weinberger, D. R. (1987). Implications of Normal Brain Development for the

Pathogenesis of Schizophrenia. *Archives of General Psychiatry*, *44*(7), 660–669. doi: 10.1001/archpsyc.1987.01800190080012

Willins, D. L., & Meltzer, H. Y. (1997). Direct injection of 5-HT2A receptor agonists into the medial prefrontal cortex produces a head-twitch response in rats. *The Journal of Pharmacology and Experimental Therapeutics*, *282*(2), 699–706.

Wilson, C., Kercher, M., Quinn, B., Murphy, A., Fiegel, C., & McLaurin, A. (2007). Effects of age and sex on ketamine-induced hyperactivity in rats. *Physiology & Behavior*, *91*(2–3), 202–207. doi: 10.1016/j.physbeh.2007.02.010

Won, H., de la Torre-Ubieta, L., Stein, J. L., Parikshak, N. N., Huang, J., Opland, C. K., … Geschwind, D. H. (2016). Chromosome conformation elucidates regulatory relationships in developing human brain. *Nature*, *538*(7626), 523–527. doi: 10.1038/nature19847

Woods, L., Perez-Garcia, V., & Hemberger, M. (2018). Regulation of Placental Development and Its Impact on Fetal Growth—New Insights From Mouse Models. *Frontiers in Endocrinology*, *9*, 570. doi: 10.3389/fendo.2018.00570

World Health Organization. (1993). *The ICD-10 classification of mental and behavioural disorders: Diagnostic criteria for research*. Geneva.

Wu, M., Wang, P. F., Lee, J. S., Martin-Brown, S., Florens, L., Washburn, M., & Shilatifard, A. (2008). Molecular Regulation of H3K4 Trimethylation by Wdr82, a Component of Human Set1/COMPASS. *Molecular and Cellular Biology*, *28*(24), 7337–7344. doi: 10.1128/MCB.00976-08

Wynn, J. K., Green, M. F., Sprock, J., Light, G. A., Widmark, C., Reist, C., … Braff, D. L. (2007). Effects of olanzapine, risperidone and haloperidol on prepulse inhibition in schizophrenia patients: A double-blind, randomized controlled trial. *Schizophrenia Research*, *95*(1–3), 134–142. doi: 10.1016/J.SCHRES.2007.05.039

Xu, M.-Q., Sun, W.-S., Liu, B.-X., Feng, G.-Y., Yu, L., Yang, L., … He, L. (2009). Prenatal Malnutrition and Adult Schizophrenia: Further Evidence From the 1959-1961 Chinese Famine. *Schizophrenia Bulletin*, *35*(3), 568–576. doi: 10.1093/schbul/sbn168

Yamada, S., Harano, M., Annoh, N., Nakamura, K., & Tanaka, M. (1999). Involvement of serotonin 2A receptors in phencyclidine-induced disruption of prepulse inhibition of the acoustic startle in rats. *Biological Psychiatry*, *46*(6), 832–838.

doi: 10.1016/S0006-3223(98)00356-4

Yan, Q.-S., Reith, M. E. ., Jobe, P. C., & Dailey, J. W. (1997). Dizocilpine (MK-801) increases not only dopamine but also serotonin and norepinephrine transmissions in the nucleus accumbens as measured by microdialysis in freely moving rats. *Brain Research*, *765*(1), 149–158. doi: 10.1016/S0006-8993(97)00568-4

Yu, X., Yang, L., Li, J., Li, W., Li, D., Wang, R., … Zhou, W. (2019). De Novo and Inherited SETD1A Variants in Early-onset Epilepsy. *Neuroscience Bulletin*. doi: 10.1007/s12264-019-00400-w

Zandi, M. S., Irani, S. R., Lang, B., Waters, P., Jones, P. B., McKenna, P., … Lennox, B. R. (2011). Disease-relevant autoantibodies in first episode schizophrenia. *Journal of Neurology*, *258*(4), 686–688. doi: 10.1007/s00415-010-5788-9

Zechner, D., Fujita, Y., Hülsken, J., Müller, T., Walther, I., Taketo, M. M., … Birchmeier, C. (2003). beta-Catenin signals regulate cell growth and the balance between progenitor cell expansion and differentiation in the nervous system. *Developmental Biology*, *258*(2), 406–418. doi: 10.1016/s0012-1606(03)00123-4

Zhan, X., Cao, M., Yoo, A. S., Zhang, Z., Chen, L., Crabtree, G. R., & Wu, J. I. (2015). Generation of BAF53b-Cre transgenic mice with pan-neuronal Cre activities. *Genesis*, *53*(7), 440–448. doi: 10.1002/dvg.22866

Zhuang, X., Oosting, R. S., Jones, S. R., Gainetdinov, R. R., Miller, G. W., Caron, M. G., & Hen, R. (2002). Hyperactivity and impaired response habituation in hyperdopaminergic mice. *Proceedings of the National Academy of Sciences*, *98*(4), 1982–1987. doi: 10.1073/pnas.98.4.1982

**Appendix 1.** Differentially expressed genes (Benjamini Hochberg $p_{adj}$ < .05) in E13.5 *Setd1a*$^{+/-}$ brain.

| Ensembl gene ID | Entrez gene ID | Gene name | Gene biotype | log2 fold change | SE | *p* value | $p_{adj}$ |
|---|---|---|---|---|---|---|---|
| ENSMUSG00000033233 | 229644 | *Trim45* | Protein coding | -0.34921 | 0.048286 | 4.76E-13 | 8.83E-09 |
| ENSMUSG00000034371 | 225913 | *Tkfc* | Protein coding | -0.29257 | 0.045843 | 1.75E-10 | 1.36E-06 |
| ENSMUSG00000029524 | 75387 | *Sirt4* | Protein coding | -0.36778 | 0.05842 | 3.06E-10 | 1.36E-06 |
| ENSMUSG00000078867 | NA | *Gm14418* | Protein coding | 0.888915 | 0.141821 | 3.66E-10 | 1.36E-06 |
| ENSMUSG00000044475 | 69090 | *Ascc1* | Protein coding | -0.28519 | 0.045503 | 3.67E-10 | 1.36E-06 |
| ENSMUSG00000024869 | NA | *Gm49405* | Protein coding | -0.40202 | 0.064596 | 4.86E-10 | 1.42E-06 |
| ENSMUSG00000097048 | 72012 | *1600020E01Rik* | lncRNA | -0.30576 | 0.049246 | 5.34E-10 | 1.42E-06 |
| ENSMUSG00000022685 | 74108 | *Parn* | Protein coding | -0.21464 | 0.035198 | 1.07E-09 | 2.49E-06 |
| ENSMUSG00000014606 | 67863 | *Slc25a11* | Protein coding | -0.19498 | 0.03301 | 3.49E-09 | 7.20E-06 |
| ENSMUSG00000034032 | 68925 | *Rpap1* | Protein coding | -0.23763 | 0.040532 | 4.56E-09 | 7.71E-06 |
| ENSMUSG00000024871 | 60425 | *Doc2g* | Protein coding | -0.44336 | 0.075631 | 4.57E-09 | 7.71E-06 |
| ENSMUSG00000007777 | 66050 | *0610009B22Rik* | Protein coding | -0.31995 | 0.05478 | 5.20E-09 | 8.05E-06 |
| ENSMUSG00000039048 | 235169 | *Foxred1* | Protein coding | -0.30068 | 0.05166 | 5.87E-09 | 8.39E-06 |
| ENSMUSG00000013622 | 381629 | *Atraid* | Protein coding | -0.26682 | 0.04627 | 8.09E-09 | 1.06E-05 |
| ENSMUSG00000059540 | 21400 | *Tcea2* | Protein coding | -0.31618 | 0.054924 | 8.57E-09 | 1.06E-05 |
| ENSMUSG00000073096 | 243371 | *Lrrc61* | Protein coding | -0.40306 | 0.071239 | 1.53E-08 | 1.78E-05 |
| ENSMUSG00000078864 | 626802 | *Gm14322* | Protein coding | 0.692545 | 0.122871 | 1.74E-08 | 1.84E-05 |
| ENSMUSG00000025188 | 192236 | *Hps1* | Protein coding | -0.30295 | 0.053796 | 1.79E-08 | 1.84E-05 |
| ENSMUSG00000037363 | 270035 | *Letm2* | Protein coding | -0.34534 | 0.06152 | 1.98E-08 | 1.94E-05 |
| ENSMUSG00000041881 | 66416 | *Ndufa7* | Protein coding | -0.16476 | 0.029509 | 2.36E-08 | 2.19E-05 |
| ENSMUSG00000025142 | 68938 | *Aspscr1* | Protein coding | -0.16641 | 0.030017 | 2.96E-08 | 2.61E-05 |
| ENSMUSG00000052369 | 380967 | *Tmem106c* | Protein coding | -0.29373 | 0.053938 | 5.16E-08 | 4.35E-05 |
| ENSMUSG00000045211 | 213484 | *Nudt18* | Protein coding | -0.38152 | 0.070713 | 6.84E-08 | 5.52E-05 |
| ENSMUSG00000048920 | 243853 | *Fkrp* | Protein coding | -0.25413 | 0.047172 | 7.15E-08 | 5.53E-05 |

| Ensembl gene ID | Entrez gene ID | Gene name | Gene biotype | log2 fold change | SE | *p* value | $p_{adj}$ |
|---|---|---|---|---|---|---|---|
| ENSMUSG00000039795 | 66361 | *Zfand1* | Protein coding | -0.21884 | 0.041165 | 1.06E-07 | 7.86E-05 |
| ENSMUSG00000042404 | 229541 | *Dennd4b* | Protein coding | -0.21019 | 0.039593 | 1.10E-07 | 7.88E-05 |
| ENSMUSG00000003423 | 68845 | *Pih1d1* | Protein coding | -0.1898 | 0.03592 | 1.26E-07 | 8.52E-05 |
| ENSMUSG00000018554 | 53422 | *Ybx2* | Protein coding | -0.30843 | 0.058405 | 1.29E-07 | 8.52E-05 |
| ENSMUSG00000007783 | 78070 | *Cpt1c* | Protein coding | -0.1701 | 0.032363 | 1.47E-07 | 9.43E-05 |
| ENSMUSG00000028158 | 17777 | *Mttp* | Protein coding | -0.34283 | 0.065566 | 1.71E-07 | 0.000104 |
| ENSMUSG00000027259 | 75894 | *Adal* | Protein coding | -0.29732 | 0.056944 | 1.78E-07 | 0.000104 |
| ENSMUSG00000030301 | 67015 | *Ccdc91* | Protein coding | -0.28969 | 0.055546 | 1.84E-07 | 0.000104 |
| ENSMUSG00000002910 | 70807 | *Arrdc2* | Protein coding | -0.42196 | 0.080919 | 1.84E-07 | 0.000104 |
| ENSMUSG00000001100 | 67811 | *Poldip2* | Protein coding | -0.14768 | 0.028424 | 2.04E-07 | 0.000111 |
| ENSMUSG00000035595 | 69770 | *1600002K03Rik* | Protein coding | -0.62757 | 0.121327 | 2.31E-07 | 0.000122 |
| ENSMUSG00000027737 | 26570 | *Slc7a11* | Protein coding | 0.562082 | 0.110346 | 3.51E-07 | 0.000181 |
| ENSMUSG00000109274 | NA | *Gm45133* | TEC | -0.26569 | 0.052398 | 3.97E-07 | 0.000199 |
| ENSMUSG00000033021 | 69080 | *Gmppa* | Protein coding | -0.22587 | 0.044654 | 4.23E-07 | 0.000207 |
| ENSMUSG00000026792 | 227738 | *Lrsam1* | Protein coding | -0.25453 | 0.05075 | 5.29E-07 | 0.000252 |
| ENSMUSG00000028047 | 21827 | *Thbs3* | Protein coding | -0.16946 | 0.03389 | 5.73E-07 | 0.000266 |
| ENSMUSG00000018570 | 70419 | *2810408A11Rik* | Protein coding | -0.44198 | 0.089262 | 7.36E-07 | 0.000333 |
| ENSMUSG00000032952 | 67489 | *Ap4b1* | Protein coding | -0.24184 | 0.049047 | 8.19E-07 | 0.000362 |
| ENSMUSG00000068264 | 69596 | *Ap5s1* | Protein coding | -0.32959 | 0.066939 | 8.49E-07 | 0.000366 |
| ENSMUSG00000026356 | 226414 | *Dars* | Protein coding | -0.1531 | 0.031143 | 8.83E-07 | 0.000373 |
| ENSMUSG00000017188 | 52469 | *Coa3* | Protein coding | -0.19849 | 0.040498 | 9.52E-07 | 0.000393 |
| ENSMUSG00000022339 | 55960 | *Ebag9* | Protein coding | -0.30065 | 0.061424 | 9.85E-07 | 0.000397 |
| ENSMUSG00000016940 | 70382 | *Kctd2* | Protein coding | -0.20458 | 0.042126 | 1.20E-06 | 0.000472 |
| ENSMUSG00000022828 | 74197 | *Gtf2e1* | Protein coding | -0.18528 | 0.038362 | 1.37E-06 | 0.000529 |
| ENSMUSG00000042632 | 53357 | *Pla2g6* | Protein coding | -0.3047 | 0.063312 | 1.49E-06 | 0.000564 |

| Ensembl gene ID | Entrez gene ID | Gene name | Gene biotype | log2 fold change | SE | *p* value | $p_{adj}$ |
|---|---|---|---|---|---|---|---|
| ENSMUSG00000047921 | 76510 | *Trappc9* | Protein coding | -0.15541 | 0.032329 | 1.53E-06 | 0.000569 |
| ENSMUSG00000002781 | 70209 | *Tmem143* | Protein coding | -0.34756 | 0.072579 | 1.68E-06 | 0.000609 |
| ENSMUSG00000116138 | 223665 | *C030006K11Rik* | Protein coding | -0.36807 | 0.076916 | 1.71E-06 | 0.000609 |
| ENSMUSG00000034757 | 72053 | *Tmub2* | Protein coding | -0.17567 | 0.036761 | 1.76E-06 | 0.000617 |
| ENSMUSG00000097287 | NA | *D130017N08Rik* | lncRNA | -0.33992 | 0.071196 | 1.80E-06 | 0.00062 |
| ENSMUSG00000046463 | NA | *5930403N24Rik* | lncRNA | 0.279275 | 0.059386 | 2.57E-06 | 0.000861 |
| ENSMUSG00000039246 | 226791 | *Lyplal1* | Protein coding | -0.37695 | 0.080194 | 2.60E-06 | 0.000861 |
| ENSMUSG00000028085 | 229487 | *Gatb* | Protein coding | -0.25471 | 0.054254 | 2.67E-06 | 0.000869 |
| ENSMUSG00000078866 | 628308 | *Zfp970* | Protein coding | 0.381367 | 0.08134 | 2.75E-06 | 0.000881 |
| ENSMUSG00000042642 | 319945 | *Flad1* | Protein coding | -0.23795 | 0.051193 | 3.35E-06 | 0.001049 |
| ENSMUSG00000051007 | 213350 | *Gatd1* | Protein coding | -0.31046 | 0.06683 | 3.39E-06 | 0.001049 |
| ENSMUSG00000105053 | NA | *Gm43064* | Protein coding | -0.24188 | 0.052163 | 3.54E-06 | 0.00106 |
| ENSMUSG00000003308 | 50868 | *Keap1* | Protein coding | -0.16419 | 0.035412 | 3.54E-06 | 0.00106 |
| ENSMUSG00000002280 | 67563 | *Narfl* | Protein coding | -0.23162 | 0.050033 | 3.67E-06 | 0.00106 |
| ENSMUSG00000053111 | 66930 | *Fank1* | Protein coding | -0.58497 | 0.126541 | 3.79E-06 | 0.00106 |
| ENSMUSG00000031641 | 234309 | *Cbr4* | Protein coding | -0.2725 | 0.058961 | 3.81E-06 | 0.00106 |
| ENSMUSG00000034121 | 380718 | *Mks1* | Protein coding | -0.27606 | 0.059734 | 3.81E-06 | 0.00106 |
| ENSMUSG00000073684 | 67513 | *Faap20* | Protein coding | -0.20789 | 0.044991 | 3.82E-06 | 0.00106 |
| ENSMUSG00000021913 | 239017 | *Ogdhl* | Protein coding | -0.28956 | 0.062749 | 3.94E-06 | 0.001075 |
| ENSMUSG00000094786 | NA | *Gm14403* | Protein coding | 0.837328 | 0.182417 | 4.43E-06 | 0.001191 |
| ENSMUSG00000078656 | 28084 | *Vps25* | Protein coding | -0.19941 | 0.04356 | 4.70E-06 | 0.001246 |
| ENSMUSG00000033111 | 218734 | *3830406C13Rik* | Protein coding | -0.27783 | 0.060801 | 4.89E-06 | 0.001278 |
| ENSMUSG00000031158 | 21855 | *Timm17b* | Protein coding | -0.18384 | 0.040267 | 4.98E-06 | 0.00128 |
| ENSMUSG00000020287 | 268395 | *Mpg* | Protein coding | -0.24293 | 0.053236 | 5.03E-06 | 0.00128 |
| ENSMUSG00000051154 | 12238 | *Commd3* | Protein coding | -0.18249 | 0.040233 | 5.73E-06 | 0.001425 |

| Ensembl gene ID | Entrez gene ID | Gene name | Gene biotype | log2 fold change | SE | *p* value | $p_{adj}$ |
|---|---|---|---|---|---|---|---|
| ENSMUSG00000011382 | 71755 | *Dhdh* | Protein coding | -0.35505 | 0.078288 | 5.76E-06 | 0.001425 |
| ENSMUSG00000027281 | 74243 | *Slx4ip* | Protein coding | -0.4188 | 0.092754 | 6.33E-06 | 0.001535 |
| ENSMUSG00000105345 | NA | *BC030343* | lncRNA | -0.51934 | 0.115054 | 6.37E-06 | 0.001535 |
| ENSMUSG00000045039 | 269878 | *Megf8* | Protein coding | -0.16501 | 0.03666 | 6.76E-06 | 0.001608 |
| ENSMUSG00000019864 | 170728 | *Rtn4ip1* | Protein coding | -0.24567 | 0.054671 | 7.01E-06 | 0.001646 |
| ENSMUSG00000006850 | 71983 | *Tmco6* | Protein coding | -0.30185 | 0.067788 | 8.47E-06 | 0.001966 |
| ENSMUSG00000078877 | 100039123 | *Gm14295* | Protein coding | 0.381522 | 0.085733 | 8.58E-06 | 0.001967 |
| ENSMUSG00000006010 | 226499 | *Odr4* | Protein coding | -0.2035 | 0.0458 | 8.86E-06 | 0.002006 |
| ENSMUSG00000009281 | 71660 | *Rarres2* | Protein coding | -0.38378 | 0.086558 | 9.26E-06 | 0.00207 |
| ENSMUSG00000026709 | 226539 | *Dars2* | Protein coding | -0.29535 | 0.067053 | 1.06E-05 | 0.00234 |
| ENSMUSG00000021902 | 71838 | *Phf7* | Protein coding | -0.28201 | 0.06448 | 1.22E-05 | 0.002668 |
| ENSMUSG00000040586 | 237222 | *Ofd1* | Protein coding | -0.17755 | 0.040871 | 1.40E-05 | 0.003018 |
| ENSMUSG00000032565 | 75686 | *Nudt16* | Protein coding | -0.31388 | 0.072514 | 1.50E-05 | 0.003203 |
| ENSMUSG00000017286 | 67201 | *Glod4* | Protein coding | -0.13644 | 0.031557 | 1.53E-05 | 0.003235 |
| ENSMUSG00000061046 | 68977 | *Haghl* | Protein coding | -0.25549 | 0.05919 | 1.59E-05 | 0.003297 |
| ENSMUSG00000007216 | 243372 | *Zfp775* | Protein coding | -0.27751 | 0.064342 | 1.61E-05 | 0.003297 |
| ENSMUSG00000021792 | 70564 | *Prxl2a* | Protein coding | -0.21665 | 0.050247 | 1.62E-05 | 0.003297 |
| ENSMUSG00000001755 | 71743 | *Coasy* | Protein coding | -0.23088 | 0.053591 | 1.65E-05 | 0.003297 |
| ENSMUSG00000039701 | 99526 | *Usp53* | Protein coding | 0.293955 | 0.068245 | 1.65E-05 | 0.003297 |
| ENSMUSG00000032067 | 19286 | *Pts* | Protein coding | -0.18906 | 0.044044 | 1.77E-05 | 0.003489 |
| ENSMUSG00000015542 | 66176 | *Nat9* | Protein coding | -0.30798 | 0.072183 | 1.98E-05 | 0.003838 |
| ENSMUSG00000085615 | NA | *A330035P11Rik* | lncRNA | -0.4127 | 0.096728 | 1.99E-05 | 0.003838 |
| ENSMUSG00000020289 | 17168 | *Nprl3* | Protein coding | -0.16804 | 0.039424 | 2.02E-05 | 0.003864 |
| ENSMUSG00000024253 | 213575 | *Dync2li1* | Protein coding | -0.2472 | 0.058021 | 2.04E-05 | 0.003864 |
| ENSMUSG00000095677 | 100040531 | *Dynlt1f* | Protein coding | -0.2102 | 0.04941 | 2.10E-05 | 0.003933 |

| Ensembl gene ID | Entrez gene ID | Gene name | Gene biotype | log2 fold change | SE | *p* value | $p_{adj}$ |
|---|---|---|---|---|---|---|---|
| ENSMUSG00000013997 | 27045 | *Nit1* | Protein coding | -0.14112 | 0.033204 | 2.14E-05 | 0.003964 |
| ENSMUSG00000003344 | 208198 | *Btbd2* | Protein coding | -0.15313 | 0.036112 | 2.23E-05 | 0.004104 |
| ENSMUSG00000021013 | 76260 | *Ttc8* | Protein coding | -0.19918 | 0.047022 | 2.28E-05 | 0.004144 |
| ENSMUSG00000038838 | 68915 | *Vars2* | Protein coding | -0.17722 | 0.041876 | 2.32E-05 | 0.004174 |
| ENSMUSG00000059851 | 232811 | *Kmt5c* | Protein coding | -0.2241 | 0.05311 | 2.45E-05 | 0.004358 |
| ENSMUSG00000018669 | 80280 | *Cdk5rap3* | Protein coding | -0.16083 | 0.038128 | 2.46E-05 | 0.004358 |
| ENSMUSG00000001751 | 27419 | *Naglu* | Protein coding | -0.38673 | 0.09207 | 2.66E-05 | 0.004665 |
| ENSMUSG00000020752 | 170472 | *Recql5* | Protein coding | -0.20338 | 0.048459 | 2.70E-05 | 0.004691 |
| ENSMUSG00000024666 | 72982 | *Tmem138* | Protein coding | -0.20587 | 0.049147 | 2.80E-05 | 0.004817 |
| ENSMUSG00000048755 | 223722 | *Mcat* | Protein coding | -0.27658 | 0.066121 | 2.88E-05 | 0.004899 |
| ENSMUSG00000048550 | 208967 | *Thnsl1* | Protein coding | -0.29015 | 0.069417 | 2.92E-05 | 0.004923 |
| ENSMUSG00000110949 | 66387 | *Nudt8* | Protein coding | -0.31167 | 0.074852 | 3.13E-05 | 0.005234 |
| ENSMUSG00000078519 | NA | *2310026L22Rik* | lncRNA | -0.57117 | 0.137348 | 3.20E-05 | 0.005285 |
| ENSMUSG00000035722 | 27403 | *Abca7* | Protein coding | -0.21145 | 0.050863 | 3.22E-05 | 0.005285 |
| ENSMUSG00000023939 | 68463 | *Mrpl14* | Protein coding | -0.26355 | 0.063422 | 3.25E-05 | 0.005285 |
| ENSMUSG00000024958 | 107173 | *Gpr137* | Protein coding | -0.22844 | 0.055034 | 3.31E-05 | 0.005347 |
| ENSMUSG00000108555 | NA | *Gm18310* | TEC | -0.29977 | 0.072255 | 3.34E-05 | 0.005348 |
| ENSMUSG00000018733 | 103737 | *Pex12* | Protein coding | -0.20043 | 0.04842 | 3.48E-05 | 0.005526 |
| ENSMUSG00000024592 | 77422 | *C330018D20Rik* | Protein coding | -0.27096 | 0.065501 | 3.52E-05 | 0.005543 |
| ENSMUSG00000107040 | NA | *Gm43791* | lncRNA | -0.21331 | 0.051628 | 3.60E-05 | 0.005617 |
| ENSMUSG00000016344 | 66496 | *Ppdpf* | Protein coding | -0.20984 | 0.051185 | 4.14E-05 | 0.006384 |
| ENSMUSG00000003731 | 16650 | *Kpna6* | Protein coding | 0.121994 | 0.029767 | 4.16E-05 | 0.006384 |
| ENSMUSG00000078570 | 68920 | *1110065P20Rik* | Protein coding | -0.21352 | 0.052298 | 4.45E-05 | 0.006772 |
| ENSMUSG00000053870 | 75540 | *Fpgt* | Protein coding | -0.19725 | 0.048339 | 4.49E-05 | 0.00678 |
| ENSMUSG00000020747 | 71947 | *Tmem94* | Protein coding | -0.14658 | 0.035991 | 4.65E-05 | 0.006959 |

| Ensembl gene ID | Entrez gene ID | Gene name | Gene biotype | log2 fold change | SE | *p* value | $p_{adj}$ |
|---|---|---|---|---|---|---|---|
| ENSMUSG00000024325 | 19763 | *Ring1* | Protein coding | -0.20048 | 0.049414 | 4.97E-05 | 0.007375 |
| ENSMUSG00000110611 | NA | *Gm20163* | lncRNA | -0.36493 | 0.090044 | 5.06E-05 | 0.007458 |
| ENSMUSG00000037773 | 319513 | *Pced1a* | Protein coding | -0.14904 | 0.036873 | 5.30E-05 | 0.007748 |
| ENSMUSG00000046567 | 68281 | *4930430F08Rik* | Protein coding | -0.24653 | 0.061266 | 5.72E-05 | 0.0083 |
| ENSMUSG00000034744 | 56174 | *Nagk* | Protein coding | -0.23652 | 0.058853 | 5.85E-05 | 0.008415 |
| ENSMUSG00000110980 | NA | *Gm47204* | lncRNA | -0.41824 | 0.104117 | 5.89E-05 | 0.008417 |
| ENSMUSG00000060380 | NA | *C030014I23Rik* | lncRNA | -0.42397 | 0.105792 | 6.13E-05 | 0.008691 |
| ENSMUSG00000041936 | 11603 | *Agrn* | Protein coding | -0.17229 | 0.043035 | 6.24E-05 | 0.008744 |
| ENSMUSG00000108461 | NA | *AV356131* | lncRNA | -0.60935 | 0.152239 | 6.27E-05 | 0.008744 |
| ENSMUSG00000066829 | 235050 | *Zfp810* | Protein coding | -0.18767 | 0.04704 | 6.62E-05 | 0.009168 |
| ENSMUSG00000051977 | 213389 | *Prdm9* | Protein coding | -0.31508 | 0.079112 | 6.81E-05 | 0.00937 |
| ENSMUSG00000043251 | 277978 | *Exoc3l* | Protein coding | -0.27556 | 0.069295 | 6.99E-05 | 0.009539 |
| ENSMUSG00000074158 | 208111 | *Zfp976* | Protein coding | 0.237299 | 0.059742 | 7.13E-05 | 0.009656 |
| ENSMUSG00000029782 | 72649 | *Tmem209* | Protein coding | -0.22904 | 0.05793 | 7.69E-05 | 0.010347 |
| ENSMUSG00000021918 | 23955 | *Nek4* | Protein coding | -0.16928 | 0.042902 | 7.95E-05 | 0.010623 |
| ENSMUSG00000096990 | NA | *Gm26790* | lncRNA | -0.17106 | 0.043441 | 8.22E-05 | 0.010853 |
| ENSMUSG00000024959 | 12015 | *Bad* | Protein coding | -0.19586 | 0.049746 | 8.24E-05 | 0.010853 |
| ENSMUSG00000034903 | 319876 | *Cobll1* | Protein coding | 0.264273 | 0.067209 | 8.42E-05 | 0.011006 |
| ENSMUSG00000087523 | NA | *Gm12319* | lncRNA | -0.48619 | 0.123944 | 8.76E-05 | 0.011314 |
| ENSMUSG00000037151 | 216011 | *Lrrc20* | Protein coding | -0.27095 | 0.069083 | 8.78E-05 | 0.011314 |
| ENSMUSG00000025500 | 72000 | *Lmntd2* | Protein coding | -0.37699 | 0.096301 | 9.05E-05 | 0.011588 |
| ENSMUSG00000029713 | 14693 | *Gnb2* | Protein coding | -0.16081 | 0.041208 | 9.52E-05 | 0.012059 |
| ENSMUSG00000048100 | 99730 | *Taf13* | Protein coding | -0.24306 | 0.062295 | 9.55E-05 | 0.012059 |
| ENSMUSG00000032842 | 224814 | *Abcc10* | Protein coding | -0.19074 | 0.048912 | 9.64E-05 | 0.012069 |
| ENSMUSG00000030380 | 109889 | *Mzf1* | Protein coding | -0.31017 | 0.079566 | 9.69E-05 | 0.012069 |

| Ensembl gene ID | Entrez gene ID | Gene name | Gene biotype | log2 fold change | SE | *p* value | $p_{adj}$ |
|---|---|---|---|---|---|---|---|
| ENSMUSG00000046947 | 57869 | *Adck2* | Protein coding | -0.16379 | 0.042047 | 9.80E-05 | 0.01213 |
| ENSMUSG00000022022 | 211253 | *Mtrf1* | Protein coding | -0.30697 | 0.07898 | 0.000102 | 0.012474 |
| ENSMUSG00000030649 | 75430 | *Anapc15* | Protein coding | -0.24667 | 0.063486 | 0.000102 | 0.012474 |
| ENSMUSG00000055660 | 76781 | *Mettl4* | Protein coding | -0.18127 | 0.046757 | 0.000106 | 0.012802 |
| ENSMUSG00000057181 | 70591 | *5730455P16Rik* | Protein coding | -0.17376 | 0.04483 | 0.000106 | 0.012802 |
| ENSMUSG00000073647 | NA | *Gm10557* | Processed pseudogene | 0.288825 | 0.074668 | 0.00011 | 0.013136 |
| ENSMUSG00000054931 | 544922 | *Zkscan4* | Protein coding | -0.31046 | 0.080693 | 0.000119 | 0.0142 |
| ENSMUSG00000039623 | 231855 | *Ap5z1* | Protein coding | -0.18033 | 0.046888 | 0.00012 | 0.0142 |
| ENSMUSG00000024799 | 73166 | *Tm7sf2* | Protein coding | -0.17738 | 0.046196 | 0.000123 | 0.014288 |
| ENSMUSG00000041354 | 19732 | *Rgl2* | Protein coding | -0.15137 | 0.039436 | 0.000124 | 0.014288 |
| ENSMUSG00000096983 | NA | *2010015M23Rik* | lncRNA | -0.42533 | 0.110852 | 0.000125 | 0.014288 |
| ENSMUSG00000022558 | 223658 | *Mroh1* | Protein coding | -0.19825 | 0.051676 | 0.000125 | 0.014288 |
| ENSMUSG00000031534 | 102032 | *Smim19* | Protein coding | -0.21539 | 0.056176 | 0.000126 | 0.014288 |
| ENSMUSG00000073609 | 98314 | *D2hgdh* | Protein coding | -0.22051 | 0.057519 | 0.000126 | 0.014288 |
| ENSMUSG00000018405 | 217038 | *Mrm1* | Protein coding | -0.32512 | 0.084813 | 0.000126 | 0.014288 |
| ENSMUSG00000015013 | 59005 | *Trappc2l* | Protein coding | -0.21088 | 0.05503 | 0.000127 | 0.014288 |
| ENSMUSG00000032579 | 69536 | *Hemk1* | Protein coding | -0.27837 | 0.072896 | 0.000134 | 0.014998 |
| ENSMUSG00000117055 | NA | *Gm9805* | Processed pseudogene | 0.716735 | 0.187948 | 0.000137 | 0.015232 |
| ENSMUSG00000038593 | 654470 | *Tctn1* | Protein coding | -0.1134 | 0.029763 | 0.000139 | 0.015355 |
| ENSMUSG00000087687 | 100503890 | *Pet100* | Protein coding | -0.26837 | 0.070603 | 0.000144 | 0.015819 |
| ENSMUSG00000021376 | 22017 | *Tpmt* | Protein coding | -0.21988 | 0.057879 | 0.000145 | 0.015871 |
| ENSMUSG00000074220 | 233060 | *Zfp382* | Protein coding | 0.307904 | 0.081283 | 0.000152 | 0.016481 |
| ENSMUSG00000019577 | 27273 | *Pdk4* | Protein coding | 0.542745 | 0.143586 | 0.000157 | 0.016796 |
| ENSMUSG00000033467 | 57914 | *Crlf2* | Protein coding | -0.47617 | 0.125995 | 0.000157 | 0.016796 |
| ENSMUSG00000024169 | 106633 | *Ift140* | Protein coding | -0.15185 | 0.040181 | 0.000157 | 0.016796 |

| Ensembl gene ID | Entrez gene ID | Gene name | Gene biotype | log2 fold change | SE | *p* value | $p_{adj}$ |
|---|---|---|---|---|---|---|---|
| ENSMUSG00000033728 | 223664 | *Lrrc14* | Protein coding | -0.21042 | 0.055907 | 0.000167 | 0.017705 |
| ENSMUSG00000051224 | 245695 | *Tceanc* | Protein coding | -0.25192 | 0.066946 | 0.000168 | 0.017705 |
| ENSMUSG00000027366 | 66552 | *Sppl2a* | Protein coding | 0.106947 | 0.028454 | 0.000171 | 0.017922 |
| ENSMUSG00000055991 | 22757 | *Zkscan5* | Protein coding | -0.16965 | 0.045171 | 0.000173 | 0.018033 |
| ENSMUSG00000003762 | 76889 | *Coq8b* | Protein coding | -0.16852 | 0.044901 | 0.000175 | 0.018111 |
| ENSMUSG00000023873 | 66931 | *1700010I14Rik* | Protein coding | -0.49306 | 0.131604 | 0.000179 | 0.018435 |
| ENSMUSG00000078878 | 668030 | *Gm14305* | Protein coding | 0.246224 | 0.065732 | 0.00018 | 0.018435 |
| ENSMUSG00000078878 | 100043387 | *Gm14305* | Protein coding | 0.246224 | 0.065732 | 0.00018 | 0.018435 |
| ENSMUSG00000020621 | 105014 | *Rdh14* | Protein coding | -0.23661 | 0.063204 | 0.000181 | 0.018502 |
| ENSMUSG00000006463 | 70605 | *Zdhhc24* | Protein coding | -0.21869 | 0.058651 | 0.000193 | 0.01953 |
| ENSMUSG00000034667 | 73192 | *Xpot* | Protein coding | 0.103968 | 0.027963 | 0.000201 | 0.020248 |
| ENSMUSG00000074519 | 626848 | *Zfp971* | Protein coding | 0.307206 | 0.082939 | 0.000212 | 0.021294 |
| ENSMUSG00000110424 | 75479 | *1700012D14Rik* | lncRNA | -0.29807 | 0.080514 | 0.000214 | 0.021343 |
| ENSMUSG00000057729 | 19152 | *Prtn3* | Protein coding | -0.35034 | 0.094708 | 0.000216 | 0.021374 |
| ENSMUSG00000022940 | 56176 | *Pigp* | Protein coding | -0.17073 | 0.046157 | 0.000216 | 0.021374 |
| ENSMUSG00000043257 | 230801 | *Pigv* | Protein coding | -0.256 | 0.069493 | 0.00023 | 0.022572 |
| ENSMUSG00000007122 | 12372 | *Casq1* | Protein coding | 0.575813 | 0.156425 | 0.000232 | 0.02266 |
| ENSMUSG00000035048 | 69010 | *Anapc13* | Protein coding | -0.25425 | 0.069089 | 0.000233 | 0.02266 |
| ENSMUSG00000097718 | NA | *Gm26896* | lncRNA | -0.27462 | 0.074734 | 0.000238 | 0.023023 |
| ENSMUSG00000026203 | 56812 | *Dnajb2* | Protein coding | -0.17459 | 0.047542 | 0.00024 | 0.023114 |
| ENSMUSG00000032657 | 68521 | *Fam189b* | Protein coding | -0.28548 | 0.077967 | 0.000251 | 0.02399 |
| ENSMUSG00000029101 | 71729 | *Rgs12* | Protein coding | -0.16731 | 0.045757 | 0.000256 | 0.024341 |
| ENSMUSG00000041966 | 75763 | *Dcaf17* | Protein coding | -0.15339 | 0.042004 | 0.00026 | 0.024663 |
| ENSMUSG00000022472 | 28075 | *Desi1* | Protein coding | -0.13418 | 0.036762 | 0.000262 | 0.024709 |
| ENSMUSG00000062944 | 100043133 | *9130023H24Rik* | Protein coding | -0.17711 | 0.048541 | 0.000264 | 0.024712 |

| Ensembl gene ID | Entrez gene ID | Gene name | Gene biotype | log2 fold change | SE | *p* value | $p_{adj}$ |
|---|---|---|---|---|---|---|---|
| ENSMUSG00000059142 | 240041 | *Zfp945* | Protein coding | 0.146552 | 0.040257 | 0.000272 | 0.02539 |
| ENSMUSG00000024319 | 224705 | *Vps52* | Protein coding | -0.14174 | 0.038963 | 0.000275 | 0.025528 |
| ENSMUSG00000020056 | 67282 | *Washc3* | Protein coding | -0.22261 | 0.061502 | 0.000295 | 0.027251 |
| ENSMUSG00000034673 | 18515 | *Pbx2* | Protein coding | -0.20887 | 0.057727 | 0.000297 | 0.027256 |
| ENSMUSG00000015474 | 54397 | *Ppt2* | Protein coding | -0.16003 | 0.044264 | 0.0003 | 0.0274 |
| ENSMUSG00000051705 | 71599 | *Senp8* | Protein coding | -0.24519 | 0.067837 | 0.000301 | 0.0274 |
| ENSMUSG00000107336 | NA | *Gm43461* | TEC | -0.4366 | 0.120873 | 0.000304 | 0.027503 |
| ENSMUSG00000097439 | NA | *Gm16754* | lncRNA | -0.19052 | 0.052822 | 0.00031 | 0.02793 |
| ENSMUSG00000021661 | 68558 | *Ankra2* | Protein coding | -0.25906 | 0.071854 | 0.000312 | 0.027956 |
| ENSMUSG00000006019 | 71723 | *Dhx34* | Protein coding | -0.19496 | 0.054105 | 0.000314 | 0.028023 |
| ENSMUSG00000040374 | 19302 | *Pex2* | Protein coding | -0.21951 | 0.060937 | 0.000316 | 0.028023 |
| ENSMUSG00000035829 | 241289 | *Ppp1r26* | Protein coding | -0.16423 | 0.045662 | 0.000322 | 0.028484 |
| ENSMUSG00000023923 | 72238 | *Tbc1d5* | Protein coding | -0.18742 | 0.052195 | 0.00033 | 0.029001 |
| ENSMUSG00000043140 | 66690 | *Tmem186* | Protein coding | -0.17507 | 0.048944 | 0.000348 | 0.030447 |
| ENSMUSG00000025486 | 64384 | *Sirt3* | Protein coding | -0.19837 | 0.055627 | 0.000362 | 0.031582 |
| ENSMUSG00000030861 | 66885 | *Acadsb* | Protein coding | 0.111857 | 0.031405 | 0.000368 | 0.031882 |
| ENSMUSG00000038312 | 108687 | *Edem2* | Protein coding | -0.16048 | 0.045065 | 0.000369 | 0.031882 |
| ENSMUSG00000072772 | 14790 | *Grcc10* | Protein coding | -0.17513 | 0.04925 | 0.000377 | 0.032359 |
| ENSMUSG00000015468 | 18132 | *Notch4* | Protein coding | -0.19895 | 0.05618 | 0.000398 | 0.03405 |
| ENSMUSG00000007033 | 15482 | *Hspa1l* | Protein coding | -0.30457 | 0.086218 | 0.000412 | 0.035045 |
| ENSMUSG00000097174 | NA | *Gm4890* | lncRNA | -0.37506 | 0.106326 | 0.00042 | 0.035568 |
| ENSMUSG00000007682 | 13371 | *Dio2* | Protein coding | 1.197192 | 0.339726 | 0.000425 | 0.035629 |
| ENSMUSG00000040795 | 230767 | *Iqcc* | Protein coding | -0.16082 | 0.045655 | 0.000427 | 0.035629 |
| ENSMUSG00000068250 | 232566 | *Amn1* | Protein coding | -0.20026 | 0.056864 | 0.000429 | 0.035629 |
| ENSMUSG00000002846 | 76916 | *Timmdc1* | Protein coding | -0.17235 | 0.048947 | 0.00043 | 0.035629 |

| Ensembl gene ID | Entrez gene ID | Gene name | Gene biotype | log2 fold change | SE | *p* value | $p_{adj}$ |
|---|---|---|---|---|---|---|---|
| ENSMUSG00000024579 | 240334 | *Pcyox1l* | Protein coding | -0.20715 | 0.058842 | 0.000431 | 0.035629 |
| ENSMUSG00000098597 | 102465227 | *Mir6418* | miRNA | -0.14987 | 0.04258 | 0.000432 | 0.035629 |
| ENSMUSG00000019813 | 103268 | *Cep57l1* | Protein coding | -0.21386 | 0.060866 | 0.000442 | 0.036307 |
| ENSMUSG00000035898 | 231380 | *Uba6* | Protein coding | 0.134961 | 0.038533 | 0.000461 | 0.037497 |
| ENSMUSG00000031079 | 245368 | *Zfp300* | Protein coding | 0.28019 | 0.080014 | 0.000462 | 0.037497 |
| ENSMUSG00000039059 | 99296 | *Hrh3* | Protein coding | -0.37335 | 0.106626 | 0.000463 | 0.037497 |
| ENSMUSG00000028876 | 230735 | *Epha10* | Protein coding | -0.46956 | 0.134145 | 0.000465 | 0.037497 |
| ENSMUSG00000046603 | 382117 | *Tcaim* | Protein coding | -0.23144 | 0.066296 | 0.000481 | 0.038616 |
| ENSMUSG00000101225 | 629159 | *1700008J07Rik* | lncRNA | -0.2734 | 0.078334 | 0.000483 | 0.038616 |
| ENSMUSG00000048410 | 240476 | *Zfp407* | Protein coding | 0.1936 | 0.05552 | 0.000488 | 0.038694 |
| ENSMUSG00000004698 | 79221 | *Hdac9* | Protein coding | 0.151772 | 0.043535 | 0.00049 | 0.038694 |
| ENSMUSG00000068130 | 668923 | *Zfp442* | Protein coding | 0.379337 | 0.108842 | 0.000492 | 0.038694 |
| ENSMUSG00000074807 | NA | *Gm10762* | lncRNA | -0.2259 | 0.064817 | 0.000492 | 0.038694 |
| ENSMUSG00000040771 | 106821 | *Oard1* | Protein coding | -0.2411 | 0.069403 | 0.000513 | 0.039968 |
| ENSMUSG00000078630 | 791260 | *Tomt* | Protein coding | -0.2162 | 0.062242 | 0.000514 | 0.039968 |
| ENSMUSG00000014850 | 17686 | *Msh3* | Protein coding | 0.127811 | 0.036801 | 0.000515 | 0.039968 |
| ENSMUSG00000035285 | 269854 | *Nat14* | Protein coding | -0.29898 | 0.086227 | 0.000526 | 0.040537 |
| ENSMUSG00000111080 | 100504586 | *Gm20300* | lncRNA | -0.28311 | 0.081658 | 0.000526 | 0.040537 |
| ENSMUSG00000026154 | 68002 | *Sdhaf4* | Protein coding | -0.37553 | 0.108363 | 0.000529 | 0.040607 |
| ENSMUSG00000015095 | 30839 | *Fbxw5* | Protein coding | -0.13437 | 0.038806 | 0.000535 | 0.040843 |
| ENSMUSG00000035206 | 73218 | *Sppl2b* | Protein coding | -0.16119 | 0.046683 | 0.000555 | 0.042006 |
| ENSMUSG00000042066 | 68875 | *Tmcc2* | Protein coding | -0.1897 | 0.054953 | 0.000556 | 0.042006 |
| ENSMUSG00000111977 | NA | *Gm47163* | lncRNA | -0.29357 | 0.085047 | 0.000557 | 0.042006 |
| ENSMUSG00000052566 | 170833 | *Hook2* | Protein coding | -0.1902 | 0.055128 | 0.00056 | 0.04211 |
| ENSMUSG00000040502 | 216438 | *March9* | Protein coding | -0.25584 | 0.074188 | 0.000564 | 0.0422 |

| Ensembl gene ID | Entrez gene ID | Gene name | Gene biotype | log2 fold change | SE | *p* value | $p_{adj}$ |
|---|---|---|---|---|---|---|---|
| ENSMUSG00000047507 | 545192 | *Baiap3* | Protein coding | -0.2922 | 0.084942 | 0.000582 | 0.04315 |
| ENSMUSG00000021038 | 104799 | *Vipas39* | Protein coding | -0.11517 | 0.033484 | 0.000583 | 0.04315 |
| ENSMUSG00000022671 | 72083 | *Mzt2* | Protein coding | -0.2012 | 0.058501 | 0.000583 | 0.04315 |
| ENSMUSG00000064364 | NA | *mt-Th* | Mt_tRNA | 0.634031 | 0.184602 | 0.000593 | 0.043718 |
| ENSMUSG00000060261 | 14886 | *Gtf2i* | Protein coding | -0.07321 | 0.021373 | 0.000614 | 0.045026 |
| ENSMUSG00000031755 | 67378 | *Bbs2* | Protein coding | -0.2195 | 0.064192 | 0.000628 | 0.045683 |
| ENSMUSG00000008855 | 15184 | *Hdac5* | Protein coding | -0.1389 | 0.040621 | 0.000628 | 0.045683 |
| ENSMUSG00000030811 | 233902 | *Fbxl19* | Protein coding | -0.15385 | 0.045054 | 0.000638 | 0.046282 |
| ENSMUSG00000002797 | 110175 | *Ggct* | Protein coding | 0.296215 | 0.086824 | 0.000646 | 0.046633 |
| ENSMUSG00000056753 | NA | *C330011M18Rik* | lncRNA | -0.28651 | 0.084105 | 0.000658 | 0.047342 |
| ENSMUSG00000090290 | 212728 | *Tarbp1* | Protein coding | 0.180664 | 0.0531 | 0.000668 | 0.047808 |
| ENSMUSG00000021773 | 69156 | *Comtd1* | Protein coding | -0.28442 | 0.083612 | 0.00067 | 0.047808 |
| ENSMUSG00000112880 | 100504661 | *Gm20337* | lncRNA | -0.579 | 0.170289 | 0.000674 | 0.047906 |
| ENSMUSG00000022664 | 74102 | *Slc35a5* | Protein coding | -0.22951 | 0.067575 | 0.000683 | 0.048372 |
| ENSMUSG00000039577 | 260305 | *Nphp4* | Protein coding | -0.16984 | 0.050052 | 0.000691 | 0.048649 |
| ENSMUSG00000027163 | 76501 | *Commd9* | Protein coding | -0.15681 | 0.046217 | 0.000692 | 0.048649 |
| ENSMUSG00000033065 | 18642 | *Pfkm* | Protein coding | -0.14205 | 0.041894 | 0.000697 | 0.04882 |
| ENSMUSG00000073415 | NA | *Gm10501* | lncRNA | -0.2775 | 0.081929 | 0.000707 | 0.049304 |